A HYBRID ADJOINT APPROACH FOR SYSTEMS OF ARBITRARILY COMPLEX PARTIAL DIFFERENTIAL EQUATIONS

A DISSERTATION
SUBMITTED TO THE DEPARTMENT OF
AERONAUTICS AND ASTRONAUTICS
AND THE COMMITTEE ON GRADUATE STUDIES
OF STANFORD UNIVERSITY
IN PARTIAL FULFILLMENT OF THE REQUIREMENTS
FOR THE DEGREE OF
DOCTOR OF PHILOSOPHY

Thomas William Richard Taylor
July 2013

© 2013 by Thomas William Richard Taylor. All Rights Reserved.
Re-distributed by Stanford University under license with the author.

This work is licensed under a Creative Commons Attribution-Noncommercial 3.0 United States License.
http://creativecommons.org/licenses/by-nc/3.0/us/

This dissertation is online at: http://purl.stanford.edu/rn446zs4833

I certify that I have read this dissertation and that, in my opinion, it is fully adequate in scope and quality as a dissertation for the degree of Doctor of Philosophy.

Juan Alonso, Primary Adviser

I certify that I have read this dissertation and that, in my opinion, it is fully adequate in scope and quality as a dissertation for the degree of Doctor of Philosophy.

Francisco Palacios, Co-Adviser

I certify that I have read this dissertation and that, in my opinion, it is fully adequate in scope and quality as a dissertation for the degree of Doctor of Philosophy.

Karthikeyan Duraisamy

I certify that I have read this dissertation and that, in my opinion, it is fully adequate in scope and quality as a dissertation for the degree of Doctor of Philosophy.

Gianluca Iaccarino

I certify that I have read this dissertation and that, in my opinion, it is fully adequate in scope and quality as a dissertation for the degree of Doctor of Philosophy.

Antony Jameson

Approved for the Stanford University Committee on Graduate Studies.

Patricia J. Gumport, Vice Provost Graduate Education

This signature page was generated electronically upon submission of this dissertation in electronic format. An original signed hard copy of the signature page is on file in University Archives.

To everyone who ever believed in me,

Abstract

The adjoint method was first developed for fluid dynamics and aerospace applications in the 1970s and 1980s, and has since been applied to an increasingly varied set of problems. Adjoint-based techniques can provide the sensitivity of an objective function to any number of parameters of a simulation inexpensively at roughly the cost of a single additional flow calculation. This information can be used to perform sensitivity analyses, aerodynamic shape optimization and to estimate the error in the objective function due to numerical discretization.

Existing approaches to derive adjoint formalisms involve the so-called discrete and continuous methods, which differ in the order of performing the discretization and linearization steps. They have both strengths and weaknesses over each other in the form of complexity of the formulation and computational expense of the solution, and the choice of which method to use is not always obvious. In this work, an alternative hybrid adjoint approach is proposed with the aim of combining the relative advantages of the continuous and discrete methods, and thus making it easier to apply the adjoint approach to complex problems.

The adjoint method can, in general, be derived via a Lagrange multiplier approach, where the governing equations of the primal problem are enforced in the objective function through the adjoint variables. The new hybrid method works by enforcing some parts of the governing equations discretely and others continuously, and intends to leverage the advantages of the existing two approaches whilst avoiding their drawbacks. The exact choice of which parts to handle discretely/continuously depends on the the specific equation set and the characteristics desired in the resultant hybrid. Where possible, the intention is also to be able to reuse existing development and implementation of the two standard adjoint methods.

The specific hybrid approach developed in this dissertation treats the flow conservation equations in a continuous manner and additional models, such as those handling turbulence or combustion, discretely. This hybrid approach has been developed with application to both quasi-one-dimensional Euler flow with a simple combustion model and Reynolds-Averaged Navier-Stokes flow with a general turbulence model.

To investigate the utility of the hybrid adjoint approach, the turbulent hybrid adjoint was used to perform lift-constrained shape optimization of the coefficient of drag of the RAE 2822 airfoil under

transonic flow conditions. Where the effect of turbulence was more significant, a difference was seen between the surface sensitivities produced by the hybrid adjoint and a frozen-viscosity continuous adjoint. In the flow case that involved a thicker boundary layer, the shape optimization using the hybrid adjoint produced a significantly lower coefficient of drag (48.4% of the baseline) than that using the frozen-viscosity continuous adjoint (53.1% of the baseline) after a set number of design steps.

Potential future applications of this hybrid adjoint may include simulating the flow through jet engines (from conventional turbines to scramjets), where the effects of both turbulence and combustion are crucially important, and handling plasmas, where additional equation sets are required to model both chemical reactions and the effects of electromagnetic forces. In cases where alternative models are used to simulate a particular phenomenon, the hybrid method also offers the possibility of being able to switch between models treated discretely without requiring additional theoretical development for the continuous part.

Acknowledgements

"So long, and thanks for all the fish."

— Douglas Adams, *The Hitchhiker's Guide to the Galaxy*

There are far too many people that I could, and should, thank here, but I'm going to try and keep this as short and sweet as possible.

That afternoon back in the fall of 2002 when I first arrived on the Farm as an aspiring Masters student seems a long time ago now, and the road that has finally ended with this dissertation has been a long and bumpy one: I withdrew from the Ph.D. program twice, struggled with injury and spent a total of six years away from Stanford. But was it all worth it? Yes.

I would like to thank everyone who has supported me financially on this journey, from the donors who contributed to the departmental fellowship that funded my first year, to the help and support from the Department of Energy's Predictive Science Academic Alliance Program (PSAAP) that both brought me back to Stanford in 2009 and has played a big part in my research.

The injuries I suffered were never life threatening, but I owe a debt of gratitude to all the doctors, nurses and physiotherapists who helped me through some of the toughest times and who didn't just get me back to walking and cycling, but even to being able to play the Beautiful Game again.

Over the last 11 years the always-friendly staff in the Department of Aeronautics and Astronautics have helped me navigate my way through Stanford, and while I realize that is their job, and I might be just one more in a never-ending line of students, I am truly grateful for the help they've given me.

I could never have written this dissertation without the support, advice and friendship of my advising trio of J. F. K. — Juan, Francisco and Karthik.

It was Karthik who first encouraged me to study adjoints, and who suffered my wall-of-shame-worthy early attempts at running Computational Fluid Dynamics simulations as part of my work for PSAAP. It was also Karthik who set out to convert me to the world of American sports, and with whom I look forward to having many, many more arguments about those sports in the future.

Sin la ayuda de Francisco, no habría sido posible graduarme en, técnicamente, cinco años. Francisco es una de las personas más inteligentes que he conocido, y, afortunadamente, es también una de las más pacientes y amigables. Ahora que finalmente he terminado de escribir mi tesis, en vez de

molestarle más con cualquier pregunta sobre ingeniería, espero mejorar mi “andaluz” charlando con él.

And Juan? Back in 2004, when I left Stanford because of a lack of funding, Juan promised me that when things changed there would always be a place for me in his lab. It took more time than I think both of us expected, but I am sincerely grateful that he never forgot that. When I talked to him late last year about my plans to trade a career in engineering for one in journalism, he never even skipped a beat in encouraging me to go for it. Though he'll no longer be either my academic advisor or even a colleague, I'm hoping I'll still have a good friend.

When I returned to Stanford in 2009, Juan had only recently come back from a sabbatical, and his reborn Aerospace Design Lab (ADL) had just taken up residence in the basement of the Durand building. A few short years later, that cramped, ugly and dusty room that I first shared with Amta, Brendan, Jeff, Sean and Tom has become a bright and friendly corner of the Department of Aeronautics and Astronautics and its population has grown almost exponentially. There are now too many names to call out everyone individually, but it has been a real pleasure to share the ADL dungeon with folks both old and new, and it won't be easy surrendering my small patch of hard-earned territory down there.

There is another corner of campus I'll going to miss, too: The Lorey I. Lokey Stanford Daily Building. By accident more than design, I stumbled across that unique place on campus almost four years ago, somewhere I could cross the gaping grad-undergrad divide and live just a little bit of that true American college experience. Its ragtag band of writers and editors taught me to write, made me feel truly at home on campus and became strong friends. Thanks to The Daily I also leave here as a die-hard Stanford sports fan and finally discovered what it is I want to do with my life.

I don't want to fall into the trap of remembering life on the Farm only through rose tinted spectacles, but I must admit that I have been extremely lucky to have shared the last few years with some of the most amazing and inspiring people, some of the best friends I could ever hope for. It's been a wild ride and I hope to see much more of everyone on the other side of this dissertation.

Last but not least, none of this would have been possible without the love and support of my family. My grandparents, who gave me too many happy and unforgettable childhood memories. My father, who showed me the world and inspired me to think beyond the frontiers that too often define us. My mother, who has always been on my side and never, ever let me give up. And my brother, who, in spite of any meaningless quarrels or fights growing up, is the best and closest friend I'll ever have.

And finally, last but not least, I want to thank you, for being brave enough to read my thesis.

Nomenclature

Abbreviations

AD	= Automatic/Algorithmic Differentiation
ADOL-C	= Automatic Differentiation by Overloading in C++
AGARD	= Advisory Group for Aerospace Research and Development
CPU	= Central Processing Unit
CFD	= Computational Fluid Dynamics
PDE	= Partial Differential Equation
RAE	= Royal Aeronautical Establishment
RANS	= Reynolds-Averaged Navier-Stokes
SA	= Spalart-Allmaras turbulence model
SU^2	= Stanford University Unstructured code
UQ	= Uncertainty Quantification

Subscript and Superscript Definition

$()_e$	= Value at exit
$()_i$	= Value at inlet
$()_{i,j,k,l}$	= Spatial components, 1 to 3. Repeated index implies summation
$()_n$	= Variable on fine grid
$()_n^N$	= Variable from coarse grid interpolated onto fine grid
$()_{p,q,r}$	= Cell identifiers
$()_s$	= Value at shock
$()_{s^-}$	= Value just before shock
$()_{s^+}$	= Value just after shock
$()_A$	= Term treated with an adjoint approach
$()_C$	= Variable treated in continuous manner
$()_D$	= Variable treated in discrete manner
$()_E$	= Term from Euler governing equations

$()_{E,E}$ = Term from Euler governing equations present in Euler adjoint equations

$()_{E,\lambda}$ = Term from Euler governing equations present in combustion model adjoint equations

$()_H$ = Variable treated in hybrid manner

$()_L$ = Term from mean-flow governing equations

$()_N$ = Variable on coarse grid

$()_S$ = Value on wall boundary

$()_{SA}$ = Term treated with a sensitivity-analysis approach

$()_L$ = Term from turbulence model governing equations

$()_\epsilon$ = Variable related to energy flow

$()_\lambda$ = Term related to combustion model governing equation

$()_{\lambda,E}$ = Term from combustion model governing equation present in Euler adjoint equations

$()_{\lambda,\lambda}$ = Term from combustion model governing equation present in combustion model adjoint equations

$()_{\mu_T}$ = Term from eddy viscosity equation

$()_\rho$ = Variable related to density

$()_{\rho E}$ = Variable related to energy

$()_{\rho u_i}$ = Variable related to ith component of momentum

$()_\Gamma$ = Value/operator on boundary

$()_{\Gamma_\infty}$ = Value on far field boundary

$()_\Omega$ = Value/operator in domain

Variable Definition

a, b, c = Uniform perturbations in analytic adjoint derivation

b = Constant in Heaviside combustion source term

c = Speed of sound

c_{b1} = Spalart-Allmaras model constant

c_{b2} = Spalart-Allmaras model constant

c_{w1} = Spalart-Allmaras model constant

d = Distance from nearest wall

f = Perturbing function in linear perturbation or function for eddy viscosity

f_{v1} = Spalart-Allmaras model term

f_{v2} = Spalart-Allmaras model term

f_w = Spalart-Allmaras model term

g = Source function in adjoint equations or Spalart-Allmaras model term

h = Height of duct

h^* = Height of duct at sonic conditions

j = Integrand of domain integral in objective function

j_Γ = Integrand of surface integral in objective function

j_Ω = Integrand of domain integral in objective function

m = Mass flow

n = Total number of cells on fine grid or number of incoming characteristics

$\hat{n}$ = Normal vector

p = Static pressure

p^* = Pressure constant for magnitude of pressure difference cost function

p_0 = Stagnation pressure

p_0^* = Stagnation pressure at sonic conditions

q = Specific heat release

r = Spalart-Allmaras model term

t = Time coordinate

u = Flow velocity

v = Adjoint variable

x = Spatial coordinates

C = Constant in exponential combustion source term

C_p = Specific heat capacity under constant pressure

E = Internal energy

F = Convective flux

F^{v1} = First viscous flux term

F^{v2} = Second viscous flux term

G = Adjoint flux term

H = Stagnation enthalpy

ΔH_w = Stagnation enthalpy change due to heat flux across a wall

L = Primal problem linear operator

L^* = Adjoint problem linear operator

M = Mach number

N = Total number of cells, number of cells on coarse grid or number of dimensions

P = Pressure source vector in quasi-one-dimensional Euler equations

Pr = Laminar Prandtl number

Pr_T = Turbulent Prandtl number

Q = Combustion source vector

R = Specific gas constant

S = Wall boundary

$\hat{S}$ = Spalart-Allmaras model term

S_R = Rayleigh flow heat source vector

T = Static temperature

T^* = Initiation temperature in Heaviside combustion source term

T_0 = Stagnation temperature

T_0^* = Stagnation temperature at sonic conditions

T^{cv} = Spalart-Allmaras turbulence model flux term

T^s = Spalart-Allmaras turbulence model source term

U = Vector of conservative flow variables

W = Vector of characteristics

$(W)_+$ = Vector of incoming characteristics

W_∞ = Vector of characteristics at the far field

$\mathcal{A}_i,\ \mathcal{B}_i,\ \mathcal{C}_i$ = Substitutions used to simplify mathematical working

$\mathcal{B}$ = Boundary conditions

$\mathcal{G}$ = Governing equations

$\mathcal{I}$ = Perturbation to objective function in analytic adjoints

$\mathcal{J}$ = Objective function

$\mathcal{L}$ = Lagrangian

$\mathcal{N}$ = Flow governing equations

$\mathcal{R}$ = Numerical residual

$\mathcal{R}^*$ = Numerical residual in a boundary cell without the flux across the boundary

$\mathcal{R}^{(*)}$ = General symbol for $\mathcal{R}$ (internally) or $\mathcal{R}^*$ (on boundary)

$\mathcal{V}$ = General adjoint variable

α = General parameter under which perturbations are considered

β = Switching variable in hybrid objective function

γ = Ratio of specific heats

ϵ = Energy flow

κ = Spalart-Allmaras model constant

λ = Combustion flow variable

μ = Laminar viscosity or momentum term in Rayleigh analytic adjoint

μ_1 = First constant in Sutherland's law

μ_2 = Second constant in Sutherland's law

μ_T = Turbulent viscosity

μ^{v1} = First viscosity combination

μ^{v2} = Second viscosity combination

ν = Kinematic viscosity

$\hat{\nu}$ = Spalart-Allmaras turbulence model variable

ξ = Location of point source in Green's function approach

$\xi^{\pm}$ = Locations either side of point source in Green's function approach

ρ = Density

σ = Spalart-Allmaras model constant

τ = Stress tensor

ϕ = Continuous adjoint variable

φ = Hybrid adjoint variable

χ = Spalart-Allmaras model term

ψ = Discrete adjoint variable

ω = Combustion source term or vorticity

Γ = Flow domain boundary

Γ_p = Cell domain boundary

Γ_∞ = Far field boundary

Λ = Reaction progress variable

Ψ = Adjoint variable used for error estimation

Ω = Flow domain

Ω_p = Cell domain

Mathematical Notation

$\emptyset$ = Empty set

$\{\}$ = Set of

$()'$ = Perturbed value

$[(), ()]$ = Bounding limits

$|()|$ = 2-norm

$\widehat{()}$ = Numerical flux

$\widetilde{()}$ = Roe flux

$()^T$ = Transpose

$\delta()$ = Dirac delta function

δ_{ij} = Kronecker delta function

$\mathcal{H}()$ = Heaviside function

$\delta()$ = Continuous perturbation

$\Delta()$ = Discrete perturbation

$\{\delta, \Delta\}()$ = Hybrid perturbation

$\partial_i()$ = Gradient in x_i direction, i.e., $\dfrac{\partial()}{\partial x_i}$

$\dfrac{\partial()}{\partial()}$ = Analytical Jacobian

$\dfrac{\mathfrak{D}()}{\mathfrak{D}()}$ = Numerical Jacobian

ϵ_{ijk} = Levi-Civita tensor

$\in$ = Element of

Contents

List of Tables

List of Figures

Chapter 1

Introduction

"Fourteen years in the professor dodge have taught me that one can argue ingeniously on behalf of any theory, applied to any piece of literature. This is rarely harmful, because normally no one reads such essays."

— Robert Parker

The adjoint variables can be interpreted as the sensitivity of a chosen objective function to perturbations in the conserved flow variables at any point within a domain. This sensitivity information can be used in a wide range of applications, from shape optimization of aerodynamic designs to the estimation of error in simulations. The main focus of this dissertation is to introduce the idea of a hybrid adjoint approach in a way that is consistent with the existing discrete and continuous adjoint methods, and which, where possible, will leverage the best features and reuse the theoretical and practical development of these standard approaches.

1.1 Background and motivation

1.1.1 The adjoint method in aerospace design

Using ideas adapted from Lions[1] on optimal control of systems governed by partial differential equations (PDEs), the adjoint method was first developed for fluid dynamic shape optimization applications through the use of control theory by Pironneau[2]. In the 1980s and 1990s Jameson pioneered the application of adjoints in computational fluid dynamics (CFD) applications, handling first the potential flow and Euler equations[3] and then the laminar Navier-Stokes equations[4]. More recent work by Zymaris et al.[5] and Bueno-Orovio et al.[6], among others, has further extended the theory to the Reynolds-Averaged Navier-Stokes equations coupled with the one-equation Spalart-Allmaras turbulence model[7, 8].

There are two broad classifications of the adjoint method, the continuous and discrete approaches, and whilst the short history outlined above discussed the development of the continuous adjoint, the discrete method has also been widely used and investigated, including work by Elliot and Peraire[9] and Giles et al.[10, 11], among others.

Over the past two decades, adjoint methods have been used in a variety of applications including sensitivity analysis[12, 13], shape optimization of wing geometries[14, 15, 16, 17], goal-oriented numerical error estimation and mesh adaptation[10, 18, 19, 20, 21, 22], and uncertainty quantification[7, 23, 24, 25].

The adjoint equations are traditionally derived either using Lagrange multipliers or through the Primal-Dual Equivalence Theorem[26, 27]. The key assumption made is that the primal equations can be linearized, though attempts have been made to apply the theory in the case of non-linear operators[26]. Like other approaches within the wider topic of gradient-based optimization, adjoint methods are generally subject to the limitations that the underlying flow variables must be continuous and that there is no guarantee that an optimization process will converge to the global minimum[26]. In general, the adjoint is most applicable to a situation in which there are few objective functions and many design variables[28]. In comparison to traditional sensitivity analysis methods such as finite differencing[29], adjoint methods are seen to be considerably cheaper, requiring roughly the cost of just one additional flow solution to compute sensitivities to arbitrary

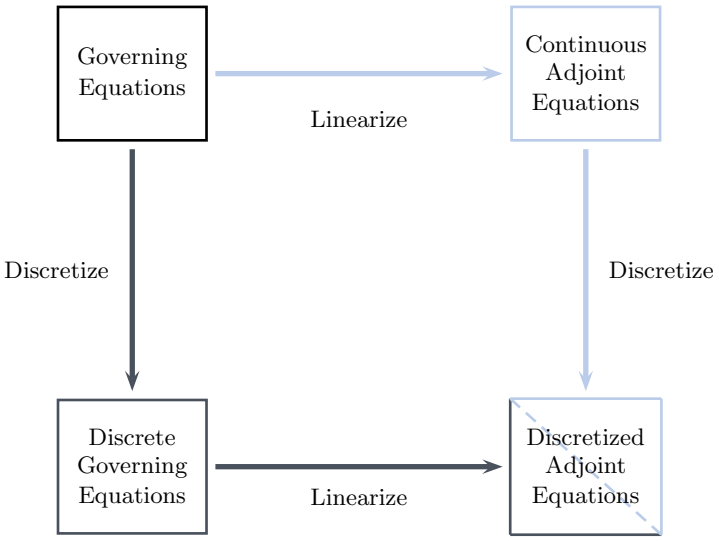

Figure 1.1: General derivation scheme for the discrete and continuous adjoint equations.

numbers of parameters[30].

The adjoint variables, obtained from the solution of the adjoint equations, can be considered as more than just a mathematical construct and have a deeper connection to the physical problem[31, 26], i.e., they represent the sensitivity of an objective function to changes in the conserved flow variables at any point within a domain. Thus, for example, the density-adjoint variable for a lift objective function at a specific point will indicate how a change purely to the density at that location would affect the overall lift.

1.1.2 The discrete and continuous approaches

Depending on the approach followed for the derivation of the adjoint equations, the method is conventionally characterized as either discrete or continuous. The difference arises from the order of discretization and linearization of the governing equations. In the discrete adjoint method, the already-discretized governing equations — from the numerical solution of the flow — are used to derive the *discrete* adjoint equations. In the continuous adjoint method, the *continuous* adjoint equations are derived from the analytical form of the PDE and then discretized to obtain a discrete representation of the adjoint equations. This key difference is shown in Figure 1.1.

The effect of these contrasting approaches is that the development and implementation of the two adjoint methods are considerably different. The continuous adjoint requires significant mathematical development before any code can be written, but can then be solved using standard approaches for PDEs. In contrast, the development required for the discrete adjoint is much less complicated and,

if employing algorithmic differentiation (AD)[30], either via source code transformation, e.g., using TAPENADE[32], or operator overloading, e.g., using ADOL-C[33], to calculate partial derivatives, this process can be considered to be relatively automatic, and independent of the complexity of the primal PDE. The discrete linear system, however, cannot be solved using the same techniques as either the continuous adjoint or the primal flow problem.

Though we might expect that on an infinitely fine grid the two methods will converge to the same, analytic, solution, unless we have dual consistency[34] the discretized equations and their resultant adjoint variables will not be consistent. A reason for this is that the discrete adjoint is closely tied to the numerical solution method of the flow equations used, including any limiters and artificial dissipation added, whereas the continuous adjoint is not. As even a difference in the solution process of two identical flow problems can lead to marginally different solutions, it is therefore to be expected that discrete and continuous adjoint solutions found by different numerical methods will not perfectly agree.

1.1.3 The pros and cons of the discrete and continuous adjoint approaches

It is important to note that both the continuous and the discrete approaches have advantages and disadvantages over one another, making the choice of which method to use both partially dependent on the particular problem to be solved, but also on the experience and preference of the researcher[26]. There may often be only small differences in the results from shape optimization obtained via either approach[35], but there is usually little comparison made between the actual adjoint solutions themselves[36], making it harder to understand which of the approaches is better.

As noted previously, the discrete is in theory easier to develop, especially when using AD to find partial derivatives, and PDEs of arbitrary complexity can be handled with very little mathematical development. However, this can be much more expensive computationally, and the resulting linear system can be highly stiff or ill-conditioned and difficult to solve, with little freedom to tailor the scheme for the numerical solution of the problem. The development of the discrete adjoint also generally relies on the condition that the numerical flow residuals are zero, and thus that the flow solution has fully converged. When this is not true, the correct approach, in theory, would be to apply the discrete adjoint to the entire flow solution process, but that is usually not possible due to the large memory demands of doing so. Though improvements have been made to reduce both the CPU cost and memory requirements[10], it remains difficult to apply the discrete approach to higher order schemes, due to the complexity of handling the limiters and artificial dissipation present in the numerical scheme and the stiffness of the linear system created. While it is also possible to analytically derive the required partial derivative terms (by hand) and then develop code based on those formulae, this requires a large amount of development, possibly more than that generally required in the continuous method[35].

The continuous adjoint, in comparison, provides much more freedom to the solution process,

allowing us to analyze the adjoint PDE and select an appropriate discretization scheme, independent of that used to solve the flow-field system, ensuring the problem is well-posed. However, this approach requires significant mathematical work, and it may not always be possible to perform the required mathematical manipulations on the governing equation sets, boundary conditions and objective functions of interest. Moreover, the cost functionals are generally limited to weighted integrals of specific quantities — for Euler flow, just the weighted integral of the linearized perturbation to the pressure —, though Arian and Salas[37] have shown that it is possible to extend the continuous adjoint to "inadmissible" cost functionals.

Some of the most interesting challenges for aeronautical engineers involve flows with turbulence and/or combustion. Applying adjoint methods to these is not necessarily straightforward and simplifications are generally made. A common one applied to the continuous adjoint being that the viscosity is considered *frozen*, removing the need to develop an adjoint form of any turbulence models, though the eddy viscosity remains in the problem as a constant term. Duraisamy and Alonso[7] applied this assumption to the discrete adjoint, making comparison to full turbulent adjoint and finite difference results, and Bueno-Orovio et al.[6] compared the frozen-viscosity and full turbulent continuous adjoint solutions, with the caveat that some terms were still neglected to aid stability. Both of these indicated an appreciable difference in the results, with Duraisamy and Alonso highlighting cases where the sensitivity was significantly wrong.

Simplifications are also sometimes made when using the discrete adjoint. One of these is that it is often applied only to first-order schemes in order to avoid the problem of having to consider contributions from a point's next-neighbors in higher order schemes, and thus reducing the stiffness in the resulting linear system. This contribution exists due to the dependence of the residual within a cell on the gradient in neighboring cells. Nielsen and Anderson[38] showed that the error due to this assumption was significant, perhaps as much as 100%.

When dealing with shape optimization, and thus surface sensitivities, a further simplification may also be required for the discrete approach. Using differential geometry it is possible to derive an analytic formula for the surface sensitivity for the continuous adjoint such that the sensitivity depends only on the surface mesh, but this is not true with the discrete adjoint. Here we generally must calculate the mesh sensitivity of the entire grid in order to find the required surface sensitivity. The assumption that we need only consider cells out to a certain distance from the surface eases the expense, but can create errors in the results[38].

However, the discrete adjoint can provide the *exact* gradient of the discretized objective function and as a result this helps optimization problems to converge. On the other hand, though the gradient from the continuous should be more consistent with that of the underlying model, providing greater physical insight, it will not generally agree perfectly with that from the numerical solution of the flow, potentially causing problems for the optimization procedure.

An additional problem with the discrete adjoint is that it can create highly oscillatory solutions

	Discrete	Continuous	Hybrid
Ease of development[11, 26, 30, 35, 39]	+	−	±
Compatibility of numerical gradients:			
- with the discretized PDE[7, 6, 26, 30, 35]	+	−	−
- with the continuous PDE[26, 36]	−	+	+
Surface formulation for gradients[6, 40]	−	+	+
Ability to handle:			
- arbitrary functionals[30, 39]	+	−	±
- non-differentiability[26, 30, 39, 41]	+	−	+
Computational cost[10, 26, 30, 35]	−	+	±
Flexibility in solution[26, 35, 36, 38, 39]	−	+	±

Table 1.1: Simple comparison between the discrete, continuous and hybrid adjoint approaches.

near surfaces where strong boundary conditions are enforced. Giles et al.[10] overcame this problem by reintroducing surface momentum residuals, usually discarded in imposing the strong conditions. Sharp shock discontinuities can also lead to instabilities, though an increased amount of smoothing in the numerical flow solution generally removes this issue.

1.1.4 A new hybrid adjoint approach

As discussed above, there are relative advantages and disadvantages of using either the discrete or continuous adjoint methods. These are summarized in the second and third columns of Table 1.1. Where an approach has been given a + sign, this indicates it has more favorable characteristics in this respect, and a − sign indicates less favorable characteristics. The *hybrid* approach that is introduced in this thesis, which mixes aspects of the discrete and continuous, aims to try and capture the positive aspects of the standard methods and minimize their drawbacks.

Some previous work has attempted to hybridize the adjoint approach to simplify the solution process or to improve results, but without introducing the concept of a full hybrid adjoint methodology. This includes using the continuous adjoint variables in a discrete sensitivity formulation[36], incorporating a more continuous-like wall boundary condition in the discrete adjoint[10] and a continuous adjoint formulation that discretizes the adjoint equations in a way consistent with the discrete approach[28].

However, these methods are relatively limited and are mostly adjustments made to one or the other of the adjoint approaches in order to make them easier to use or more accurate. Instead, a more general approach is developed here[39, 42, 43], which aims to allow us to handle parts of the governing equations continuously and other parts discretely, in a way that is consistent with the fundamentals of adjoint theory and does not necessarily favor one approach over the other. The choice between which terms will be enforced discretely or continuously is intended to be made such that non-differentiable or highly complex functions will be removed from the continuous part of the

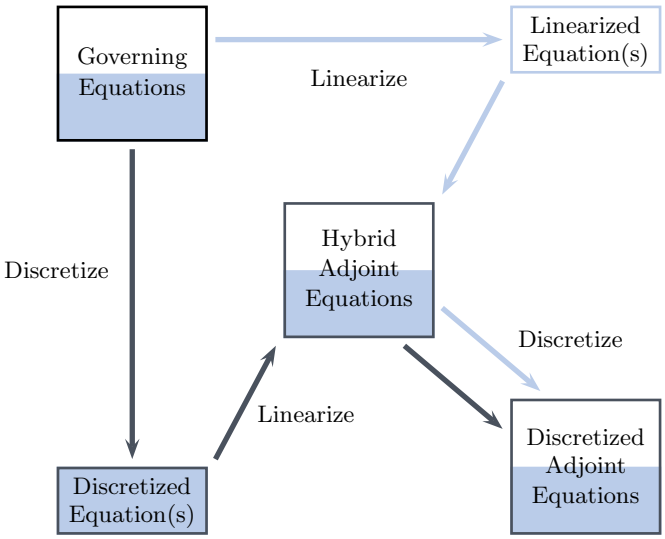

Figure 1.2: General derivation scheme for continuous–discrete hybrid adjoint equations.

formulation, and so as to reduce the mathematical development time usually associated with the continuous adjoint. The general approach for this continuous-discrete hybrid is shown in Figure 1.2.

This hybrid adjoint approach is intended for problems involving very complex PDEs, such as those involving two- (or more) equation turbulence models, combustion including look-up tables and multi-species simulations such as those seen in multi-species, multi-phase problems. The idea is to use a continuous formulation for those portions of the flow equations for which such formulations already exist (in the form of code or as previously published equations), but to treat discretely those portions of the governing equations that are difficult (or impossible) to handle analytically. This aims to leverage the properties of the discrete adjoint approach to build the adjoint equations and the properties of the continuous adjoint approach to solve them. The result is intended to be an approach that produces a high-quality adjoint solution and one that inherits the favorable characteristics of the original methods, including the ability to relax the solution process, while overcoming their drawbacks.

In this dissertation, the hybrid approach is applied to quasi-one-dimensional Euler flow with a simple combustion model and to Reynolds-Averaged Navier-Stokes flow with a general turbulence model. Returning to Table 1.1, the final column illustrates how well the hybrid adjoint method used here has performed in our goal of capturing the advantages of the existing two approaches.

1.2 Thesis Overview

As explained in the previous section, the key focus of this thesis is to develop a hybrid adjoint approach for situations in which the fully discrete or fully continuous adjoint methods alone are no longer ideal. The hybrid aims to appropriately combine the approaches of both of the traditional adjoint methods, and possibly of other sensitivity-analysis methods, in order to take advantage of the positive characteristics of these standard techniques, whilst avoiding their drawbacks. To understand how to create such a hybrid, and in order to evaluate its performance, it is also necessary to investigate and make comparisons between the existing approaches.

The following two sections detail the main contributions of this work and provide an outline of this dissertation.

1.2.1 Contributions

The main contribution of this work is to introduce the general idea of a hybrid approach aimed at both simplifying the development and solution process, and also improving the quality of the adjoint solution obtained.

In many cases, the standard approach for applying adjoint methods to complex flow simulations is to start from either the discrete or continuous adjoint and then make assumptions and simplifications such that the resultant system can be solved. However, a key drawback to that process is that we are no longer solving the real (continuous or discrete) equations and thus may not obtain accurate adjoint solutions. Instead of introducing assumptions or simplifications, the continuous-discrete hybrid introduced here remains mathematically consistent with the adjoint derivation process, and thus we expect the adjoint variables obtained to be (numerically) accurate. By appropriately segregating the governing equation set, however, we can simplify both the development and solution process, e.g., treating turbulence and combustion models discretely (and using AD) reduces the development cost, especially when new models are added, and treating the mean flow continuously allows greater flexibility in the numerical solution process.

We also show that within the general hybrid derivation, decisions can be made to improve its usefulness and applicability. These include the decision of how to treat each governing equation (i.e., discretely or continuously), if we should consider a discrete or continuous form for the objective function and whether it is possible to extract terms from the discrete or continuous governing equation sets and treat them in the opposite manner.

To fully justify the decisions made in creating a hybrid adjoint, and to be able to analyze the performance of this new approach, it was important to develop the discrete and continuous methods side-by-side and compare and contrast not just their solutions, but also their underlying theory and implementation. In addition to helping justify and design the hybrid approach, this analysis can also help indicate when and where the discrete should be used over the continuous, and vice versa.

1.2.2 Outline

Chapter 2 explains the general features of the adjoint method, using a Lagrange multiplier approach, and shows how both the discrete and continuous adjoint equations can be derived according to this same general approach. It is important to make this connection so that later in this thesis the two parts of a continuous-discrete hybrid can be treated in a similar, though not identical, way. Finally it introduces several different applications of the adjoint variables.

Chapter 3 introduces the process of creating a hybrid adjoint, first briefly discussing existing, limited, approaches and then developing the general strategy for two different hybrids, an adjoint-sensitivity analysis method and a continuous-discrete hybrid. However, the latter approach, combining the continuous and discrete adjoint methodologies, is the key focus of this thesis, and the adjoint-sensitivity analysis method is not discussed further.

Chapter 4 applies the three different adjoint approaches (discrete, continuous and hybrid) to quasi-one-dimensional flow. The discrete and continuous methods are first developed for standard quasi-one-dimensional Euler flow, and then extended to include a simple combustion model. The hybrid approach is then developed, making key reference to the parts of the derivation that it inherits from the standard two methods, and finally results from numerical simulations are used as a means to compare the three approaches.

Chapter 5 extends the hybrid theory and development from the preceding chapters to the more complicated cases of two- and three-dimensional flows. Again we intend to provide detailed development, and thus start from Euler flow before extending this to Navier-Stokes and then Reynolds-Averaged Navier-Stokes (RANS) flows. When considering this latter situation we first consider using the Spalart-Allmaras one-equation model and then attempt to create a hybrid whose mathematical development is essentially independent of the turbulence model. Results from transonic simulations of the RAE 2822 airfoil are used to understand how effective the hybrid adjoint approach has been. These include optimization studies of AGARD AR 138 cases 9 and 10[44] that indicate improved performance of the hybrid approach over the frozen-viscosity continuous adjoint when the effects of turbulence are greater.

In the Conclusions (Chapter 6), we return to the comparison between the discrete, continuous and hybrid adjoints (Table 1.1), discussing in more detail where this new approach achieves the goal of capturing the positive characteristics of the traditional two methods, whilst avoiding their drawbacks. We also discuss the possible applications of the hybrid and the future development that may be required to better understand and improve the hybrid adjoint approach.

To help explain and justify the development of the hybrid adjoint approach, considerable effort has been paid to writing the derivations in this thesis in as much detail as possible. However, where appropriate, the derivations within the main body of this document have been condensed and the more detailed mathematical development moved to the Appendices.

Chapter 2

General adjoint theory

"You didn't understand this at first, but my CONVINCING USE OF CAPITAL LETTERS HAS MADE IT ALL CLEAR TO YOU."

— J. Nairn

BEFORE considering the problem of a hybrid adjoint approach we will first introduce the general adjoint method. This will then allow us to apply a consistent approach to the development of both the discrete and continuous adjoint methods in this chapter, and then, in the following chapter, the hybrid.

2.1 Introduction to adjoint methods

The adjoint equations can conveniently be formulated in a framework to calculate the sensitivity of a given objective function $\mathcal{J}$ to parameters α in a problem governed by the set of equations which can be represented by $\mathcal{G}(U, \alpha) = 0$, where U is the solution. The adjoint variables that solve these equations can be used purely as a mathematical tool to find the required sensitivities, but, as discussed by Giles and Pierce[26] and Belegundu and Arora[31], they can also be interpreted as representing the sensitivity of the objective function to perturbations in the governing equations/conserved variables, or the influence on the objective function of an arbitrary source function.

The additional computational cost of solving the adjoint problem is of the order of one additional flow solution, and the adjoint variables can be used to compute the sensitivities of $\mathcal{J}$ to changes in all of the parameters that define the problem at any point in the domain, without requiring additional flow solutions. In contrast, though finite-difference or complex-step methods[29] can also be used to find these sensitivities, they are in general significantly more expensive, requiring at least one additional flow solution to find the gradient of the objective function with respect to each parameter in the domain and, in the case of finite differencing, these methods can potentially be less accurate.

There are two main approaches used to derive the adjoint equations: the Primal-Dual Equivalence Theorem and an optimization framework using Lagrange multipliers[26, 31]. In this dissertation we consider the latter method, and present the discrete, continuous and then hybrid derivations in an identical context. To demonstrate the basic method we will consider the model problem of the objective function

$$\mathcal{J}(U, \alpha), \quad \text{on } \Omega \text{ or } \Gamma, \tag{2.1}$$

defined on the domain or boundary shown in Figure 2.1, and subject to the constraints

$$\mathcal{G}(U, \alpha) = 0, \quad \text{on } \Omega \text{ and } \Gamma, \tag{2.2}$$

which are the governing equations, including both the flow equations, $\mathcal{N} = 0$, on Ω, and the boundary conditions, $\mathcal{B} = 0$, on Γ.

The general derivation process follows these steps:

1. Introduce a Lagrangian, $\mathcal{L}$, to enforce the governing equations in the objective function via a set of Lagrange multipliers,

$$\mathcal{L} = \mathcal{J} + \mathcal{V}^T \mathcal{G}, \tag{2.3}$$

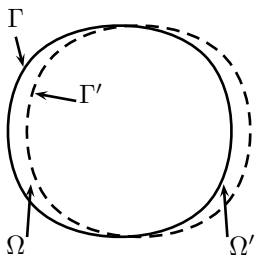

Figure 2.1: Unperturbed and perturbed domain and boundary surface.

where $\mathcal{V}$ are the Lagrange multipliers, which we will later denote as the adjoint variables, and we note that as $\mathcal{G} = 0$, $\mathcal{L} \equiv \mathcal{J}$ for any value of $\mathcal{V}$.

2. Write down the perturbation of the Lagrangian, $\delta\mathcal{L}$, relative to a small change in some parameter α (which may induce perturbations in the flow, domain and boundary),

$$\delta\mathcal{L} = \delta\mathcal{J} + \mathcal{V}^T\delta\mathcal{G}, \tag{2.4}$$

noting that we have constrained $\mathcal{V}$ such that it does not depend on α.

3. Expand and mathematically manipulate the terms in $\delta\mathcal{L}$ so as to group those dependent on the flow perturbation, δU. Neglecting domain or surface perturbations, this gives

$$\begin{aligned} \delta\mathcal{L} &= \frac{\partial\mathcal{J}}{\partial\alpha}\delta\alpha + \frac{\partial\mathcal{J}}{\partial U}\delta U + \mathcal{V}^T\left(\frac{\partial\mathcal{G}}{\partial\alpha}\delta\alpha + \frac{\partial\mathcal{G}}{\partial U}\delta U\right) \\ &= \left(\frac{\partial\mathcal{J}}{\partial\alpha} + \mathcal{V}^T\frac{\partial\mathcal{G}}{\partial\alpha}\right)\delta\alpha + \left(\frac{\partial\mathcal{J}}{\partial U} + \mathcal{V}^T\frac{\partial\mathcal{G}}{\partial U}\right)\delta U. \end{aligned} \tag{2.5}$$

4. Identify the Lagrange multipliers as the adjoint variables and introduce constraints on these variables, including adjoint equations and boundary conditions, such that any explicit dependence of $\delta\mathcal{L}$ on δU is removed. Here we note that through definition of the adjoint equations

$$\frac{\partial\mathcal{J}}{\partial U} + \mathcal{V}^T\frac{\partial\mathcal{G}}{\partial U} = 0, \tag{2.6}$$

the perturbation to the Lagrangian can then be written

$$\delta\mathcal{L} = \left(\frac{\partial\mathcal{J}}{\partial\alpha} + \mathcal{V}^T\frac{\partial\mathcal{G}}{\partial\alpha}\right)\delta\alpha. \tag{2.7}$$

5. Equate $\delta\mathcal{L}$ to the perturbation to the objective function, $\delta\mathcal{J}$, allowing us to easily find, once

the adjoint problem has been solved, the sensitivities of $\mathcal{J}$ relative to any system parameter, i.e.,

$$\frac{d\mathcal{J}}{d\alpha} = \frac{\delta\mathcal{J}}{\delta\alpha} = \frac{\partial\mathcal{J}}{\partial\alpha} + \mathcal{V}^T\frac{\partial\mathcal{G}}{\partial\alpha}. \tag{2.8}$$

For the case where there is no explicit dependence of $\mathcal{J}$ on α we can write this as the simple inner product

$$\frac{d\mathcal{J}}{d\alpha} = \mathcal{V}^T\frac{\partial\mathcal{G}}{\partial\alpha}. \tag{2.9}$$

2.1.1 Discrete adjoint approach

Starting from the discrete objective function, $\mathcal{J}_D$, in the discrete adjoint approach the governing equations that we wish to enforce are the residuals, at every point in the domain, that come from the flow solution process, $\mathcal{R}_p$, i.e., $\mathcal{G} = \{\mathcal{R}_p\} = 0$. We note that these residuals include the boundary conditions from the primal solution. This gives the Lagrangian

$$\mathcal{L} = \mathcal{J}_D + \sum_{p=1}^{N}\psi_p^T\mathcal{R}_p, \tag{2.10}$$

where ψ are the Lagrange multipliers, or discrete adjoint variables. The perturbation to this is

$$\Delta\mathcal{L} = \Delta\mathcal{J}_D + \sum_{p=1}^{N}\psi_p^T\Delta\mathcal{R}_p. \tag{2.11}$$

The terms on the right hand side can then be linearized and expanded as

$$\Delta\mathcal{J}_D = \sum_{q=1}^{N}\frac{\mathfrak{D}\mathcal{J}_D}{\mathfrak{D}U_q}\Delta U_q + \frac{\mathfrak{D}\mathcal{J}_D}{\mathfrak{D}\alpha}\Delta\alpha, \tag{2.12}$$

and

$$\Delta\mathcal{R}_p = \sum_{q=1}^{N}\frac{\mathfrak{D}\mathcal{R}_p}{\mathfrak{D}U_q}\Delta U_q + \frac{\mathfrak{D}\mathcal{R}_p}{\mathfrak{D}\alpha}\Delta\alpha = 0, \tag{2.13}$$

which gives, after rearrangement,

$$\Delta\mathcal{L} = \sum_{p=1}^{N}\psi_p^T\frac{\mathfrak{D}\mathcal{R}_p}{\mathfrak{D}\alpha}\Delta\alpha + \sum_{p=1}^{N}\left(\frac{\mathfrak{D}\mathcal{J}_D}{\mathfrak{D}U_p} + \sum_{q=1}^{N}\psi_q^T\frac{\mathfrak{D}\mathcal{R}_q}{\mathfrak{D}U_p}\right)\Delta U_p + \frac{\mathfrak{D}\mathcal{J}_D}{\mathfrak{D}\alpha}\Delta\alpha. \tag{2.14}$$

Then finally we may define the adjoint equations as

$$\sum_{q=1}^{N}\left(\frac{\mathfrak{D}\mathcal{R}_q}{\mathfrak{D}U_p}\right)^T\psi_q = -\left(\frac{\mathfrak{D}\mathcal{J}_D}{\mathfrak{D}U_p}\right)^T, \tag{2.15}$$

which removes the dependence on the flow perturbation and allows us to write

$$\Delta\mathcal{J}_D = \Delta\mathcal{L} = \sum_{p=1}^{N} \psi_p^T \frac{\mathfrak{D}\mathcal{R}_p}{\mathfrak{D}\alpha}\Delta\alpha + \frac{\mathfrak{D}\mathcal{J}_D}{\mathfrak{D}\alpha}\Delta\alpha, \tag{2.16}$$

or, in terms purely of the sensitivity to α,

$$\frac{d\mathcal{J}_D}{d\alpha} = \sum_{p=1}^{N} \psi_p^T \frac{\mathfrak{D}\mathcal{R}_p}{\mathfrak{D}\alpha} + \frac{\mathfrak{D}\mathcal{J}_D}{\mathfrak{D}\alpha}, \tag{2.17}$$

where it is seen that once the adjoint equations are solved, we can determine sensitivities of the objective function to changes in any α relatively cheaply, needing only to consider the explicit dependence of $\mathcal{J}_D$ and $\mathcal{R}_p$ on α.

2.1.2 Continuous adjoint approach

In the continuous adjoint approach we enforce the analytical form of the flow equations, $\mathcal{N}$, i.e. $\mathcal{G} = \{\mathcal{N}\} = 0$. The Lagrangian is thus

$$\mathcal{L} = \mathcal{J}_C - \int_\Omega \phi^T \mathcal{N} d\Omega, \tag{2.18}$$

where ϕ are the Lagrange multipliers, or continuous adjoint variables, and the continuous objective function $\mathcal{J}_C$ can be defined over either the entire domain or just the boundary, i.e.,

$$\mathcal{J}_C = \int_\Omega j d\Omega \quad \text{or} \quad \mathcal{J}_C = \int_\Gamma j d\Gamma. \tag{2.19}$$

Also, we note that the sign of the terms introduced to enforce the constraints is negative. This ensures that after the mathematical derivation steps, the final continuous adjoint variables are of the same sign as the discrete adjoint variables.

The perturbation to the Lagrangian now becomes

$$\delta\mathcal{L} = (\mathcal{J}_C' - \mathcal{J}_C) - \left(\int_{\Omega'} \phi^T \mathcal{N}' d\Omega - \int_\Omega \phi^T \mathcal{N} d\Omega \right), \tag{2.20}$$

where we note that perturbations to the parameter α may cause perturbations to both the flow U, and the domain Ω and its bounding surface Γ.

The next step is to manipulate and rearrange terms such that the direct dependence of this quantity on the flow perturbations δU is removed, whilst retaining those terms dependent on perturbations to α and/or the domain and boundary surface. As these remaining terms are either known or easily calculated, the perturbation to the objective function can then be found with respect to

those perturbations. This process will lead to the continuous adjoint equations and boundary conditions, but the derivation and final form are intimately connected to the form of the governing equations, the objective function and the boundary conditions, and cannot be shown generally as in the discrete case above.

2.1.3 Analytic adjoint approach

In the same way that some flow situations have analytical solutions, the continuous adjoint equations can be solved exactly for a limited number of cases. Giles and Pierce demonstrated that a Green's function approach can be used to derive exact forms for the adjoint variables for quasi-one-dimensional[45] and two-dimensional[46] Euler flows. This approach can be shown by considering the objective function

$$\mathcal{J} = \int_{\Omega} j d\Omega, \tag{2.21}$$

and its perturbation

$$\mathcal{I} = \int_{\Omega} g^T \delta U d\Omega, \tag{2.22}$$

subject to the linearized primal problem

$$L(\delta U) - f = 0, \tag{2.23}$$

where

$$g^T = \frac{\partial j}{\partial U}. \tag{2.24}$$

Noting that for simplicity in this example we are not considering the presence of boundary conditions, derivation of the continuous adjoint equation gives

$$L^*(\phi) - g = 0, \tag{2.25}$$

and the perturbation to the objective function becomes

$$\mathcal{I} = \int_{\Omega} \phi^T f d\Omega, \tag{2.26}$$

Considering a point source f_p located at ξ that induces a perturbation in the objective function, we can write

$$L(\delta U_p(x,\xi)) - f_p(x,\xi) = L(\delta U_p) - \delta(x-\xi) f_p(\xi), \tag{2.27}$$

and thus the perturbation becomes

$$\mathcal{I}_p(\xi) = \int g^T(x)\, \delta U_p(x,\xi)\, d\Omega = \phi^T(\xi)\, f_p(\xi). \tag{2.28}$$

This can then be rearranged to give the adjoint variables without having to solve the adjoint problem itself

$$\phi^T(\xi) = I_p f_p^{-1}, \tag{2.29}$$

assuming we can find the appropriate $\mathcal{I}_p$ and f_p.

To determine analytical solutions for these terms, we can consider the solution $\delta U_p(x, \xi)$ to the inhomogeneous linearized governing equations (2.27), and expand the solution in terms of perturbations to quantities that would be constant if the equations were homogeneous (e.g., for quasi-one-dimensional Euler flow these would be mass flow, stagnation pressure and stagnation enthalpy). Note that on either side of the point sources, where the linearized equations are homogeneous, the perturbations to these constant quantities must be uniform. To find f_p we first integrate the inhomogeneous equation in the small region around ξ, and then use this information to appropriately choose the f_p point sources that will simplify the working, and this process is applied to one-dimensional flows in Appendix D.

2.2 Application of adjoints

2.2.1 Sensitivity analysis

Sensitivity analysis involves the determination of the sensitivity of a given objective function to one or more parameters in a simulation. These parameters can be anything that would affect the value of the flow variables at one or more points within the domain, e.g., they could be the boundary conditions or the values of the flow variables at specific points, and typical choices of objective functions include the lift and drag of a model. The traditional approach is to either consider analytical functions, or to use either finite differencing or a complex-step approach[29]. However, as noted previously, the adjoint variables can also be used to do this.

The general adjoint sensitivity formula (2.8) includes a contribution due to the explicit dependence of the objective function on the relevant parameter (the first term on the right hand side) and an implicit contribution through the adjoint variables (the second term). It is also common to find that the parameters only explicitly affect the flow in a relatively small region of the full domain, e.g., in the case of boundary sensitivities we only expect the flow variables at the relevant boundary to be directly dependent on changes there, and thus in calculating these sensitivities we often need only integrate or sum over limited parts of the boundary.

The exact form of the sensitivity formula depends intimately on both the objective function and the parameters being considered, and cannot be shown more generally here. However, it can be noted that given these formulae, and given the adjoint variables have already been obtained, the cost of calculating these sensitivities is minimal, especially in comparison to finite differencing[30].

2.2.2 Shape optimization

Adjoint sensitivity analysis can be used to find the sensitivity of an objective function to the actual shape of, for instance, an airfoil. As the adjoint variables represent the sensitivity of the objective function to infinitesimal changes in the flow variables at any location throughout the domain, the surface sensitivity can be found by considering infinitesimal perturbations to the surface of the airfoil, and how these will affect the flow quantities at that surface.

Though the adjoint equation itself is general for a specific objective function and set of governing equations, to determine the formula for the sensitivity of an objective function with respect to changes in the surface shape we usually must re-derive the adjoint equation allowing for domain and surface perturbations. There is a key difference between the continuous and discrete adjoint approaches here: the continuous can produce a sensitivity formulation that depends purely on the values of the flow and adjoint variables on the surface and the shape perturbation considered, whereas the discrete formulation depends not just on the flow and adjoint variables at the surface or some additional internal points, but we also must consider how the shape perturbation physically perturbs the entire computational mesh. As such, the continuous, rather than the discrete, is usually preferred for surface sensitivity analysis.

Once surface sensitivities have been found, shape optimization proceeds by automatically making small adjustments to the shape of the surface of interest so as to obtain a better value of the objective function. In an iterative process, the flow and adjoint solutions are then recomputed on this new grid and used to further optimize the shape, and so on.

2.2.3 Error estimation and grid adaptation

The basis for two-grid error estimation is derived here via a similar approach to that used previously in the discrete adjoint approach. This is presented here in a slightly different way than in standard papers on the subject[20, 47], but yields identical results.

We consider two domains, a baseline (or coarse) grid Ω_N of N cells, and a fine grid Ω_n of n cells. After solving both the primal and adjoint problems on the coarse mesh we will have both the flow variables, U_N, and adjoint variables, Ψ_N, on that domain. We do not know their exact values on the fine grid but can use an appropriate interpolation method to find approximations to these, U_n^N and Ψ_n^N.

On the fine grid we can also define the objective function $\mathcal{J}_n(U_n)$ and the residuals $\mathcal{R}_{n_p}(U_n)$. Using the method of Lagrange multipliers we can enforce these residuals by introducing the Lagrangian

$$\mathcal{L} = \mathcal{J}_n(U_n) + \sum_{p=1}^{n} \Psi_{n_p}^T \mathcal{R}_{n_p}(U_n), \tag{2.30}$$

where we see that the Lagrange multiplier $\Psi_{n,i}$ is exactly the discrete adjoint since equations (2.10) and (2.30) consider the same objective function and the same residuals. We now consider the effect of evaluating the fine grid objective function using the flow solution interpolated from the coarse grid. This can be considered as a perturbation to the functional value due to the perturbation in the flow $(U_n^N - U_n)$. The change in the Lagrangian thus becomes

$$\Delta\mathcal{L} = \Delta\mathcal{J}_n + \sum_{p=1}^{n} \Psi_{n_p}^T \Delta\mathcal{R}_{n_p}. \tag{2.31}$$

Using linearity the perturbations on the right hand side can be written as

$$\begin{aligned} \Delta\mathcal{J}_n &= \mathcal{J}_n(U_n^N) - \mathcal{J}_n(U_n) \\ &= \sum_{p=1}^{n} \left.\frac{\mathfrak{D}\mathcal{J}_n}{\mathfrak{D}U_p}\right|_{U_n^N} (U_{n_p}^N - U_{n_p}), \end{aligned} \tag{2.32}$$

and

$$\begin{aligned} \Delta\mathcal{R}_{n_p}(U_n) &= \mathcal{R}_{n_p}(U_n^N) - \mathcal{R}_{n_p}(U_n) \\ &= \sum_{q=1}^{n} \left.\frac{\mathfrak{D}\mathcal{R}_{n_p}}{\mathfrak{D}U_{n_q}}\right|_{U_n^N} (U_{n_q}^N - U_{n_q}), \end{aligned} \tag{2.33}$$

giving

$$\Delta\mathcal{L} = \sum_{p=1}^{n} \left.\frac{\mathfrak{D}\mathcal{J}_n}{\mathfrak{D}U_p}\right|_{U_n^N} (U_{n_p}^N - U_{n_p}) + \sum_{p=1}^{n} \Psi_{n_p}^T \sum_{q=1}^{n} \left.\frac{\mathfrak{D}\mathcal{R}_{n_p}}{\mathfrak{D}U_{n_q}}\right|_{U_n^N} (U_{n_q}^N - U_{n_q}). \tag{2.34}$$

Noting that we expect the numerical scheme to give, to machine accuracy, $\mathcal{R}_{n_p}(U_n) = 0$, we can also rewrite (2.33) as

$$\sum_{q=1}^{n} \left.\frac{\mathfrak{D}\mathcal{R}_{n_p}}{\mathfrak{D}U_{n_q}}\right|_{U_n^N} (U_{n_q}^N - U_{n_q}) = \mathcal{R}_{n_p}(U_n^N), \tag{2.35}$$

and thus finally, using $\Delta\mathcal{J}_n = \Delta\mathcal{L}$, we get

$$\Delta\mathcal{J}_n = \sum_{p=1}^{n} \left.\frac{\mathfrak{D}\mathcal{J}_n}{\mathfrak{D}U_{n_p}}\right|_{U_n^N} (U_{n_p}^N - U_{n_p}) + \sum_{p=1}^{n} \Psi_{n_p}^T \mathcal{R}_{n_p}(U_n^N), \tag{2.36}$$

which is the error in the objective function on the fine grid when it is evaluated using flow variables interpolated from the coarse grid. The first term cannot be calculated since we do not know U_n, and to find the second term we must make the assumption that $\Psi_n^N \approx \Psi_n$ and perform a single residual iteration on U_n^N. To be able to accurately estimate the error it is thus desirable that the first term is relatively small in comparison to the second.

Using the formula for error estimation given in (2.36) it also becomes possible to approximate

not just the error from the entire domain, but the contribution from individual cells. This can be seen by considering just the last term on the right hand side, i.e., the term that we can calculate to predict the error, and removing the summation sign to get the error value from each cell

$$\Delta\mathcal{J}_{n_p} \approx \Psi_{n_p}^T \mathcal{R}_{n_p}(U_n^N). \tag{2.37}$$

We can then apply an appropriate refinement strategy, using this information, to improve the quality of further solutions, leading to a mesh with spacing optimized for the functional of interest.

2.2.4 Uncertainty Quantification (UQ)

Uncertainty Quantification (UQ) aims to predict the amount of error or uncertainty present in an experiment or numerical simulation. This is an important step, because it allows us to know how much confidence we can place in a result, and even may help us refine the experiment or simulation such as to reduce the uncertainty.

It is often divided into two broad groups, aleatoric uncertainty, meaning the statistical uncertainty present because quantities change each time an experiment is run, and epistemic uncertainty, due to quantities that we either do not know or that we neglect.

Since the adjoint variables can be used to predict how sensitive an objective function is to any parameter, it is thus possible to determine how sensitive this functional is to any type of uncertainty that would affect the flow variables in a simulation, therefore, with appropriate estimates of these input uncertainties, we can quantify the uncertainty in the value of the objective function produced by the simulation.

The previous section on estimating the error due to the coarseness of a computational grid is an example of the application of adjoints to epistemic UQ, and Duraisamy[23] used adjoint methods to enable aleatoric UQ, reducing the error in statistics based on the random sampling of stochastic space.

Chapter 3

Hybrid adjoint theory

"We are not retreating, merely advancing in another direction."

— Douglas Adams

HAVING now motivated why we are interested in a hybrid approach and introduced both the main concepts of the general adjoint method and how these apply to the existing adjoint approaches, we now proceed to develop the core theory of a hybrid approach.

3.1 A general hybrid approach

The overall aim of the hybrid adjoint approach is to be able to compute adjoint solutions in a more desirable way than through existing methods by combining together the approaches of two or more of these methods. It is intended for problems involving very complex PDEs (such as those involving two-, or more, equation turbulence models, combustion including look-up tables, and multi-species simulations such as those seen in multi-species, multi-phase problems).

Exactly how the process of hybridizing should be done and exactly what are the most desirable features that a hybrid method should exhibit remain open questions. However, we will present below the broad theory for two possible approaches, one which combines an adjoint method (which could be continuous or discrete) with sensitivity analysis, and another which combines the continuous and discrete adjoint methods, though in later sections of this thesis we will concentrate solely on this second approach. The basic idea of this latter method is to use a continuous formulation for those portions of the flow equations for which such formulations already exist (in the form of a program or as previously published equations), but to treat discretely those portions of the governing equations that are difficult (or impossible) to handle analytically.

We will also use Table 1.1, given in the Introduction (Chapter 1) to motivate which features are of most interest to us, and aim to try and create an approach that inherits the favorable characteristics, overcomes the drawbacks and produces high-quality adjoint (and thus sensitivity) information.

3.2 Existing hybrid methods

Though the broad approach described in this thesis is new, some existing work has made reference to attempts to apply a limited hybrid-like strategy to help improve certain features of the numerical solution process or results. Lozano and Ponsin[36] showed that if the sensitivity is obtained by using the continuous adjoint variables for the quasi-one-dimensional Euler equations in a discrete adjoint framework, the accuracy of the resultant gradients was improved with respect to those obtained from both finite differencing and a pure discrete adjoint approach. Giles and Duta et al.[10], meanwhile, argued that if strong wall boundary conditions are imposed at surface nodes on an Euler wall or viscous wall, i.e., the normal velocity here is fixed to zero (Euler) or the entire velocity here is set as zero (viscous), the quality of the adjoint solution near the wall suffers. Their solution to this problem is to include terms that represent the linearized surface momentum residuals on the boundary, in a manner that more closely resembles the derivation of the boundary conditions in the continuous

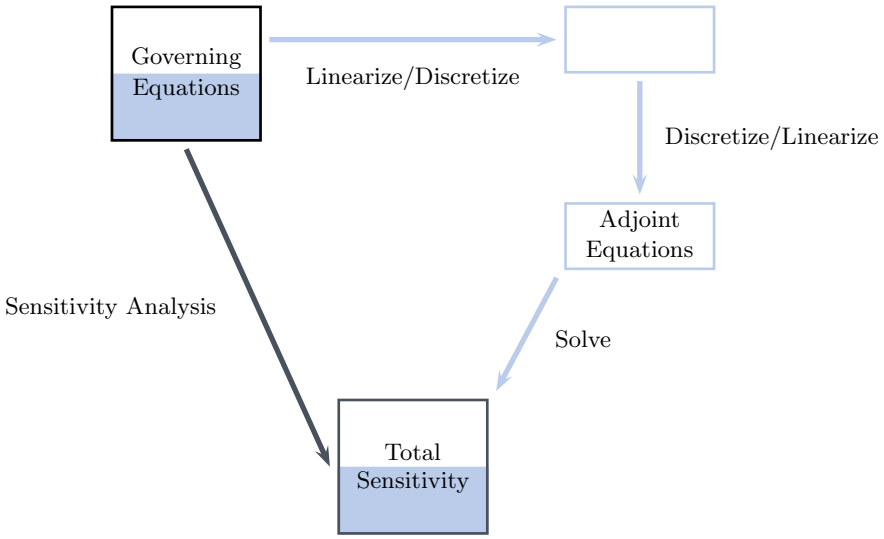

Figure 3.1: General scheme for adjoint–sensitivity analysis hybrid approach.

approach. Anderson and Venkatakrishnan[28] also presented a continuous adjoint formulation that discretizes the adjoint equations for viscous and inviscid flow in a way that corresponds exactly to a discrete adjoint for first-order accuracy, differing only in the artificial dissipation schemes.

However, neither of these existing methods create truly hybrid approaches, modifying only a small part of the procedure, e.g., the sensitivity calculation or the boundary condition treatment, and in this work we instead attempt to take the idea much further.

3.3 An adjoint–sensitivity analysis hybrid

It is possible to consider an approach that mixes an adjoint method with a non-adjoint sensitivity analysis method. This second method could include analytical formulations of the sensitivity, finite differencing and applying automatic differentiation. The general approach is shown in Figure 3.1 and can be derived by modifying the general adjoint approach explained above in Chapter 2. This particular approach is not investigated further in this thesis, but is presented here for completeness.

We split the governing equations into those that will be treated via an adjoint method, $\mathcal{G}_A$, and those that will be treated via a sensitivity analysis method, $\mathcal{G}_{SA}$. Enforcing $\mathcal{G}_A$ we can write the Lagrangian

$$\mathcal{L} = \mathcal{J} + \mathcal{V}^T \mathcal{G}_A, \tag{3.1}$$

where $\mathcal{V}$ will be the adjoint variables. The perturbation of this relative to a small change in some

parameter α then becomes

$$\delta\mathcal{L} = \delta\mathcal{J} + \mathcal{V}^T\delta\mathcal{G}_A. \tag{3.2}$$

Expanding these perturbations we have

$$\delta\mathcal{J} = \frac{\partial\mathcal{J}}{\partial\alpha}\delta\alpha + \frac{\partial\mathcal{J}}{\partial U_A}\delta U_A + \frac{\partial\mathcal{J}}{\partial U_{SA}}\delta U_{SA}, \tag{3.3}$$

and

$$\delta\mathcal{G}_A = \frac{\partial\mathcal{G}_A}{\partial\alpha}\delta\alpha + \frac{\partial\mathcal{G}_A}{\partial U_A}\delta U_A + \frac{\partial\mathcal{G}_A}{\partial U_{SA}}\delta U_{SA}, \tag{3.4}$$

where we note the flow vector U has been separated into those variables given by $\mathcal{G}_A$ and those given by $\mathcal{G}_{SA}$.

Inserting these into the Lagrangian perturbation, and rearranging, gives

$$\delta\mathcal{L} = \left(\frac{\partial\mathcal{J}}{\partial\alpha} + \mathcal{V}^T\frac{\partial\mathcal{G}_A}{\partial\alpha}\right)\delta\alpha + \left(\frac{\partial\mathcal{J}}{\partial U_A} + \mathcal{V}^T\frac{\partial\mathcal{G}_A}{\partial U_A}\right)\delta U_A + \left(\frac{\partial\mathcal{J}}{\partial U_{SA}} + \mathcal{V}^T\frac{\partial\mathcal{G}_A}{\partial U_{SA}}\right)\delta U_{SA}. \tag{3.5}$$

We then define the adjoint equation (and boundary conditions), such that any explicit dependence of $\delta\mathcal{L}$ on δU_A is removed,

$$\frac{\partial\mathcal{J}}{\partial U_A} + \mathcal{V}^T\frac{\partial\mathcal{G}_A}{\partial U_A} = 0, \tag{3.6}$$

giving the perturbation to the objective function

$$\delta\mathcal{J} = \delta\mathcal{L} = \left(\frac{\partial\mathcal{J}}{\partial\alpha} + \mathcal{V}^T\frac{\partial\mathcal{G}_A}{\partial\alpha}\right)\delta\alpha + \left(\frac{\partial\mathcal{J}}{\partial U_{SA}} + \mathcal{V}^T\frac{\partial\mathcal{G}_A}{\partial U_{SA}}\right)\delta U_{SA}, \tag{3.7}$$

and noting that $\delta U_{SA} = \dfrac{\partial U_{SA}}{\partial\alpha}\delta\alpha$ this becomes

$$\delta\mathcal{J} = \delta\mathcal{L} = \left(\frac{\partial\mathcal{J}}{\partial\alpha} + \mathcal{V}^T\frac{\partial\mathcal{G}}{\partial\alpha} + \left(\frac{\partial\mathcal{J}}{\partial U_{SA}} + \mathcal{V}^T\frac{\partial\mathcal{G}_A}{\partial U_{SA}}\right)\frac{\partial U_{SA}}{\partial\alpha}\right)\delta\alpha. \tag{3.8}$$

We can also obtain from this the sensitivity to α,

$$\frac{d\mathcal{J}}{d\alpha} = \frac{\partial\mathcal{J}}{\partial\alpha} + \mathcal{V}^T\frac{\partial\mathcal{G}}{\partial\alpha} + \left(\frac{\partial\mathcal{J}}{\partial U_{SA}} + \mathcal{V}^T\frac{\partial\mathcal{G}_A}{\partial U_{SA}}\right)\frac{\partial U_{SA}}{\partial\alpha}. \tag{3.9}$$

However, this approach requires that the terms $\dfrac{\partial\mathcal{J}}{\partial U_{SA}}$, $\dfrac{\partial\mathcal{G}_A}{\partial U_{SA}}$ and $\dfrac{\partial U_{SA}}{\partial\alpha}$ can all be found easily (at least more easily than applying a full adjoint approach) via an appropriate sensitivity analysis method.

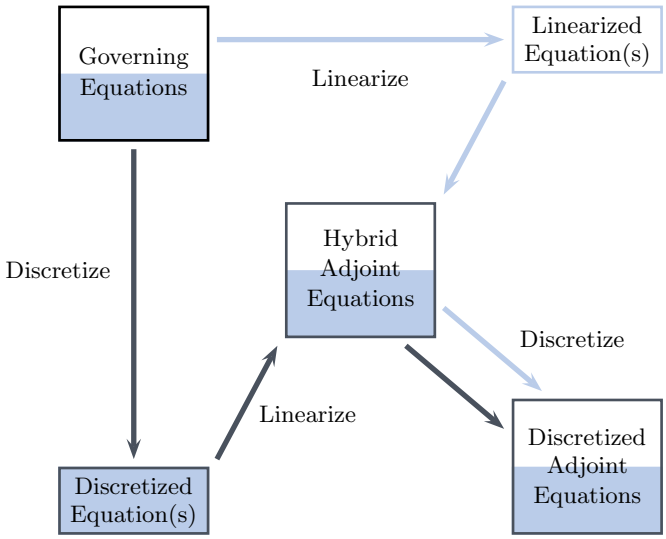

Figure 1.2: General derivation scheme for continuous–discrete hybrid adjoint equations.

3.4 A continuous–discrete adjoint hybrid

In this approach, we split the governing equations into a set that will be incorporated continuously and a set that will be incorporated discretely, i.e., $\mathcal{G} = \{\{\mathcal{N}\}_C, \{\mathcal{R}_p\}_D\} = 0$. The general approach is shown in Figure 1.2, and repeated again in this chapter, and this particular hybrid method is the main focus of this thesis.

The equations that will be treated continuously will be those that will not change when minor adjustments are made to the flow equations, such as altering the source terms, and that are easily differentiable (e.g., the Euler equations for a perfect gas or even the laminar Navier-Stokes equations). The terms that will be treated discretely will include those that are not easily differentiable, and those that we may wish to change and experiment with (e.g., chemical source terms and turbulence models). One of the main intentions is that once the derivation of the continuous part is performed, substantial changes do not need to be made in the future, thus significantly lowering the development cost for additional problems and allowing the re-use of existing code.

Additionally, we will define the objective function as either a discrete or continuous objective function. We combine these by writing them as a sum:

$$\mathcal{J}_H = \beta \mathcal{J}_C + (1 - \beta)\mathcal{J}_D, \tag{3.10}$$

where β can be set equal to 0 or 1 in order to recover either the discrete or continuous functionals, respectively. Writing it in this way is useful so that both types of objective function can be carried

through the derivations simultaneously, though we do not to intend to combine them as a weighted sum.

The reason behind considering two types of objective function is to attempt to broaden the applicability of the resultant adjoint equations. For example, the purely continuous adjoint for viscous flows is typically restricted to functionals that depend on the pressure, temperature and/or shear stress along a surface, whereas the discrete adjoint can be developed for any functional of interest. Whilst any continuous objective function must eventually be discretized in order to solve the adjoint equations numerically, being able to manipulate the functional analytically before choosing an appropriate discretization scheme may also add greater flexibility to the development of a hybrid adjoint.

However, the idea of blending discrete and continuous objective functions together as a weighted sum does not appear to be helpful because instead of avoiding the potential disadvantages of either, it would combine the drawbacks of both functionals. There may, though, be situations in which it would be beneficial to use different definitions of a functional at different points within a domain, for example, changing the functional definition in the region around a shock.

The Lagrangian now becomes

$$\mathcal{L} = \beta\mathcal{J}_C + (1-\beta)\mathcal{J}_D - \int_\Omega \varphi_C^T \mathcal{N}_C d\Omega + \sum_{p=1}^{N} \varphi_{D_p}^T \mathcal{R}_{D_p}, \tag{3.11}$$

and its perturbation can be written as

$$\{\delta,\Delta\}\mathcal{L} = \beta\left(\mathcal{J}_C' - \mathcal{J}_C\right) + (1-\beta)\Delta\mathcal{J}_D - \left(\int_{\Omega'} \varphi_C^T \mathcal{N}_C' d\Omega - \int_\Omega \varphi_C^T \mathcal{N}_C d\Omega\right) + \sum_{p=1}^{N} \varphi_{D_p}^T \Delta\mathcal{R}_{D_p}. \tag{3.12}$$

The next steps in this derivation mirror those introduced previously for the discrete and continuous parts, mathematically manipulating the equation so as to remove the explicit dependence of the perturbation on the discrete and continuous flow perturbations, ΔU and δU, respectively, and in so doing generating the hybrid adjoint equation and hybrid boundary conditions for φ_C and φ_D. It is important to note that unlike for the discrete adjoint, the hybrid approach explicitly includes boundary conditions on the discrete adjoint variables.

When deriving and calculating the hybrid adjoint for a specific problem, two important choices will need to be made. The first deals with the selection of which governing equations will be treated discretely and continuously, and the second is to decide whether to use the discrete or continuous objective function. An interesting feature that can be inferred from (3.11) is that the discrete and continuous approaches are in fact special cases of the more general hybrid approach. By setting $\beta = 0$ and defining $\{\mathcal{R}\}_D = \mathcal{R}$ and thus $\{\mathcal{N}\}_C = \emptyset$ we recover the pure discrete method, and by setting $\beta = 1$ and defining $\{\mathcal{N}\}_C = \mathcal{N}$ and thus $\{\mathcal{R}\}_D = \emptyset$ we get the pure continuous.

However, we are no longer limited to just those two options. It is now possible to create a

continuous adjoint that has a discrete functional, allowing non-differentiable cost functions to be considered in the continuous approach, or vice versa, and many other combinations in between.

3.5 Discussion

The freedom of the general hybrid approach means that there is significant flexibility within the development of a particular hybrid adjoint. Not only can we consider adjoint-sensitivity analysis hybrids and continuous-discrete adjoint hybrids, but within each of these approaches we must make choices about how the objective functions and each of the governing equations is to be treated. Further still, it is even possible to treat different terms within a single governing equation via different approaches.

The hybrid adjoints developed in the following parts of this dissertation provide an example of this, treating the Euler and mean flow equations continuously and the included models discretely, and, in the case of the turbulent hybrid adjoint, separating out the eddy viscosity term from the mean flow equations and handling it in a discrete way. However, there may be many alternatives or modifications to these two specific approaches that are worth consideration. For example, it might be possible to instead handle the convective terms of the Reynolds-Averaged Navier-Stokes equations continuously, and all of the viscous terms discretely (instead of just the eddy viscosity and turbulence model).

The decision as to how to exactly hybridize the adjoint approach for a specific problem is likely to be influenced by several competing factors and there isn't necessarily a single correct answer. It will depend on the amount of mathematical development that can be performed up-front, the computational resources available, the existing implementations of the discrete and continuous adjoint approaches, the functionals of interest, the governing equation sets, whether or not generality is important, etc. It is therefore important to have a clear idea of the motivation behind using a hybrid adjoint in a particular situation before proceeding with its development.

Chapter 4

Quasi-one-dimensional flows

"Why a four-year-old child could understand this report. Run out and find me a four-year-old child. I can't make head nor tail out of it."

— Groucho Marx

To better understand the adjoint theory introduced in the preceding chapters, we now apply the discrete, continuous and hybrid adjoint approaches to a demonstrative model of a multi-physics flow situation, quasi-one-dimensional Euler flow both with and without a combustion model. The simplified combustion model chosen simulates the heat release into the flow as reaction proceeds and was chosen so that key concepts of the hybrid methodology could be developed and explored.

4.1 Quasi-one-dimensional Euler flow

The theory for quasi-one-dimensional Euler flow is developed here in order to show how the general adjoint steps outlined in Chapter 2 are applied to the discrete and continuous methods, and as a basis for the development of a hybrid adjoint for quasi-one-dimensional Euler flow with combustion later in this chapter. It is important to note that one of the aims of the hybrid approach is to reuse existing theory and thus reduce the cost of derivation and implementation of the new strategy.

4.1.1 Flow problem

4.1.1.1 Definition

We consider quasi-one-dimensional Euler flow (smooth or shocked) in the duct $x \in [x_i, x_e]$ with height $h(x)$ as shown in Figure 4.1.

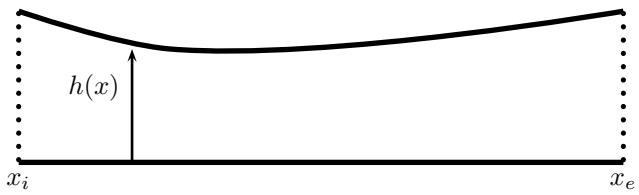

Figure 4.1: General quasi-one-dimensional duct.

The analytical governing equations for this are

$$\mathcal{N} \equiv \frac{d}{dx}(hF) - \frac{dh}{dx}P = 0, \quad x \in [x_i, x_e], \tag{4.1}$$

where the vectors of flow variables, fluxes and the pressure source term are given by

$$U = \begin{pmatrix} \rho \\ m \\ \epsilon \end{pmatrix}, \quad F = \begin{pmatrix} m \\ \frac{m^2}{\rho} + p \\ mH \end{pmatrix}, \quad P = \begin{pmatrix} 0 \\ p \\ 0 \end{pmatrix}, \tag{4.2}$$

respectively, the stagnation enthalpy is given by

$$H = \frac{\epsilon + p}{\rho}, \tag{4.3}$$

and the pressure is given by

$$p = (\gamma - 1)(\epsilon - \frac{m^2}{2\rho}). \tag{4.4}$$

We also define the functional as an integral over the duct,

$$\mathcal{J} = \int_{x_i}^{x_e} j dx. \tag{4.5}$$

4.1.1.2 Boundary conditions

The number of boundary conditions required to solve for the flow can be determined by considering the characteristics of the problem. When a characteristic is incoming at a boundary, that implies that a condition is required at that boundary, and when it is outgoing, no condition is required. For quasi-one-dimensional Euler flow there are three characteristic variables, with the velocities $\frac{m}{\rho} - c$, $\frac{m}{\rho}$ and $\frac{m}{\rho} + c$, where the speed of sound is given by $c = \sqrt{\gamma \frac{p}{\rho}}$.

Subsonic For subsonic flow, two of the characteristics are incoming at the inlet, and the third is incoming at the outlet. This means two boundary conditions are required at the inlet, where we fix stagnation enthalpy and stagnation pressure, and one at the outlet, where we fix static pressure.

Supersonic For supersonic flow, all three of the characteristics are incoming at the inlet. This means three boundary conditions are required at the inlet, where we fix Mach number, stagnation enthalpy and stagnation pressure, and none at the outlet.

Transonic For transonic flow, we have subsonic conditions at the inlet, thus two of the characteristics are incoming there, and supersonic conditions at the outlet, thus no characteristics are incoming there. This means two boundary conditions are required at the inlet, where we fix stagnation enthalpy and stagnation pressure, and the third boundary condition comes from the requirement that the flow is sonic at the throat.

Shocked For shocked flow, we may have either purely supersonic or transonic conditions ahead of the shock and subsonic conditions after it. This means three boundary conditions are required ahead of the shock (for supersonic flow, again fixing all conditions at the inlet, and for transonic flow fixing two conditions at the inlet plus the sonic condition at the throat) and one boundary condition is required at the outlet (again fixing the pressure). The total of four boundary conditions fixes both the profiles of the flow variables through the duct and also the position of the shock.

4.1.2 Discrete adjoint problem

4.1.2.1 Derivation

Writing the objective function in a discrete form,

$$\mathcal{J}_D = \sum_{p=1}^{N} j_p \Delta x_p, \tag{4.6}$$

and then following the general discrete approach outlined in Section 2.1.1 we can reuse the discrete adjoint equations,

$$\sum_{q=1}^{N} \left(\frac{\mathfrak{D}\mathcal{R}_q}{\mathfrak{D}U_p} \right)^T \psi_q = - \left(\frac{\mathfrak{D}\mathcal{J}_D}{\mathfrak{D}U_p} \right)^T, \tag{2.15}$$

and the perturbation to the objective function,

$$\Delta\mathcal{J}_D = \sum_{p=1}^{N} \psi_p^T \frac{\mathfrak{D}\mathcal{R}_p}{\mathfrak{D}\alpha} \Delta\alpha + \frac{\mathfrak{D}\mathcal{J}_D}{\mathfrak{D}\alpha} \Delta\alpha, \tag{2.16}$$

developed previously, where the residuals, $\mathcal{R}_p$, are given in the solution strategy to the primal problem.

4.1.2.2 Boundary conditions

In the discrete adjoint approach, no boundary conditions are explicitly used, with the boundary conditions on the problem implicitly applied through the boundary conditions used to solve the flow problem.

4.1.2.3 Sensitivity formulae

If there is no explicit dependence of $\mathcal{J}_D$ on α then we can write the sensitivity to changes in this parameter as

$$\frac{d\mathcal{J}_D}{d\alpha} = \frac{\Delta\mathcal{J}_D}{\Delta\alpha} = \sum_{p=1}^{N} \psi_p^T \frac{\mathfrak{D}\mathcal{R}_p}{\mathfrak{D}\alpha}, \tag{4.7}$$

and though it is possible to obtain the term $\frac{\mathfrak{D}\mathcal{R}_p}{\mathfrak{D}\alpha}$ by automatic differentiation, this can be further expanded to give

$$\frac{d\mathcal{J}_D}{d\alpha} = \frac{\Delta\mathcal{J}_D}{\Delta\alpha} = \sum_{p=1}^{N}\sum_{q=1}^{N} \psi_p^T \frac{\mathfrak{D}\mathcal{R}_p}{\mathfrak{D}U_q}\frac{\partial U_q}{\partial\alpha}, \tag{4.8}$$

where $\frac{\partial U_q}{\partial\alpha}$, can be found either via automatic differentiation or analytically, and the term $\frac{\mathfrak{D}\mathcal{R}_p}{\mathfrak{D}U_q}$ is already calculated as part of the discrete adjoint method.

When considering possible choices for α that are only defined at just one point, say r, in the flow, such as boundary conditions, the term $\frac{\partial U_q}{\partial\alpha}$ becomes zero everywhere except at this point, giving the simple result

$$\frac{d\mathcal{J}_D}{d\alpha} = \psi_r^T \frac{\mathfrak{D}\mathcal{R}_r}{\mathfrak{D}U_r}\frac{\partial U_r}{\partial\alpha}. \tag{4.9}$$

4.1.3 Continuous adjoint problem

4.1.3.1 Derivation

We can derive the continuous adjoint equation via the Lagrange multiplier approach demonstrated by Giles and Pierce[45]. We continuously enforce the analytical flow equations, $\mathcal{N}$, and in the case of shocked flow we must also continuously enforce the Rankine-Hugoniot conditions at the internal shock boundary,

$$[hF]_{x_{s^-}}^{x_{s^+}} = 0, \tag{4.10}$$

noting that this step will later help remove the dependence of the objective function perturbation on the shock displacement.

For this case we have the Lagrangian

$$\mathcal{L} = \int_{x_i}^{x_s} j dx + \int_{x_s}^{x_e} j dx - \int_{x_i}^{x_s} \phi^T\mathcal{N} dx - \int_{x_s}^{x_e} \phi^T\mathcal{N} dx - \phi_s^T \left[hF\right]_{x_{s^-}}^{x_{s^+}}, \tag{4.11}$$

where ϕ are the Lagrange multipliers.

The perturbation then becomes

$$\begin{aligned}\delta\mathcal{L} \quad = \quad & \int_{x_i}^{x_s} \delta j dx + \int_{x_s}^{x_e} \delta j dx - [j]_{x_{s^-}}^{x_{s^+}} \delta x_s \\ & - \int_{x_i}^{x_s} \phi^T \delta\mathcal{N} dx - \int_{x_s}^{x_e} \phi^T \delta\mathcal{N} dx - \phi_s^T \delta\left(\left[hF\right]_{x_{s^-}}^{x_{s^+}}\right).\end{aligned} \tag{4.12}$$

Using linearity, the integrand in the perturbed objective function can be evaluated as

$$\delta j = \frac{\partial j}{\partial U}\delta U + \frac{\partial j}{\partial\alpha}\delta\alpha. \tag{4.13}$$

The governing equation term can also be linearized to give

$$\delta\mathcal{N} = L(\delta U) - \frac{\partial \mathcal{N}}{\partial \alpha}\delta\alpha = 0, \tag{4.14}$$

where the linear operator, L, is given by

$$L(\delta U) = \frac{d}{dx}\left(h\left(\frac{\partial F}{\partial U}\delta U\right)\right) - \frac{dh}{dx}\left(\frac{\partial P}{\partial U}\delta U\right). \tag{4.15}$$

Finally, the perturbation to the Rankine-Hugoniot conditions is

$$\delta\left([hF]_{x_{s^-}}^{x_{s^+}}\right) = h_s\left[\frac{\partial F}{\partial U}\delta U\right]_{x_{s^-}}^{x_{s^+}} - h_s\left[\frac{dF}{dx}\right]_{x_{s^-}}^{x_{s^+}}\delta x_s. \tag{4.16}$$

Incorporating these into the perturbation to the Lagrangian (4.12) and performing integration by parts, followed by rearrangement, we obtain

$$\begin{aligned}
\delta\mathcal{L} \;=\; & \int_{x_i}^{x_s}\phi^T\frac{\partial\mathcal{N}}{\partial\alpha}\delta\alpha dx + \int_{x_s}^{x_e}\phi^T\frac{\partial\mathcal{N}}{\partial\alpha}\delta\alpha dx + \int_{x_i}^{x_s}\frac{\partial j}{\partial\alpha}\delta\alpha dx + \int_{x_s}^{x_e}\frac{\partial j}{\partial\alpha}\delta\alpha dx \\
& - \int_{x_i}^{x_s}\left(L^*(\phi)-g\right)^T\delta U dx - \int_{x_s}^{x_e}\left(L^*(\phi)-g\right)^T\delta U dx \\
& - \left(h_s\phi_s^T\left[\frac{dF}{dx}\right]_{x_{s^-}}^{x_{s^+}} + [j]_{x_{s^-}}^{x_{s^+}}\right)\delta x_s \\
& - h_s\left(\phi_s^T - \phi^T\left(x_{s^+}\right)\right)\left(\frac{\partial F}{\partial U}\delta U\right)\Big|_{x_{s^-}} + h_s\left(\phi_s^T - \phi^T\left(x_{s^-}\right)\right)\left(\frac{\partial F}{\partial U}\delta U\right)\Big|_{x_{s^+}} \\
& - \left[h\phi^T\frac{\partial F}{\partial U}\delta U\right]_{x_i}^{x_e},
\end{aligned} \tag{4.17}$$

where the adjoint linear operator, L^*, is defined by

$$L^*(\phi) = -h\left(\frac{\partial F}{\partial U}\right)^T\frac{d\phi}{dx} - \frac{dh}{dx}\left(\frac{\partial P}{\partial U}\right)^T\phi, \tag{4.18}$$

and

$$g^T = \frac{\partial j}{\partial U}. \tag{4.19}$$

We then proceed by appropriately restricting the adjoint variables such that the explicit dependence of the Lagrangian perturbation on the flow perturbation and shock movement can be removed. Canceling the last three lines leads to

$$\phi_s = \phi, \tag{4.20}$$

the internal shock boundary condition,

$$h_s \phi_s^T \left[\frac{dF}{dx}\right]_{x_{s^-}}^{x_{s^+}} = -\left[j\right]_{x_{s^-}}^{x_{s^+}}, \tag{4.21}$$

and the inlet/outlet boundary condition,

$$\left[h\phi^T \frac{\partial F}{\partial U}\delta U\right]_{x_i}^{x_e} = 0. \tag{4.22}$$

The remaining lines that depend on the flow perturbation can then be removed by introducing the continuous adjoint equations,

$$L^*(\phi) - g = 0, \quad x \in [x_i, x_e], \tag{4.23}$$

and thus the perturbation to the objective function can be written

$$\delta\mathcal{J} = \delta\mathcal{L} = \int_{x_i}^{x_s} \phi^T \frac{\partial \mathcal{N}}{\partial \alpha}\delta\alpha dx + \int_{x_i}^{x_s} \frac{\partial j}{\partial \alpha}\delta\alpha dx + \int_{x_s}^{x_e} \frac{\partial j}{\partial \alpha}\delta\alpha dx. \tag{4.24}$$

4.1.3.2 Boundary conditions

The continuous adjoint equations for quasi-one-dimensional flow are subject to the boundary conditions (4.22) at the inlet and outlet and, if present, (4.21) at the shock.

Considering the first of these two, we note that the boundary condition will be satisfied if the term in square brackets is zero at both the inlet and outlet. The consequence of this for quasi-one-dimensional flow is that if at an inlet/outlet boundary we have n incoming flow characteristics, we must have $3 - n$ incoming adjoint characteristics, i.e., we must have $3 - n$ adjoint boundary conditions to remove the dependence of the functional on the same number of flow quantities that are not fixed by the flow boundary conditions.

The derivation of these adjoint boundary conditions proceeds by expanding the term in square brackets at just one of these locations, noting that we can cancel out the height dependence, to get

$$\begin{pmatrix} \phi_\rho & \phi_m & \phi_\epsilon \end{pmatrix} \frac{\partial F}{\partial U} \begin{pmatrix} \delta\rho \\ \delta m \\ \delta\epsilon \end{pmatrix} = 0, \tag{4.25}$$

and then appropriately applying the flow boundary conditions to determine the required condition on the adjoint variables.

This process is summarized below, first for inlets, then outlets, and finally for the shock boundary condition.

Inlet boundary conditions

Subsonic At a subsonic inlet we have two incoming flow characteristics and thus one incoming adjoint characteristic, and so one adjoint boundary condition is required. We can write both H and p_0 as functions of the flow variables ρ, m and ϵ, and since we fix the stagnation pressure and stagnation enthalpy at the inlet we can then use the conditions $\delta H = 0$ and $\delta p_0 = 0$ to remove the dependence on two of the flow perturbations, δm and $\delta\epsilon$, giving, after rearrangement,

$$\begin{aligned} \left(\left(\frac{m}{\rho} - \gamma\frac{p}{m}\right)\phi_\rho + \left(\left(\frac{m}{\rho}\right)^2 - \frac{\gamma p}{\rho}\right)\phi_m \right. \\ \left. + \left(\frac{m^3}{2\rho^3} - \frac{\gamma m p(\gamma-3)}{2\rho^2(\gamma-1)} - \frac{\gamma^2 p^2}{\rho m(\gamma-1)}\right)\phi_\epsilon\right)\delta\rho &= 0, \end{aligned} \tag{4.26}$$

which implies that to remove the dependence on $\delta\rho$ we require the adjoint boundary condition

$$\begin{aligned} \left(\frac{m}{\rho} - \gamma\frac{p}{m}\right)\phi_\rho + \left(\left(\frac{m}{\rho}\right)^2 - \frac{\gamma p}{\rho}\right)\phi_m \\ + \left(\frac{m^3}{2\rho^3} - \frac{\gamma m p(\gamma-3)}{2\rho^2(\gamma-1)} - \frac{\gamma^2 p^2}{\rho m(\gamma-1)}\right)\phi_\epsilon &= 0 \end{aligned} \tag{4.27}$$

Supersonic At a supersonic inlet, all flow characteristics are incoming and thus $\delta U = 0$. This immediately implies that no boundary conditions need to be set for the adjoint variables.

Outlet boundary conditions

Subsonic At a subsonic outlet we have one incoming flow characteristic and thus two incoming adjoint characteristics, and so two adjoint boundary conditions are required. We can write p as a function of the flow variables ρ, m and ϵ, and since we fix the static pressure at the outlet we can then use the condition $\delta p = 0$ to remove the dependence on one of the flow perturbations, $\delta\epsilon$, giving, after rearrangement,

$$\begin{aligned} -\left(\left(\frac{m}{\rho}\right)^2\phi_m + \left(\frac{m}{\rho}H + \frac{1}{2}\left(\frac{m}{\rho}\right)^3\right)\phi_\epsilon\right)\delta\rho \\ + \left(\phi_\rho + 2\frac{m}{\rho}\phi_m + \left(H + \left(\frac{m}{\rho}\right)^2\right)\phi_\epsilon\right)\delta m &= 0, \end{aligned} \tag{4.28}$$

which implies that to remove the dependence on $\delta\rho$ and δm we require the adjoint boundary conditions

$$-\left(\frac{m}{\rho}\right)^2 \phi_m - \left(\frac{m}{\rho}H + \frac{1}{2}\left(\frac{m}{\rho}\right)^3\right)\phi_\epsilon = 0, \tag{4.29}$$

and

$$\phi_\rho + 2\frac{m}{\rho}\phi_m + \left(H + \left(\frac{m}{\rho}\right)^2\right)\phi_\epsilon = 0. \tag{4.30}$$

Supersonic At a supersonic outlet we have no incoming flow characteristics and thus three incoming adjoint characteristics, and so three adjoint boundary conditions are required. However, due to the direction of the flow characteristics in supersonic flow we interpret that changes at the exit will not propagate upstream, and thus changes at this point will not effect the functional. This implies that all the adjoint variables will be zero here.

Shock boundary condition If the objective function is an integral of pressure, the adjoint boundary condition at the shock, (4.21), can be shown to reduce to a condition solely on the second adjoint variable,

$$\phi_m = -\left(\frac{dh}{dx}\right)^{-1}. \tag{4.31}$$

4.1.3.3 Sensitivity formulae

Assuming no explicit dependence of $\mathcal{J}$ on α, the sensitivity of the functional to α can be written as

$$\frac{d\mathcal{J}}{d\alpha} = \frac{\delta\mathcal{J}}{\delta\alpha} = \int_{x_i}^{x_e} \phi^T \frac{\partial\mathcal{N}}{\partial\alpha} dx, \tag{4.32}$$

and we can further expand the integrand

$$\frac{d\mathcal{J}}{d\alpha} = \frac{\delta\mathcal{J}}{\delta\alpha} = \int_{x_i}^{x_e} \phi^T \frac{\partial\mathcal{N}}{\partial U}\frac{\partial U}{\partial\alpha} dx. \tag{4.33}$$

Thus the only additional information needed to calculate this sensitivity is the term $\dfrac{\partial U}{\partial\alpha}$, noting that the terms that make up $\dfrac{\partial\mathcal{N}}{\partial U}$ are already required by the continuous adjoint equation.

When considering possible choices for α that are only defined at just one point in the flow, such as boundary conditions, the term $\dfrac{\partial U}{\partial\alpha}$ becomes zero everywhere except at this point, giving the simple result

$$\frac{d\mathcal{J}}{d\alpha} = h\phi^T \frac{\partial F}{\partial U}\frac{\partial U}{\partial\alpha}. \tag{4.34}$$

4.1.4 Discussion

The above section has concentrated on the theory of the discrete and continuous adjoints without presenting or comparing numerical results, with the main goal simply to provide some of the tools that will be used in the following section. However, a couple of important points can now be understood about the difference between the two approaches. The mathematical development of the discrete is seen to be much simpler than that of the continuous, and also to be general (i.e., we did not need to look at the form of the residual, $\mathcal{R}$, in order to derive the adjoint equation), and thus able to be applied to arbitrary equation sets and objective functions. The continuous in contrast requires significant derivation just for this simple quasi-one-dimensional flow case. However, since the discrete uses the same residual as the flow problem, we will have less freedom in its solution method than the continuous.

4.2 Quasi-one-dimensional Euler flow with combustion

The theory of quasi-one-dimensional flow is now extended to include a simplified combustion model, and we will then combine the discrete and continuous approaches to develop a discrete-continuous hybrid adjoint for this case. We will also consider a typical simplification used when developing multi-physics continuous adjoints, neglecting the contributions from the perturbations or sensitivities of certain quantities. In this example we will consider freezing the combustion source terms.

4.2.1 Flow problem

4.2.1.1 Definition

We now consider quasi one-dimensional Euler flow (smooth or shocked) in the duct $x \in [x_i, x_e]$ with height $h(x)$ as shown previously in Figure 4.1, with the addition, inspired by Powers[48], of a simplified combustion model. We introduce the reaction progress variable Λ and the combustion flow variable $\lambda = \rho\Lambda$.

The analytical governing equations are

$$\mathcal{N} \equiv \frac{d}{dx}(hF) - \frac{dh}{dx}P - hQ = 0, \quad x \in [x_i, x_e], \tag{4.35}$$

where the vectors of the flow variables, fluxes and source terms are given by

$$U = \begin{pmatrix} U_E \\ U_\lambda \end{pmatrix}, \quad F = \begin{pmatrix} F_E \\ F_\lambda \end{pmatrix}, \quad P = \begin{pmatrix} P_E \\ P_\lambda \end{pmatrix}, \quad Q = \begin{pmatrix} Q_E \\ Q_\lambda \end{pmatrix}, \tag{4.36}$$

noting that U_E, F_E and P_E were previously given in (4.2), and also defining

$$U_\lambda = \lambda, \quad F_\lambda = m\Lambda, \quad P_\lambda = 0, \quad Q_E = \begin{pmatrix} 0 \\ 0 \\ 0 \end{pmatrix}, \quad Q_\lambda = \omega. \tag{4.37}$$

We can reuse the equation for the stagnation enthalpy (4.3), but must now include an additional term in the pressure to account for the heat released during reaction,

$$p = (\gamma - 1)(\epsilon - \frac{m^2}{2\rho} + \lambda q), \tag{4.38}$$

where q is the specific heat release, a constant, and the temperature is given by

$$T = \frac{p}{\rho R}. \tag{4.39}$$

We again consider the general objective function (4.5), but will later consider both smooth and non-smooth source and objective functions to investigate the impact of this on the adjoint equations.

4.2.1.2 Boundary conditions

For this case we still have the three characteristic variables from quasi-one-dimensional Euler flow, but with the addition of another characteristic variable from the simple combustion model, with velocity $\frac{m}{\rho}$. The boundary conditions for all flow cases are therefore similar to those detailed previously for quasi-one-dimensional Euler flow, but with an extra condition, fixing the combustion progress variable, required at the inlet.

4.2.1.3 Numerical implementation

The steady-state problem can be solved by discretizing and then iterating the following equation until the variation in U between each time-step is sufficiently small:

$$h\frac{\partial U}{\partial t} = -\frac{\partial}{\partial x}(hF) + \frac{dh}{dx}P + hQ. \tag{4.40}$$

In this case, to make use of existing methods we first split this equation into a set of coupled equations, one for the Euler variables,

$$h\frac{\partial U_E}{\partial t} = -\frac{\partial}{\partial x}(hF_E) + \frac{dh}{dx}P_E, \tag{4.41}$$

and the other for the combustion variable,

$$h\frac{\partial U_\lambda}{\partial t} = -\frac{\partial}{\partial x}\left(hF_\lambda\right) + hQ_\lambda, \tag{4.42}$$

and then solved these together by treating them in an uncoupled way within each iteration.

Applying a finite volume method for the cell p we can obtain

$$h_p\frac{\Delta U_{E_p}}{\Delta t}\Delta x + \mathcal{R}_{E_p} = 0, \tag{4.43}$$

and

$$h_p\frac{\Delta U_{\lambda_p}}{\Delta t}\Delta x + \mathcal{R}_{\lambda_p} = 0, \tag{4.44}$$

where the numerical residuals are given by

$$\mathcal{R}_{E_p} = \widehat{hF}_{E_{p+\frac{1}{2}}} - \widehat{hF}_{E_{p-\frac{1}{2}}} - \Delta h_p P_{E_p}, \tag{4.45}$$

and

$$\mathcal{R}_{\lambda_p} = \widehat{hF}_{\lambda_{p+\frac{1}{2}}} - \widehat{hF}_{\lambda_{p-\frac{1}{2}}} - h_p Q_{\lambda_p}\Delta x, \tag{4.46}$$

and also the numerical fluxes for the Euler variables are given via the Roe scheme[49]

$$\widehat{hF}_{E_{p+\frac{1}{2}}} = \frac{1}{2}\left(hF_{E_{p+1}} + hF_{E_p}\right) - \frac{1}{2}\left|\widetilde{\frac{\partial F_E}{\partial U_E}}\right|_{p+\frac{1}{2}}\left(hU_{E_{p+1}} - hU_{E_p}\right), \tag{4.47}$$

and those for the combustion variable are given by a simple upwinding scheme:

$$\widehat{hF}_{\lambda_{p+\frac{1}{2}}} = \frac{1}{2}\left(hF_{\lambda_{p+1}} + hF_{\lambda_p}\right) - \frac{1}{2}\left|\frac{\partial F_\lambda}{\partial U_\lambda}\right|_{p+\frac{1}{2}}\left(hU_{\lambda_{p+1}} - hU_{\lambda_p}\right). \tag{4.48}$$

We discretized the domain into a uniform mesh of cells of width Δx and wrapped each iteration within a fourth-order Runge-Kutta step.

4.2.2 Discrete adjoint problem

The form of the discrete adjoint problem is identical to that shown previously in Section 2.1.1 and discussed above in Section 4.1.2, since it is independent of the form of the residuals.

4.2.2.1 Numerical implementation

The required discrete Jacobians were computed by applying automatic differentiation via the software tool ADOL-C[33], and then the following equation was solved directly using the forward Euler method until the variation in ψ between each time-step was sufficiently small (equivalent to solving

the linear system iteratively):

$$\frac{\Delta\psi_p}{\Delta t}\Delta x = -\sum_{q=1}^{N}\left(\frac{\mathfrak{D}\mathcal{R}_q}{\mathfrak{D}U_p}\right)^T\psi_q - \left(\frac{\mathfrak{D}\mathcal{J}_D}{\mathfrak{D}U_p}\right)^T, \tag{4.49}$$

where we note that the Δx term is required because the Jacobians are obtained from applying ADOL-C to a finite volume method.

4.2.3 Continuous adjoint problem

4.2.3.1 Derivation

The derivation of the continuous adjoint for this case mirrors closely the process used above for simple quasi-one-dimensional flow. We will not show this in full here since the results can be found by inspection, noting an additional flow variable and source term from the combustion.

We find the same continuous adjoint equations as previously, (4.23), but note that the adjoint linear operator (4.18) now contains an additional combustion source term:

$$L^*(\phi) = -h\left(\frac{\partial F}{\partial U}\right)^T\frac{d\phi}{dx} - \left(\frac{dh}{dx}\left(\frac{\partial P}{\partial U}\right)^T + h\left(\frac{\partial Q}{\partial U}\right)^T\right)\phi. \tag{4.50}$$

The inlet, outlet and shock boundary conditions are the same as (4.22) and (4.21), respectively.

This also gives virtually the same formula for the perturbation to the objective function, (4.24),

$$\delta\mathcal{J}_C = \int_{x_i}^{x_e}\phi^T\frac{\partial\mathcal{N}}{\partial\alpha}\delta\alpha dx + \int_{x_i}^{x_s}\frac{\partial j}{\partial\alpha}\delta\alpha dx + \int_{x_s}^{x_e}\frac{\partial j}{\partial\alpha}\delta\alpha dx. \tag{4.51}$$

It is also possible to consider a frozen-combustion continuous adjoint, mirroring a standard approach used when dealing with the eddy viscosity in turbulent flows. This fixes the combustion source term in the continuous adjoint development and effectively leads to the same adjoint equations developed for quasi-one-dimensional flow in Section 4.1.3.1, but with the modified pressure given by (4.38).

4.2.3.2 Boundary conditions

As explained above, the continuous adjoint equations for quasi-one-dimensional flow with a simple combustion model are subject to effectively the same boundary conditions as the continuous adjoint equations for quasi-one-dimensional Euler flow. The only real difference is that when we have n incoming flow characteristics we now require $4-n$ incoming adjoint characteristics, i.e., that we must have $4-n$ adjoint boundary conditions.

Expanding the term in square brackets in equation (4.18) at either the inlet or outlet, and noting

that we can cancel out the height dependence, we get

$$\left(\begin{array}{cccc} \phi_\rho & \phi_m & \phi_\epsilon & \phi_\lambda \end{array} \right) \frac{\partial F}{\partial U} \left(\begin{array}{c} \delta\rho \\ \delta m \\ \delta\epsilon \\ \delta\lambda \end{array} \right) = 0, \tag{4.52}$$

and then we can appropriately apply the flow boundary conditions to determine the required condition on the adjoint variables, as shown previously for quasi-one-dimensional flow. The major differences in the boundary conditions are summarized below.

Inlet boundary conditions

Subsonic At a subsonic inlet we now have an additional incoming flow characteristic, making a total of three, and thus still need just one incoming adjoint characteristic, and so one adjoint boundary condition. Fixing the combustion progress variable, Λ, at the inlet we can now also use the condition $\delta\Lambda = 0$ to help remove the dependence on three of the flow perturbations, δm, $\delta\epsilon$ and $\delta\lambda$, giving, after rearrangement,

$$\begin{aligned} &\left(\left(\frac{m}{\rho} - \gamma\frac{p}{m} + q\frac{\lambda}{m} \right) \phi_\rho + \left(\left(\frac{m}{\rho} \right)^2 - \frac{\gamma p}{\rho} + 2q\frac{\lambda}{\rho} \right) \phi_m \right. \\ &+ \left(\frac{m}{2\rho^2} \left(\frac{m^2}{\rho} + q\lambda \right) - \frac{\gamma p}{\rho(\gamma-1)} \left(\frac{m(\gamma-3)}{2\rho} - q\frac{\lambda}{m} \right) - \frac{\gamma^2 p^2}{\rho m(\gamma-1)} \right) \phi_\epsilon \\ &\left. + \left(\frac{\lambda}{\rho} \left(\frac{m}{\rho} - \gamma\frac{p}{m} + q\frac{\lambda}{m} \right) \right) \phi_\lambda \right) \delta\rho \quad = \quad 0, \end{aligned} \tag{4.53}$$

which implies that to remove the dependence on $\delta\rho$ we require the adjoint boundary condition

$$\begin{aligned} &\left(\frac{m}{\rho} - \gamma\frac{p}{m} + q\frac{\lambda}{m} \right) \phi_\rho + \left(\left(\frac{m}{\rho} \right)^2 - \frac{\gamma p}{\rho} + 2q\frac{\lambda}{\rho} \right) \phi_m \\ &+ \left(\frac{m}{2\rho^2} \left(\frac{m^2}{\rho} + q\lambda \right) - \frac{\gamma p}{\rho(\gamma-1)} \left(\frac{m(\gamma-3)}{2\rho} - q\frac{\lambda}{m} \right) - \frac{\gamma^2 p^2}{\rho m(\gamma-1)} \right) \phi_\epsilon \\ &+ \left(\frac{\lambda}{\rho} \left(\frac{m}{\rho} - \gamma\frac{p}{m} + q\frac{\lambda}{m} \right) \right) \phi_\lambda \quad = \quad 0, \end{aligned} \tag{4.54}$$

Supersonic At a supersonic inlet, all flow characteristics are incoming and thus again $\delta U = 0$, implying that no boundary conditions need to be set for the adjoint variables.

Outlet boundary conditions

Subsonic At a subsonic outlet we have one incoming flow characteristic and thus now have three incoming adjoint characteristics, and so three adjoint boundary conditions are required. We can again use the condition $\delta p = 0$ to remove the dependence on one of the flow perturbations, $\delta\epsilon$, giving, after rearrangement

$$\begin{aligned} -\left(\left(\frac{m}{\rho}\right)^2\phi_m + \left(\frac{m}{\rho}H + \frac{1}{2}\left(\frac{m}{\rho}\right)^3 + \frac{m}{\rho^2}\lambda(\gamma-1)q\right)\phi_\epsilon + \frac{m}{\rho^2}\lambda\phi_\lambda\right)\delta\rho \\ + \left(\phi_\rho + 2\frac{m}{\rho}\phi_m + \left(H + \left(\frac{m}{\rho}\right)^2 + \frac{\lambda}{\rho}(\gamma-1)q\right)\phi_\epsilon + \frac{\lambda}{\rho}\phi_\lambda\right)\delta m \\ - \left(\frac{m}{\rho}(\gamma\phi_\epsilon + \phi_\lambda)\right)\delta\lambda \quad = \quad 0, \end{aligned} \tag{4.55}$$

which implies that to remove the dependence on $\delta\rho$, δm and $\delta\lambda$ we require the three adjoint boundary conditions

$$-\left(\frac{m}{\rho}\right)^2\phi_m - \left(\frac{m}{\rho}H + \frac{1}{2}\left(\frac{m}{\rho}\right)^3 + \frac{m}{\rho^2}\lambda(\gamma-1)q\right)\phi_\epsilon - \frac{m}{\rho^2}\lambda\phi_\lambda = 0, \tag{4.56}$$

$$\phi_\rho + 2\frac{m}{\rho}\phi_m + \left(H + \left(\frac{m}{\rho}\right)^2 + \frac{\lambda}{\rho}(\gamma-1)q\right)\phi_\epsilon + \frac{\lambda}{\rho}\phi_\lambda = 0, \tag{4.57}$$

and

$$-\frac{m}{\rho}(\gamma\phi_\epsilon + \phi_\lambda) = 0. \tag{4.58}$$

Supersonic At a supersonic outlet we again have no incoming flow characteristics and thus four incoming adjoint characteristics, and so four adjoint boundary conditions are required. As before, due to the direction of the flow characteristics in supersonic flow we interpret that all the adjoint variables will be zero here.

Shock boundary condition The adjoint boundary condition at the shock (4.21) now reduces to a condition on the second and fourth adjoint variables,

$$\phi_m \frac{dh_s}{dx}\left[p\right]_{x_{s^-}}^{x_{s^+}} + \phi_\lambda\left[\omega\right]_{x_{s^-}}^{x_{s^+}} = -\left[j\right]_{x_{s^-}}^{x_{s^+}}, \tag{4.59}$$

noting that this depends on the jumps in p, ω and j across the shock.

4.2.3.3 Sensitivity formulae

The sensitivity of the functional to a parameter α can be written in exactly the same way as for quasi-one-dimensional Euler flow, outlined in Section 4.1.3.3.

4.2.3.4 Numerical implementation

Similar to the direct problem, the steady-state problem can be solved by discretizing and then iterating the following equation until the variation in ϕ between each time-step was sufficiently small:

$$h\frac{\partial \phi}{\partial t} + L^*(\phi) - \left(\frac{\partial j}{\partial U}\right)^T = 0, \tag{4.60}$$

and we again can make use of existing methods by first splitting this equation into a set of coupled equations, one for the Euler adjoint variables, and another for the combustion adjoint variable. However, care should be given to the explicit coupling existing between the two sets of equations. For the Euler part we have

$$h\frac{\partial \phi}{\partial t} + L_E^*(\phi) - \left(\frac{\partial j}{\partial U}\right)^T = 0, \tag{4.61}$$

where

$$L_E^*(\phi) = -h\left(\frac{\partial F}{\partial U_E}\right)^T \frac{d\phi}{dx} - \left(\frac{dh}{dx}\left(\frac{\partial P}{\partial U_E}\right)^T + h\left(\frac{\partial Q}{\partial U_E}\right)^T\right)\phi, \tag{4.62}$$

and for the combustion part

$$h\frac{\partial \phi}{\partial t} + L_\lambda^*(\phi) - \left(\frac{\partial j}{\partial U}\right)^T = 0, \tag{4.63}$$

where

$$L_\lambda^*(\phi) = -h\left(\frac{\partial F}{\partial U_\lambda}\right)^T \frac{d\phi}{dx} - \left(\frac{dh}{dx}\left(\frac{\partial P}{\partial U_\lambda}\right)^T + h\left(\frac{\partial Q}{\partial U_\lambda}\right)^T\right)\phi. \tag{4.64}$$

Applying a finite volume method to the cell p, and noting that unlike the flow equations, the continuous equations are not conservative, we can then obtain

$$\begin{aligned} \frac{\Delta\phi_{E_p}}{\Delta t}\Delta x - h_{p+\frac{1}{2}}\widehat{G}_{E_{p,p+\frac{1}{2}}} + h_{p-\frac{1}{2}}\widehat{G}_{E_{p,p-\frac{1}{2}}} - h_p\left(\frac{\partial F_\lambda}{\partial U_E}\right)_p^T \Delta\phi_{\lambda_p} \\ - \left(\frac{dh}{dx}\left(\frac{\partial P}{\partial U_E}\right)^T + h\left(\frac{\partial Q}{\partial U_E}\right)^T\right)_p \phi_p\Delta x - \left(\frac{\partial j}{\partial U_E}\right)_p^T \Delta x &= 0, \end{aligned} \tag{4.65}$$

and

$$\begin{aligned} \frac{\Delta\phi_{\lambda_p}}{\Delta t}\Delta x - h_{p+\frac{1}{2}}\widehat{G}_{\lambda_{p,p+\frac{1}{2}}} + h_{p-\frac{1}{2}}\widehat{G}_{\lambda_{p,p-\frac{1}{2}}} - h_p\left(\frac{\partial F_E}{\partial U_\lambda}\right)_p^T \Delta\phi_{E_p} \\ - \left(\frac{dh}{dx}\left(\frac{\partial P}{\partial U_\lambda}\right)^T + h\left(\frac{\partial Q}{\partial U_\lambda}\right)^T\right)_p \phi_p\Delta x - \left(\frac{\partial j}{\partial U_\lambda}\right)_p^T \Delta x &= 0, \end{aligned} \tag{4.66}$$

where the numerical fluxes for the Euler adjoint variables are given via a method based on the Roe

scheme[28]

$$\widehat{G}_{E_{p,p+\frac{1}{2}}} = \frac{1}{2}\left(\frac{\partial F_E}{\partial U_E}\right)_p^T (\phi_{p+1}+\phi_p) + \frac{1}{2}\left|\widetilde{\left(\frac{\partial F_E}{\partial U_E}\right)}_{p+\frac{1}{2}}^T\right| (\phi_{p+1}-\phi_p)\,, \tag{4.67}$$

and those for the combustion adjoint variable are given by a simple upwinding scheme

$$\widehat{G}_{\lambda_{p,p+\frac{1}{2}}} = \frac{1}{2}\left(\frac{\partial F_\lambda}{\partial U_\lambda}\right)_p^T (\phi_{p+1}+\phi_p) + \frac{1}{2}\left|\left(\frac{\partial F_\lambda}{\partial U_\lambda}\right)_{p+\frac{1}{2}}^T\right| (\phi_{p+1}-\phi_p)\,. \tag{4.68}$$

Each complete iteration is again wrapped within a fourth-order Runge-Kutta step.

4.2.4 Hybrid adjoint approach

4.2.4.1 Derivation

In the hybrid adjoint approach for this case, we choose to continuously enforce the analytical form of the Euler part of the flow equations, $\mathcal{N}_E$, and to discretely enforce the residual for the solution of the combustion model, $\mathcal{R}_{\lambda_p}$, i.e. $\mathcal{G} = \{\{\mathcal{N}_E\}_C, \{\mathcal{R}_{\lambda_p}\}_D\}$.

In the case of shocked flow we must also continuously enforce the Euler Rankine-Hugoniot conditions (4.10) at the internal shock boundary. However, it is not necessary to include a shock-jump condition for the combustion model, as would be the case for the continuous adjoint, since that equation is being treated discretely (and we note that in the discrete adjoint no such condition was needed).

For this case we have the Lagrangian

$$\begin{aligned}\mathcal{L} &= \beta\left(\int_{x_i}^{x_s} j dx + \int_{x_s}^{x_e} j dx\right) + (1-\beta)\mathcal{J}_D \\ &\quad - \int_{x_i}^{x_s} \varphi_C^T \mathcal{N}_E dx - \int_{x_s}^{x_e} \varphi_C^T \mathcal{N}_E dx - \varphi_{C_s}^T \left[hF_E\right]_{x_s^-}^{x_s^+} + \sum_{p=1}^{N} \varphi_{D_p}^T \mathcal{R}_{\lambda_p},\end{aligned} \tag{4.69}$$

where $\varphi = \{\varphi_C, \varphi_D\}$ and φ_{C_s} are the Lagrange multipliers.

The perturbation then becomes

$$\begin{aligned}\{\delta,\Delta\}\mathcal{L} &= \beta\left(\int_{x_i}^{x_s} \delta j dx + \int_{x_s}^{x_e} \delta j dx - [j]_{x_s^-}^{x_s^+} \delta x_s\right) + (1-\beta)\Delta\mathcal{J}_D \\ &\quad - \int_{x_i}^{x_s} \varphi_C^T \delta\mathcal{N}_E dx - \int_{x_s}^{x_e} \varphi_C^T \delta\mathcal{N}_E dx - \varphi_{C_s}^T \delta\left(\left[hF_E\right]_{x_s^-}^{x_s^+}\right) + \sum_{p=1}^{N} \varphi_{D_p}^T \Delta\mathcal{R}_{\lambda_p}.\end{aligned} \tag{4.70}$$

The perturbed objective function terms can be evaluated as previously for the discrete and continuous adjoints, and the Euler and Rankine-Hugoniot equations can be linearized in the same

way as for quasi-one-dimensional Euler flow. We also can write the discrete perturbation to the combustion residuals as

$$\Delta\mathcal{R}_{D_p} = \sum_{q=1}^{N} \frac{\mathfrak{D}\mathcal{R}_{D_p}}{\mathfrak{D}U_q}\Delta U_q + \frac{\mathfrak{D}\mathcal{R}_{D_p}}{\mathfrak{D}\alpha}\Delta\alpha = 0. \tag{4.71}$$

Incorporating these into (4.70) and performing integration by parts on the continuous terms, followed by rearrangement, we obtain

$$\begin{aligned}
\{\delta,\Delta\}\mathcal{L} \quad = \quad & \int_{x_i}^{x_s} \varphi_C^T \frac{\partial \mathcal{N}_E}{\partial\alpha}\delta\alpha dx + \int_{x_s}^{x_e} \varphi_C^T \frac{\partial \mathcal{N}_E}{\partial\alpha}\delta\alpha dx + \sum_{p=1}^{N} \varphi_{D_p}^T \frac{\mathfrak{D}\mathcal{R}_{\lambda_p}}{\mathfrak{D}\alpha}\Delta\alpha \\
& + \beta\left(\int_{x_i}^{x_s} \frac{\partial j}{\partial\alpha}\delta\alpha dx + \int_{x_s}^{x_e} \frac{\partial j}{\partial\alpha}\delta\alpha dx\right) + (1-\beta)\frac{\mathfrak{D}\mathcal{R}_{\lambda_p}}{\mathfrak{D}\alpha}\Delta\alpha \\
& - \int_{x_i}^{x_s} \left(L_E^*(\varphi_C) - \beta\left(\frac{\partial j}{\partial U}\right)^T\right)^T \delta U dx \\
& - \int_{x_s}^{x_e} \left(L_E^*(\varphi_C) - \beta\left(\frac{\partial j}{\partial U}\right)^T\right)^T \delta U dx \\
& + \sum_{p=1}^{N}\left((1-\beta)\frac{\mathfrak{D}\mathcal{J}_D}{\mathfrak{D}U_p} + \sum_{q=1}^{N}\varphi_{D_p}^T\frac{\mathfrak{D}\mathcal{R}_{\lambda_q}}{\mathfrak{D}U_p}\right)\Delta U_p \\
& - \left(h_s\varphi_{C_s}^T\left[\frac{dF_E}{dx}\right]_{x_{s-}}^{x_{s+}} + [j]_{x_{s-}}^{x_{s+}}\right)\delta x_s \\
& - h_s\left(\varphi_{C_s}^T - \varphi_C^T(x_{s^+})\right)\left(\frac{\partial F_E}{\partial U}\delta U\right)\Big|_{x_{s-}} \\
& + h_s\left(\varphi_{C_s}^T - \varphi_C^T(x_{s^-})\right)\left(\frac{\partial F_E}{\partial U}\delta U\right)\Big|_{x_{s+}} \\
& - \left[h\varphi_C^T\frac{\partial F_E}{\partial U}\delta U\right]_{x_i}^{x_e},
\end{aligned} \tag{4.72}$$

where the adjoint linear operator is the same as that for quasi-one-dimensional flow, given in equation (4.18),

$$L_E^*(\varphi_C) = -h\left(\frac{\partial F_E}{\partial U}\right)^T\frac{d\varphi_C}{dx} - \frac{dh}{dx}\left(\frac{\partial P_E}{\partial U}\right)^T\varphi_C, \tag{4.73}$$

though noting the additional flow variable in U.

We then proceed by appropriately restricting the adjoint variables $\varphi = \{\varphi_C, \varphi_D\}$ and φ_{C_s} such that the explicit dependence of the Lagrangian perturbation on the flow perturbation and shock movement can be removed. Canceling the penultimate three lines leads to the condition that

$$\varphi_{C_s} = \varphi_C, \tag{4.74}$$

and the internal shock boundary condition,

$$h_s \varphi_s^T \left[\frac{dF}{dx}\right]_{x_{s-}}^{x_{s+}} = -\left[j\right]_{x_{s-}}^{x_{s+}}. \tag{4.75}$$

The remaining lines that depend on the flow perturbation can then be removed by introducing the combined hybrid adjoint equations and boundary conditions,

$$\begin{aligned} \int_{x_i}^{x_e} \left(L_E^*(\varphi_C) - \beta \left(\frac{\partial j}{\partial U}\right)^T \right)^T \delta U \, dx - \left[h \varphi_C^T \frac{\partial F_E}{\partial U} \delta U \right]_{x_i}^{x_e} \\ = \sum_{p=1}^{N} \left((1-\beta) \frac{\mathfrak{D}\mathcal{J}_D}{\mathfrak{D}U_p} + \sum_{q=1}^{N} \varphi_{D_q}^T \frac{\mathfrak{D}\mathcal{R}_{\lambda_q}}{\mathfrak{D}U_p} \right) \Delta U_p, \end{aligned} \tag{4.76}$$

and thus the perturbation to the objective function can be written

$$\begin{aligned} \{\delta, \Delta\}\mathcal{J}_H = \{\delta, \Delta\}\mathcal{L} \quad = \quad & \int_{x_i}^{x_s} \varphi_C^T \frac{\partial \mathcal{N}_E}{\partial \alpha} \delta\alpha dx + \sum_{p=1}^{N} \mu_p^T \frac{\mathfrak{D}\mathcal{R}_{\lambda_p}}{\mathfrak{D}\alpha} \Delta\alpha \\ & + \beta \int_{x_i}^{x_s} \frac{\partial j}{\partial \alpha} \delta\alpha dx + \beta \int_{x_s}^{x_e} \frac{\partial j}{\partial \alpha} \delta\alpha dx + (1-\beta) \frac{\mathfrak{D}\mathcal{J}_D}{\mathfrak{D}\alpha} \Delta\alpha. \end{aligned} \tag{4.77}$$

However, we need to segregate the adjoint equations and boundary conditions from the combined equation (4.76) in order to remove the dependence on the linear flow perturbations. This process is not quite as simple as the step in the continuous adjoint derivation, because we cannot simply equate the term in square brackets to zero. The reason for this complication is that this term still involves four flow perturbations, δU, but now only three adjoint variables, φ_C, making it impossible to guarantee that through appropriate choice of the adjoint variables the dependence on all four flow perturbations can be removed.

The solution to this problem is to incorporate some of the discrete terms, creating truly hybrid boundary conditions. We split the residual in the boundary cells into the part due to the flux across the boundary and the part due to internal fluxes and sources, i.e.,

$$\mathcal{R}_{\lambda_p} = (\widehat{hF}_\lambda)_{\Gamma_p} + \mathcal{R}^*_{\lambda_p}, \tag{4.78}$$

and to simplify the working, use the notation that

$$\mathcal{R}^{(*)}_{\lambda_p} = \begin{cases} \mathcal{R}_{\lambda_p} & \text{for internal cells,} \\ \mathcal{R}^*_{\lambda_p} & \text{for boundary cells,} \end{cases} \tag{4.79}$$

The combined equations can then be written

$$\begin{aligned}\int_{x_i}^{x_e}\left(L_E^*(\varphi_C)-\beta\left(\frac{\partial j}{\partial U}\right)^T\right)^T\delta U\,dx-\left[h\varphi_C^T\frac{\partial F_E}{\partial U}\delta U\right]_{x_i}^{x_e}\\ =\sum_{p=1}^{N}\left((1-\beta)\frac{\mathfrak{D}\mathcal{J}_D}{\mathfrak{D}U_p}+\sum_{q=1}^{N}\varphi_{D_q}^T\frac{\mathfrak{D}\mathcal{R}_{\lambda_q}^{(*)}}{\mathfrak{D}U_p}\right)\Delta U_p\\ +\varphi_{D_1}^T\frac{\mathfrak{D}(\widehat{hF}_\lambda)_{\Gamma_1}}{\mathfrak{D}U_1}\Delta U_1+\varphi_{D_N}^T\frac{\mathfrak{D}(\widehat{hF}_\lambda)_{\Gamma_N}}{\mathfrak{D}U_N}\Delta U_N,\end{aligned}\tag{4.80}$$

which can then be split into the hybrid adjoint equations

$$\int_{x_i}^{x_e}\left(L_E^*(\varphi_C)-\beta\left(\frac{\partial j}{\partial U}\right)^T\right)^T\delta U\,dx=\sum_{p=1}^{N}\left((1-\beta)\frac{\mathfrak{D}\mathcal{J}_D}{\mathfrak{D}U_p}+\sum_{q=1}^{N}\varphi_{D_q}^T\frac{\mathfrak{D}\mathcal{R}_{\lambda_q}^{(*)}}{\mathfrak{D}U_p}\right)\Delta U_p,\tag{4.81}$$

and boundary conditions

$$\left[h\varphi_C^T\frac{\partial F_E}{\partial U}\delta U\right]_{x_i}^{x_e}+\varphi_{D_1}^T\frac{\mathfrak{D}(\widehat{hF}_\lambda)_{\Gamma_1}}{\mathfrak{D}U_1}\Delta U_1+\varphi_{D_N}^T\frac{\mathfrak{D}(\widehat{hF}_\lambda)_{\Gamma_N}}{\mathfrak{D}U_N}\Delta U_N=0.\tag{4.82}$$

However, it can be seen that the hybrid equations (4.80) still retain a dependency on the flow perturbation through δU and ΔU. To remove this we first write the integral over the domain as a sum of the integrals over each cell

$$\sum_{p=1}^{N}\int_p\left(L_E^*(\varphi_C)-\beta\left(\frac{\partial j}{\partial U}\right)^T\right)^T\delta U\,dx=\sum_{p=1}^{N}\left((1-\beta)\frac{\mathfrak{D}\mathcal{J}_D}{\mathfrak{D}U_p}+\sum_{q=1}^{N}\varphi_{D_q}^T\frac{\mathfrak{D}\mathcal{R}_{\lambda_q}^{(*)}}{\mathfrak{D}U_p}\right)\Delta U_p,\tag{4.83}$$

and then impose the condition that as well as this being valid over the whole domain, this is also true over each cell, allowing us to drop the leading summation signs and write

$$\int_p\left(L_E^*(\varphi_C)-\beta\left(\frac{\partial j}{\partial U}\right)^T\right)^T\delta U\,dx=\left((1-\beta)\frac{\mathfrak{D}\mathcal{J}_D}{\mathfrak{D}U_p}+\sum_{q=1}^{N}\varphi_{D_q}^T\frac{\mathfrak{D}\mathcal{R}_{\lambda_q}^{(*)}}{\mathfrak{D}U_p}\right)\Delta U_p,\tag{4.84}$$

We also now assume that the flow perturbation is in general small, and thus only varies gradually over the domain. This means that as the cell width decreases it can be treated as constant within each cell, allowing us to factor δU out of the integral,

$$\left(\int_p\left(L_E^*(\varphi_C)-\beta\left(\frac{\partial j}{\partial U}\right)^T\right)^T dx\right)\delta U_p=\left((1-\beta)\frac{\mathfrak{D}\mathcal{J}_D}{\mathfrak{D}U_p}+\sum_{q=1}^{N}\varphi_{C_q}^T\frac{\mathfrak{D}\mathcal{R}_{\lambda_q}^{(*)}}{\mathfrak{D}U_p}\right)\Delta U_p.\tag{4.85}$$

Finally asserting that $\delta U_p\to\Delta U_p$ as $\Delta x\to 0$, we factor out the flow perturbation and arrive at

the final hybrid adjoint equations,

$$\int_p \left(L_E^*(\varphi_C) - \beta \left(\frac{\partial j}{\partial U} \right)^T \right)^T dx = (1-\beta) \frac{\mathfrak{D}\mathcal{J}_D}{\mathfrak{D}U_p} + \sum_{q=1}^{N} \varphi_{C_q}^T \frac{\mathfrak{D}\mathcal{R}_{\lambda_q}^{(*)}}{\mathfrak{D}U_p}, \quad x \in [x_i, x_e]. \tag{4.86}$$

4.2.4.2 Boundary conditions

The hybrid adjoint equations for quasi-one-dimensional flow with a simple combustion model are subject to the boundary conditions (4.82) at the inlet and outlet and, if present, (4.75) at the shock.

Considering the first of these two, we can split the boundary condition into two, one part for the inlet,

$$\left(h \varphi_C^T \frac{\partial F_E}{\partial U} \delta U \right)_{x_i} + \varphi_{D_1}^T \frac{\mathfrak{D}(\widehat{hF}_\lambda)_{\Gamma_1}}{\mathfrak{D}U_1} \Delta U_1 = 0, \tag{4.87}$$

and another for the outlet,

$$\left(h \varphi_C^T \frac{\partial F_E}{\partial U} \delta U \right)_{x_e} + \varphi_{D_N}^T \frac{\mathfrak{D}(\widehat{hF}_\lambda)_{\Gamma_N}}{\mathfrak{D}U_N} \Delta U_N = 0. \tag{4.88}$$

Noting the similarity between these two we will treat a generalized boundary condition on the cell p. We also use the assumption that the values are constant within each cell, giving,

$$h_{\Gamma_p} \varphi_{C_p}^T \left(\frac{\partial F_E}{\partial U} \right)_{\Gamma_p} \delta U_p + \varphi_{D_p}^T \frac{\mathfrak{D}(\widehat{hF}_\lambda)_{\Gamma_p}}{\mathfrak{D}U_p} \Delta U_p = 0. \tag{4.89}$$

Equating δU_p and ΔU_p, and dividing through by the height of the boundary, this can be rewritten to closely resemble the continuous version, (4.52),

$$\begin{pmatrix} \varphi_{C_\rho} & \varphi_{C_m} & \varphi_{C_\epsilon} & \varphi_D \end{pmatrix}_p \begin{pmatrix} \left(\frac{\partial F_E}{\partial U} \right)_{\Gamma_p} \\ \frac{1}{h_{\Gamma_p}} \frac{\mathfrak{D}(\widehat{hF}_\lambda)_{\Gamma_p}}{\mathfrak{D}U_p} \end{pmatrix} \begin{pmatrix} \delta\rho \\ \delta m \\ \delta\epsilon \\ \delta\lambda \end{pmatrix}_p = 0. \tag{4.90}$$

We thus require the same number of adjoint boundary conditions as before for the continuous adjoint, in order to remove the dependence on the boundary flow perturbations. To derive the specific adjoint boundary conditions we now consider the different types of flow boundaries.

Inlet boundary conditions

Subsonic As for the continuous adjoint, we can use the conditions $\delta H = 0$, $\delta p_0 = 0$ and $\delta\Lambda = 0$ to remove the dependence on three of the flow perturbations, δm, $\delta\epsilon$ and $\delta\lambda$, giving

$$\begin{aligned}
&\left(\left(\frac{m}{\rho} - \gamma\frac{p}{m} + q\frac{\lambda}{m}\right)\varphi_{C_\rho} + \left(\left(\frac{m}{\rho}\right)^2 - \frac{\gamma p}{\rho} + 2q\frac{\lambda}{\rho}\right)\varphi_{C_m}\right.\\
&+\left(\frac{m}{2\rho^2}\left(\frac{m^2}{\rho} + q\lambda\right) - \frac{\gamma p}{\rho(\gamma-1)}\left(\frac{m(\gamma-3)}{2\rho} - q\frac{\lambda}{m}\right) - \frac{\gamma^2 p^2}{\rho m(\gamma-1)}\right)\varphi_{C_\epsilon}\\
&+\frac{1}{h_{\Gamma_1}}\left(\frac{\mathfrak{D}(\widehat{hF}_\lambda)_{\Gamma_1}}{\mathfrak{D}\rho_1} + \left(\frac{m}{\rho} - \gamma\frac{p}{m} + q\frac{\lambda}{m}\right)\frac{\mathfrak{D}(\widehat{hF}_\lambda)_{\Gamma_1}}{\mathfrak{D}\rho_1}\right.\\
&\left.\left.+\left(H - \gamma\frac{\lambda}{\rho}\right)\frac{\mathfrak{D}(\widehat{hF}_\lambda)_{\Gamma_1}}{\mathfrak{D}\epsilon_1} + \frac{\lambda}{\rho}\frac{\mathfrak{D}(\widehat{hF}_\lambda)_{\Gamma_1}}{\mathfrak{D}\lambda_1}\right)\varphi_D\right)\delta\rho \;=\; 0,
\end{aligned} \tag{4.91}$$

which implies that to remove the dependence on $\delta\rho$ we require the adjoint boundary condition,

$$\begin{aligned}
&\left(\left(\frac{m}{\rho} - \gamma\frac{p}{m} + q\frac{\lambda}{m}\right)\varphi_{C_\rho} + \left(\left(\frac{m}{\rho}\right)^2 - \frac{\gamma p}{\rho} + 2q\frac{\lambda}{\rho}\right)\varphi_{C_m}\right.\\
&+\left(\frac{m}{2\rho^2}\left(\frac{m^2}{\rho} + q\lambda\right) - \frac{\gamma p}{\rho(\gamma-1)}\left(\frac{m(\gamma-3)}{2\rho} - q\frac{\lambda}{m}\right) - \frac{\gamma^2 p^2}{\rho m(\gamma-1)}\right)\varphi_{C_\epsilon}\\
&+\frac{1}{h_{\Gamma_1}}\left(\frac{\mathfrak{D}(\widehat{hF}_\lambda)_{\Gamma_1}}{\mathfrak{D}\rho_1} + \left(\frac{m}{\rho} - \gamma\frac{p}{m} + q\frac{\lambda}{m}\right)\frac{\mathfrak{D}(\widehat{hF}_\lambda)_{\Gamma_1}}{\mathfrak{D}\rho_1}\right.\\
&\left.\left.+\left(H - \gamma\frac{\lambda}{\rho}\right)\frac{\mathfrak{D}(\widehat{hF}_\lambda)_{\Gamma_1}}{\mathfrak{D}\epsilon_1} + \frac{\lambda}{\rho}\frac{\mathfrak{D}(\widehat{hF}_\lambda)_{\Gamma_1}}{\mathfrak{D}\lambda_1}\right)\varphi_D\right) \;=\; 0.
\end{aligned} \tag{4.92}$$

Supersonic Again, no boundary conditions need to be set for the adjoint variables.

Outlet boundary conditions

Subsonic We can again use the condition $\delta p = 0$ to remove the dependence on one of the flow perturbations, $\delta\epsilon$, giving, after rearrangement,

$$\begin{aligned}
-\left(\left(\frac{m}{\rho}\right)^2\varphi_{C_m} + \left(\frac{m}{\rho}H + \frac{1}{2}\left(\frac{m}{\rho}\right)^3 + \frac{m}{\rho^2}\lambda(\gamma-1)q\right)\varphi_{C_\epsilon}\right.\\
\left. + \frac{1}{h_{\Gamma_N}}\left(\frac{\mathfrak{D}(\widehat{hF}_\lambda)_{\Gamma_N}}{\mathfrak{D}\rho_N} - \frac{m^2}{2\rho^2}\frac{\mathfrak{D}(\widehat{hF}_\lambda)_{\Gamma_N}}{\mathfrak{D}\epsilon_N}\right)\varphi_D\right)\delta\rho\\
+\left(\varphi_{C_\rho} + 2\frac{m}{\rho}\varphi_{C_m} + \left(H + \left(\frac{m}{\rho}\right)^2 + \frac{\lambda}{\rho}(\gamma-1)q\right)\varphi_{C_\epsilon}\right.\\
\left. + \frac{1}{h_{\Gamma_N}}\left(\frac{\mathfrak{D}(\widehat{hF}_\lambda)_{\Gamma_N}}{\mathfrak{D}m_N} + \frac{m}{\rho}\frac{\mathfrak{D}(\widehat{hF}_\lambda)_{\Gamma_N}}{\mathfrak{D}\epsilon_N}\right)\varphi_D\right)\delta m\\
+\left(\frac{1}{h_{\Gamma_N}}\left(\frac{\mathfrak{D}(\widehat{hF}_\lambda)_{\Gamma_N}}{\mathfrak{D}\lambda_N} - q\frac{\mathfrak{D}(\widehat{hF}_\lambda)_{\Gamma_N}}{\mathfrak{D}\epsilon_N}\right)\varphi_D - \frac{m}{\rho}\gamma\varphi_{C_\epsilon}\right)\delta\lambda \quad = \quad 0,
\end{aligned} \tag{4.93}$$

which implies that to remove the dependence on $\delta\rho$, δm and $\delta\lambda$, we require the three adjoint boundary conditions,

$$\begin{aligned}
-\left(\frac{m}{\rho}\right)^2\varphi_{C_m} - \left(\frac{m}{\rho}H + \frac{1}{2}\left(\frac{m}{\rho}\right)^3 + \frac{m}{\rho^2}\lambda(\gamma-1)q\right)\varphi_{C_\epsilon}\\
-\frac{1}{h_{\Gamma_N}}\left(\frac{\mathfrak{D}(\widehat{hF}_\lambda)_{\Gamma_N}}{\mathfrak{D}\rho_N} - \frac{m^2}{2\rho^2}\frac{\mathfrak{D}(\widehat{hF}_\lambda)_{\Gamma_N}}{\mathfrak{D}\epsilon_N}\right)\varphi_D \quad = \quad 0,
\end{aligned} \tag{4.94}$$

$$\begin{aligned}
\varphi_{C_\rho} + 2\frac{m}{\rho}\varphi_{C_m} + \left(H + \left(\frac{m}{\rho}\right)^2 + \frac{\lambda}{\rho}(\gamma-1)q\right)\varphi_{C_\epsilon}\\
+\frac{1}{h_{\Gamma_N}}\left(\frac{\mathfrak{D}(\widehat{hF}_\lambda)_{\Gamma_N}}{\mathfrak{D}m_N} + \frac{m}{\rho}\frac{\mathfrak{D}(\widehat{hF}_\lambda)_{\Gamma_N}}{\mathfrak{D}\epsilon_N}\right)\varphi_D \quad = \quad 0,
\end{aligned} \tag{4.95}$$

and

$$\frac{1}{h_{\Gamma_N}}\left(\frac{\mathfrak{D}(\widehat{hF}_\lambda)_{\Gamma_N}}{\mathfrak{D}\lambda_N} - q\frac{\mathfrak{D}(\widehat{hF}_\lambda)_{\Gamma_N}}{\mathfrak{D}\epsilon_N}\right)\varphi_D - \frac{m}{\rho}\gamma\varphi_{C_\epsilon} = 0. \tag{4.96}$$

Supersonic As previously, all the adjoint variables will be zero here.

Shock boundary condition The hybrid adjoint boundary condition at the shock (4.75) gives the value of the mass flow-adjoint variable

$$\varphi_{C_m} = -\frac{[j]_{x_{s^-}}^{x_{s^+}}}{[p]_{x_{s^-}}^{x_{s^+}}}\left(\frac{dh_s}{dx}\right)^{-1}, \tag{4.97}$$

noting that this now only depends on the jumps in p and j across the shock, and not ω as previously in the continuous adjoint.

4.2.4.3 Sensitivity formulae

Assuming no explicit dependence of $\mathcal{J}_H$ on the parameter α, then we can write the sensitivity as

$$\frac{d\mathcal{J}_H}{d\alpha} = \int_{x_i}^{x_s} \varphi_C^T \frac{\partial \mathcal{N}_E}{\partial U}\frac{\partial U}{\partial \alpha} dx + \sum_{p=1}^{N} \varphi_{D_p}^T \frac{\mathfrak{D}\mathcal{R}_{\lambda_p}}{\mathfrak{D}U}\frac{\partial U}{\partial \alpha}. \tag{4.98}$$

When considering possible choices for α that are only defined at just one point in the flow, such as boundary conditions, this can again be simplified to give

$$\frac{d\mathcal{J}_H}{d\alpha} = h\varphi_C^T \frac{\partial F_E}{\partial U}\frac{\partial U}{\partial \alpha} + \varphi_{D_p}^T \frac{\mathfrak{D}\mathcal{R}_{\lambda_p}}{\mathfrak{D}U}\frac{\partial U}{\partial \alpha}. \tag{4.99}$$

4.2.4.4 Numerical implementation

Similar to the continuous method, the steady-state problem can be solved by discretizing and then iterating the following equations, noting that the hybrid equation is already presented in a semi-discretized format, until the variation in the adjoint variables $\varphi = \{\varphi_C, \varphi_D\}$ between each time-step is sufficiently small:

$$h_p \frac{\Delta \varphi_p}{\Delta t} + \int_p \left(L_E^*(\varphi_C) - \beta \left(\frac{\partial j}{\partial U} \right)^T \right) dx = (1-\beta) \left(\frac{\mathfrak{D}\mathcal{J}_D}{\mathfrak{D}U_p} \right)^T + \sum_{q=1}^{N} \left(\frac{\mathfrak{D}\mathcal{R}_{\lambda_q}^{(*)}}{\mathfrak{D}U_p} \right)^T \varphi_{D_q}, \tag{4.100}$$

with the appropriate hybrid boundary conditions for the given flow case.

We can immediately simplify this equation by noting that the combustion model residuals were calculated via first-order upwinding, and thus $\mathcal{R}_{D_p}$ explicitly depends only on the flow variables at $p-1$, p and $p+1$:

$$h_p \frac{\Delta \varphi_p}{\Delta t} + \int_p \left(L_E^*(\varphi_C) - \beta \left(\frac{\partial j}{\partial U} \right)^T \right) dx (1-\beta) \left(\frac{\mathfrak{D}\mathcal{J}_D}{\mathfrak{D}U_p} \right)^T + \sum_{q=p-1}^{p+1} \left(\frac{\mathfrak{D}\mathcal{R}_{\lambda_q}^{(*)}}{\mathfrak{D}U_p} \right)^T \varphi_{D_q}, \tag{4.101}$$

noting that at the boundaries $p = 1$ and $p = N$ we must restrict the summation region further to include just p and $p+1$ or $p-1$ and p, respectively.

We again intend to make use of existing methods by first splitting these equations into sets of coupled equations, for the Euler adjoint variables and for the combustion adjoint variable. However, we must be careful due to the explicit coupling between the two sets of equations. First for the

Euler part we have

$$\begin{aligned} h_p \frac{\Delta \varphi_p}{\Delta t} + \int_p \left(L^*_{E,E}(\varphi_C) - \beta \left(\frac{\partial j}{\partial U_E} \right)^T \right) dx \\ = (1-\beta) \left(\frac{\mathfrak{D} \mathcal{J}_D}{\mathfrak{D} U_{E_p}} \right)^T + \sum_{q=p-1}^{p+1} \left(\frac{\mathfrak{D} \mathcal{R}^{(*)}_{\lambda_q}}{\mathfrak{D} U_{E_p}} \right)^T \varphi_{D_q}, \end{aligned} \tag{4.102}$$

where

$$L^*_{E,E}(\varphi_C) = -h \left(\frac{\partial F_E}{\partial U_E} \right)^T \frac{d\varphi_C}{dx} - \frac{dh}{dx} \left(\frac{\partial P_E}{\partial U_E} \right)^T \varphi_C. \tag{4.103}$$

Next for the combustion part we have

$$\begin{aligned} h_p \frac{\Delta \varphi_p}{\Delta t} + \int_p \left(L^*_{E,\lambda}(\varphi_C) - \beta \left(\frac{\partial j}{\partial U_\lambda} \right)^T \right) dx \\ = (1-\beta) \left(\frac{\mathfrak{D} \mathcal{J}_D}{\mathfrak{D} U_{\lambda_p}} \right)^T + \sum_{q=p-1}^{p+1} \left(\frac{\mathfrak{D} \mathcal{R}^{(*)}_{\lambda_q}}{\mathfrak{D} U_{\lambda_p}} \right)^T \varphi_{D_q}, \end{aligned} \tag{4.104}$$

where

$$L^*_{E,\lambda}(\varphi_C) = -h \left(\frac{\partial F_E}{\partial U_\lambda} \right)^T \frac{d\varphi_C}{dx} - \frac{dh}{dx} \left(\frac{\partial P_E}{\partial U_\lambda} \right)^T \varphi_C. \tag{4.105}$$

Identifying the integrals as the equivalent of applying a finite volume method to the cell p, we can then obtain for the Euler part,

$$\begin{aligned} \frac{\Delta \varphi_{C_p}}{\Delta t} \Delta x - h_{p+\frac{1}{2}} \widehat{G}_{E_{p,p+\frac{1}{2}}} - h_{p-\frac{1}{2}} \widehat{G}_{E_{p,p-\frac{1}{2}}} - \frac{dh_p}{dx} \left(\frac{\partial P_E}{\partial U_E} \right)^T_p \varphi_{C_p} \Delta x - \beta \left(\frac{\partial j}{\partial U_E} \right)^T_p \Delta x \\ = (1-\beta) \left(\frac{\mathfrak{D} \mathcal{J}_D}{\mathfrak{D} U_{E_p}} \right)^T + \sum_{q=p-1}^{p+1} \left(\frac{\mathfrak{D} \mathcal{R}^{(*)}_{\lambda_q}}{\mathfrak{D} U_{E_p}} \right)^T \varphi_{D_q}, \end{aligned} \tag{4.106}$$

and for the combustion part,

$$\begin{aligned} \frac{\Delta \varphi_{D_p}}{\Delta t} \Delta x - h_p \left(\frac{\partial F_E}{\partial U_\lambda} \right)^T_p \Delta \varphi_{C_p} - \frac{dh_p}{dx} \left(\frac{\partial P_E}{\partial U_\lambda} \right)^T_p \varphi_{C_p} \Delta x - \beta \left(\frac{\partial j}{\partial U_\lambda} \right)^T_p \Delta x \\ = (1-\beta) \left(\frac{\mathfrak{D} \mathcal{J}_D}{\mathfrak{D} U_{\lambda_p}} \right)^T + \sum_{q=p-1}^{p+1} \left(\frac{\mathfrak{D} \mathcal{R}^{(*)}_{\lambda_q}}{\mathfrak{D} U_{\lambda_p}} \right)^T \varphi_{D_q}, \end{aligned} \tag{4.107}$$

where the numerical fluxes for the Euler adjoint variables are again given via a method based on

the Roe scheme[28]:

$$\widehat{G}_{E_{p,p+\frac{1}{2}}} = \frac{1}{2}\left(\frac{\partial F_E}{\partial U_E}\right)_p^T \left(\varphi_{C_{p+1}} + \varphi_{C_p}\right) + \frac{1}{2}\left|\widetilde{\left(\frac{\partial F_E}{\partial U_E}\right)}_{p+\frac{1}{2}}^T\right| \left(\varphi_{C_{p+1}} - \varphi_{C_p}\right). \tag{4.108}$$

Each complete iteration is again wrapped within a fourth-order Runge-Kutta step.

4.2.5 Results

4.2.5.1 Theoretical analysis

Careful analysis of the numerical implementation of the three different adjoint methods used here highlights certain key differences between the approaches:

1. The primal problem was solved by first decoupling the Euler and combustion variable parts of the governing equations. Considering the general upwind formulation for the numerical flux:

$$\widehat{hF}_{p+\frac{1}{2}} = \frac{1}{2}\left(hF_{p+1} + hF_p\right) - \frac{1}{2}\left|\frac{\partial F}{\partial U}\right|_{p+\frac{1}{2}} \left(hU_{p+1} - hU_p\right). \tag{4.109}$$

For the fully coupled system this would expand to give

$$\begin{aligned}\begin{pmatrix} \widehat{hF}_E \\ \widehat{hF}_\lambda \end{pmatrix}_{p+\frac{1}{2}} &= \tfrac{1}{2}\left(\begin{pmatrix} hF_E \\ hF_\lambda \end{pmatrix}_{p+1} + \begin{pmatrix} hF_E \\ hF_\lambda \end{pmatrix}_p\right) \\ &\quad -\tfrac{1}{2}\begin{vmatrix} \dfrac{\partial F_E}{\partial U_E} & \dfrac{\partial F_E}{\partial U_\lambda} \\ \dfrac{\partial F_\lambda}{\partial U_E} & \dfrac{\partial F_\lambda}{\partial U_\lambda} \end{vmatrix}_{p+\frac{1}{2}} \left(\begin{pmatrix} hU_E \\ hU_\lambda \end{pmatrix}_{p+1} - \begin{pmatrix} hU_E \\ hU_\lambda \end{pmatrix}_p\right),\end{aligned} \tag{4.110}$$

but for the uncoupled approach, gathering the two uncoupled equations into one, we have

$$\begin{aligned}\begin{pmatrix} \widehat{hF}_E \\ \widehat{hF}_\lambda \end{pmatrix}_{p+\frac{1}{2}} &= \tfrac{1}{2}\left(\begin{pmatrix} hF_E \\ hF_\lambda \end{pmatrix}_{p+1} + \begin{pmatrix} hF_E \\ hF_\lambda \end{pmatrix}_p\right) \\ &\quad -\tfrac{1}{2}\begin{vmatrix} \dfrac{\partial F_E}{\partial U_E} & 0 \\ 0 & \dfrac{\partial F_\lambda}{\partial U_\lambda} \end{vmatrix}_{p+\frac{1}{2}} \left(\begin{pmatrix} hU_E \\ hU_\lambda \end{pmatrix}_{p+1} - \begin{pmatrix} hU_E \\ hU_\lambda \end{pmatrix}_p\right),\end{aligned} \tag{4.111}$$

where it can be seen that the cross terms in the artificial dissipation in Equation (4.110) are absent.

This difference is expected to affect the discrete adjoint, which depends explicitly on the form of the flow residuals, and also parts of the hybrid adjoint. However, assuming that the methods are consistent and the same flow solution is obtained, the continuous adjoint should be unaffected.

2. The Jacobian, $\dfrac{\mathfrak{D}()}{\mathfrak{D}()}$, at any point in the discrete adjoint equation is a derivative of some quantity at that point relative to parameters defined at every other point throughout the domain. In contrast, in the continuous adjoint, the Jacobian, $\dfrac{\partial()}{\partial()}$, at any point is a derivative of the quantity at that point with respect to parameters only at that same point. This immediately implies that the Jacobians in the discrete formulation are much larger matrices than for the continuous, though the actual stencil used in the flow residual calculation is likely to mean the Jacobian matrix will mostly contain zeros. As it includes both discrete and continuous Jacobians, the hybrid approach lies somewhere between the discrete and continuous in terms of the memory requirements that would be needed to store these terms.

3. When applying automatic differentiation to find the discrete Jacobians, additional terms that give the sensitivity of the artificial dissipation of the Roe flux splitting and upwinding schemes to the flow variables will be automatically included. For example, considering the following numerical flux:

$$\widehat{hF}_{E,p+\frac{1}{2}} = \frac{1}{2}\left(hF_{E,p+1} + hF_{E,p}\right) - \frac{1}{2}\left|\widetilde{\frac{\partial F_E}{\partial U_E}}\right|_{p+\frac{1}{2}} \left(hU_{E,p+1} - hU_{E,p}\right), \tag{4.112}$$

we can see that taking derivatives with respect to $U_{E,p}$ will introduce the Hessian term

$$-\frac{1}{2}\left(\frac{\mathfrak{D}}{\mathfrak{D}U_{E,p}}\left|\widetilde{\frac{\partial F_E}{\partial U_E}}\right|_{p+\frac{1}{2}}\right)\left(hU_{E,p+1} - hU_{E,p}\right). \tag{4.113}$$

Though we expect this to be small, a cumbersome term-by-term expansion of the numerical methods used to solve the continuous, discrete and hybrid adjoints in this case reveals that the only difference between them is due to such terms. The continuous has no such terms, and the hybrid has fewer than the discrete since in that case these only appear in the fluxes of the combustion adjoint variables.

4. The derivation of the hybrid reveals two important points. The first is that the terms treated continuously do not involve the combustion source term ω, and the second is that it is possible to deal with a purely discrete objective function in the definition of the adjoint equation. The implications of both of these are that once the continuous part has been derived once, it will not be altered by modifications to the source term, and that it will be valid for non-smooth

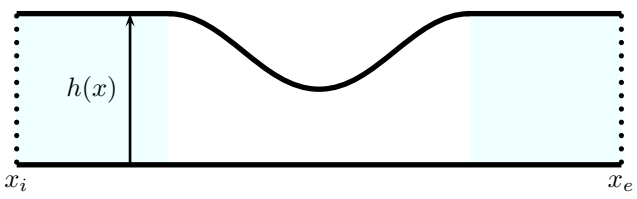

Figure 4.2: Converging-diverging nozzle.

source and objective functions. Additionally, it implies that at least part of any code developed for the continuous adjoint can be reused.

4.2.5.2 Flow test case

The test case used to investigate the characteristics of the hybrid adjoint method was supersonic flow through the converging-diverging nozzle used by Giles and Pierce[45]. Shown in Figure 4.2, this has the height

$$h(x) = \begin{cases} 2 & \text{for } x \leq -\frac{1}{2} \text{ or } x \geq -\frac{1}{2}, \\ 1 + \sin^2(\pi x) & \text{for } -\frac{1}{2} < x < \frac{1}{2}. \end{cases} \tag{4.114}$$

We consider two possible forms for the combustion source term ω:

1. A smooth, exponential form,
$$\omega_e = \rho(1-\Lambda)e^{-\frac{C}{RT}}. \tag{4.115}$$

2. A non-smooth, Heaviside form,
$$\omega_{\mathcal{H}} = b\rho(1-\Lambda)\mathcal{H}\left(T - T^*\right). \tag{4.116}$$

where C, b and T^* are constants relevant to each source term.

We also define two objective functions as integrals over the domain:

1. A smooth form, the 'lift' over the duct,
$$\mathcal{J}_p = \int_{x_i}^{x_e} p dx. \tag{4.117}$$

2. A non-smooth form, the magnitude of a pressure difference,
$$\mathcal{J}_{\Delta p} = \int_{x_i}^{x_e} \left|p - p^*\right| dx. \tag{4.118}$$

where p^* is a constant baseline pressure.

Note, the reason for choosing both smooth and non-smooth source and objective functions is to allow the hybrid method to be developed, investigated and applied to situations where using the continuous adjoint may be problematic, rather than, in this case, to choose the most useful objective functions for engineering applications. It should be noted, however, that norms of pressure differences similar to (4.118) have been used to predict unstart in scramjet engines[50].

The flow conditions and mesh used in this paper are:

- Inlet Mach number, $M_i = 4.0$
- Inlet stagnation enthalpy, $H_i = 4.0$
- Inlet stagnation pressure, $p_{0i} = 2.0$
- CFL number = 0.5
- Number of mesh cells = 100
- Exponential source term constant, $C = 0.1$
- Gas constant, $R = 1.0$
- Ratio of specific heats, $\gamma = 1.4$
- Heaviside source term constant, $b = 1.0$
- Specific heat release, $q = 1.0$
- Heaviside initiation temperature, $T^* = 0.3$
- Baseline pressure for non-smooth fuctional, $p^* = 0.03$

Figures 4.3 and 4.4 show the pressure and progress variables for the flow solutions with the exponential and Heaviside source terms, respectively. Of note, the step nature of the Heaviside source function can be seen in Figure 4.4 b), where the combustion progress variable remains constant until the duct height has changed sufficiently to cause the temperature to rise above T^*.

4.2.5.3 Adjoint results

Adjoint variables The density- and combustion progress-adjoint variables computed by the different adjoint approaches are shown in the following graphs for the cases: exponential source term and integral of pressure functional (Figure 4.5), Heaviside source term and integral of pressure functional (Figure 4.6), and exponential source term and the magnitude of a pressure difference functional (Figure 4.7). In all three, close agreement is seen between the adjoint variables produced by the different methods.

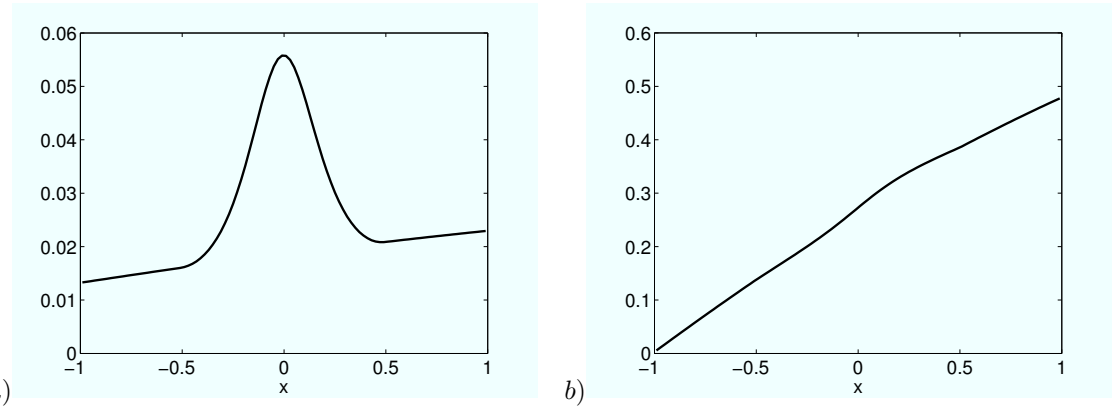

Figure 4.3: Flow solution along converging-diverging nozzle with exponential combustion source term: a) pressure, b) combustion progress variable.

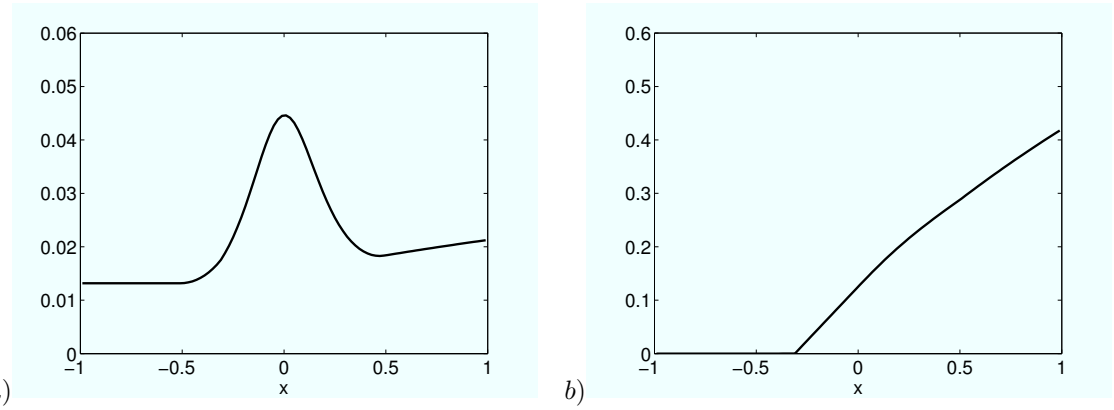

Figure 4.4: Flow solution along converging-diverging nozzle with Heaviside combustion source term: a) pressure, b) combustion progress variable.

In Figure 4.5, close agreement is seen between the adjoint variables produced by the discrete, continuous and hybrid methods, but not with those from the frozen continuous adjoint.

In Figure 4.6 the lack of smoothness of the source term makes it difficult to apply the full continuous adjoint approach, and so only the discrete, frozen continuous and hybrid adjoint variables can be evaluated. Again it is seen that whilst the discrete and hybrid match each other, the frozen-combustion continuous adjoint does not.

Finally, in Figure 4.7 the non-smooth objective function means that none of the two continuous adjoint approaches can be used, but the discrete and hybrid adjoints still give very good agreement with each other.

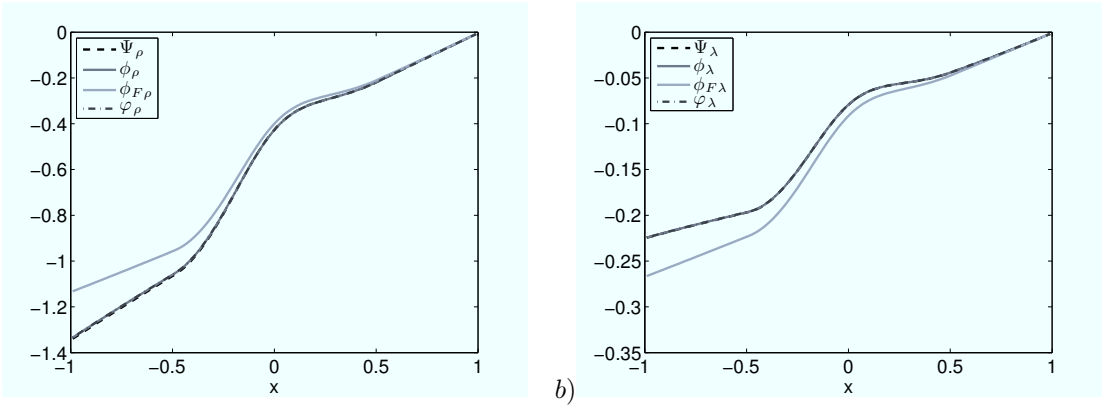

Figure 4.5: Adjoint variables (discrete (ψ), continuous (ϕ), frozen continuous (ϕ_F) and hybrid (φ)) for the exponential combustion source term and the integral of pressure functional: a) density-adjoint variable, b) combustion progress-adjoint variable.

Figure 4.8 shows the difference between the hybrid and discrete, and hybrid and full continuous variables for the density and combustion adjoint variables for the exponential source term and integral of pressure functional, and Figures 4.9 and 4.10 show the difference between the hybrid and discrete for the Heaviside source term and integral of pressure functional, and the exponential source term and the magnitude of a pressure difference functional, respectively. This shows, in general, closer agreement between the hybrid and continuous approaches where the continuous exists (Figure 4.8). It is also possible to see that this difference fluctuates most where the duct height changes most rapidly ($x = \pm 0.25$).

Sensitivity The sensitivity of the objective function, $\mathcal{J}$, to the inlet Mach number, M_i, neglecting any explicit dependence of the functional on M_i, can be written:

- Discrete approach:

$$\frac{d\mathcal{J}_D}{dM_i} = \psi_i^T \frac{\mathfrak{D}}{\mathfrak{D}M_i} \frac{\mathcal{R}_i}{\Delta x}. \tag{4.119}$$

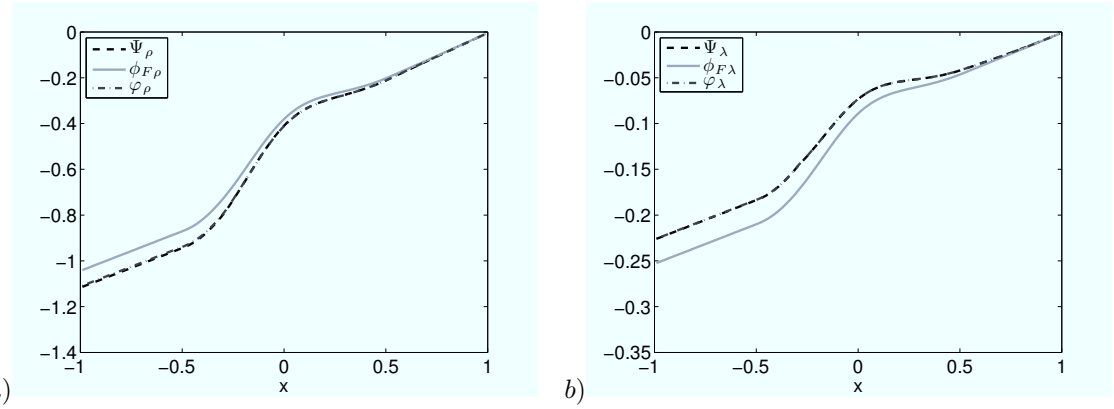

Figure 4.6: Adjoint variables (discrete (ψ), frozen continuous (ϕ_F) and hybrid (φ)) for the Heaviside combustion source term and the integral of pressure functional: a) density-adjoint variable, b) combustion progress-adjoint variable.

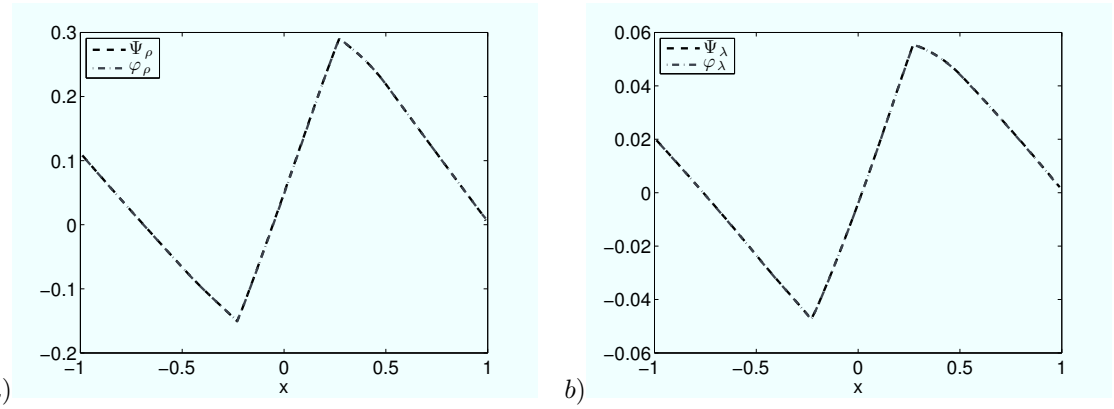

Figure 4.7: Adjoint variables (discrete (ψ) and hybrid (φ)) for the exponential combustion source term and the magnitude of a pressure difference functional: a) density-adjoint variable, b) combustion progress-adjoint variable.

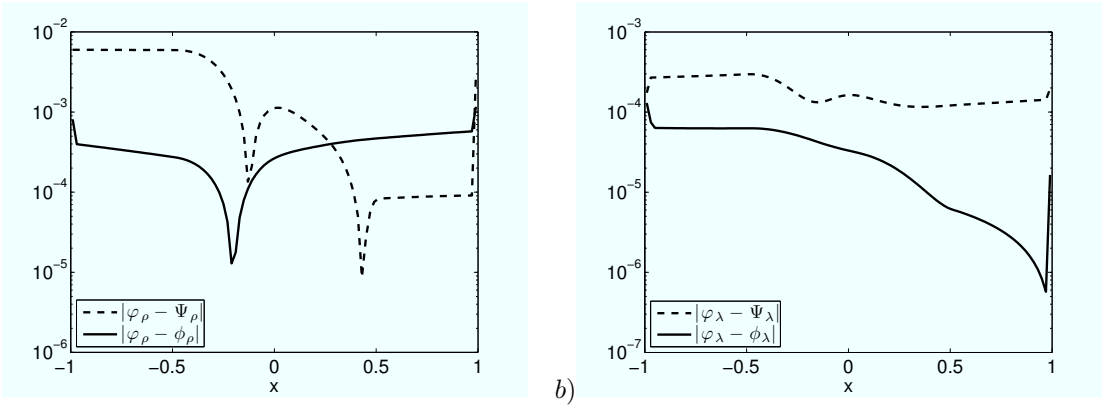

Figure 4.8: Size of the difference in adjoint variables (the hybrid and discrete ($|\varphi - \psi|$), and the hybrid and continuous ($|\varphi - \phi|$)) for the exponential combustion source term and integral of pressure functional: a) density-adjoint variable, b) combustion progress-adjoint variable.

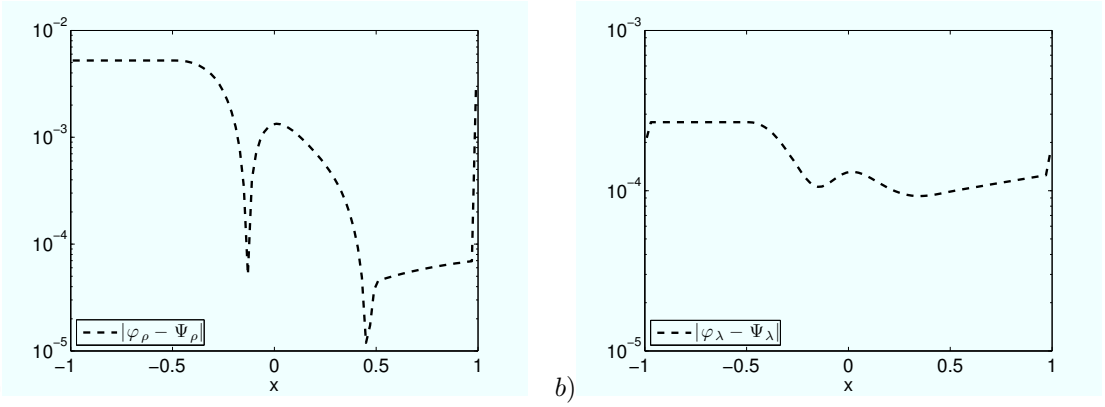

Figure 4.9: Size of the difference in adjoint variables (the hybrid and discrete ($|\varphi - \psi|$)) for the Heaviside combustion source term and the integral of pressure functional: a) density-adjoint variable, b) combustion progress-adjoint variable.

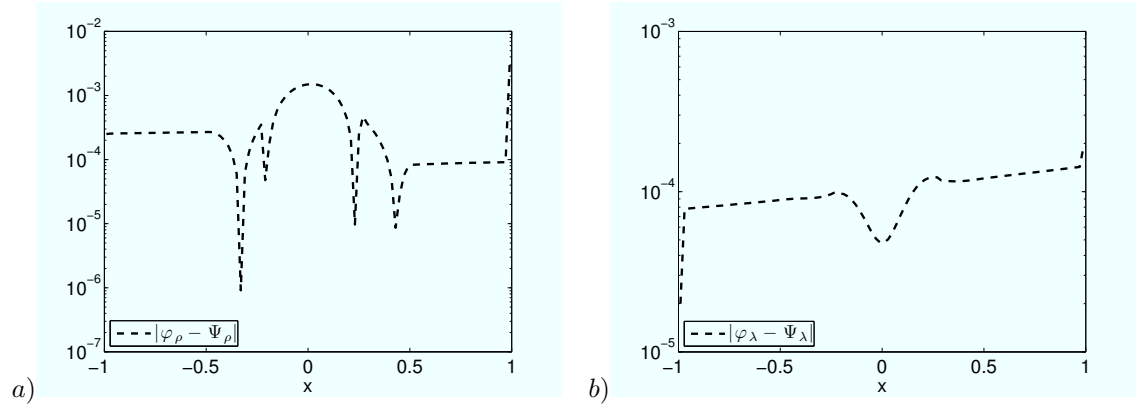

Figure 4.10: Size of difference in adjoint variables (the hybrid and discrete ($|\varphi - \psi|$)) for the exponential combustion source term and the magnitude of a pressure difference functional: a) density-adjoint variable, b) combustion progress-adjoint variable.

- Continuous approach:

$$\frac{d\mathcal{J}_C}{dM_i} = \phi_i^T \frac{\partial \mathcal{N}_i}{\partial M_i}. \tag{4.120}$$

- Hybrid approach:

$$\frac{d\mathcal{J}_H}{dM_i} = \varphi_{C_i}^T \frac{\partial \mathcal{N}_{E,i}}{\partial M_i} + \varphi_{D_i}^T \frac{\mathfrak{D}}{\mathfrak{D} M_i} \frac{\mathcal{R}_{\lambda,i}}{\Delta x}. \tag{4.121}$$

where we note that as $\Delta x \to 0$, and in the absence of shocks, we expect $\frac{\mathcal{R}}{\Delta x} \to \mathcal{N}$ and the equations to become consistent.

Figure 4.11 shows the variation of the sensitivity to the inlet Mach number over a range of Mach numbers calculated by finite differencing and the different adjoint methods for all four combinations of source and objective function considered here. It can be seen that for all the cases considered, there is good agreement between all of the methods except the frozen continuous adjoint, which is expected since, apart from the frozen adjoint, the adjoint variables shown previously in Figures 4.5, 4.6 and 4.7 demonstrate very good agreement over the domain, including at the inlet. It also should be noted that combinations b), c) and d) include non-smooth terms, and thus again confirm the applicability of the hybrid to cases that are problematic for the continuous adjoint.

Figures 4.11 c) and d), however, exhibit an interesting feature. The sensitivity of the magnitude of a pressure difference functional is seen to switch sign around $M_i = 4$, and to investigate this the form of the integrand along the duct was plotted at different Mach numbers and using the exponential source term and the the magnitude of a pressure difference functional. The result of this is shown in Figure 4.12. This picture shows that within this region of flow conditions the general shape of the magnitude of a pressure difference integrand becomes inverted as the pressure in the duct drops below $p^* = 0.03$, and this change in the integrand explains the shape of figures 4.11 c)

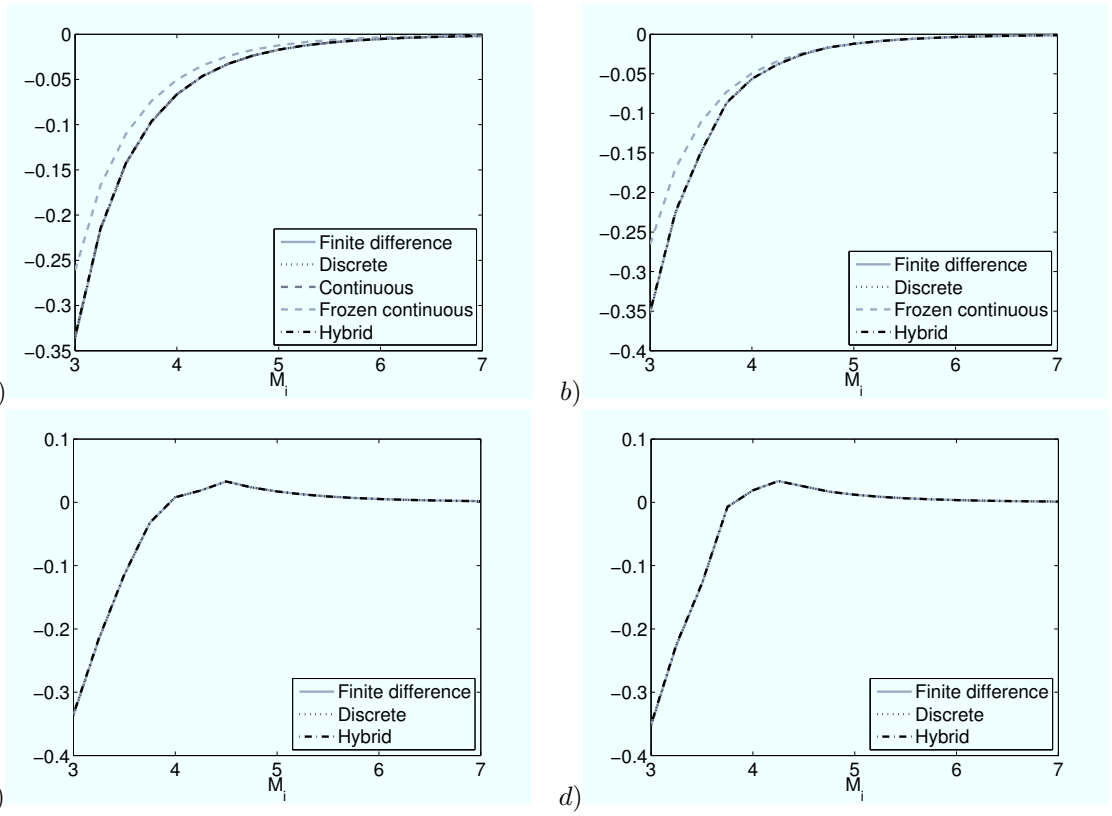

Figure 4.11: Sensitivity of functional to incoming Mach number at a range of Mach numbers: a) exponential source term and integral of pressure functional, b) Heaviside source term and integral of pressure functional, c) exponential source term and the magnitude of a pressure difference functional, d) Heaviside source term and the magnitude of a pressure difference functional.

and d).

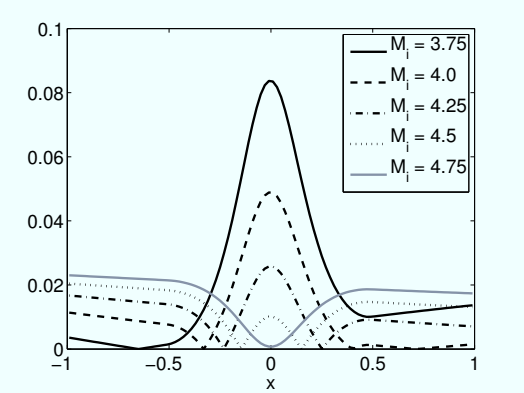

Figure 4.12: Shape of the integrand along the converging-diverging nozzle for the exponential source term and the magnitude of a pressure difference functional at a range of Mach numbers.

Grid convergence Using the formulae for the sensitivity of the objective function to the inlet Mach number, a grid refinement study of all four combinations of source and objective functions is shown in Figure 4.13. From Figures 4.13 a) and b) it can be seen that the finite difference and discrete adjoint compare very well, as do the hybrid and full continuous adjoint methods. However, the latter two methods appear to give a better approximation to the fine grid sensitivity on coarser meshes.

In Figures 4.13c) and d), which consider the magnitude of a pressure difference functional, the computed sensitivities do not reach a steady value in a monotonic fashion as the grid is refined though the three methods agree well with each other. To investigate this feature the integrands of the magnitude of a pressure difference objective function along the duct for the exponential source term were plotted for the coarsest and finest levels. The result of this is shown in Figure 4.14. The coarse integrand does not match the fine integrand well and with few points the sharp turning points where the integrand is zero are not well resolved. It is also inferred that these sharp turning points will cause problems for the simple trapezoidal quadrature used to evaluate the integral in the objective function.

4.2.6 Discussion

The above numerical experiments indicate that the hybrid adjoint approach can be used in this simple case to estimate the sensitivity of an objective function to different parameters, showing generally good agreement with finite differencing, discrete adjoints and continuous adjoints. It is also seen to better match the continuous adjoint result where available, but, perhaps most importantly can

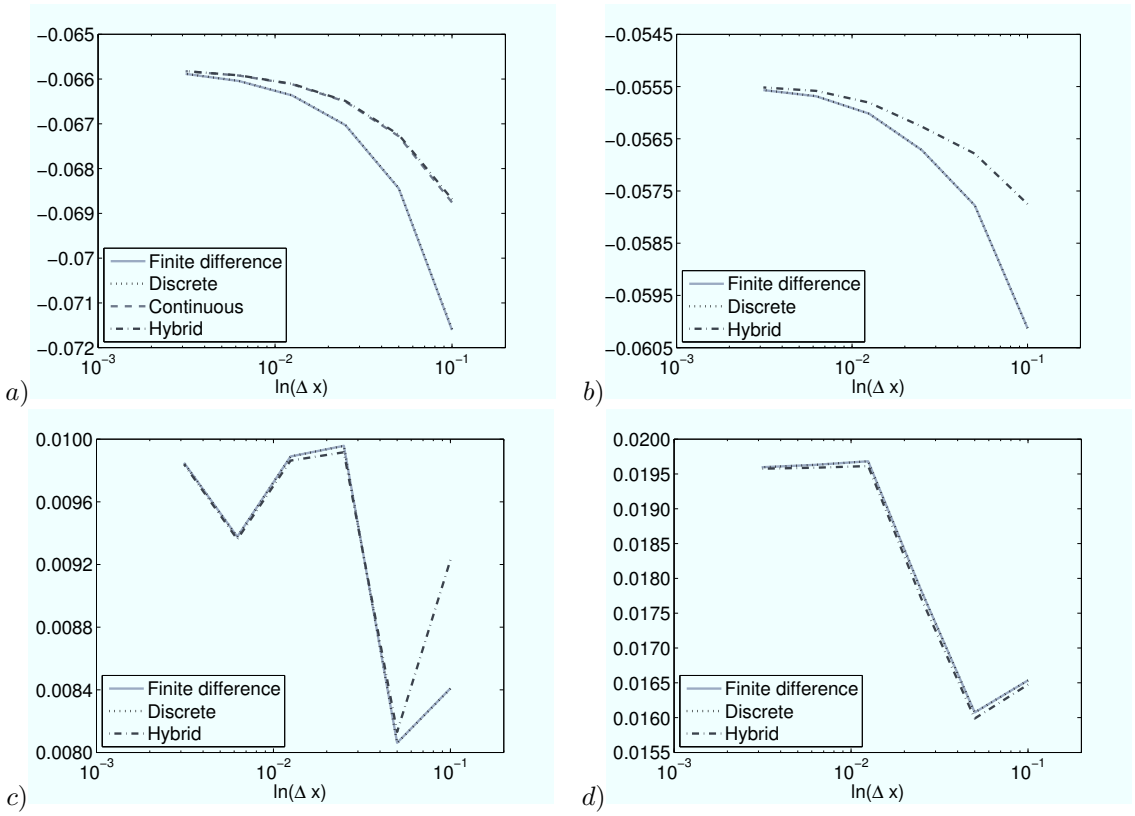

Figure 4.13: Sensitivity of functional to incoming Mach number at different grid refinement levels: a) exponential source term and integral of pressure functional, b) Heaviside source term and integral of pressure functional, c) exponential source term and v functional, d) Heaviside source term and the magnitude of a pressure difference functional.

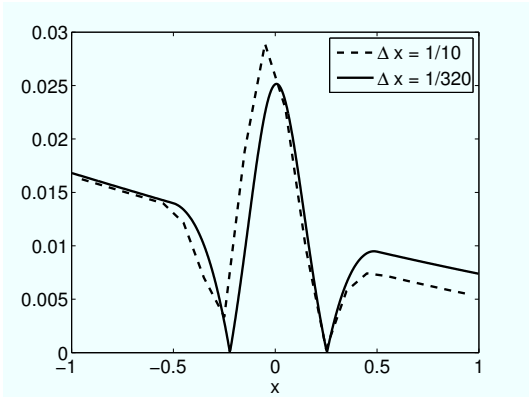

Figure 4.14: Shape of the integrand along the converging-diverging nozzle for the exponential source term and the magnitude of a pressure difference functional on coarse and fine grids.

be applied to problems where the development and application of the continuous method would be difficult. In terms of the ease of development, the initial hybrid derivation is of a similar level of complexity to that of the continuous adjoint, but once derived, can easily be applied to more complex problems with minimal mathematical development.

However, to better understand and investigate the hybrid adjoint approach presented in this thesis we will now apply it to the more complicated cases of two- and three-dimensional turbulent flows in the following chapter.

It should also be noted that the hybrid developed above retained a dependency of the form of the combustion model in the continuous part of the adjoint equations, present due to the model dependence in the pressure given by (4.38). When developing the turbulent hybrid adjoint in the following chapter, one of the aims will be to create a model-independent hybrid.

Chapter 5

Two- and three-dimensional flows

"Of all forty-two alternatives, running away is best."

— Will Rogers

HAVING applied adjoint theory to quasi-one-dimensional flows in the preceding chapter, we now extend the continuous and hybrid approaches to the more complex cases of two- and three-dimensional flows, starting with the Euler equations, the Navier-Stokes equations, and finally the Reynolds-Averaged Navier-Stokes (RANS) equations with a general turbulence model. One of the key goals in developing the hybrid adjoint for this last case is to create a formulation whose continuous part is independent of the form of the turbulence model used.

5.1 Euler flow

We first develop adjoint theory for two- and three-dimensional Euler flow, with the intention of reusing these concepts when developing the theory for laminar Navier-Stokes and Reynolds-Averaged Navier-Stokes flows. The key parts of this development will be outlined below, with the full detail provided in Appendices B and C.

5.1.1 Flow problem

5.1.1.1 Definition

We consider smooth Euler flow in the general domain Ω with the boundary Γ divided into a far-field, Γ_∞ and an Euler wall, S. This general definition can be used to represent a variety of geometries, including both the duct and the airfoil shown in Figure 5.1.

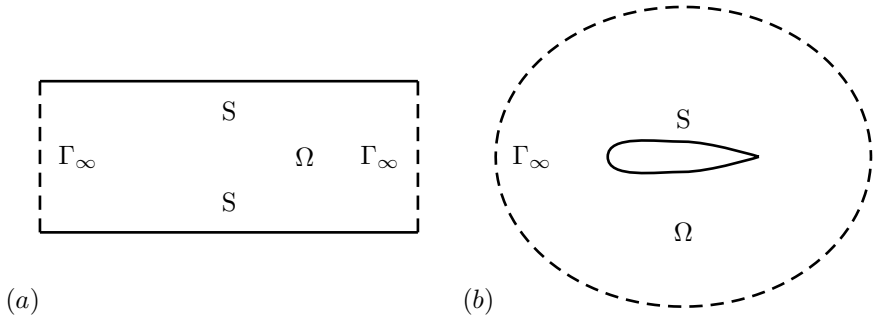

Figure 5.1: Two possible general flow domains: (a) duct, (b) airfoil.

The analytical governing equations for this are

$$\mathcal{N}(U,\alpha) = \partial_i F_i = 0, \quad \text{in } \Omega, \tag{5.1}$$

subject to the boundary conditions

$$\begin{aligned} u_i \hat{n}_i &= 0, && \text{on } S, \\ (W)_+ &= W_\infty, && \text{on } \Gamma_\infty, \end{aligned} \tag{5.2}$$

where the vectors of flow variables and fluxes are

$$U = \begin{pmatrix} \rho \\ \rho u_i \\ \rho E \end{pmatrix}, \quad F_i = \begin{pmatrix} \rho u_i \\ \rho u_i u_j + p\delta_{ij} \\ \rho u_i H \end{pmatrix}, \tag{5.3}$$

and the stagnation enthalpy and pressure are given by

$$H = E + \frac{p}{\rho}, \quad p = (\gamma - 1)(\rho E - \frac{\rho}{2} u_i u_i), \tag{5.4}$$

and also W is the vector of characteristics.

The objective function is defined as the sum of an integral over the domain and an integral over the bounding surface,

$$\mathcal{J} = \int_\Omega j_\Omega d\Omega + \int_\Gamma j_\Gamma d\Gamma, \tag{5.5}$$

noting that, through appropriate definition of the j_Ω and j_Γ, we may consider objective functions that are purely domain or surface integrals, and that are only over part of the relevant domain or surface.

5.1.1.2 Boundary conditions

At a boundary, the number of conditions required can again be determined by considering the characteristics of the problem. For N-dimensional flow there are $N + 2$ characteristic variables, one with the velocity normal to the boundary $u_i \hat{n}_i - c$, one with velocity $u_i \hat{n}_i + c$ and N with velocity $u_i \hat{n}_i$, where c is the speed of sound.

The Euler wall boundary condition given places the condition on the velocity vector such that the flow here is parallel to the wall surface. The consequence of this is that there can only be one flow characteristic entering or leaving the wall, i.e., with non-zero normal velocity, and thus only one boundary condition is needed on the flow equation.

At the far field, the normal velocity can instead be either subsonic or supersonic:

Flow velocity normal to far field is subsonic For incoming subsonic flow, $N + 1$ of the characteristics are incoming at the boundary, thus requiring $N + 1$ boundary conditions on the flow. For outgoing subsonic flow, one of the characteristics is incoming at the boundary, requiring one boundary condition.

Flow velocity normal to far field is supersonic For incoming supersonic flow, all $N+2$ of the characteristics are incoming at the boundary, thus requiring $N+2$ boundary conditions on the flow. For outgoing supersonic flow, none of the characteristics is incoming at the boundary, requiring no boundary conditions.

5.1.2 Continuous adjoint problem

5.1.2.1 Derivation

Starting from the continuous objective function, (5.5), we can enforce the governing equations $\mathcal{N}$ by introducing the Lagrangian

$$\mathcal{L} = \int_\Omega j_\Omega d\Omega + \int_\Gamma j_\Gamma d\Gamma - \int_\Omega \phi^T \mathcal{N} d\Omega, \tag{5.6}$$

where ϕ are the Lagrange multipliers (or continuous adjoint variables).

Taking the perturbation of this to a change in some parameter α, noting that to simplify the derivation of the adjoint equations we neglect shape perturbations (without affecting generality), we then get

$$\delta\mathcal{L} = \int_\Omega \delta j_\Omega d\Omega + \int_\Gamma \delta j_\Gamma d\Gamma - \int_\Omega \phi^T \delta\mathcal{N} d\Omega. \tag{5.7}$$

We can then linearize the integrands and perform integration by parts to give

$$\begin{aligned} \delta\mathcal{L} \quad = \quad & \int_\Omega \frac{\partial j_\Omega}{\partial \alpha}\delta\alpha d\Omega + \int_\Gamma \frac{\partial j_\Gamma}{\partial \alpha}\delta\alpha d\Gamma - \int_\Omega \phi^T \partial_i \left(\frac{\partial F_i}{\partial \alpha}\delta\alpha\right) d\Omega \\ & - \int_\Omega \left(L^*_\Omega(\phi) - \left(\frac{\partial j_\Omega}{\partial U}\right)^T\right)^T \delta U d\Omega - \int_\Gamma \left(L^*_\Gamma(\phi) - \left(\frac{\partial j_\Gamma}{\partial U}\right)^T\right)^T \delta U d\Gamma, \end{aligned} \tag{5.8}$$

where we define the adjoint linear operators

$$L^*_\Omega(\phi) = -\left(\frac{\partial F_i}{\partial U}\right)^T \partial_i \phi, \tag{5.9}$$

and

$$L^*_\Gamma(\phi) = \left(\frac{\partial F_i}{\partial U}\hat{n}_i\right)^T \phi. \tag{5.10}$$

This process is shown in complete detail in Appendix B.

We can then remove the dependence on the flow perturbation through the continuous adjoint equations,

$$L^*_\Omega(\phi) - \left(\frac{\partial j_\Omega}{\partial U}\right)^T = 0, \quad \text{in } \Omega, \tag{5.11}$$

and boundary conditions,

$$\int_\Gamma \left(L_\Gamma^*(\phi) - \left(\frac{\partial j_\Gamma}{\partial U} \right)^T \right)^T \delta U d\Gamma = 0, \tag{5.12}$$

giving the perturbation to the objective function as

$$\delta \mathcal{J}_C = \delta \mathcal{L} = \int_\Omega \frac{\partial j_\Omega}{\partial \alpha} \delta\alpha d\Omega + \int_\Gamma \frac{\partial j_\Gamma}{\partial \alpha} \delta\alpha d\Gamma - \int_\Omega \phi^T \partial_i \left(\frac{\partial F_i}{\partial \alpha} \delta\alpha \right) d\Omega. \tag{5.13}$$

5.1.2.2 Boundary conditions

For an Euler wall the adjoint boundary conditions reduce to

$$\frac{\partial j_\Gamma}{\partial U} - \phi_{\rho u_j}^T \frac{\partial p}{\partial U} \hat{n}_j = 0, \tag{5.14}$$

and at the far field they become

$$- \int_{\Gamma_\infty} \phi^T \frac{\partial F_i}{\partial U} \hat{n}_i \delta U d\Gamma = 0. \tag{5.15}$$

A detailed derivation of these conditions is shown in Appendix C.

5.1.3 Discussion

The previous section illustrated how the continuous adjoint approach is applied to two- and three-dimensional flows. It should be noted that the discrete adjoint formulae developed in Section 2.1.1 are general, and thus no additional work would have been needed to apply them to two- or three-dimensional flow, whilst the continuous adjoint equations had to be derived again for this situation. However, though we were considering only Euler flow above, the general continuous adjoint procedure and some of the results can be used in the following sections on viscous flows, especially with respect to handling the convective terms.

5.2 Laminar Navier-Stokes flow

We now consider two- and three-dimensional laminar Navier-Stokes flow, extending the theory developed above for Euler flow. This theory and derivation will then help when developing the adjoints for Reynolds-Averaged Navier-Stokes flow.

A typical simplification made in the derivation and solution of the continuous adjoint problem, particularly when considering turbulent flows, is to neglect perturbations of the viscosity, and thus neglect the sensitivity of the laminar viscosity. We therefore develop both the frozen-viscosity and full continuous adjoints below.

5.2.1 Flow problem

5.2.1.1 Definition

We consider smooth, laminar Navier-Stokes flow in the general domain shown previously in Figure 5.1.

The analytical governing equations for this are

$$\mathcal{N}(U, \partial_j U, \alpha) = \partial_i \left(F_i - \mu^{v1} F_i^{v1} - \mu^{v2} F_i^{v2} \right) = 0, \quad \text{in } \Omega, \tag{5.16}$$

subject to the boundary conditions

$$\begin{aligned} u_i &= 0, && \text{on } S, \\ \hat{n}_i \partial_i T &= 0, && \text{on } S, \\ (W)_+ &= W_\infty, && \text{on } \Gamma_\infty, \end{aligned} \tag{5.17}$$

where U and F_i have the same form as given previously for Euler flow, and the viscous flux vectors are

$$F_i^{v1} = \begin{pmatrix} 0 \\ \tau_{ij} \\ u_k \tau_{ik} \end{pmatrix}, \quad F_i^{v2} = \begin{pmatrix} 0 \\ 0 \\ C_p \partial_i T \end{pmatrix}, \tag{5.18}$$

also now we define the temperature and stress,

$$T = \frac{p}{R\rho}, \quad \tau_{ij} = (\partial_j u_i + \partial_i u_j) - \frac{2}{3} \delta_{ij} \partial_k u_k, \tag{5.19}$$

and

$$\mu^{v1} = \mu, \quad \mu^{v2} = \frac{\mu}{Pr}, \tag{5.20}$$

where Pr is the Prandtl number and the laminar viscosity, μ, is given by Sutherland's law,

$$\mu = \frac{\mu_1 T^{\frac{3}{2}}}{T + \mu_2}. \tag{5.21}$$

The objective function is again defined as the sum of an integral over the domain and an integral over the bounding surface as in (5.5).

5.2.1.2 Boundary conditions

The Navier-Stokes wall boundary condition given above requires that each component of the velocity vector at the wall is zero. The consequence of this is that there can only be one flow characteristic entering or leaving the wall, i.e., with non-zero normal velocity here, and thus only one boundary condition is needed on the flow equations.

At the far field, the characteristics, and thus the number of boundary conditions required, are the same as for Euler flow.

5.2.2 Frozen-viscosity continuous adjoint problem

5.2.2.1 Derivation

Starting from the same general continuous objective function as used for Euler flow, (5.5), we can again enforce the governing equations $\mathcal{N}$ through the Lagrangian, (5.6).

However, to derive the perturbation to this Lagrangian we note that the governing equations, (5.16), are now different. The process of expanding and manipulating these terms is shown in full in Appendix B, but here we simply state the result that the perturbation can be written as

$$\begin{aligned}\delta\mathcal{L} &= \int_\Omega \left(\frac{\partial j_\Omega}{\partial\alpha}\delta\alpha - \phi^T\partial_i\left(\left(\frac{\partial F_i}{\partial\alpha} - \mathcal{A}_1\right)\delta\alpha\right)\right)d\Omega + \int_\Gamma \frac{\partial j_\Gamma}{\partial\alpha}\delta\alpha d\Gamma \\ &\quad - \int_\Omega \left(L^*_\Omega(\phi) - \left(\frac{\partial j_\Omega}{\partial U}\right)^T\right)^T \delta U d\Omega \\ &\quad - \int_\Gamma \left(\left(L^*_\Gamma(\phi) - \left(\frac{\partial j_\Gamma}{\partial U}\right)^T\right)^T \delta U - \phi^T\mathcal{A}_3\delta(\partial_j U)\hat{n}_i\right)d\Gamma,\end{aligned} \tag{5.22}$$

where the adjoint linear operators are

$$L^*_\Omega(\phi) = -\left(\frac{\partial F_i}{\partial U} - \mathcal{A}_2\right)^T \partial_i\phi - \partial_j\left(\mathcal{A}_3^T\partial_i\phi\right), \tag{5.23}$$

and

$$L^*_\Gamma(\phi) = \left(\left(\frac{\partial F_i}{\partial U} - \mathcal{A}_2\right)\hat{n}_i\right)^T \phi + \left(\mathcal{A}_3\hat{n}_j\right)^T\partial_i\phi, \tag{5.24}$$

and we have introduced the substitutions

$$\mathcal{A}_1 = \mu\left(\frac{\partial F_i^{v1}}{\partial\alpha} + \left(\frac{1}{Pr}\right)\frac{\partial F_i^{v2}}{\partial\alpha}\right), \tag{5.25}$$

$$\mathcal{A}_2 = \mu\left(\frac{\partial F_i^{v1}}{\partial U} + \left(\frac{1}{Pr}\right)\frac{\partial F_i^{v2}}{\partial U}\right), \tag{5.26}$$

and

$$\mathcal{A}_3 = \mu\left(\frac{\partial F_i^{v1}}{\partial(\partial_j U)} + \left(\frac{1}{Pr}\right)\frac{\partial F_i^{v2}}{\partial(\partial_j U)}\right). \tag{5.27}$$

We can then remove the dependence on the flow perturbation through the continuous adjoint

equations, (5.11), and boundary conditions,

$$\int_\Gamma \left(\left(L^*_\Gamma(\phi) - \left(\frac{\partial j_\Gamma}{\partial U} \right)^T \right)^T \delta U - \phi^T \mathcal{A}_3 \delta(\partial_j U) \hat{n}_i \right) d\Gamma = 0, \tag{5.28}$$

giving the perturbation to the objective function as

$$\delta \mathcal{J}_C = \delta \mathcal{L} = \int_\Omega \left(\frac{\partial j_\Omega}{\partial \alpha} \delta\alpha - \phi^T \partial_i \left(\left(\frac{\partial F_i}{\partial \alpha} - \mathcal{A}_1 \right) \delta\alpha \right) \right) d\Omega + \int_\Gamma \frac{\partial j_\Gamma}{\partial \alpha} \delta\alpha d\Gamma. \tag{5.29}$$

5.2.2.2 Boundary conditions

For a viscous wall the adjoint boundary conditions reduce to

$$\frac{\partial j_\Gamma}{\partial U} \delta U - \phi^T_{\rho u_j} \hat{n}_i \delta p + \phi^T_{\rho u_j} \mu \hat{n}_i \delta \tau_{ij} + \mu \left(\partial_i \phi_{\rho E} \right)^T \frac{C_p}{Pr} \hat{n}_i \delta T = 0, \tag{5.30}$$

which implies that we must consider objective functions for which we can write the perturbation in the form

$$\frac{\partial j_\Gamma}{\partial U} \delta U = \frac{\partial j_\Gamma}{\partial p} \delta p + \frac{\partial j_\Gamma}{\partial \tau_{ij}} \delta \tau_{ij} + \frac{\partial j_\Gamma}{\partial T} \delta T, \tag{5.31}$$

allowing the δp, $\delta \tau_{ij}$ and δT dependencies to be removed.

At the far field the boundary conditions are the same as for Euler flow, (5.15), neglecting gradients in the flow variables and viscous contributions at this boundary. The derivation of these conditions is shown in detail in Appendix C.

5.2.3 Full continuous adjoint problem

5.2.3.1 Derivation

The Lagrangian is now modified slightly to include dependence on the sensitivity of the viscosity, giving the perturbation

$$\begin{aligned} \delta \mathcal{L} \quad = \quad & \int_\Omega \left(\frac{\partial j_\Omega}{\partial \alpha} \delta\alpha - \phi^T \partial_i \left(\left(\frac{\partial F_i}{\partial \alpha} - \mathcal{A}_1 - \mathcal{A}_4 \right) \delta\alpha \right) \right) d\Omega + \int_\Gamma \frac{\partial j_\Gamma}{\partial \alpha} \delta\alpha d\Gamma \\ & - \int_\Omega \left(L^*_\Omega(\phi) - \left(\frac{\partial j_\Omega}{\partial U} \right)^T \right)^T \delta U d\Omega \\ & - \int_\Gamma \left(\left(L^*_\Gamma(\phi) - \left(\frac{\partial j_\Gamma}{\partial U} \right)^T \right)^T \delta U - \phi^T \mathcal{A}_3 \delta(\partial_j U) \hat{n}_i \right) d\Gamma, \end{aligned} \tag{5.32}$$

where

$$L^*_\Omega(\phi) = - \left(\frac{\partial F_i}{\partial U} - \mathcal{A}_2 - \mathcal{A}_5 \right)^T \partial_i \phi - \partial_j \left(\mathcal{A}_3^T \partial_i \phi \right), \tag{5.33}$$

and

$$L_\Gamma^*(\phi) = \left(\left(\frac{\partial F_i}{\partial U} - \mathcal{A}_2 - \mathcal{A}_5 \right) \hat{n}_i \right)^T \phi + \left(\mathcal{A}_3 \hat{n}_j \right)^T \partial_i \phi, \tag{5.34}$$

and we have introduced the additional substitutions

$$\mathcal{A}_4 = \left(F_i^{v1} + \left(\frac{1}{Pr} \right) F_i^{v2} \right) \frac{\partial \mu}{\partial \alpha}, \tag{5.35}$$

$$\mathcal{A}_5 = \left(F_i^{v1} + \left(\frac{1}{Pr} \right) F_i^{v2} \right) \frac{\partial \mu}{\partial U}. \tag{5.36}$$

We can then remove the dependence on the flow perturbation by again using the continuous adjoint equations, (5.11), and boundary conditions, (5.28), giving the perturbation to the objective function as

$$\delta \mathcal{J}_C = \delta \mathcal{L} = \int_\Omega \left(\frac{\partial j_\Omega}{\partial \alpha} \delta \alpha - \phi^T \partial_i \left(\left(\frac{\partial F_i}{\partial \alpha} - \mathcal{A}_1 - \mathcal{A}_4 \right) \delta \alpha \right) \right) d\Omega + \int_\Gamma \frac{\partial j_\Gamma}{\partial \alpha} \delta \alpha d\Gamma. \tag{5.37}$$

5.2.3.2 Boundary conditions

The adjoint boundary conditions for a viscous wall now include an additional term for the viscosity sensitivity,

$$\frac{\partial j_\Gamma}{\partial U} \delta U - \phi_{\rho u_j}^T \hat{n}_i \delta p + \phi_{\rho u_j}^T \mu \hat{n}_i \delta \tau_{ij} + \left(\phi_{\rho u_j}^T \tau_{ij} \frac{\partial \mu}{\partial T} + \mu \left(\partial_i \phi_{\rho E} \right) \frac{C_p}{Pr} \right) \hat{n}_i \delta T = 0, \tag{5.38}$$

and thus we must still consider objective functions of the same form as (5.31).

At the far field the boundary conditions are again the same as for Euler flow, (5.15), neglecting gradients in the flow variables and viscous contributions at this boundary.

The derivation of these conditions is shown in detail in Appendix C.

5.2.4 Discussion

The theory introduced above shows how the continuous adjoint approach can be extended to viscous flows, noting that some of the development from the Euler treatment can be reused. It also illustrates the difference between the frozen-viscosity and full continuous adjoint equations. The assumption of frozen-viscosity is a widely used simplification applied when dealing with turbulent flows, and will be used in the following section on Reynolds-Averaged Navier-Stokes flow.

5.3 Reynolds-Averaged Navier-Stokes flow

In the following section we extend the two- and three-dimensional adjoint theory developed above for Euler and laminar Navier-Stokes flows to a fully turbulent Reynolds-Averaged Navier-Stokes

case, where we add an unspecified turbulence model to the mean-flow governing equations. Though we develop a general hybrid approach for any turbulence model, in order to produce results and experiment with the adjoint methods, we will consider the Spalart-Allmaras one-equation turbulence model[8].

We also will follow the assumption introduced in the previous section, where the continuous adjoint can be solved through a frozen viscosity assumption. Use of this assumption makes the purely continuous formulation independent of the turbulence model form. However, the hybrid does not need this restriction

5.3.1 Flow problem

5.3.1.1 Definition

We consider smooth, turbulent Reynolds-Averaged Navier-Stokes flow with an unspecified turbulence model in the general domain shown previously in Figure 5.1.

The mean-flow analytical governing equations for this, which we now denote $\mathcal{N}_L$, are almost the same as that for laminar flow, given by (5.16), subject to the boundary conditions (5.17), but with the modification that we now have additional turbulence model flow variables, thus the vector of conservative variables becomes

$$U = \begin{pmatrix} U_L \\ U_T \end{pmatrix}, \tag{5.39}$$

where the laminar flow variables, U_L, are given by (5.3), and the form and number of turbulence model flow variables, U_T, will depend on the exact turbulence model used.

We also must include an eddy viscosity, μ_T, such that

$$\mu^{v1} = \mu + \mu_T, \quad \mu^{v2} = \frac{\mu}{Pr} + \frac{\mu_T}{Pr_T}, \tag{5.40}$$

where Pr_T is now the turbulent Prandtl number.

We make the simplifying assumption that there is no direct dependence of the sensitivity of the mean-flow terms on the sensitivity of the turbulence model variables except through the eddy viscosity, μ_T, and assume that μ_T is a general function of U_L, U_T and possibly their gradients, i.e.,

$$\mu_T = f(U, \partial_m U). \tag{5.41}$$

The exact form of μ_T will depend on the specific turbulence model being used, and thus it is possible to see that the form of the mean-flow governing equations (5.16) now depends on the turbulence model. To remove this model dependence from the mean-flow adjoint equations in the

general hybrid approach, we will write a dummy governing equation for the eddy viscosity,

$$\mathcal{N}_{\mu_T} = \mu_T - f(U, \partial_m U) = 0, \quad \text{in } \Omega. \tag{5.42}$$

The variables U_T can be given by a general turbulence model, with the governing equations

$$\mathcal{N}_T = \partial_i \left(F_T\right) - S_T = 0, \quad \text{in } \Omega, \tag{5.43}$$

subject to boundary conditions on S and Γ_∞.

We again define the objective function as the sum of an integral over the domain and an integral over the bounding surface as in (5.5).

5.3.1.2 Boundary conditions

Flow boundary conditions The mean-flow boundary conditions are the same as for laminar flow, while the turbulence model boundary conditions will depend on the exact model being used.

5.3.1.3 Numerical implementation

The numerical solution method for the mean-flow and turbulence equations was implemented in the open-source code SU^2[51]. For the mean flow, the convective terms were discretized using the Jameson-Schmidt-Turkel (JST) central-differencing scheme and the viscous terms were discretized by averaging the gradients and including a correction based on the directional derivative.

Within each major iteration of the flow solver, an implicit backward Euler scheme was used for the pseudo-time integration of the mean-flow step and subsequently, the turbulence model step.

5.3.2 Spalart-Allmaras turbulence model problem

5.3.2.1 Definition

The one-equation Spalart-Allmaras turbulence model[8], has the governing equation

$$\mathcal{N}_T = \partial_i T_i^{cv} - T^s = 0, \quad \text{in } \Omega, \tag{5.44}$$

subject to the boundary conditions

$$\begin{aligned} \hat{\nu} &= 0, && \text{on } S, \\ \hat{\nu}_\infty &= \sigma_\infty \nu_\infty, && \text{on } \Gamma_\infty, \end{aligned} \tag{5.45}$$

where the convective flux is given by

$$T_i^{cv} = -\frac{\nu + \hat{\nu}}{\sigma} \partial_i \hat{\nu} + u_i \hat{\nu}, \tag{5.46}$$

and the source term is

$$T^s = c_{b1}\hat{S}\hat{\nu} - c_{w1}f_w\left(\frac{\hat{\nu}}{d_s}\right)^2 + \frac{c_{b2}}{\sigma}\left(\partial_i\hat{\nu}\right)\left(\partial_i\hat{\nu}\right). \tag{5.47}$$

We identify the turbulence flow variable for this model as

$$U_T = \hat{\nu}, \tag{5.48}$$

and note that the eddy viscosity is given by

$$\mu_T = \rho\hat{\nu}f_{v1}. \tag{5.49}$$

In the above formula we must define the following terms

$$\begin{aligned}
&f_{v1} = \frac{\chi^3}{\chi^3 + c_{v1}^3}, \quad \chi = \frac{\hat{\nu}}{\nu}, \quad \nu = \frac{\mu}{\rho},\\
&\hat{S} = \sqrt{\omega_i\omega_i} + \frac{\hat{\nu}}{\kappa^2 d_s^2}f_{v2}, \quad \omega_k = \epsilon_{ijk}\partial_i u_j,\\
&f_{v2} = 1 - \frac{\chi}{1+\chi f_{v1}}, \qquad f_w = g\left(\frac{1+c_{w3}^6}{g^6+c_{w3}^6}\right)^{\frac{1}{6}},\\
&g = r + c_{w2}(r^6 - r), \qquad r = \frac{\hat{\nu}}{\hat{S}\kappa^2 d_s^2},
\end{aligned} \tag{5.50}$$

where the model constants are

$$\begin{aligned}
&\sigma = \frac{2}{3}, && c_{b1} = 0.1355,\\
&c_{b2} = 0.622, && \kappa = 0.41,\\
&c_{w1} = \frac{c_{b1}}{\kappa^2} + \frac{1+c_{b2}}{\sigma}, && c_{w2} = 0.3,\\
&c_{w3} = 2, && c_{v1} = 7.1.
\end{aligned} \tag{5.51}$$

5.3.2.2 Numerical implementation

As noted above, the open-source code SU^2[51] was used for the numerical solution of the mean-flow and turbulence equations. For the Spalart-Allmaras one-equation model, the convective terms were discretized using first order upwinding, the viscous terms were handled by averaging the gradients and the source terms were treated in a piece-wise manner.

It is to be noted that the coupling of the turbulence model into the mean flow is only through the eddy viscosity, while the turbulence model requires density, velocity and laminar viscosity information from the mean flow.

5.3.3 Frozen-viscosity continuous adjoint problem

5.3.3.1 Derivation

With the laminar and turbulent viscosity both frozen, we effectively have the same Lagrangian given for Euler or laminar Navier-Stokes flow, given by equation (5.6), noting that we do not need to enforce either the eddy viscosity or turbulence model governing equations, or consider perturbations to the eddy viscosity or turbulence model variables. After linearization and mathematical manipulation we can write

$$\begin{aligned}\delta\mathcal{L} &= \int_\Omega \left(\frac{\partial j_\Omega}{\partial\alpha}\delta\alpha - \phi_L^T\partial_i\left(\left(\frac{\partial F_i}{\partial\alpha} - \mathcal{A}_1 - \mathcal{B}_1\right)\delta\alpha\right)\right)d\Omega + \int_\Gamma \frac{\partial j_\Gamma}{\partial\alpha}\delta\alpha d\Gamma \\ &\quad - \int_\Omega \left(L_\Omega^*(\phi) - \left(\frac{\partial j_\Omega}{\partial U_L}\right)^T\right)^T \delta U_L d\Omega \\ &\quad - \int_\Gamma \left(\left(L_\Gamma^*(\phi) - \left(\frac{\partial j_\Gamma}{\partial U_L}\right)^T\right)^T \delta U_L - \phi^T\left(\mathcal{A}_3 + \mathcal{B}_3\right)\delta(\partial_j U_L)\hat{n}_i\right)d\Gamma,\end{aligned} \tag{5.52}$$

where

$$L_\Omega^*(\phi) = -\left(\frac{\partial F_i}{\partial U_L} - \mathcal{A}_2 - \mathcal{B}_2\right)^T\partial_i\phi - \partial_j\left(\left(\mathcal{A}_3 + \mathcal{B}_3\right)^T\partial_i\phi\right), \tag{5.53}$$

and

$$L_\Gamma^*(\phi) = \left(\left(\frac{\partial F_i}{\partial U_L} - \mathcal{A}_2 - \mathcal{B}_2\right)\hat{n}_i\right)^T\phi + \left(\left(\mathcal{A}_3 + \mathcal{B}_3\right)\hat{n}_j\right)^T\partial_i\phi, \tag{5.54}$$

where we introduce the substitutions

$$\mathcal{B}_1 = \mu_T\left(\frac{\partial F_i^{v1}}{\partial\alpha} + \left(\frac{1}{Pr_T}\right)\frac{\partial F_i^{v2}}{\partial\alpha}\right), \tag{5.55}$$

$$\mathcal{B}_2 = \mu_T\left(\frac{\partial F_i^{v1}}{\partial U_L} + \left(\frac{1}{Pr_T}\right)\frac{\partial F_i^{v2}}{\partial U_L}\right), \tag{5.56}$$

and

$$\mathcal{B}_3 = \mu_T\left(\frac{\partial F_i^{v1}}{\partial(\partial_j U_L)} + \left(\frac{1}{Pr_T}\right)\frac{\partial F_i^{v2}}{\partial(\partial_j U_L)}\right). \tag{5.57}$$

We can then remove the dependence on the flow perturbation through the continuous adjoint equations, (5.11), and boundary conditions,

$$\int_\Gamma \left(\left(L_\Gamma^*(\phi) - \left(\frac{\partial j_\Gamma}{\partial U_L}\right)^T\right)^T \delta U_L - \phi^T\left(\mathcal{A}_3 + \mathcal{B}_3\right)\delta(\partial_j U_L)\hat{n}_i\right)d\Gamma = 0, \tag{5.58}$$

giving the perturbation to the objective function as

$$\delta\mathcal{J}_C = \delta\mathcal{L} = \int_\Omega \left(\frac{\partial j_\Omega}{\partial \alpha}\delta\alpha - \phi_L^T \partial_i \left(\left(\frac{\partial F_i}{\partial \alpha} - \mathcal{A}_1 - \mathcal{B}_1 \right) \delta\alpha \right) \right) d\Omega + \int_\Gamma \frac{\partial j_\Gamma}{\partial \alpha}\delta\alpha d\Gamma. \tag{5.59}$$

Note that the above results can in fact be found from inspection by considering Laminar Navier-Stokes flow with the modification that $\mathcal{A}_i \Rightarrow (\mathcal{A}_i + \mathcal{B}_i)$, or alternatively by considering $\mu \Rightarrow (\mu + \mu_T)$.

5.3.3.2 Boundary conditions

The boundary conditions for the frozen-viscosity continuous adjoint equation are given by (5.58), however, we must manipulate this so as to remove the dependence on the flow perturbation.

Since the eddy viscosity at a viscous wall must be zero, the boundary conditions for the frozen-viscosity RANS adjoint will be identical to those for the frozen-viscosity. laminar Navier-Stokes flow, given by equation (5.30).

At the far field, if the flow gradients and viscosity contributions are neglected, we again have the condition (5.15).

5.3.3.3 Numerical implementation

The SU^2 code was also used to solve the frozen continuous adjoint problem, again using the same approach as Bueno-Orovio[6], and as discussed above for laminar Navier-Stokes flow. Given the frozen viscosity assumption, there are no additional coupling terms from the turbulence model, and the adjoint system being solved is effectively the same, though with different values of the viscosities, as the laminar Navier-Stokes problem.

5.3.4 Hybrid adjoint problem

5.3.4.1 Derivation

Starting from a hybrid version of the general continuous objective function used for Euler flow, (5.5), that can be either continuous or discrete, we now enforce the mean-flow governing equations $\mathcal{N}_L$ and the eddy viscosity and turbulence model numerical residuals $\mathcal{R}_{\mu_T}$ and $\mathcal{R}_T$ by introducing the modified Lagrangian

$$\begin{aligned} \mathcal{L} \;=\; & \beta \left(\int_\Omega j d\Omega + \int_\Gamma j_\Gamma d\Gamma \right) + (1-\beta)\, \frac{\mathfrak{D}\mathcal{J}_D}{\mathfrak{D}\alpha}\Delta\alpha \\ & - \int_\Omega \varphi_C^T \mathcal{N}_L d\Omega - \sum_{p=1}^{N} \varphi_{\mu_{T_p}}^T \mathcal{N}_{\mu_{T_p}} \Omega_p + \sum_{p=1}^{N} \varphi_{D_p}^T \mathcal{R}_{T_p}, \end{aligned} \tag{5.60}$$

where $\varphi = \{\varphi_C, \varphi_{\mu_T}, \varphi_D\}$ are the Lagrange multipliers (or hybrid adjoint variables).

Taking the perturbation of $\mathcal{L}$ to a change in some parameter α we then get, after linearization and appropriate manipulation,

$$\begin{aligned}
\{\delta,\Delta\}\mathcal{L} \quad = \quad & \int_\Omega \left(\beta \frac{\partial j_\Omega}{\partial \alpha}\delta\alpha - \varphi_C^T \partial_i \left(\left(\frac{\partial F_i}{\partial \alpha} - \mathcal{A}_1 - \mathcal{A}_4 - \mathcal{B}_1 \right) \delta\alpha \right) \right) d\Omega \\
& + \int_\Gamma \beta \frac{\partial j_\Gamma}{\partial \alpha}\delta\alpha d\Gamma + (1-\beta)\frac{\mathfrak{D}\mathcal{J}_D}{\mathfrak{D}\alpha}\Delta\alpha \\
& + \sum_{p=1}^{N} \varphi_{\mu_{T_p}}^T \frac{\mathfrak{D}f_p}{\mathfrak{D}\alpha}\Delta\alpha\Omega_p + \sum_{p=1}^{N} \varphi_{D_p}^T \frac{\mathfrak{D}\mathcal{R}_{T_p}}{\mathfrak{D}\alpha}\Delta\alpha \\
& - \int_\Omega \left(L_\Omega^*(\varphi_C) - \beta \left(\frac{\partial j_\Omega}{\partial U} \right)^T \right)^T \delta U d\Omega \\
& - \int_\Gamma \left(\left(L_\Gamma^*(\varphi_C) - \beta \left(\frac{\partial j_\Gamma}{\partial U} \right)^T \right)^T \delta U - \varphi_C^T \left(\mathcal{A}_3 + \mathcal{B}_3 \right) \delta(\partial_j U)\hat{n}_i \right) d\Gamma \\
& - \int_\Omega \left(\partial_i \varphi_C^T \right) \mathcal{C}_1 \delta\mu_T d\Omega + \int_\Gamma \varphi_C^T \mathcal{C}_1 \hat{n}_i \delta\mu_T d\Gamma \\
& + (1-\beta)\sum_{p=1}^{N} \frac{\mathfrak{D}\mathcal{J}_D}{\mathfrak{D}U_p}\Delta U_p + \sum_{p=1}^{N}\sum_{q=1}^{N} \varphi_{D_q}^T \frac{\mathfrak{D}\mathcal{R}_{T_q}}{\mathfrak{D}U_p}\Delta U_p \\
& + \sum_{p=1}^{N}\sum_{q=1}^{N} \varphi_{\mu_{T_q}}^T \frac{\mathfrak{D}f_q}{\mathfrak{D}U_p}\Delta U_p\Omega_q - \sum_{p=1}^{N} \varphi_{\mu_{T_p}}^T \Delta\mu_{T_p}\Omega_p,
\end{aligned} \tag{5.61}$$

where the adjoint linear operators are

$$L_\Omega^*(\varphi_C) = -\left(\frac{\partial F_i}{\partial U} - \mathcal{A}_2 - \mathcal{A}_5 - \mathcal{B}_2 \right)^T \partial_i\varphi_C - \partial_j \left(\left(\mathcal{A}_3 + \mathcal{B}_3 \right)^T \partial_i\varphi_C \right), \tag{5.62}$$

and

$$L_\Gamma^*(\varphi_C) = \left(\left(\frac{\partial F_i}{\partial U} - \mathcal{A}_2 - \mathcal{A}_5 - \mathcal{B}_2 \right)\hat{n}_i \right)^T \varphi_C + \left(\left(\mathcal{A}_3 + \mathcal{B}_3 \right)\hat{n}_j \right)^T \partial_i\varphi_C, \tag{5.63}$$

where we have introduced the additional substitution,

$$\mathcal{C}_1 = \left(F_i^{v1} + \left(\frac{1}{Pr_T} \right) F_i^{v2} \right). \tag{5.64}$$

We can then remove the dependence on the flow perturbation through the combined hybrid

adjoint equations and boundary conditions,

$$\begin{aligned}
&\int_\Omega \left(L_\Omega^*(\varphi_C) - \beta \left(\frac{\partial j_\Omega}{\partial U} \right)^T \right)^T \delta U d\Omega \\
+ \int_\Gamma \Bigg(&\left(\left(L_\Gamma^*(\varphi_C) - \beta \left(\frac{\partial j_\Gamma}{\partial U} \right)^T \right)^T \delta U - \varphi_C^T \left(\mathcal{A}_3 + \mathcal{B}_3 \right) \delta(\partial_j U) \hat{n}_i \right) d\Gamma \\
&- (1-\beta) \sum_{p=1}^N \frac{\mathfrak{D}\mathcal{J}_D}{\mathfrak{D}U_p} \Delta U_p - \sum_{p=1}^N \sum_{q=1}^N \varphi_{D_q}^T \frac{\mathfrak{D}\mathcal{R}_{T_q}}{\mathfrak{D}U_p} \Delta U_p \\
&- \sum_{p=1}^N \sum_{q=1}^N \varphi_{\mu_{T_q}}^T \frac{\mathfrak{D}f_q}{\mathfrak{D}U_p} \Delta U_p \Omega_q \quad = \quad 0,
\end{aligned} \tag{5.65}$$

and

$$\int_\Omega \left(\partial_i \varphi_C^T \right) \mathcal{C}_1 \delta \mu_T d\Omega + \sum_{p=1}^N \varphi_{\mu_{T_p}}^T \Delta \mu_{T_p} \Omega_p - \int_\Gamma \varphi_C^T \mathcal{C}_1 \hat{n}_i \delta \mu_T d\Gamma = 0, \tag{5.66}$$

giving the perturbation to the objective function as

$$\begin{aligned}
\{\delta, \Delta\}\mathcal{L} \quad = \quad & \int_\Omega \left(\beta \frac{\partial j_\Omega}{\partial \alpha} \delta\alpha - \varphi_C^T \partial_i \left(\left(\frac{\partial F_i}{\partial \alpha} - \mathcal{A}_1 - \mathcal{A}_4 - \mathcal{B}_1 \right) \delta\alpha \right) \right) d\Omega \\
& + \int_\Gamma \beta \frac{\partial j_\Gamma}{\partial \alpha} \delta\alpha d\Gamma + (1-\beta) \frac{\mathfrak{D}\mathcal{J}_D}{\mathfrak{D}\alpha} \Delta\alpha \\
& + \sum_{p=1}^N \varphi_{\mu_{T_p}}^T \frac{\mathfrak{D}f_p}{\mathfrak{D}\alpha} \Delta\alpha \Omega_p + \sum_{p=1}^N \varphi_{D_p}^T \frac{\mathfrak{D}\mathcal{R}_{T_p}}{\mathfrak{D}\alpha} \Delta\alpha.
\end{aligned} \tag{5.67}$$

As previously in quasi-one-dimensional flow, we now separate the combined equations and boundary conditions. The hybrid equations are then

$$\begin{aligned}
&\int_\Omega \left(L_\Omega^*(\varphi_C) - \beta \left(\frac{\partial j_\Omega}{\partial U} \right)^T \right)^T \delta U d\Omega \\
&- (1-\beta) \sum_{p=1}^N \sum_{q=1}^N \frac{\mathfrak{D}j_q}{\mathfrak{D}U_p} \Omega_q \Delta U_p - \sum_{p=1}^N \sum_{q=1}^N \varphi_{D_q}^T \frac{\mathfrak{D}\mathcal{R}_{T_q}^{(*)}}{\mathfrak{D}U_p} \Delta U_p \\
&- \sum_{p=1}^N \sum_{q=1}^N \varphi_{\mu_{T_q}}^T \frac{\mathfrak{D}f_q}{\mathfrak{D}U_p} \Delta U_p \Omega_q \quad = \quad 0,
\end{aligned} \tag{5.68}$$

and

$$\int_\Omega \left(\partial_i \varphi_C^T \right) \mathcal{C}_1 \delta \mu_T d\Omega + \sum_{p=1}^N \varphi_{\mu_{T_p}}^T \Delta \mu_T \Omega_p = 0, \tag{5.69}$$

and the hybrid boundary conditions are

$$\begin{aligned}\int_\Gamma \left(\left(L^*_\Gamma(\varphi_C) - \beta \left(\frac{\partial j_\Gamma}{\partial U} \right)^T \right)^T \delta U - \varphi_C^T \left(\mathcal{A}_3 + \mathcal{B}_3 \right) \delta(\partial_j U) \hat{n}_i \right) d\Gamma \\ - (1-\beta) \sum_{p=1}^{N_\Gamma} \sum_{q=1}^{N_\Gamma} \frac{\mathfrak{D} j_{\Gamma_q}}{\mathfrak{D} U_p} \Gamma_q \Delta U_p - \sum_{p=1}^{N_\Gamma} \sum_{q=1}^{N_\Gamma} \varphi_{D_q}^T \frac{\mathfrak{D}(\hat{F}_T)_{\Gamma_q}}{\mathfrak{D} U_p} \Delta U_p &= 0,\end{aligned} \tag{5.70}$$

and

$$\int_\Gamma \varphi_C^T \mathcal{C}_1 \hat{n}_i \delta \mu_T d\Gamma = 0, \tag{5.71}$$

where we note that the boundary objective function should only explicitly depend on the boundary cells, and we have again separated out the flux across the boundary from the residual in the boundary cell where appropriate

$$\mathcal{R}_{T_p} = (\hat{F}_T)_{\Gamma_p} + \mathcal{R}^*_{T_p}. \tag{5.72}$$

Next we must cancel out the flow perturbations by discretizing the integrals and assuming the perturbations are piece-wise constant within each cell, giving, from equation (5.68),

$$\begin{aligned}\int_{\Omega_p} \left(L^*_\Omega(\varphi_C) - \beta \left(\frac{\partial j_\Omega}{\partial U} \right)^T \right) d\Omega - (1-\beta) \sum_{q=1}^{N} \left(\frac{\mathfrak{D} j_q}{\mathfrak{D} U_p} \right)^T \Omega_q \\ - \sum_{q=1}^{N} \left(\frac{\mathfrak{D} \mathcal{R}^{(*)}_{T_q}}{\mathfrak{D} U_p} \right)^T \varphi_{D_q} - \sum_{q=1}^{N} \left(\frac{\mathfrak{D} f_q}{\mathfrak{D} U_p} \right)^T \varphi_{\mu_{T_q}} \Omega_q &= 0,\end{aligned} \tag{5.73}$$

and from equation (5.69),

$$\int_{\Omega_p} \mathcal{C}_1^T \partial_i \varphi_C d\Omega + \varphi_{\mu_{T_p}} \Omega_p = 0. \tag{5.74}$$

We can now substitute equation (5.74) into equation (5.73) to remove the variable φ_{μ_T} and produce just one set of adjoint equations,

$$\begin{aligned}\int_{\Omega_p} \left(L^*_\Omega(\varphi_C) - \beta \left(\frac{\partial j_\Omega}{\partial U} \right)^T \right) d\Omega - (1-\beta) \sum_{q=1}^{N} \left(\frac{\mathfrak{D} j_q}{\mathfrak{D} U_p} \right)^T \Omega_q \\ - \sum_{q=1}^{N} \left(\frac{\mathfrak{D} \mathcal{R}^{(*)}_{T_q}}{\mathfrak{D} U_p} \right)^T \varphi_{D_q} + \sum_{q=1}^{N} \left(\frac{\mathfrak{D} f_q}{\mathfrak{D} U_p} \right)^T \int_{\Omega_q} \mathcal{C}_1^T \partial_i \varphi_C d\Omega &= 0.\end{aligned} \tag{5.75}$$

This hybrid derivation process is explained in full detail in Appendix B.

5.3.4.2 Boundary conditions

The boundary conditions for the adjoint equations are given by (5.70) and (5.71), however, we must manipulate these so as to remove the dependence on the flow perturbation. This is shown in greater detail in Appendix C, but is summarized below.

Viscous wall First considering equation (5.71), we note that at the wall the flow should be laminar and thus the eddy viscosity must be zero, implying $\delta\mu_T = 0$ and thus satisfying this condition.

For the other condition, given by (5.70), we can handle the mean flow in the same way as for laminar flow, but must also now consider discrete perturbations in the flow variables.

The result is the condition

$$\begin{aligned}
&\left(\int_{S_p} \frac{\partial j_\Gamma}{\partial U} d\Gamma\right) \delta U_p + (1-\beta) \sum_{q=1}^{N_S} \frac{\mathfrak{D} j_{\Gamma_q}}{\mathfrak{D} U_p} \Gamma_q \Delta U_p \\
&- \left(\int_{S_p} \phi^T_{\rho u_j} \hat{n}_i\right) \delta p_p + \sum_{q=1}^{N_S} \varphi^T_{D_q} \left(\frac{\rho_p}{p_p} \frac{\mathfrak{D}(\hat{F}_T)_{\Gamma_q}}{\mathfrak{D}\rho_p} + \frac{1}{\gamma - 1} \frac{\mathfrak{D}(\hat{F}_T)_{\Gamma_q}}{\mathfrak{D}(\rho E)_p}\right) \Delta p_p \\
&+ \left(\int_{S_p} \left(\phi^T_{\rho u_j} \tau_{ij} \frac{\partial \mu}{\partial T} + \mu \left(\partial_i \phi_{\rho E}\right) \frac{C_p}{Pr}\right) \hat{n}_i d\Gamma\right) \delta T_p - \sum_{q=1}^{N_S} \frac{\rho_p}{T_p} \varphi^T_{D_q} \frac{\mathfrak{D}(\hat{F}_T)_{\Gamma_q}}{\mathfrak{D}\rho_p} \Delta T_p \\
&+ \left(\int_{S_p} \phi^T_{\rho u_j} \mu \hat{n}_i d\Gamma\right) \delta \tau_{ij_p} \\
&+ (1-\beta) \sum_{q=1}^{N_S} \frac{\mathfrak{D} j_{\Gamma_q}}{\mathfrak{D} U_{T_p}} \Gamma_q \Delta U_{T_p} + \sum_{q=1}^{N_S} \varphi^T_{D_q} \frac{\mathfrak{D}(\hat{F}_T)_{\Gamma_q}}{\mathfrak{D} U_{T_p}} \Delta U_{T_p} \quad = \quad 0,
\end{aligned} \tag{5.76}$$

and thus also the requirement that we must consider objective functions for which we can write the perturbation in the form

$$\frac{\partial j_\Gamma}{\partial U} \delta U = \frac{\partial j_\Gamma}{\partial p} \delta p + \frac{\partial j_\Gamma}{\partial \tau_{ij}} \delta \tau_{ij} + \frac{\partial j_\Gamma}{\partial T} \delta T + \frac{\partial j_\Gamma}{\partial U_T} \delta U_T, \tag{5.77}$$

allowing the δp, $\delta \tau_{ij}$, δT and δU_T dependencies to be removed.

Far field First considering equation (5.71), we note that at a true far field we expect the eddy viscosity to be constant and unperturbed, implying $\delta\mu_T = 0$ and thus satisfying this condition.

For the other boundary condition, (5.70), again considering objective functions not defined along the far field boundary and neglecting flow gradients and viscosity contributions we have simply equation (5.15).

5.3.4.3 Numerical implementation

As for the flow, the solution method for the hybrid adjoint equations was implemented into the SU^2 CFD and design code[51]. In the same way as the primal problem, the adjoint was also solved by stepping through first the mean-flow part and then the turbulence model part.

For the mean-flow adjoint, the convective terms were discretized using the Jameson-Schmidt-Turkel[52] central-differencing scheme (noting the absence of the shock-related artificial dissipation as no shocks are present in the adjoint solution) and the viscous terms were discretized through a combination of average gradients and piece-wise source terms, following the method used by Bueno-Orovio et al.[6]. However, there were also additional discrete coupling terms added in as sources to the mean-flow adjoint.

To obtain the required Jacobians for the turbulence variable-adjoint, the Spalart-Allmaras one-equation model routines from the flow solution method were differentiated using the TAPENADE source code transformation AD tool[32]. Since SU^2 is written in C++ and TAPENADE works only on Fortran or C, this process was automated by creating a series of Python routines to convert the raw source code from C++ to C, run TAPENADE and then convert the differentiated routines back to C++. On the very first iteration of the hybrid adjoint code, a set of wrapping routines in SU^2 extracted the required discrete Jacobians from the differentiated code and stored them both to solve the adjoint turbulence model problem and to couple back into the mean-flow adjoint equations.

Within each major iteration of the hybrid adjoint solver, an implicit backward Euler scheme was used for the pseudo-time integration of the mean-flow step and then the turbulence model linear system was solved completely, noting that after each mean-flow adjoint solution step the mixed coupling source term would alter this linear system.

5.3.5 Results

5.3.5.1 Theoretical analysis

Before applying the turbulent hybrid adjoint approach developed above to an appropriate test case, it is useful to first make some observations based on the theory:

1. The hybrid adjoint equations (5.75) are already written in finite volume form because of the need to discretize the domain integral.

2. Considering a continuous objective function defined on a surface, which does not explicitly depend on the turbulence model variables, such as the drag on an airfoil, and splitting equation (5.75) into the adjoint equations for the mean flow and for the turbulence model gives a

continuous-like adjoint PDE with discrete and mixed source terms for the mean flow,

$$\int_{\Omega_p} L^*_\Omega(\varphi_C)d\Omega = \sum_{q=1}^{N}\left(\frac{\mathfrak{D}\mathcal{R}^{(*)}_{T_q}}{\mathfrak{D}U_p}\right)^T \varphi_{D_q} - \sum_{q=1}^{N}\left(\frac{\mathfrak{D}f_q}{\mathfrak{D}U_p}\right)^T \int_{\Omega_q} \mathcal{C}_1^T \partial_i \varphi_C d\Omega, \tag{5.78}$$

and a discrete-like linear system with mixed source terms for the turbulence model,

$$\sum_{q=1}^{N}\left(\frac{\mathfrak{D}\mathcal{R}^{(*)}_{T_q}}{\mathfrak{D}U_p}\right)^T \varphi_{D_q} = \sum_{q=1}^{N}\left(\frac{\mathfrak{D}f_q}{\mathfrak{D}U_p}\right)^T \int_{\Omega_q} \mathcal{C}_1^T \partial_i \varphi_C d\Omega, \tag{5.79}$$

noting that the chosen objective function influences the coupled system only through the hybrid boundary conditions on the viscous wall, i.e.,

$$\int_{S_p}\left(\frac{\partial j_\Gamma}{\partial p} - \varphi^T_{C_{\rho u_j}}\hat{n}_i\right)d\Gamma + \sum_{q=1}^{N_S}\varphi^T_{D_q}\left(\frac{\rho_p}{p_p}\frac{\mathfrak{D}(\hat{F}_T)_{\Gamma_q}}{\mathfrak{D}\rho_p} + \frac{1}{\gamma-1}\frac{\mathfrak{D}(\hat{F}_T)_{\Gamma_q}}{\mathfrak{D}(\rho E)_p}\right) = 0, \tag{5.80}$$

$$\int_{S_p}\left(\frac{\partial j_\Gamma}{\partial T} + \left(\varphi^T_{C_{\rho u_j}}\tau_{ij}\frac{\partial \mu}{\partial T} + \mu\left(\partial_i\varphi_{C_{\rho E}}\right)\frac{C_p}{Pr}\right)\hat{n}_i\right)d\Gamma - \sum_{q=1}^{N_S}\frac{\rho_p}{T_p}\varphi^T_{D_q}\frac{\mathfrak{D}(\hat{F}_T)_{\Gamma_q}}{\mathfrak{D}\rho_p} = 0, \tag{5.81}$$

$$\int_{S_p}\left(\frac{\partial j_\Gamma}{\partial \tau_{ij}} + \varphi^T_{C_{\rho u_j}}\mu\hat{n}_i\right)d\Gamma = 0, \tag{5.82}$$

and

$$\sum_{q=1}^{N_S}\varphi^T_{D_q}\frac{\mathfrak{D}(\hat{F}_T)_{\Gamma_q}}{\mathfrak{D}U_{T_p}} = 0. \tag{5.83}$$

The form of equations (5.78) and (5.79) implies that the former should be solved as a PDE and the second as a linear system.

3. While the summation signs in the hybrid adjoint equations (5.75) and wall boundary conditions (5.76) are written as either over all the cells in the mesh, or all the cells along the surface, it is not typically required to consider the explicit dependence of every cell in the mesh to every other cell. The numerical scheme usually considers a smaller stencil for calculating the flow (and gradients) for any particular cell, and it is this stencil that is most important when handling parts of the hybrid approach discretely. The same is generally true of the calculation of the eddy viscosity.

4. The continuous-like treatment of the boundary conditions in the hybrid adjoint derivation

implies that, at least on a viscous wall, the choice of objective function in the hybrid adjoint is restricted in a similar way as the continuous adjoint. This means that only functionals of the pressure, temperature, stress and turbulence adjoint variable should be considered. However, within the domain, there is the possibility of using a more varied selection of objective functions.

5. An important result from the hybrid derivation shown previously is that no derivatives of the eddy viscosity appear in the continuously-treated parts of the hybrid adjoint equations or boundary conditions, and instead these model-dependent derivatives are handled discretely. Since the turbulence model is treated discretely, and all required derivatives in the discrete implementation are derived using Automatic Differentiation (AD), this means that, given the only coupling from the turbulence model to the mean flow is via μ_T, the mathematical form of the hybrid adjoint is general for any turbulence model.

6. The derivation of the hybrid adjoint in this paper considered only viscous wall and far field boundary conditions. Some additional work therefore may be required to apply the resulting PDE to other boundary conditions, such as inlets and outlets, and if the outer boundary is not sufficiently far away that viscous terms cannot be neglected.

7. Though shape of the wall S was held fixed in the above derivations of the frozen-viscosity continuous adjoint and hybrid adjoint, the adjoint equations derived, and the adjoint variables that come from their solution, are in fact general and can be used to evaluate the sensitivities to changes in this shape. Assuming there is no explicit dependence of the objective function on the turbulence variables, the objective function depends only on the forces on S and some constant projection vector, and that the surface is either smooth or δS is zero where it is singular, it is possible to write the perturbation to the objective function with respect to shape perturbations as[6]

$$\begin{aligned}\delta\mathcal{J} \quad = \quad & \int_S \Bigg(\hat{n}_i \left(\partial_j \phi_{\rho u_i} + \partial_i \phi_{\rho u_j} - \frac{2}{3}\delta_{ij}\partial_l \phi_{\rho u_l} \right) \partial_k u_k \hat{n}_j \\ & -\mu^{v2} C_p \left(\partial_i(\phi_{\rho E}) - \partial_j(\phi_{\rho E})\hat{n}_j\hat{n}_i \right) \left(\partial_i(T) - \partial_j(T)\hat{n}_j\hat{n}_i \right) \Bigg) \delta S d\Gamma.\end{aligned} \tag{5.84}$$

This result can be used to evaluate the sensitivity of objective functions such as the coefficients of lift and drag on an airfoil with respect to changes in its surface shape.

5.3.5.2 Flow test case

The test cases used to investigate the frozen continuous and full hybrid adjoints were transonic flow over the RAE 2822 airfoil at non-zero angle-of-attack. The flow conditions used, corresponding to AGARD AR 138 cases 9 and 10[44, 53], were:

- Freestream Mach number, $M_\infty = 0.734$ (case 9) and $M_\infty = 0.754$ (case 10)
- Freestream temperature, $T_\infty = 273.15K$
- Angle-of-attack, $\alpha = 2.54^o$ (case 9) and $\alpha = 2.57^o$ (case 10)
- Reynolds number, $Re = 6.5 \times 10^6$ (case 9) and $Re = 6.2 \times 10^6$ (case 10)
- Gas constant, $R = 287.87 Jkg^{-1}K^{-1}$
- Ratio of specific heats, $\gamma = 1.4$

and the grid for this case contains a total of $13,937$ points, including 192 on the surface of the airfoil, and is given in Figure 5.2. The flow simulations were converged to machine precision (residual values of $1e^{-16}$), and the adjoint simulations until an approximation of the geometric sensitivity of the functional changed by less than $1e^{-6}$ over 100 iterations.

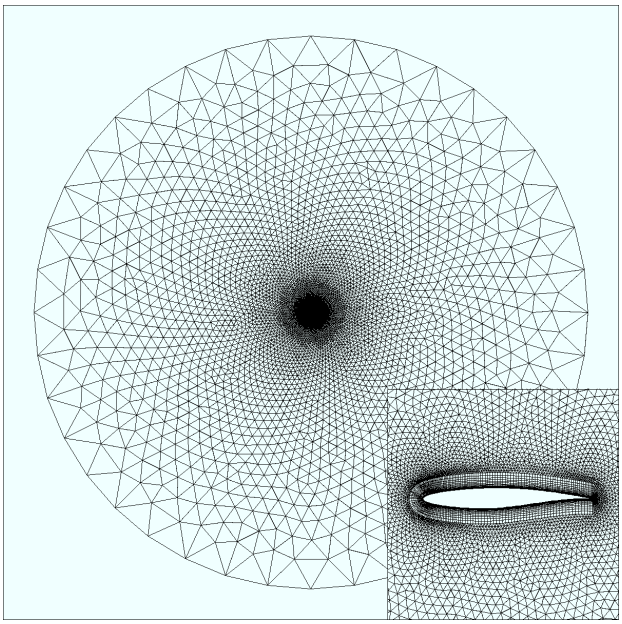

Figure 5.2: Computational mesh for the RAE 2822 airfoil used for the AGARD AR 138 turbulent flow cases 9 and 10[44, 53].

The turbulence model used was the Spalart-Allmaras one-equation turbulence model, and the resulting surface pressure coefficients are shown in Figures 5.3 and 5.4. The simulation of case 9 matches the pressure coefficients from experiment along the lower surface and upstream of the shock well, and also predicts the shock location. However, downstream of the shock there is a difference between the values obtained using simulation and experiment. Case 10 also shows good agreement on the lower surface, but on the upper surface the pressure coefficients from simulation and experiment

now match more closely after the shock, whilst there is a difference between the shock location and values upstream.

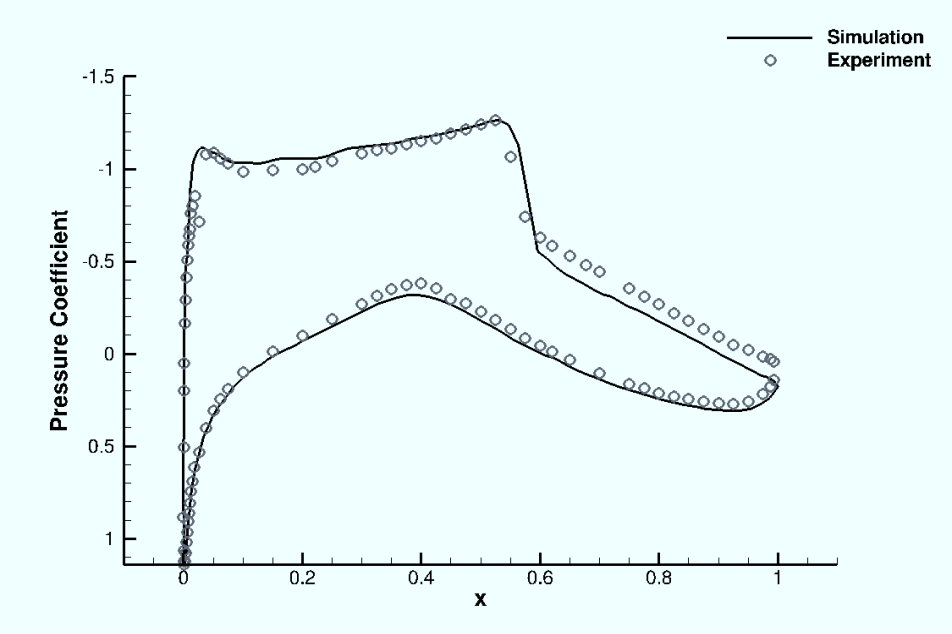

Figure 5.3: Pressure coefficient along the RAE 2822 airfoil for AGARD AR 138 case 9[44].

5.3.5.3 Adjoint results

Surface sensitivity Figures 5.5 and 5.6 show the sensitivity of the coefficient of drag to changes in the surface of the RAE 2822 airfoil obtained using the frozen continuous and hybrid adjoint approaches for cases 9 and 10, respectively. It can be seen that for case 9 there is very little difference between the frozen continuous and hybrid results. For case 10, there is also no significant difference in the sensitivity on the lower surface, but on the upper surface, near the location of the shock, the frozen continuous and hybrid results noticeably differ. It should also be noted that for case 10 the drag is seen to be in general much more sensitive to changes on the upper surface, where the effects of turbulence are expected to be greatest.

Shape sensitivity The airfoil shape was parameterized using 38 Hicks-Henne bump functions[54] and the sensitivity of the airfoil drag to changes in the surface was then calculated by projecting these bump functions onto the surface of the airfoil. These bumps were numbered from the lower side of the trailing edge clockwise towards the leading edge (0 to 18) and then backwards from the leading edge along the upper surface to the trailing edge (19 to 37), and positioned at intervals

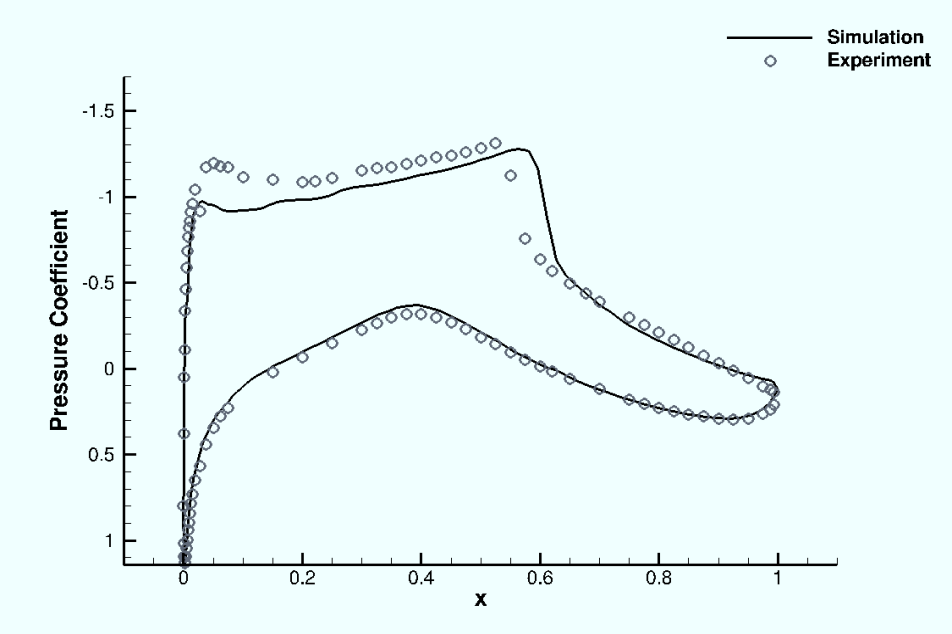

Figure 5.4: Pressure coefficient along the RAE 2822 airfoil for AGARD AR 138 case 10[44].

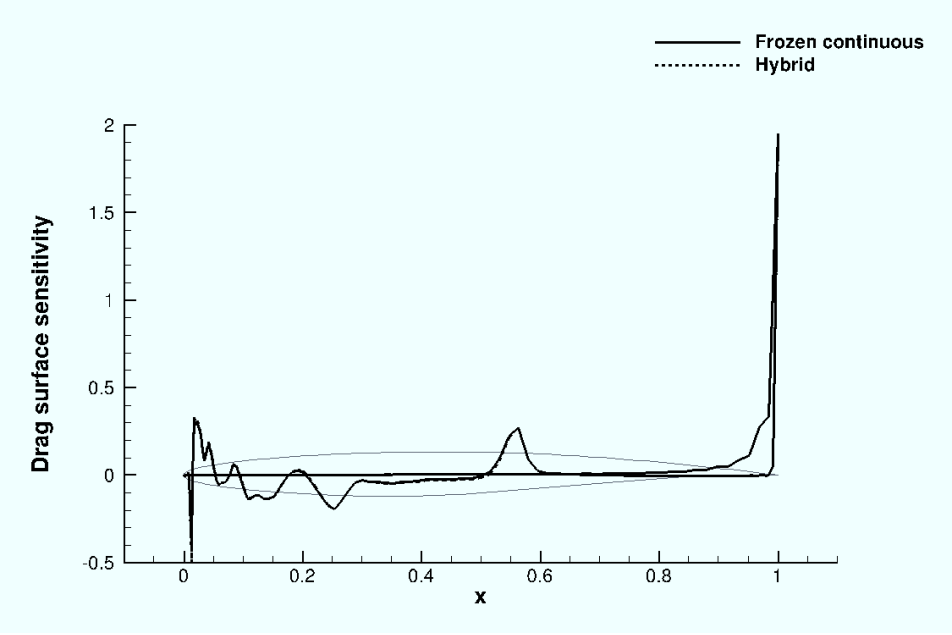

Figure 5.5: Surface sensitivity of coefficient of drag along the RAE 2822 airfoil for AGARD AR 138 case 9[44].

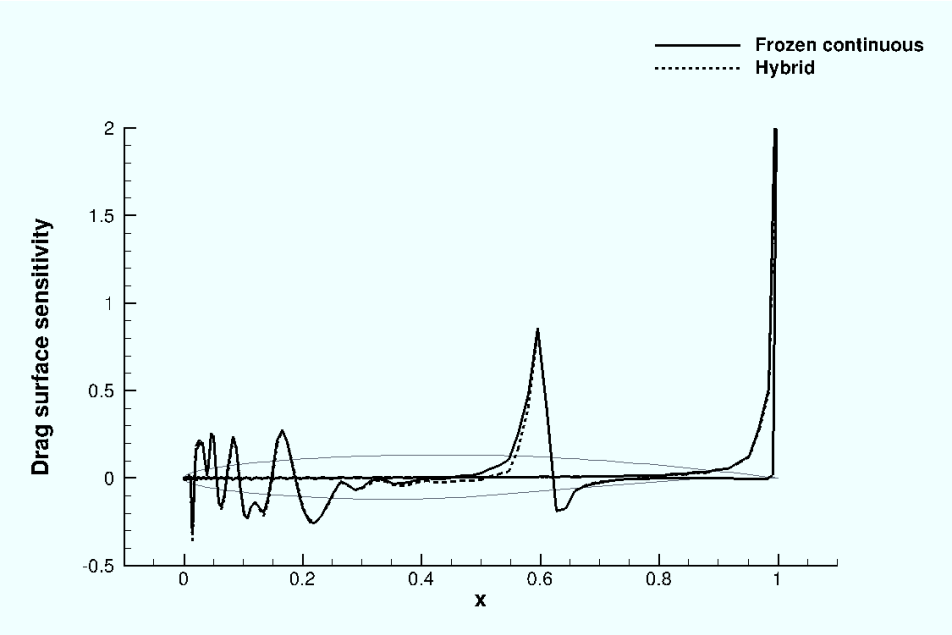

Figure 5.6: Surface sensitivity of coefficient of drag along the RAE 2822 airfoil for AGARD AR 138 case 10[44].

of 0.05 of the chord along the x-axis. The sensitivities obtained by finite differencing, the frozen-viscosity continuous adjoint and the hybrid adjoint are shown in Figures 5.7 and 5.8 for cases 9 and 10, respectively. For case 9, the two adjoints are seen to give relatively similar results, and neither agrees perfectly with finite differencing. For case 10, however, a marked difference is seen between the frozen-viscosity continuous adjoint, the hybrid adjoint and the results from finite differencing on the upper surface of the airfoil.

To validate the finite difference results for case 10, the finite difference step in the shape was varied from $1e^{-2}$ to $1e^{-8}$, but over this range no significant change was seen in the finite difference results.

Shape optimization Using the above results for surface sensitivities, and the parametrization of the airfoil using 38 Hicks-Henne bump functions, both adjoint methods were then applied to a problem of gradient-based optimization of the shape of the RAE 2822 airfoil with the objective of reducing the drag, whilst keeping the lift constant. A simple quasi-newton method was used to enable the optimization.

Figures 5.9 and 5.10 show the evolution of the drag and lift values at each design step. Case 9 shows only a small difference between using the two adjoint approaches, as might be expected from the very similar surface sensitivities in Figure 5.5. After 10 design steps the frozen-viscosity

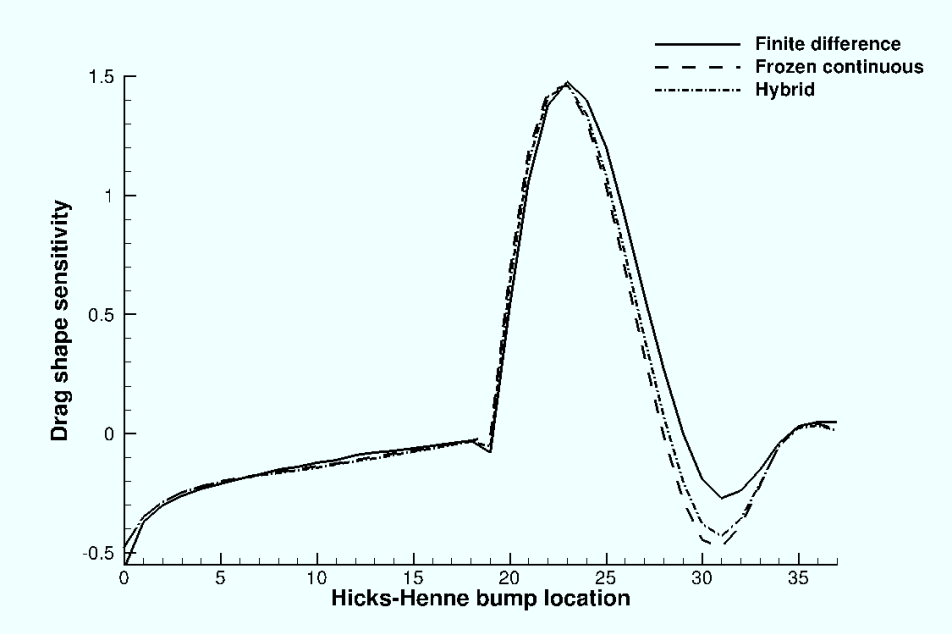

Figure 5.7: Shape sensitivity of coefficient of drag along the RAE 2822 airfoil for AGARD AR 138 case 9[44].

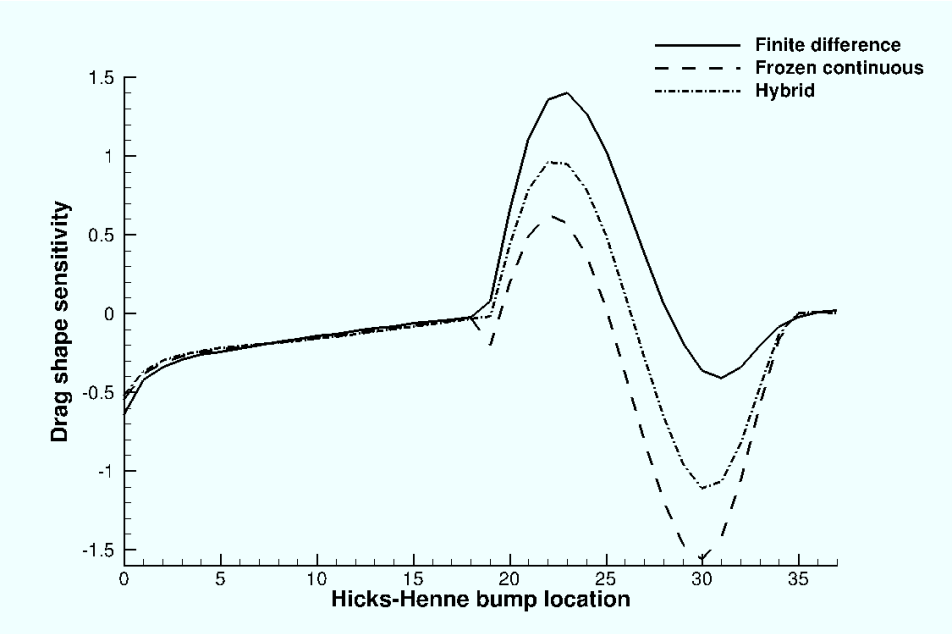

Figure 5.8: Shape sensitivity of coefficient of drag along the RAE 2822 airfoil for AGARD AR 138 case 10[44].

continuous adjoint reduced the drag coefficient to 63.1% of the original value, increasing the lift-to-drag ratio to 73.2 (the baseline was 46.4). In comparison, the hybrid adjoint reduced the drag coefficient to 64.5% and raised the lift-to-drag ratio to 71.5.

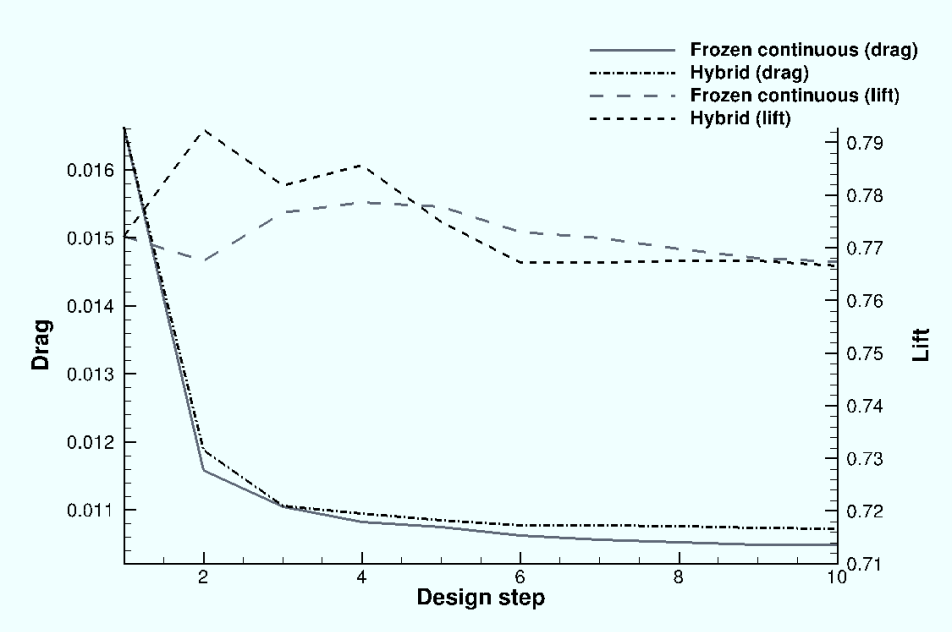

Figure 5.9: Shape optimization of the RAE 2822 airfoil for AGARD AR 138 case 9[44], aiming to minimize the coefficient of drag whilst constraining the coefficient of lift above 0.77.

Application of the hybrid adjoint to the optimization of case 10, however, showed a more significant difference to the frozen-viscosity continuous method. After 15 design steps the frozen-viscosity approach gave a drag coefficient of 53.1% of the original value with a lift-to-drag ratio of 55.6 (the baseline was 28.6), and the hybrid gave a drag coefficient of 48.4% and a lift-to-drag ratio of 61.8.

The resulting surface pressures are shown in Figures 5.11 and 5.12, indicating that the optimizer is able to reduce the strong shock on the upper surface. However, in case 10 the hybrid adjoint appears to have more substantially reduced the strength of the pressure jump on the upper surface of the airfoil than the frozen-viscosity continuous adjoint method.

The oscillatory nature of the coefficient of pressure profiles is expected to be caused by the relatively coarse discretization of the airfoil into 38 Hicks-Henne bump functions. Using a greater number of bumps would be expected to smooth out the profiles.

Finally, Figures 5.13 and 5.14 show the modified airfoil surfaces produced. Again, the difference between the frozen-viscosity and hybrid adjoint results for case 9 is small, but in the case 10 result it is possible to see a significant difference between the shapes produced on the upper surface of the airfoil.

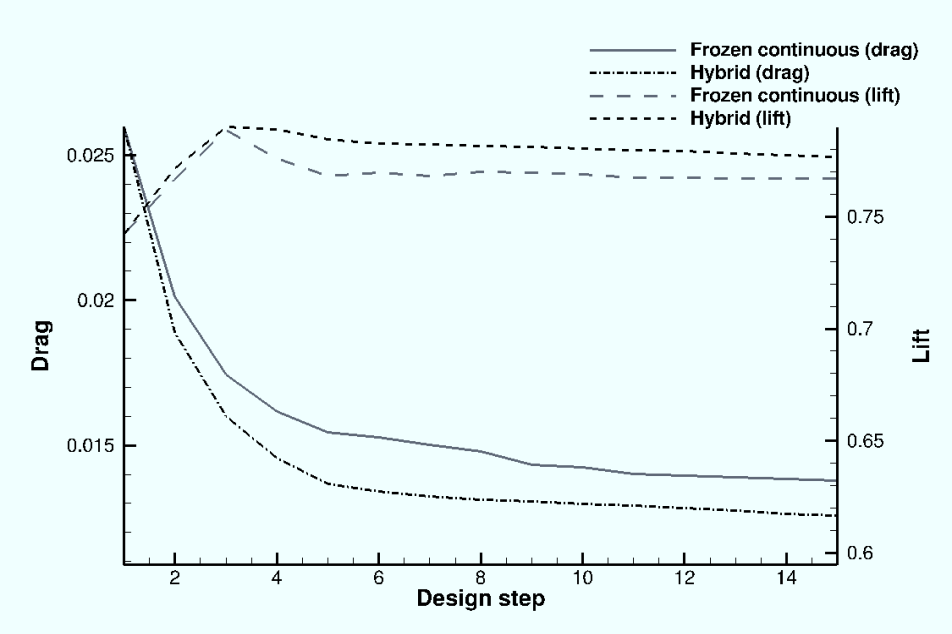

Figure 5.10: Shape optimization of the RAE 2822 airfoil for AGARD AR 138 case 9[44], aiming to minimize the coefficient of drag whilst constraining the coefficient of lift above 0.74.

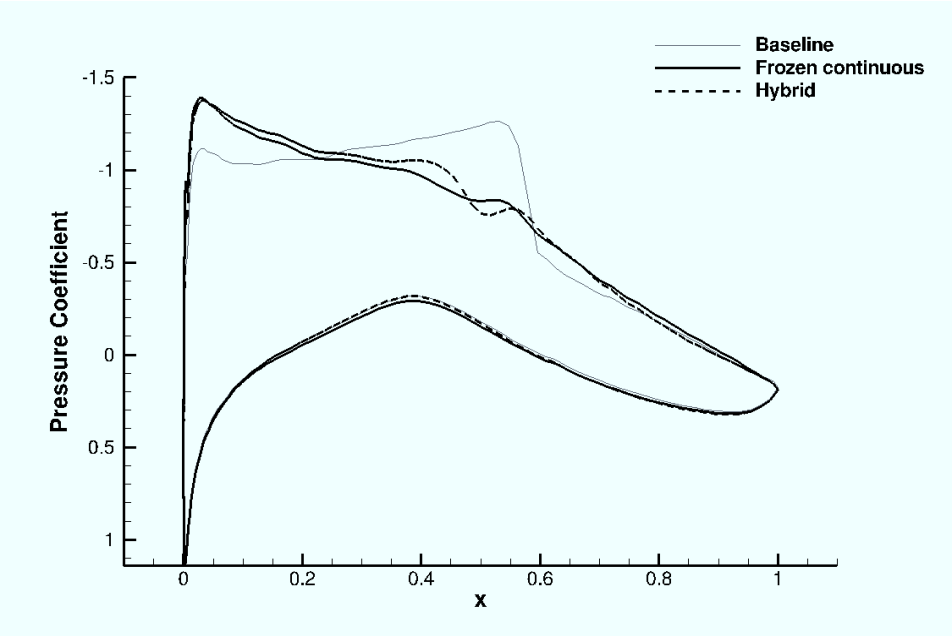

Figure 5.11: Coefficient of pressure along baseline and optimized (10th design step) RAE 2822 airfoils for AGARD AR 138 case 9[44].

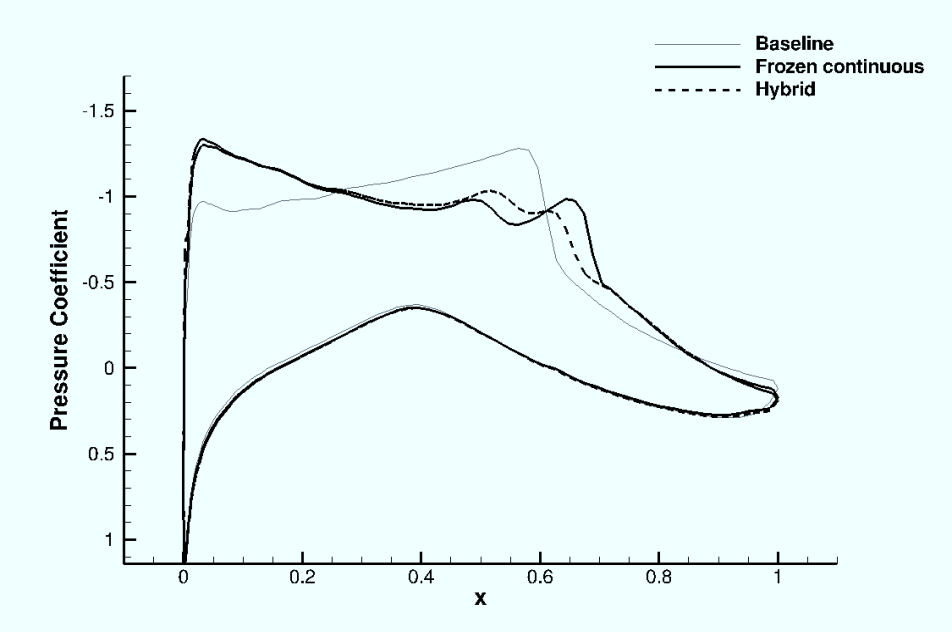

Figure 5.12: Coefficient of pressure along baseline and optimized (15th design step) RAE 2822 airfoils for AGARD AR 138 case 10[44].

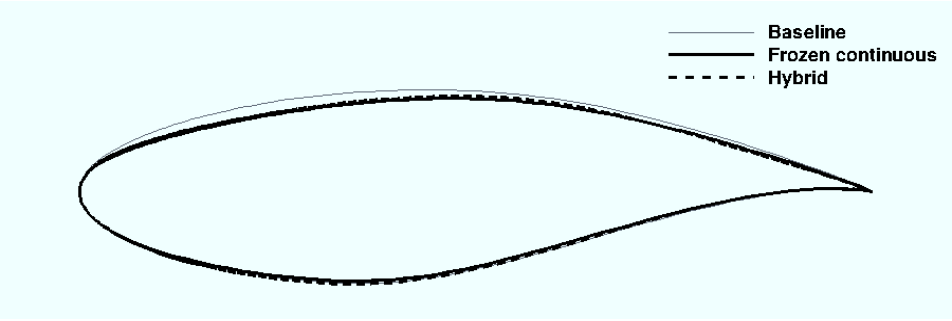

Figure 5.13: Shape comparison of baseline and optimized (10th design step) RAE 2822 airfoils for AGARD AR 138 case 9[44]. Note that the shape has been stretched so that $x : y = 0.5 : 1$ to make the shape differences clearer.

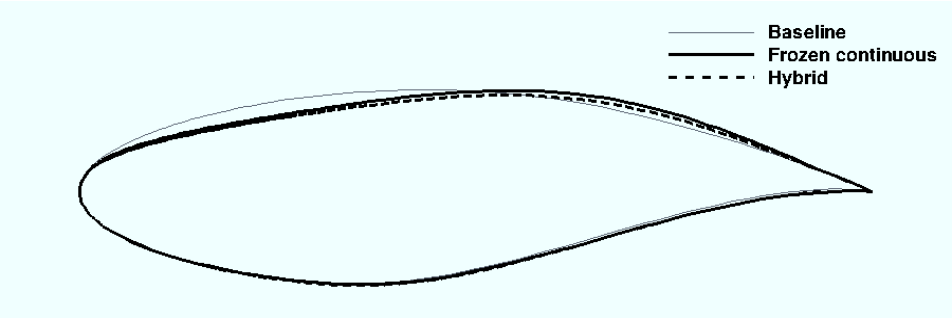

Figure 5.14: Shape comparison of baseline and optimized (10th design step) RAE 2822 airfoils for AGARD AR 138 case 10[44]. Note that the shape has been stretched so that $x : y = 0.5 : 1$ to make the shape differences clearer.

5.3.6 Discussion

The theory developed above shows how the hybrid adjoint approach can be applied in a way that means the continuous part of the formulation is independent of the turbulence model form. However, the choice of objective functions defined on a viscous wall may be restricted to the same functions of pressure, temperature and shear stress as the continuous adjoint.

The continuous and discrete parts of the hybrid are seen to be able to reuse both the existing development and implementation of continuous and discrete adjoints, respectively. The development produces a PDE for the mean-flow adjoint with discrete and mixed source terms, and a linear system for the turbulence model with a mixed source vector. This allows the mean-flow adjoint to be solved using a wide range of PDE solution techniques, whilst solving the turbulence-model adjoint as a linear system.

In situations of high turbulence, such as in the separation zone in case 10, a significant difference is seen between the frozen continuous and hybrid adjoint results, but in the lower turbulence conditions of case 9 it is not clear whether the frozen continuous or hybrid gives a better surface sensitivity result, and which method is more suitable for performing optimization.

Chapter 6

Conclusions

"A computer lets you make more mistakes faster than any invention in human history; with the possible exceptions of handguns and tequila."

— Mitch Ratliffe

In this dissertation we have introduced the general theory for a hybrid adjoint approach that seeks to improve both the solution process of the adjoint system and the quality of the sensitivity information generated by combining existing methods of sensitivity analysis. We have developed this idea by concentrating on a hybrid between the continuous and discrete adjoint approaches, with application to both quasi-one-dimensional flow with a simplified combustion model and Reynolds-Averaged Navier-Stokes flow with a general turbulence model.

The existing continuous and discrete adjoint approaches differ primarily in the order of the linearization and discretization steps, and this new continuous-discrete adjoint hybrid works by splitting the governing equations and handling some parts in the continuous framework (linearization, then discretization) and others in the discrete framework (discretization, then linearization). Prior to this work, previous hybrid approaches used have been much more limited, including attempts to improve the quality of the discrete adjoint solution by using continuous-like boundary conditions[10] and to use the continuous adjoint variables in a discrete sensitivity framework[36].

In complex engineering applications, whilst it is always possible to build the discrete adjoint system using Automatic Differentiation (AD), the resulting linear system can be large and stiff, making solution difficult or impossible. On the other hand, though it may not be possible to apply a full continuous adjoint to such problems, were it possible to build the continuous adjoint PDEs, it is expected that these could be solved using the wide range of techniques that exist for solving such systems of equations. Therefore, the motivation of developing a hybrid for such physical problems can be summarized as using the discrete approach to build the adjoint equations, and the continuous approach to solve them.

The specific hybrid approach investigated in this dissertation treats the conservation equations of mass, momentum and energy in a continuous manner and additional models, such as turbulence or combustion, discretely. Through appropriate comparison to the pure discrete and continuous approaches it is possible to understand whether or not the hybrid adjoint approach succeeds in capturing the advantages of the existing methods whilst mitigating their disadvantages. We can return to Table 1.1, originally shown in the Introduction, to understand how successful the hybrid has been in this respect.

The hybrid derivation is of a similar complexity to the continuous, but for both the quasi-one-dimensional and RANS cases, was seen to be unaltered by either new source terms or combustion models as these models were treated in a discrete framework. This, combined with the ability of AD to handle arbitrary terms (which may not be smooth or continuous, thus causing problems for analytic differentiation), means that it is possible to change the turbulence or combustion models without affecting the development of the continuous part. Additionally, large parts of existing continuous adjoint implementations can be reused when developing hybrid code.

In the quasi-one-dimensional cases, the hybrid gradients were shown to match the full continuous gradients much better than those obtained via the discrete adjoint or finite differencing, indicating

	Discrete	Continuous	Hybrid
Ease of development[11, 26, 30, 35, 39]	+	−	±
Compatibility of numerical gradients:			
- with the discretized PDE[7, 6, 26, 30, 35]	+	−	−
- with the continuous PDE[26, 36]	−	+	+
Surface formulation for gradients[6, 40]	−	+	+
Ability to handle:			
- arbitrary functionals[30, 39]	+	−	±
- non-differentiability[26, 30, 39, 41]	+	−	+
Computational cost[10, 26, 30, 35]	−	+	±
Flexibility in solution[26, 35, 36, 38, 39]	−	+	±

Table 1.1: Simple comparison between the discrete, continuous and hybrid adjoint approaches.

that it is able to better predict the fine grid sensitivity on coarser meshes. In situations where the full continuous adjoint was no longer possible or easy to obtain, the hybrid could still be used, and performed significantly better than a frozen-combustion continuous adjoint.

In the RANS cases, little difference was seen between the hybrid adjoint and frozen-viscosity adjoint derived sensitivities where the effect of turbulence was small (AGARD AR 138 case 9[44, 53]), and an optimization study of this flow case did not show a significant difference between using either method. However, where the effect of turbulence was greater (AGARD AR 138 case 10[44, 53], and particularly on the upper surface of the airfoil), a marked difference was seen between the sensitivities produced by either method. A lift-contrained optimization study of the RAE 2822 airfoil under these flow conditions produced a lower overall drag coefficient using the hybrid adjoint approach compared to the frozen-viscosity adjoint approach (48.4% of the baseline compared to 53.1%)

Though in the quasi-one-dimensional example the hybrid approach allowed the possibility of using any objective function, including one that would usually not be admissible in the continuous adjoint formulation, the required hybrid boundary condition treatment in RANS flow introduced restrictions on the choice of the objective function at the wall similar to those in the development of the continuous adjoint.

Finally, when solving the hybrid, the memory requirements of the hybrid can be seen by inspection to be much lower than for the full discrete approach, since only the discrete Jacobians of the turbulence model must be stored, and not of the entire flow equations, and much of the flexibility still remains in how we can solve the continuous PDE part of the system.

One of the key remaining questions in the hybrid implementation developed in this dissertation is how to optimize the numerical solution process of the hybrid to reduce the computational cost and improve the solution quality. Currently only relatively conservative PDE solution methods have been applied to the continuous part of the RANS hybrid adjoint system, and the turbulent discrete linear system has been solved completely at each major iteration step. Ideally, though, acceleration techniques can be applied to the solution of the continuous PDE, and it may prove better to relax

the solution of the linear system at each step.

Further work is also required to investigate the applicability of the hybrid adjoint methods developed here. Whilst the quasi-one-dimensional hybrid was developed for subsonic, transonic and shocked flows, it has not been tested with these conditions. It will also be important to test the generality of the RANS hybrid by running it with other turbulence models and to apply it to situations where the effects of turbulence are more significant.

Other open areas of research include the validity of assumptions made in deriving the hybrid adjoint and the question of exactly how the hybrid adjoint should be constructed. There may be many other alternatives to the approaches used in this research, such as treating all of the viscous terms of the RANS equations discretely, instead of just the eddy viscosity and turbulence model.

The final goal of this new approach will be to apply it to complex multi-physics flow cases, creating, for example, a hybrid adjoint that is able to handle both general turbulence models and general combustion models and that allows the adjoint approach to be applied to situations that are currently too computationally expensive for the discrete method or simply not possible with the full continuous method.

Appendix A

Useful formulae and results

This appendix presents a list of useful mathematical formulae and results used in the adjoint derivations elsewhere in this thesis.

A.1 Mathematical formulae

Integration by parts:

$$\int_{\Omega} a\left(\partial_i b\right) d\Omega = \int_{\Gamma} ab\hat{n}_i d\Gamma - \int_{\Omega} \left(\partial_i a\right) b d\Omega. \tag{A.1}$$

A.2 Useful results

A.2.1 One-dimensional flows

A.2.1.1 Quasi-one-dimensional Euler flow

Pressure-flow derivative:

$$\frac{\partial p}{\partial U} = \begin{pmatrix} \frac{(\gamma-1)}{2}\left(\frac{m}{\rho}\right)^2 & (1-\gamma)\frac{m}{\rho} & (\gamma-1) \end{pmatrix}. \tag{A.2}$$

Convective flux Jacobian:

$$\frac{\partial F}{\partial U} = \begin{pmatrix} 0 & 1 & 0 \\ \frac{(\gamma-3)}{2}\left(\frac{m}{\rho}\right)^2 & (3-\gamma)\frac{m}{\rho} & (\gamma-1) \\ -\frac{m}{\rho}H + \frac{(\gamma-1)}{2}\left(\frac{m}{\rho}\right)^3 & H + (1-\gamma)\left(\frac{m}{\rho}\right)^2 & \gamma\frac{m}{\rho} \end{pmatrix}. \tag{A.3}$$

Pressure source Jacobian:

$$\frac{\partial P}{\partial U} = \begin{pmatrix} 0 & 0 & 0 \\ \frac{(\gamma-1)}{2}\left(\frac{m}{\rho}\right)^2 & (1-\gamma)\frac{m}{\rho} & (\gamma-1) \\ 0 & 0 & 0 \end{pmatrix}. \tag{A.4}$$

Flow-Mach number derivative:

$$\left.\frac{\partial U}{\partial M}\right|_{H,p_0} = \frac{1}{1+\frac{\gamma-1}{2}M^2}\begin{pmatrix} -\rho M \\ \frac{m}{M}\left(1-M^2\right) \\ \frac{m^2}{\rho M} - \rho H M \end{pmatrix}. \tag{A.5}$$

Flow-pressure derivative:

$$\left.\frac{\partial U}{\partial p}\right|_{H,p_0} = -\frac{1}{\gamma p M}\begin{pmatrix} -\rho M \\ \frac{m}{M}\left(1-M^2\right) \\ \frac{m^2}{\rho M} - \rho H M \end{pmatrix}. \tag{A.6}$$

A.2.1.2 Rayleigh flow

Mass flux-flow derivative:

$$\frac{\partial m}{\partial U} = \begin{pmatrix} 0 & 1 & 0 \end{pmatrix}. \tag{A.7}$$

Heat addition Jacobian:

$$\frac{\partial S_R}{\partial U} = \begin{pmatrix} 0 & 0 & 0 \\ 0 & 0 & 0 \\ 0 & \Delta H_w & 0 \end{pmatrix}. \tag{A.8}$$

A.2.1.3 Quasi-one-dimensional Euler flow with combustion

Pressure-flow derivative:

$$\frac{\partial p}{\partial U} = \begin{pmatrix} \frac{\partial p}{\partial U_E} & \frac{\partial p}{\partial U_\lambda} \end{pmatrix}, \tag{A.9}$$

where $\frac{\partial p}{\partial U_E}$ is given by (A.2) and

$$\frac{\partial p}{\partial U_\lambda} = (\gamma-1)q. \tag{A.10}$$

Convective flux Jacobian:

$$\frac{\partial F}{\partial U} = \begin{pmatrix} \frac{\partial F_E}{\partial U_E} & \frac{\partial F_E}{\partial U_\lambda} \\ \frac{\partial F_\lambda}{\partial U_E} & \frac{\partial F_\lambda}{\partial U_\lambda} \end{pmatrix}, \tag{A.11}$$

where $\frac{\partial F_E}{\partial U_E}$ is given by (A.3) and

$$\frac{\partial F_E}{\partial U_\lambda} = \begin{pmatrix} 0 \\ (\gamma-1)q \\ (\gamma-1)\frac{m}{\rho}q \end{pmatrix}, \quad \frac{\partial F_\lambda}{\partial U_E} = \begin{pmatrix} -m\frac{\lambda}{\rho^2} & \frac{\lambda}{\rho} & 0 \end{pmatrix}, \quad \frac{\partial F_\lambda}{\partial U_\lambda} = \frac{m}{\rho}. \tag{A.12}$$

Pressure source Jacobian:

$$\frac{\partial P}{\partial U} = \begin{pmatrix} \frac{\partial P_E}{\partial U_E} & \frac{\partial P_E}{\partial U_\lambda} \\ \frac{\partial P_\lambda}{\partial U_E} & \frac{\partial P_\lambda}{\partial U_\lambda} \end{pmatrix}, \tag{A.13}$$

where $\frac{\partial P_E}{\partial U_E}$ is given by (A.4) and

$$\frac{\partial P_E}{\partial U} = \begin{pmatrix} 0 \\ (\gamma-1)q \\ 0 \end{pmatrix}, \quad \frac{\partial P_\lambda}{\partial U_E} = \begin{pmatrix} 0 & 0 & 0 \end{pmatrix}, \quad \frac{\partial P_\lambda}{\partial U_\lambda} = 0. \tag{A.14}$$

Combustion source Jacobian:

$$\frac{\partial Q}{\partial U} = \begin{pmatrix} \frac{\partial Q_E}{\partial U} \\ \frac{\partial Q_\lambda}{\partial U} \end{pmatrix}, \tag{A.15}$$

where

$$\frac{\partial Q_E}{\partial U} = \begin{pmatrix} 0 & 0 & 0 & 0 \\ 0 & 0 & 0 & 0 \\ 0 & 0 & 0 & 0 \end{pmatrix}, \tag{A.16}$$

and

$$\frac{\partial Q_\lambda}{\partial U} = \begin{pmatrix} \frac{\partial \omega}{\partial \rho} & \frac{\partial \omega}{\partial m} & \frac{\partial \omega}{\partial \epsilon} & \frac{\partial \omega}{\partial \lambda} \end{pmatrix}. \tag{A.17}$$

Flow-Mach number derivative:

$$\left.\frac{\partial U}{\partial M}\right|_{H,p_0,\Lambda} = \begin{pmatrix} \left.\frac{\partial U_E}{\partial M}\right|_{H,p_0,\Lambda} \\ \left.\frac{\partial U_\lambda}{\partial M}\right|_{H,p_0,\Lambda} \end{pmatrix}, \tag{A.18}$$

where $\left.\frac{\partial U_E}{\partial M}\right|_{H,p_0,\Lambda}$ is given by (A.5) and

$$\left.\frac{\partial U_\lambda}{\partial M}\right|_{H,p_0,\Lambda} = -\frac{\lambda M}{1+\frac{\gamma-1}{2}M^2}. \tag{A.19}$$

Flow-pressure derivative:

$$\left.\frac{\partial U}{\partial p}\right|_{H,p_0,\Lambda} = \begin{pmatrix} \left.\frac{\partial U_E}{\partial p}\right|_{H,p_0,\Lambda} \\ \left.\frac{\partial U_\lambda}{\partial p}\right|_{H,p_0,\Lambda} \end{pmatrix}, \tag{A.20}$$

where $\left.\frac{\partial U_E}{\partial p}\right|_{H,p_0,\Lambda}$ is given by (A.6) and

$$\left.\frac{\partial U_\lambda}{\partial p}\right|_{H,p_0,\Lambda} = \frac{\lambda}{\gamma p}. \tag{A.21}$$

A.2.2 Two- and three-dimensional flows

A.2.2.1 Euler flow

Pressure-flow derivative:

$$\frac{\partial p}{\partial U} = \begin{pmatrix} \frac{(\gamma-1)}{2}u_k u_k & (1-\gamma)u_j & (\gamma-1) \end{pmatrix}. \tag{A.22}$$

Stagnation enthalpy-flow derivative:

$$\frac{\partial H}{\partial U} = \frac{1}{\rho}\begin{pmatrix} \frac{(\gamma-1)}{2}u_k u_k - H & (1-\gamma)u_j & \gamma \end{pmatrix}. \tag{A.23}$$

Convective flux Jacobian:

$$\frac{\partial F_i}{\partial U} = \begin{pmatrix} 0 & \delta_{ik} & 0 \\ -u_i u_j + \dfrac{\partial p}{\partial \rho}\delta_{ij} & u_j\delta_{ik} + u_i\delta_{jk} + \dfrac{\partial p}{\partial(\rho u_k)}\delta_{ij} & \frac{\partial p}{\partial(\rho E)}\delta_{ij} \\ \rho u_i \dfrac{\partial H}{\partial \rho} & H\delta_{ik} + \rho u_i \dfrac{\partial H}{\partial(\rho u_k)} & \rho u_i \dfrac{\partial H}{\partial(\rho E)} \end{pmatrix}. \tag{A.24}$$

Flow-Mach number derivative:

$$\left.\frac{\partial U}{\partial M}\right|_{p,T} = \begin{pmatrix} 0 \\ \frac{\rho u_j}{M} \\ \gamma M p \end{pmatrix}. \tag{A.25}$$

Flow-pressure derivative:

$$\left.\frac{\partial U}{\partial p}\right|_{M,T} = \begin{pmatrix} \frac{\rho}{p} \\ \frac{\rho u_j}{p} \\ \frac{\rho E}{p} \end{pmatrix}. \tag{A.26}$$

Flow-temperature derivative:

$$\left.\frac{\partial U}{\partial T}\right|_{M,p} = \begin{pmatrix} -\frac{\rho}{T} \\ \frac{\rho u_j}{2T} \\ \frac{\rho u_k u_k}{T} \end{pmatrix}. \tag{A.27}$$

A.2.2.2 Laminar Navier-Stokes flow

Temperature-flow derivative:

$$\frac{\partial T}{\partial U} = \frac{1}{R\rho}\begin{pmatrix} \frac{(\gamma-1)}{2}u_k u_k - \frac{p}{\rho} & (1-\gamma)u_j & (\gamma-1) \end{pmatrix}. \tag{A.28}$$

Viscosity-flow derivative:

$$\frac{\partial \mu}{\partial U} = \frac{\partial \mu}{\partial T}\frac{\partial T}{\partial U}, \tag{A.29}$$

where

$$\frac{\partial \mu}{\partial T} = \frac{\mu(T+3\mu_2)}{2T(T+\mu_2)}. \tag{A.30}$$

Shear stress:

$$\begin{aligned}\tau_{ij} &= \frac{1}{\rho}\left(\left(\partial_i(\rho u_j) - (\partial_i\rho)\frac{\rho u_j}{\rho}\right) + \left(\partial_j(\rho u_i) - (\partial_j\rho)\frac{\rho u_i}{\rho}\right)\right. \\ &\quad \left. -\frac{2}{3}\delta_{ij}\left(\partial_k(\rho u_k) - (\partial_k\rho)\frac{\rho u_k}{\rho}\right)\right).\end{aligned} \tag{A.31}$$

Shear stress-flow variable derivatives:

$$\begin{aligned}\frac{\partial\tau_{ij}}{\partial\rho} &= -\frac{1}{\rho^2}\left(\left(\partial_i(\rho u_j) - 2(\partial_i\rho)\frac{\rho u_j}{\rho}\right) + \left(\partial_j(\rho u_i) - 2(\partial_j\rho)\frac{\rho u_i}{\rho}\right)\right. \\ &\quad \left. -\frac{2}{3}\delta_{ij}\left(\partial_k(\rho u_k) - 2(\partial_k\rho)\frac{\rho u_k}{\rho}\right)\right),\end{aligned} \tag{A.32}$$

$$\frac{\partial\tau_{ij}}{\partial(\rho u_l)} = -\frac{1}{\rho^2}\left((\partial_i\rho)\delta_{jl} + (\partial_j\rho)\delta_{il} - \frac{2}{3}\delta_{ij}(\partial_l\rho)\right), \tag{A.33}$$

and

$$\frac{\partial\tau_{ij}}{\partial(\rho E)} = 0. \tag{A.34}$$

Shear stress-flow variable gradient derivatives:

$$\frac{\partial\tau_{ij}}{\partial(\partial_m\rho)} = -\frac{1}{\rho}\left(\frac{\rho u_j}{\rho}\delta_{im} + \frac{\rho u_i}{\rho}\delta_{jm} - \frac{2}{3}\delta_{ij}\frac{\rho u_k}{\rho}\delta_{km}\right), \tag{A.35}$$

$$\frac{\partial\tau_{ij}}{\partial(\partial_m(\rho u_l))} = \frac{1}{\rho}\left(\delta_{im}\delta_{jl} + \delta_{jm}\delta_{il} - \frac{2}{3}\delta_{ij}\delta_{lm}\right), \tag{A.36}$$

and

$$\frac{\partial\tau_{ij}}{\partial(\partial_m(\rho E))} = 0. \tag{A.37}$$

Temperature gradient:

$$\partial_i T = \frac{(\gamma-1)}{R}\left(\left(\frac{\rho u_k\rho u_k}{\rho^3} - \frac{\rho E}{\rho^2}\right)\partial_i\rho - \frac{\rho u_k\partial_i(\rho u_k)}{\rho^2} + \frac{1}{\rho}\partial_i(\rho E)\right). \tag{A.38}$$

Temperature gradient-flow variable derivatives:

$$\frac{\partial(\partial_i T)}{\partial\rho} = -\frac{(\gamma-1)}{R}\left(\left(3\frac{\rho u_k\rho u_k}{\rho^4} - 2\frac{\rho E}{\rho^3}\right)\partial_i\rho - 2\frac{\rho u_k\partial_i(\rho u_k)}{\rho^3} + \frac{1}{\rho^2}\partial_i(\rho E)\right), \tag{A.39}$$

$$\frac{\partial(\partial_i T)}{\partial(\rho u_l)} = \frac{(\gamma-1)}{R}\left(-\frac{\partial_i(\rho u_l)}{\rho^2} + 2\frac{\rho u_l}{\rho^3}\partial_i\rho\right), \tag{A.40}$$

and

$$\frac{\partial(\partial_i T)}{\partial(\rho E)} = -\frac{(\gamma-1)}{R}\frac{\partial_i \rho}{\rho^2}. \tag{A.41}$$

Temperature gradient-flow variable gradient derivatives:

$$\frac{\partial(\partial_i T)}{\partial(\partial_l \rho)} = \frac{(\gamma-1)}{R}\left(\frac{\rho u_k \rho u_k}{\rho^3} - \frac{\rho E}{\rho^2}\right)\delta_{il}, \tag{A.42}$$

$$\frac{\partial(\partial_i T)}{\partial(\partial_l(\rho u_m))} = -\frac{(\gamma-1)}{R}\frac{\rho u_m}{\rho^2}\delta_{il}, \tag{A.43}$$

and

$$\frac{\partial(\partial_i T)}{\partial(\partial_l(\rho E))} = \frac{(\gamma-1)}{\rho R}\delta_{il}. \tag{A.44}$$

Viscous flux Jacobians:

$$\frac{\partial F_i^{v1}}{\partial U} = \begin{pmatrix} 0 & 0 & 0 \\ \dfrac{\partial \tau_{ij}}{\partial \rho} & \dfrac{\partial \tau_{ij}}{\partial(\rho u_l)} & 0 \\ u_k\dfrac{\partial \tau_{ik}}{\partial \rho} - \dfrac{u_k}{\rho}\tau_{ik} & u_k\dfrac{\partial \tau_{ik}}{\partial(\rho u_l)} + \dfrac{1}{\rho}\tau_{il} & 0 \end{pmatrix}, \tag{A.45}$$

$$\frac{\partial F_i^{v2}}{\partial U} = \begin{pmatrix} 0 & 0 & 0 \\ 0 & 0 & 0 \\ C_p\dfrac{\partial(\partial_i T)}{\partial \rho} & C_p\dfrac{\partial(\partial_i T)}{\partial(\rho u_l)} & C_p\dfrac{\partial(\partial_i T)}{\partial(\rho E)} \end{pmatrix}, \tag{A.46}$$

$$\frac{\partial F_i^{v1}}{\partial(\partial_m U)} = \begin{pmatrix} 0 & 0 & 0 \\ \dfrac{\partial \tau_{ij}}{\partial(\partial_m \rho)} & \dfrac{\partial \tau_{ij}}{\partial(\partial_m(\rho u_l))} & 0 \\ u_k\dfrac{\partial \tau_{ik}}{\partial(\partial_m \rho)} & u_k\dfrac{\partial \tau_{ik}}{\partial(\partial_m(\rho u_l))} & 0 \end{pmatrix}, \tag{A.47}$$

and

$$\frac{\partial F_i^{v2}}{\partial(\partial_k U)} = \begin{pmatrix} 0 & 0 & 0 \\ 0 & 0 & 0 \\ C_p\dfrac{\partial(\partial_i T)}{\partial(\partial_m \rho)} & C_p\dfrac{\partial(\partial_i T)}{\partial(\partial_m(\rho u_l))} & C_p\dfrac{\partial(\partial_i T)}{\partial(\partial_m(\rho E))} \end{pmatrix}. \tag{A.48}$$

A.2.2.3 Reynolds-Averaged Navier-Stokes flow

Pressure-flow derivative:

$$\frac{\partial p}{\partial U} = \begin{pmatrix} \frac{\partial p}{\partial U_L} & \frac{\partial p}{\partial U_T} \end{pmatrix}, \tag{A.49}$$

where $\frac{\partial p}{\partial U_L}$ is given by (A.22) and

$$\frac{\partial p}{\partial U_T} = 0. \tag{A.50}$$

Temperature-flow derivative:

$$\frac{\partial T}{\partial U} = \begin{pmatrix} \frac{\partial T}{\partial U_L} & \frac{\partial T}{\partial U_T} \end{pmatrix}, \tag{A.51}$$

where $\frac{\partial T}{\partial U_L}$ is given by (A.28) and

$$\frac{\partial T}{\partial U_T} = 0. \tag{A.52}$$

Viscosity-flow derivative:

$$\frac{\partial \mu}{\partial U} = \begin{pmatrix} \frac{\partial \mu}{\partial U_L} & \frac{\partial \mu}{\partial U_T} \end{pmatrix}, \tag{A.53}$$

where $\frac{\partial \mu}{\partial U_L}$ is given by (A.29) and

$$\frac{\partial \mu}{\partial U_T} = 0. \tag{A.54}$$

Convective flux Jacobian:

$$\frac{\partial F_i}{\partial U} = \begin{pmatrix} \frac{\partial F_i}{\partial U_L} & \frac{\partial F_i}{\partial U_T} \end{pmatrix}, \tag{A.55}$$

where $\frac{\partial F_i}{\partial U_L}$ is given by (A.24) and

$$\frac{\partial F_i}{\partial U_T} = \begin{pmatrix} 0 \\ 0 \\ 0 \end{pmatrix}. \tag{A.56}$$

Viscous flux Jacobians:

$$\frac{\partial F_i^{v1}}{\partial U} = \begin{pmatrix} \frac{\partial F_i^{v1}}{\partial U_L} & \frac{\partial F_i^{v1}}{\partial U_T} \end{pmatrix}, \tag{A.57}$$

$$\frac{\partial F_i^{v2}}{\partial U} = \begin{pmatrix} \frac{\partial F_i^{v2}}{\partial U_L} & \frac{\partial F_i^{v2}}{\partial U_T} \end{pmatrix}, \tag{A.58}$$

$$\frac{\partial F_i^{v1}}{\partial (\partial_k U)} = \begin{pmatrix} \frac{\partial F_i^{v1}}{\partial (\partial_k U_L)} & \frac{\partial F_i^{v1}}{\partial (\partial_k U_T)} \end{pmatrix}, \tag{A.59}$$

and

$$\frac{\partial F_i^{v2}}{\partial(\partial_k U)} = \begin{pmatrix} \frac{\partial F_i^{v2}}{\partial(\partial_k U_L)} & \frac{\partial F_i^{v2}}{\partial(\partial_k U_T)} \end{pmatrix}, \tag{A.60}$$

where $\frac{\partial F_i^{v1}}{\partial U_L}$, $\frac{\partial F_i^{v2}}{\partial U_L}$, $\frac{\partial F_i^{v1}}{\partial(\partial_k U_L)}$ and $\frac{\partial F_i^{v2}}{\partial(\partial_k U_L)}$ are given by (A.45), (A.46), (A.47) and (A.48), respectively, and

$$\frac{\partial F_i^{v1}}{\partial U_T} = \frac{\partial F_i^{v2}}{\partial U_T} = \frac{\partial F_i^{v1}}{\partial(\partial_k U_T)} = \frac{\partial F_i^{v2}}{\partial(\partial_k U_T)} = \begin{pmatrix} 0 \\ 0 \\ 0 \end{pmatrix}. \tag{A.61}$$

Appendix B

Adjoint equation derivations

This appendix presents the derivations of the continuous and hybrid adjoint equations for two- and three-dimensional flows in full detail.

B.1 Euler flow

B.1.1 Continuous adjoint equation

Starting from the continuous objective function

$$\mathcal{J}_C = \int_\Omega j d\Omega + \int_\Gamma j_\Gamma d\Gamma, \tag{B.1}$$

we can enforce the governing equations $\mathcal{N}$ by introducing the Lagrangian

$$\mathcal{L} = \int_\Omega j_\Omega d\Omega + \int_\Gamma j_\Gamma d\Gamma - \int_\Omega \phi^T \mathcal{N} d\Omega, \tag{B.2}$$

where ϕ are the Lagrange multipliers (or continuous adjoint variables).

Taking the perturbation of this to a change in some parameter α, noting that to simplify the derivation of the adjoint equations we neglect shape perturbations (without affecting generality), we then get

$$\delta\mathcal{L} = \int_\Omega \delta j_\Omega d\Omega + \int_\Gamma \delta j_\Gamma d\Gamma - \int_\Omega \phi^T \delta\mathcal{N} d\Omega, \tag{B.3}$$

Linearizing the integrands in the objective function we can write

$$\delta j_\Omega = \frac{\partial j_\Omega}{\partial U}\delta U + \frac{\partial j_\Omega}{\partial \alpha}\delta\alpha, \tag{B.4}$$

and

$$\delta j_\Gamma = \frac{\partial j_\Gamma}{\partial U}\delta U + \frac{\partial j_\Gamma}{\partial \alpha}\delta\alpha. \tag{B.5}$$

Also, we can write the perturbation to the governing equations as

$$\delta\mathcal{N} = \partial_i(\delta F_i), \tag{B.6}$$

where the perturbation to the flux vector can be written as

$$\delta F_i = \frac{\partial F_i}{\partial U}\delta U + \frac{\partial F_i}{\partial \alpha}\delta\alpha, \tag{B.7}$$

and thus finally the perturbation to the governing equations can be written as

$$\delta\mathcal{N} = \partial_i\left(\frac{\partial F_i}{\partial U}\delta U\right) + \partial_i\left(\frac{\partial F_i}{\partial \alpha}\delta\alpha\right). \tag{B.8}$$

The perturbation to the Lagrangian can then be written, grouping terms explicitly dependent on $\delta\alpha$ and δU,

$$\begin{aligned}\delta\mathcal{L} &= \int_\Omega \frac{\partial j_\Omega}{\partial \alpha}\delta\alpha d\Omega + \int_\Gamma \frac{\partial j_\Gamma}{\partial \alpha}\delta\alpha d\Gamma - \int_\Omega \phi^T\partial_i\left(\frac{\partial F_i}{\partial \alpha}\delta\alpha\right)d\Omega \\ &\quad + \int_\Omega \frac{\partial j_\Omega}{\partial U}\delta U d\Omega + \int_\Gamma \frac{\partial j_\Gamma}{\partial U}\delta U d\Gamma - \int_\Omega \phi^T\partial_i\left(\frac{\partial F_i}{\partial U}\delta U\right)d\Omega.\end{aligned} \tag{B.9}$$

Applying integration by parts to the last term we can then write

$$\int_\Omega \phi^T\partial_i\left(\frac{\partial F_i}{\partial U}\delta U\right)d\Omega = \int_\Gamma \phi^T\frac{\partial F_i}{\partial U}\delta U\hat{n}_i d\Gamma - \int_\Omega\left(\partial_i\phi^T\right)\frac{\partial F_i}{\partial U}\delta U d\Omega, \tag{B.10}$$

and thus the perturbation to the Lagrangian becomes

$$\begin{aligned}\delta\mathcal{L} &= \int_\Omega \frac{\partial j_\Omega}{\partial \alpha}\delta\alpha d\Omega + \int_\Gamma \frac{\partial j_\Gamma}{\partial \alpha}\delta\alpha d\Gamma - \int_\Omega \phi^T\partial_i\left(\frac{\partial F_i}{\partial \alpha}\delta\alpha\right)d\Omega \\ &\quad - \int_\Omega\left(L^*_\Omega(\phi) - \left(\frac{\partial j_\Omega}{\partial U}\right)^T\right)^T\delta U d\Omega - \int_\Gamma\left(L^*_\Gamma(\phi) - \left(\frac{\partial j_\Gamma}{\partial U}\right)^T\right)^T\delta U d\Gamma,\end{aligned} \tag{B.11}$$

where we define the adjoint linear operators

$$L^*_\Omega(\phi) = -\left(\frac{\partial F_i}{\partial U}\right)^T\partial_i\phi, \tag{B.12}$$

and

$$L_\Gamma^*(\phi) = \left(\frac{\partial F_i}{\partial U}\hat{n}_i\right)^T \phi. \tag{B.13}$$

We can then remove the dependence on the flow perturbation through the continuous adjoint equations,

$$L_\Omega^*(\phi) - \left(\frac{\partial j_\Omega}{\partial U}\right)^T = 0, \quad \text{in } \Omega, \tag{B.14}$$

and boundary conditions,

$$\int_\Gamma \left(L_\Gamma^*(\phi) - \left(\frac{\partial j_\Gamma}{\partial U}\right)^T\right)^T \delta U d\Gamma = 0, \tag{B.15}$$

giving the perturbation to the objective function as

$$\delta\mathcal{J}_C = \delta\mathcal{L} = \int_\Omega \frac{\partial j_\Omega}{\partial \alpha}\delta\alpha d\Omega + \int_\Gamma \frac{\partial j_\Gamma}{\partial \alpha}\delta\alpha d\Gamma - \int_\Omega \phi^T \partial_i \left(\frac{\partial F_i}{\partial \alpha}\delta\alpha\right) d\Omega. \tag{B.16}$$

B.2 Laminar Navier-Stokes flow

B.2.1 Frozen-viscosity continuous adjoint equations

Starting from the same general continuous objective function as used for Euler flow, (B.1), we can again enforce the governing equations $\mathcal{N}$ through the Lagrangian, (B.2).

However, to derive the perturbation to this Lagrangian we note that the governing equations, (5.16), are now different. Given the form of these equations, we can rewrite them as

$$\mathcal{N} = \partial_i \left(F_i - \mu\left(F_i^{v1} + \left(\frac{1}{Pr}\right)F_i^{v2}\right)\right) = 0, \tag{B.17}$$

and thus the perturbation to these becomes

$$\delta\mathcal{N} = \partial_i \left(\delta F_i - \mu\left(\delta F_i^{v1} + \left(\frac{1}{Pr}\right)\delta F_i^{v2}\right)\right), \tag{B.18}$$

noting that perturbation to the viscosity is neglected.

The perturbation to the convective flux vector, δF_i, is the same as for Euler flow, and can be handled the same way as previously, however we must also now consider perturbation to the viscous terms. When considering the perturbations to F_i^{v1} and F_i^{v2}, we note that both of these depend not just on U, but also its derivative, $\partial_j U$, giving

$$\delta F_i^{v1} = \frac{\partial F_i^{v1}}{\partial U}\delta U + \frac{\partial F_i^{v1}}{\partial(\partial_j U)}\delta(\partial_j U) + \frac{\partial F_i^{v1}}{\partial \alpha}\delta\alpha, \tag{B.19}$$

and

$$\delta F_i^{v2} = \frac{\partial F_i^{v2}}{\partial U}\delta U + \frac{\partial F_i^{v2}}{\partial(\partial_j U)}\delta(\partial_j U) + \frac{\partial F_i^{v2}}{\partial \alpha}\delta\alpha, \tag{B.20}$$

and thus finally the perturbation to the governing equations can be written as

$$\begin{aligned}
\delta\mathcal{N} \;=\; & \partial_i\left(\frac{\partial F_i}{\partial U}\delta U\right) + \partial_i\left(\frac{\partial F_i}{\partial \alpha}\delta\alpha\right) \\
& -\partial_i\left(\mu\left(\frac{\partial F_i^{v1}}{\partial U} + \left(\frac{1}{Pr}\right)\frac{\partial F_i^{v2}}{\partial U}\right)\delta U\right) \\
& -\partial_i\left(\mu\left(\frac{\partial F_i^{v1}}{\partial(\partial_j U)} + \left(\frac{1}{Pr}\right)\frac{\partial F_i^{v2}}{\partial(\partial_j U)}\right)\delta(\partial_j U)\right) \\
& -\partial_i\left(\mu\left(\frac{\partial F_i^{v1}}{\partial \alpha} + \left(\frac{1}{Pr}\right)\frac{\partial F_i^{v2}}{\partial \alpha}\right)\delta\alpha\right).
\end{aligned} \tag{B.21}$$

To simplify slightly the working we now introduce the substitutions

$$\mathcal{A}_1 = \mu\left(\frac{\partial F_i^{v1}}{\partial \alpha} + \left(\frac{1}{Pr}\right)\frac{\partial F_i^{v2}}{\partial \alpha}\right), \tag{B.22}$$

$$\mathcal{A}_2 = \mu\left(\frac{\partial F_i^{v1}}{\partial U} + \left(\frac{1}{Pr}\right)\frac{\partial F_i^{v2}}{\partial U}\right), \tag{B.23}$$

and

$$\mathcal{A}_3 = \mu\left(\frac{\partial F_i^{v1}}{\partial(\partial_j U)} + \left(\frac{1}{Pr}\right)\frac{\partial F_i^{v2}}{\partial(\partial_j U)}\right). \tag{B.24}$$

The perturbation to the Lagrangian can thus be written, grouping terms explicitly dependent on $\delta\alpha$, δU and $\delta(\partial_j U)$,

$$\begin{aligned}
\delta\mathcal{L} \;=\; & \int_\Omega \frac{\partial j_\Omega}{\partial \alpha}\delta\alpha d\Omega + \int_\Gamma \frac{\partial j_\Gamma}{\partial \alpha}\delta\alpha d\Gamma - \int_\Omega \phi^T\partial_i\left(\frac{\partial F_i}{\partial \alpha}\delta\alpha\right)d\Omega + \int_\Omega \phi^T\partial_i\left(\mathcal{A}_1\delta\alpha\right)d\Omega \\
& + \int_\Omega \frac{\partial j_\Omega}{\partial U}\delta U d\Omega + \int_\Gamma \frac{\partial j_\Gamma}{\partial U}\delta U d\Gamma - \int_\Omega \phi^T\partial_i\left(\frac{\partial F_i}{\partial U}\delta U\right)d\Omega \\
& + \int_\Omega \phi^T\partial_i\left(\mathcal{A}_2\delta U\right)d\Omega + \int_\Omega \phi^T\partial_i\left(\mathcal{A}_3\delta(\partial_j U)\right)d\Omega.
\end{aligned} \tag{B.25}$$

We can handle the third from last term as previously for Euler flow, and, in a similar way, applying integration by parts to the last two terms, we can write

$$\int_\Omega \phi^T\partial_i\left(\mathcal{A}_2\delta U\right)d\Omega = \int_\Gamma \phi^T\mathcal{A}_2\delta U\hat{n}_i d\Gamma - \int_\Omega\left(\partial_i\phi^T\right)\mathcal{A}_2\delta U d\Omega, \tag{B.26}$$

and

$$\int_\Omega \phi^T \partial_i \left(\mathcal{A}_3 \delta(\partial_j U)\right) d\Omega = \int_\Gamma \phi^T \mathcal{A}_3 \delta(\partial_j U) \hat{n}_i d\Gamma - \int_\Omega \left(\partial_i \phi^T\right) \mathcal{A}_3 \delta(\partial_j U) d\Omega. \tag{B.27}$$

We also note that by Young's theorem the order of taking partial derivatives does not matter, so we may make the substitution $\delta(\partial_j U) = \partial_j(\delta U)$ in the domain integral on the right hand side of (B.27), giving

$$\int_\Omega \left(\partial_i \phi^T\right) \mathcal{A}_3 \delta(\partial_j U) d\Omega = \int_\Omega \left(\partial_i \phi^T\right) \mathcal{A}_3 \partial_j(\delta U) d\Omega, \tag{B.28}$$

which allows a second integration by parts to be applied, giving

$$\int_\Omega \left(\partial_i \phi^T\right) \mathcal{A}_3 \delta(\partial_j U) d\Omega = \int_\Gamma \left(\partial_i \phi^T\right) \mathcal{A}_3 \delta U \hat{n}_j d\Gamma - \int_\Omega \left(\partial_j \left(\left(\partial_i \phi^T\right) \mathcal{A}_3\right)\right) \delta U d\Omega. \tag{B.29}$$

Combining all these terms, the perturbation to the Lagrangian then becomes

$$\begin{aligned} \delta\mathcal{L} \quad = \quad & \int_\Omega \left(\frac{\partial j_\Omega}{\partial \alpha} \delta\alpha - \phi^T \partial_i \left(\left(\frac{\partial F_i}{\partial \alpha} - \mathcal{A}_1 \right) \delta\alpha \right) \right) d\Omega + \int_\Gamma \frac{\partial j_\Gamma}{\partial \alpha} \delta\alpha d\Gamma \\ & - \int_\Omega \left(L^*_\Omega(\phi) - \left(\frac{\partial j_\Omega}{\partial U} \right)^T \right)^T \delta U d\Omega \\ & - \int_\Gamma \left(\left(L^*_\Gamma(\phi) - \left(\frac{\partial j_\Gamma}{\partial U} \right)^T \right)^T \delta U - \phi^T \mathcal{A}_3 \delta(\partial_j U) \hat{n}_i \right) d\Gamma, \end{aligned} \tag{B.30}$$

where the adjoint linear operators are

$$L^*_\Omega(\phi) = -\left(\frac{\partial F_i}{\partial U} - \mathcal{A}_2 \right)^T \partial_i \phi - \partial_j \left(\mathcal{A}_3^T \partial_i \phi \right), \tag{B.31}$$

and

$$L^*_\Gamma(\phi) = \left(\left(\frac{\partial F_i}{\partial U} - \mathcal{A}_2 \right) \hat{n}_i \right)^T \phi + \left(\mathcal{A}_3 \hat{n}_j \right)^T \partial_i \phi. \tag{B.32}$$

We can then remove the dependence on the flow perturbation through the continuous adjoint equations, (B.14), and boundary conditions,

$$\int_\Gamma \left(\left(L^*_\Gamma(\phi) - \left(\frac{\partial j_\Gamma}{\partial U} \right)^T \right)^T \delta U - \phi^T \mathcal{A}_3 \delta(\partial_j U) \hat{n}_i \right) d\Gamma = 0, \tag{B.33}$$

giving the perturbation to the objective function as

$$\delta\mathcal{J}_C = \delta\mathcal{L} = \int_\Omega \left(\frac{\partial j_\Omega}{\partial \alpha} \delta\alpha - \phi^T \partial_i \left(\left(\frac{\partial F_i}{\partial \alpha} - \mathcal{A}_1 \right) \delta\alpha \right) \right) d\Omega + \int_\Gamma \frac{\partial j_\Gamma}{\partial \alpha} \delta\alpha d\Gamma. \tag{B.34}$$

B.2.2 Full continuous adjoint equations

Starting from the same Lagrangian used above for the frozen-viscosity case, we now include the perturbation to the viscosity in the perturbation to the governing equations, i.e.,

$$\delta\mathcal{N} = \partial_i \left(\delta F_i - \left(F_i^{v1} + \left(\frac{1}{Pr} \right) F_i^{v2} \right) \delta\mu - \mu \left(\delta F_i^{v1} + \left(\frac{1}{Pr} \right) \delta F_i^{v2} \right) \right). \tag{B.35}$$

The perturbation to the viscosity may be written

$$\delta\mu = \frac{\partial\mu}{\partial U}\delta U + \frac{\partial\mu}{\partial\alpha}\delta\alpha, \tag{B.36}$$

and thus the perturbation to the governing equations can now be written as

$$\begin{aligned}
\delta\mathcal{N} \;=\; & \partial_i \left(\frac{\partial F_i}{\partial U}\delta U \right) + \partial_i \left(\frac{\partial F_i}{\partial\alpha}\delta\alpha \right) \\
& -\partial_i \left(\left(F_i^{v1} + \left(\frac{1}{Pr} \right) F_i^{v2} \right) \frac{\partial\mu}{\partial U}\delta U \right) \\
& -\partial_i \left(\left(F_i^{v1} + \left(\frac{1}{Pr} \right) F_i^{v2} \right) \frac{\partial\mu}{\partial\alpha}\delta\alpha \right) \\
& -\partial_i \left(\mu \left(\frac{\partial F_i^{v1}}{\partial U} + \left(\frac{1}{Pr} \right) \frac{\partial F_i^{v2}}{\partial U} \right) \delta U \right) \\
& -\partial_i \left(\mu \left(\frac{\partial F_i^{v1}}{\partial(\partial_j U)} + \left(\frac{1}{Pr} \right) \frac{\partial F_i^{v2}}{\partial(\partial_j U)} \right) \delta(\partial_j U) \right) \\
& -\partial_i \left(\mu \left(\frac{\partial F_i^{v1}}{\partial\alpha} + \left(\frac{1}{Pr} \right) \frac{\partial F_i^{v2}}{\partial\alpha} \right) \delta\alpha \right).
\end{aligned} \tag{B.37}$$

Introducing the same substitutions as previously, and also

$$\mathcal{A}_4 = \left(F_i^{v1} + \left(\frac{1}{Pr} \right) F_i^{v2} \right) \frac{\partial\mu}{\partial\alpha}, \tag{B.38}$$

and

$$\mathcal{A}_5 = \left(F_i^{v1} + \left(\frac{1}{Pr} \right) F_i^{v2} \right) \frac{\partial\mu}{\partial U}, \tag{B.39}$$

and grouping terms explicitly dependent on $\delta\alpha$, δU and $\delta(\partial_j U)$, the perturbation to the Lagrangian

can be written

$$\begin{aligned}\delta\mathcal{L} &= \int_\Omega \frac{\partial j_\Omega}{\partial\alpha}\delta\alpha d\Omega + \int_\Gamma \frac{\partial j_\Gamma}{\partial\alpha}\delta\alpha d\Gamma - \int_\Omega \phi^T\partial_i\left(\frac{\partial F_i}{\partial\alpha}\delta\alpha\right)d\Omega \\ &+ \int_\Omega \phi^T\partial_i\left(\mathcal{A}_1\delta\alpha\right)d\Omega + \int_\Omega \phi^T\partial_i\left(\mathcal{A}_4\delta\alpha\right)d\Omega \\ &+ \int_\Omega \frac{\partial j_\Omega}{\partial U}\delta U d\Omega + \int_\Gamma \frac{\partial j_\Gamma}{\partial U}\delta U d\Gamma - \int_\Omega \phi^T\partial_i\left(\frac{\partial F_i}{\partial U}\delta U\right)d\Omega \\ &+ \int_\Omega \phi^T\partial_i\left(\mathcal{A}_2\delta U\right)d\Omega + \int_\Omega \phi^T\partial_i\left(\mathcal{A}_5\delta U\right)d\Omega \\ &+ \int_\Omega \phi^T\partial_i\left(\mathcal{A}_3\delta(\partial_j U)\right)d\Omega.\end{aligned} \tag{B.40}$$

We can handle the additional, second from last, term by again applying integration by parts, thus

$$\int_\Omega \phi^T\partial_i\left(\mathcal{A}_5\delta U\right)d\Omega = \int_\Gamma \phi^T\mathcal{A}_5\delta U\hat{n}_i d\Gamma - \int_\Omega\left(\partial_i\phi^T\right)\mathcal{A}_5\delta U d\Omega, \tag{B.41}$$

and then combining terms, including those from the frozen-viscosity derivation, the perturbation to the Lagrangian then becomes

$$\begin{aligned}\delta\mathcal{L} &= \int_\Omega\left(\frac{\partial j_\Omega}{\partial\alpha}\delta\alpha - \phi^T\partial_i\left(\left(\frac{\partial F_i}{\partial\alpha} - \mathcal{A}_1 - \mathcal{A}_4\right)\delta\alpha\right)\right)d\Omega + \int_\Gamma \frac{\partial j_\Gamma}{\partial\alpha}\delta\alpha d\Gamma \\ &- \int_\Omega\left(L^*_\Omega(\phi) - \left(\frac{\partial j_\Omega}{\partial U}\right)^T\right)^T\delta U d\Omega \\ &- \int_\Gamma\left(\left(L^*_\Gamma(\phi) - \left(\frac{\partial j_\Gamma}{\partial U}\right)^T\right)^T\delta U - \phi^T\mathcal{A}_3\delta(\partial_j U)\hat{n}_i\right)d\Gamma,\end{aligned} \tag{B.42}$$

where

$$L^*_\Omega(\phi) = -\left(\frac{\partial F_i}{\partial U} - \mathcal{A}_2 - \mathcal{A}_5\right)^T\partial_i\phi - \partial_j\left(\mathcal{A}_3^T\partial_i\phi\right), \tag{B.43}$$

and

$$L^*_\Gamma(\phi) = \left(\left(\frac{\partial F_i}{\partial U} - \mathcal{A}_2 - \mathcal{A}_5\right)\hat{n}_i\right)^T\phi + \left(\mathcal{A}_3\hat{n}_j\right)^T\partial_i\phi. \tag{B.44}$$

We can then remove the dependence on the flow perturbation through the continuous adjoint equation (B.14) and boundary conditions (B.33), giving the perturbation to the objective function as

$$\delta\mathcal{J}_C = \delta\mathcal{L} = \int_\Omega\left(\frac{\partial j_\Omega}{\partial\alpha}\delta\alpha - \phi^T\partial_i\left(\left(\frac{\partial F_i}{\partial\alpha} - \mathcal{A}_1 - \mathcal{A}_4\right)\delta\alpha\right)\right)d\Omega + \int_\Gamma \frac{\partial j_\Gamma}{\partial\alpha}\delta\alpha d\Gamma. \tag{B.45}$$

B.3 Reynolds-Averaged Navier-Stokes flow

B.3.1 Frozen-viscosity continuous adjoint problem

Starting from the same Lagrangian used above for the frozen-viscosity Navier-Stokes case, we now include the eddy viscosity terms in the mean-flow governing equations, i.e.,

$$\mathcal{N} = \partial_i \left(F_i - \mu \left(F_i^{v1} + \left(\frac{1}{Pr} \right) F_i^{v2} \right) - \mu_T \left(F_i^{v1} + \left(\frac{1}{Pr} \right) F_i^{v2} \right) \right) = 0, \tag{B.46}$$

and thus its perturbation becomes

$$\begin{aligned}
\delta\mathcal{N} \;=\; & \partial_i \left(\frac{\partial F_i}{\partial U} \delta U \right) + \partial_i \left(\frac{\partial F_i}{\partial \alpha} \delta\alpha \right) \\
& - \partial_i \left(\mu \left(\frac{\partial F_i^{v1}}{\partial U_L} + \left(\frac{1}{Pr} \right) \frac{\partial F_i^{v2}}{\partial U_L} \right) \delta U_L \right) \\
& - \partial_i \left(\mu \left(\frac{\partial F_i^{v1}}{\partial (\partial_j U_L)} + \left(\frac{1}{Pr} \right) \frac{\partial F_i^{v2}}{\partial (\partial_j U_L)} \right) \delta (\partial_j U_L) \right) \\
& - \partial_i \left(\mu \left(\frac{\partial F_i^{v1}}{\partial \alpha} + \left(\frac{1}{Pr_T} \right) \frac{\partial F_i^{v2}}{\partial \alpha} \right) \delta\alpha \right) \\
& - \partial_i \left(\mu_T \left(\frac{\partial F_i^{v1}}{\partial U_L} + \left(\frac{1}{Pr_T} \right) \frac{\partial F_i^{v2}}{\partial U_L} \right) \delta U_L \right) \\
& - \partial_i \left(\mu_T \left(\frac{\partial F_i^{v1}}{\partial (\partial_j U_L)} + \left(\frac{1}{Pr_T} \right) \frac{\partial F_i^{v2}}{\partial (\partial_j U_L)} \right) \delta (\partial_j U_L) \right) \\
& - \partial_i \left(\mu_T \left(\frac{\partial F_i^{v1}}{\partial \alpha} + \left(\frac{1}{Pr_T} \right) \frac{\partial F_i^{v2}}{\partial \alpha} \right) \delta\alpha \right),
\end{aligned} \tag{B.47}$$

noting that we have neglected perturbations to the laminar and eddy viscosities.

It can be seen form inspection that by considering the modification $\mu \Rightarrow (\mu + \mu_T)$ this follows the same derivation as laminar Navier-Stokes flow, and thus we can simply write that the perturbation to the Lagrangian becomes

$$\begin{aligned}
\delta\mathcal{L} \;=\; & \int_\Omega \left(\frac{\partial j_\Omega}{\partial \alpha} \delta\alpha - \phi_L^T \partial_i \left(\left(\frac{\partial F_i}{\partial \alpha} - \mathcal{A}_1 - \mathcal{B}_1 \right) \delta\alpha \right) \right) d\Omega + \int_\Gamma \frac{\partial j_\Gamma}{\partial \alpha} \delta\alpha \, d\Gamma \\
& - \int_\Omega \left(L_\Omega^*(\phi) - \left(\frac{\partial j_\Omega}{\partial U_L} \right)^T \right)^T \delta U_L \, d\Omega \\
& - \int_\Gamma \left(\left(L_\Gamma^*(\phi) - \left(\frac{\partial j_\Gamma}{\partial U_L} \right)^T \right)^T \delta U_L - \phi^T \left(\mathcal{A}_3 + \mathcal{B}_3 \right) \delta (\partial_j U_L) \hat{n}_i \right) d\Gamma,
\end{aligned} \tag{B.48}$$

where

$$L^*_\Omega(\phi) = -\left(\frac{\partial F_i}{\partial U_L} - \mathcal{A}_2 - \mathcal{B}_2\right)^T \partial_i\phi - \partial_j\left(\left(\mathcal{A}_3 + \mathcal{B}_3\right)^T \partial_i\phi\right), \tag{B.49}$$

and

$$L^*_\Gamma(\phi) = \left(\left(\frac{\partial F_i}{\partial U_L} - \mathcal{A}_2 - \mathcal{B}_2\right)\hat{n}_i\right)^T \phi + \left(\left(\mathcal{A}_3 + \mathcal{B}_3\right)\hat{n}_j\right)^T \partial_i\phi, \tag{B.50}$$

where we introduce the substitutions

$$\mathcal{B}_1 = \mu_T\left(\frac{\partial F_i^{v1}}{\partial\alpha} + \left(\frac{1}{Pr_T}\right)\frac{\partial F_i^{v2}}{\partial\alpha}\right), \tag{B.51}$$

$$\mathcal{B}_2 = \mu_T\left(\frac{\partial F_i^{v1}}{\partial U_L} + \left(\frac{1}{Pr_T}\right)\frac{\partial F_i^{v2}}{\partial U_L}\right), \tag{B.52}$$

and

$$\mathcal{B}_3 = \mu_T\left(\frac{\partial F_i^{v1}}{\partial(\partial_j U_L)} + \left(\frac{1}{Pr_T}\right)\frac{\partial F_i^{v2}}{\partial(\partial_j U_L)}\right). \tag{B.53}$$

We can then remove the dependence on the flow perturbation through the continuous adjoint equations, (B.14), and boundary conditions,

$$\int_\Gamma\left(\left(L^*_\Gamma(\phi) - \left(\frac{\partial j_\Gamma}{\partial U_L}\right)^T\right)^T \delta U_L - \phi^T\left(\mathcal{A}_3 + \mathcal{B}_3\right)\delta(\partial_j U_L)\hat{n}_i\right) d\Gamma = 0, \tag{B.54}$$

giving the perturbation to the objective function as

$$\delta\mathcal{J}_C = \delta\mathcal{L} = \int_\Omega\left(\frac{\partial j_\Omega}{\partial\alpha}\delta\alpha - \phi_L^T\partial_i\left(\left(\frac{\partial F_i}{\partial\alpha} - \mathcal{A}_1 - \mathcal{B}_1\right)\delta\alpha\right)\right)d\Omega + \int_\Gamma\frac{\partial j_\Gamma}{\partial\alpha}\delta\alpha d\Gamma. \tag{B.55}$$

B.3.2 Hybrid adjoint equations

Starting from a hybrid version of the general continuous objective function used for Euler flow, (5.5), that can be either continuous or discrete, we now enforce the mean-flow governing equations $\mathcal{N}_L$ and the eddy viscosity and turbulence model numerical residuals $\mathcal{R}_{\mu_T}$ and $\mathcal{R}_T$ by introducing the modified Lagrangian

$$\begin{aligned}\mathcal{L} &= \beta\left(\int_\Omega j_\Omega d\Omega + \int_\Gamma j_\Gamma d\Gamma\right) + (1-\beta)\frac{\mathfrak{D}\mathcal{J}_D}{\mathfrak{D}\alpha}\Delta\alpha \\ &\quad - \int_\Omega\varphi_C^T\mathcal{N}_L d\Omega - \sum_{p=1}^N\varphi_{\mu_{T_p}}^T\mathcal{R}_{\mu_{T_p}}\Omega_p + \sum_{p=1}^N\varphi_{D_p}^T\mathcal{R}_{T_p},\end{aligned} \tag{B.56}$$

where $\varphi = \{\varphi_C, \varphi_{\mu_T}, \varphi_D\}$ are the Lagrange multipliers (or hybrid adjoint variables).

Taking the perturbation of $\mathcal{L}$ to a change in some parameter α we then get

$$\begin{aligned}\{\delta,\Delta\}\mathcal{L} &= \beta\delta\mathcal{J}_C + (1-\beta)\Delta\mathcal{J}_D - \int_\Omega \varphi_C^T \delta\mathcal{N} d\Omega \\ &\quad - \sum_{p=1}^{N} \varphi_{\mu_{T_p}}^T \Delta\mathcal{R}_{\mu_{T_p}} \Delta\Omega_p + \sum_{p=1}^{N} \varphi_{D_p}^T \Delta\mathcal{R}_{T_p}.\end{aligned} \tag{B.57}$$

We can linearize the continuous objective function perturbations and mean-flow equations in the same way as shown previously for the laminar Navier-Stokes continuous adjoints and the RANS frozen-viscosity continuous adjoint equation, and the discrete objective function and turbulence model residuals can be discretely linearized as

$$\Delta\mathcal{J}_D = \sum_{p=1}^{N} \frac{\mathfrak{D}\mathcal{J}_D}{\mathfrak{D}U_p}\Delta U_p + \frac{\mathfrak{D}\mathcal{J}_D}{\mathfrak{D}\alpha}\Delta\alpha, \tag{B.58}$$

and

$$\Delta\mathcal{R}_{T_p} = \sum_{q=1}^{N} \frac{\mathfrak{D}\mathcal{R}_{T_p}}{\mathfrak{D}U_q}\Delta U_q + \frac{\mathfrak{D}\mathcal{R}_{T_p}}{\mathfrak{D}\alpha}\Delta\alpha. \tag{B.59}$$

We also now discretely linearize $\mathcal{R}_{\mu_T}$ so that

$$\Delta\mathcal{R}_{\mu_{T_p}} = \Delta\mu_{T_p} - \Delta f_p, \tag{B.60}$$

where

$$\Delta f_p = \sum_{q=1}^{N} \frac{\mathfrak{D}f_p}{\mathfrak{D}U_q}\Delta U_q + \frac{\mathfrak{D}f_p}{\mathfrak{D}\alpha}\Delta\alpha. \tag{B.61}$$

The perturbation to the Lagrangian can thus be written, after performing the same integration

by parts steps as previously for the laminar Navier-Stokes continuous adjoints and the RANS frozen-viscosity continuous adjoint equation,

$$\begin{aligned}
\{\delta,\Delta\}\mathcal{L} \;=\; & \int_{\Omega}\left(\beta\frac{\partial j_{\Omega}}{\partial\alpha}\delta\alpha-\varphi_{C}^{T}\partial_{i}\left(\left(\frac{\partial F_{i}}{\partial\alpha}-\mathcal{A}_{1}-\mathcal{A}_{4}-\mathcal{B}_{1}\right)\delta\alpha\right)\right)d\Omega\\
& +\int_{\Gamma}\beta\frac{\partial j_{\Gamma}}{\partial\alpha}\delta\alpha d\Gamma+\left(1-\beta\right)\frac{\mathfrak{D}\mathcal{J}_{D}}{\mathfrak{D}\alpha}\Delta\alpha\\
& +\sum_{p=1}^{N}\varphi_{\mu_{T_{p}}}^{T}\frac{\mathfrak{D}f_{p}}{\mathfrak{D}\alpha}\Delta\alpha\Omega_{p}+\sum_{p=1}^{N}\varphi_{D_{p}}^{T}\frac{\mathfrak{D}\mathcal{R}_{T_{p}}}{\mathfrak{D}\alpha}\Delta\alpha\\
& -\int_{\Omega}\left(L_{\Omega}^{*}(\varphi_{C})-\beta\left(\frac{\partial j_{\Omega}}{\partial U}\right)^{T}\right)^{T}\delta U d\Omega\\
& -\int_{\Gamma}\left(\left(L_{\Gamma}^{*}(\varphi_{C})-\beta\left(\frac{\partial j_{\Gamma}}{\partial U}\right)^{T}\right)^{T}\delta U-\varphi_{C}^{T}\left(\mathcal{A}_{3}+\mathcal{B}_{3}\right)\delta(\partial_{j}U)\hat{n}_{i}\right)d\Gamma\\
& -\int_{\Omega}\left(\partial_{i}\varphi_{C}^{T}\right)\mathcal{C}_{1}\delta\mu_{T}d\Omega+\int_{\Gamma}\varphi_{C}^{T}\mathcal{C}_{1}\hat{n}_{i}\delta\mu_{T}d\Gamma\\
& +\left(1-\beta\right)\sum_{p=1}^{N}\frac{\mathfrak{D}\mathcal{J}_{D}}{\mathfrak{D}U_{p}}\Delta U_{p}+\sum_{p=1}^{N}\sum_{q=1}^{N}\varphi_{D_{q}}^{T}\frac{\mathfrak{D}\mathcal{R}_{T_{q}}}{\mathfrak{D}U_{p}}\Delta U_{p}\\
& +\sum_{p=1}^{N}\sum_{q=1}^{N}\varphi_{\mu_{T_{q}}}^{T}\frac{\mathfrak{D}f_{q}}{\mathfrak{D}U_{p}}\Delta U_{p}\Omega_{q}-\sum_{p=1}^{N}\varphi_{\mu_{T_{p}}}^{T}\Delta\mu_{T_{p}}\Omega_{p},
\end{aligned}\tag{B.62}$$

where the adjoint linear operators are

$$L_{\Omega}^{*}(\varphi_{C})=-\left(\frac{\partial F_{i}}{\partial U}-\mathcal{A}_{2}-\mathcal{A}_{5}-\mathcal{B}_{2}\right)^{T}\partial_{i}\varphi_{C}-\partial_{j}\left(\left(\mathcal{A}_{3}+\mathcal{B}_{3}\right)^{T}\partial_{i}\varphi_{C}\right),\tag{B.63}$$

and

$$L_{\Gamma}^{*}(\varphi_{C})=\left(\left(\frac{\partial F_{i}}{\partial U}-\mathcal{A}_{2}-\mathcal{A}_{5}-\mathcal{B}_{2}\right)\hat{n}_{i}\right)^{T}\varphi_{C}+\left(\left(\mathcal{A}_{3}+\mathcal{B}_{3}\right)\hat{n}_{j}\right)^{T}\partial_{i}\varphi_{C},\tag{B.64}$$

and where we have introduced the additional substitution,

$$\mathcal{C}_{1}=\left(F_{i}^{v1}+\left(\frac{1}{Pr_{T}}\right)F_{i}^{v2}\right).\tag{B.65}$$

We can then remove the dependence on the flow perturbation through the combined hybrid

adjoint equations and boundary conditions, for the flow variables,

$$\begin{aligned}
&\int_\Omega \left(L^*_\Omega(\varphi_C) - \beta \left(\frac{\partial j_\Omega}{\partial U} \right)^T \right)^T \delta U d\Omega \\
+ \int_\Gamma \Bigg(\Bigg(L^*_\Gamma(\varphi_C) - \beta \left(\frac{\partial j_\Gamma}{\partial U} \right)^T \Bigg)^T \delta U - \varphi_C^T \left(\mathcal{A}_3 + \mathcal{B}_3 \right) \delta(\partial_j U) \hat{n}_i \Bigg) d\Gamma \\
&- (1-\beta) \sum_{p=1}^N \frac{\mathfrak{D}\mathcal{J}_D}{\mathfrak{D}U_p} \Delta U_p - \sum_{p=1}^N \sum_{q=1}^N \varphi_{D_q}^T \frac{\mathfrak{D}\mathcal{R}_{T_q}}{\mathfrak{D}U_p} \Delta U_p \\
&- \sum_{p=1}^N \sum_{q=1}^N \varphi_{\mu_{T_q}}^T \frac{\mathfrak{D}f_q}{\mathfrak{D}U_p} \Delta U_p \Omega_q \quad = \quad 0,
\end{aligned} \tag{B.66}$$

and for the eddy viscosity,

$$\int_\Omega \left(\partial_i \varphi_C^T \right) \mathcal{C}_1 \delta \mu_T d\Omega + \sum_{p=1}^N \varphi_{\mu_{T_p}}^T \Delta \mu_{T_p} \Omega_p - \int_\Gamma \varphi_C^T \mathcal{C}_1 \hat{n}_i \delta \mu_T d\Gamma = 0, \tag{B.67}$$

giving the perturbation to the objective function as

$$\begin{aligned}
\{\delta, \Delta\}\mathcal{L} \quad = \quad & \int_\Omega \left(\beta \frac{\partial j_\Omega}{\partial \alpha} \delta\alpha - \varphi_C^T \partial_i \left(\left(\frac{\partial F_i}{\partial \alpha} - \mathcal{A}_1 - \mathcal{A}_4 - \mathcal{B}_1 \right) \delta\alpha \right) \right) d\Omega \\
& + \int_\Gamma \beta \frac{\partial j_\Gamma}{\partial \alpha} \delta\alpha d\Gamma + (1-\beta) \frac{\mathfrak{D}\mathcal{J}_D}{\mathfrak{D}\alpha} \Delta\alpha \\
& + \sum_{p=1}^N \varphi_{\mu_{T_p}}^T \frac{\mathfrak{D}f_p}{\mathfrak{D}\alpha} \Delta\alpha \Omega_p + \sum_{p=1}^N \varphi_{D_p}^T \frac{\mathfrak{D}\mathcal{R}_{T_p}}{\mathfrak{D}\alpha} \Delta\alpha.
\end{aligned} \tag{B.68}$$

As previously in quasi-one-dimensional flow, we now separate the combined equations and boundary conditions. The hybrid adjoint equations are then

$$\begin{aligned}
&\int_\Omega \left(L^*_\Omega(\varphi_C) - \beta \left(\frac{\partial j_\Omega}{\partial U} \right)^T \right)^T \delta U d\Omega \\
&- (1-\beta) \sum_{p=1}^N \sum_{q=1}^N \frac{\mathfrak{D}j_q}{\mathfrak{D}U_p} \Omega_q \Delta U_p - \sum_{p=1}^N \sum_{q=1}^N \varphi_{D_q}^T \frac{\mathfrak{D}\mathcal{R}^{(*)}_{T_q}}{\mathfrak{D}U_p} \Delta U_p \\
&- \sum_{p=1}^N \sum_{q=1}^N \varphi_{\mu_{T_q}}^T \frac{\mathfrak{D}f_q}{\mathfrak{D}U_p} \Delta U_p \Omega_q \quad = \quad 0,
\end{aligned} \tag{B.69}$$

and

$$\int_\Omega \left(\partial_i \varphi_C^T \right) \mathcal{C}_1 \delta \mu_T d\Omega + \sum_{p=1}^N \varphi_{\mu_{T_p}}^T \Delta \mu_T \Omega_p = 0, \tag{B.70}$$

and the hybrid boundary conditions are

$$\begin{aligned}\int_\Gamma \left(\left(L_\Gamma^*(\varphi_C) - \beta \left(\frac{\partial j_\Gamma}{\partial U} \right)^T \right)^T \delta U - \varphi_C^T \left(\mathcal{A}_3 + \mathcal{B}_3 \right) \delta(\partial_j U) \hat{n}_i \right) d\Gamma \\ - (1-\beta) \sum_{p=1}^{N_\Gamma} \sum_{q=1}^{N_\Gamma} \frac{\mathfrak{D} j_{\Gamma_q}}{\mathfrak{D} U_p} \Gamma_q \Delta U_p - \sum_{p=1}^{N_\Gamma} \sum_{q=1}^{N_\Gamma} \varphi_{D_q}^T \frac{\mathfrak{D}(\hat{F}_T)_{\Gamma_q}}{\mathfrak{D} U_p} \Delta U_p &= 0,\end{aligned} \tag{B.71}$$

and

$$\int_\Gamma \varphi_C^T \mathcal{C}_1 \hat{n}_i \delta \mu_T d\Gamma = 0, \tag{B.72}$$

where we note that the boundary objective function should only explicitly depend on the boundary cells, and we have again separated out the flux across the boundary from the residual in the boundary cell, where appropriate,

$$\mathcal{R}_{T_p} = (\hat{F}_T)_{\Gamma_p} + \mathcal{R}_{T_p}^*. \tag{B.73}$$

The final part of this derivation is to cancel out the flow perturbations in the hybrid adjoint equations. Considering the first of these, (B.69), to do this we first note that the domain integral can be written as a sum of the domain integrals over each cell, i.e.,

$$\begin{aligned}\sum_{p=1}^{N} \int_{\Omega_p} \left(\beta \frac{\partial j_\Omega}{\partial U} - L_\Omega^T(\varphi_C) \right) \delta U d\Omega \\ + (1-\beta) \sum_{p=1}^{N} \sum_{q=1}^{N} \frac{\mathfrak{D} j_q}{\mathfrak{D} U_p} \Omega_q \Delta U_p + \sum_{p=1}^{N} \sum_{q=1}^{N} \varphi_{D_q}^T \frac{\mathfrak{D} \mathcal{R}_{T_q}^{(*)}}{\mathfrak{D} U_p} \Delta U_p \\ + \sum_{p=1}^{N} \sum_{q=1}^{N} \varphi_{\mu_{T_q}}^T \frac{\mathfrak{D} f_q}{\mathfrak{D} U_p} \Delta U_p \Delta \Omega_q &= 0.\end{aligned} \tag{B.74}$$

We then drop the leading summation terms, giving

$$\begin{aligned}\int_{\Omega_p} \left(\beta \frac{\partial j_\Omega}{\partial U} - L_\Omega^T(\varphi_C) \right) \delta U d\Omega + (1-\beta) \sum_{q=1}^{N} \frac{\mathfrak{D} j_q}{\mathfrak{D} U_p} \Omega_q \Delta U_p \\ + \sum_{q=1}^{N} \varphi_{D_q}^T \frac{\mathfrak{D} \mathcal{R}_{T_q}^{(*)}}{\mathfrak{D} U_p} \Delta U_p + \sum_{q=1}^{N} \varphi_{\mu_{T_q}}^T \frac{\mathfrak{D} f_q}{\mathfrak{D} U_p} \Delta U_p \Delta \Omega_q &= 0.\end{aligned} \tag{B.75}$$

The next step is to assume the flow perturbation is piecewise constant within each cell, allowing

δU_p to be factored out of the integral, giving

$$\begin{aligned}\left(\int_{\Omega_p}\left(\beta\frac{\partial j_\Omega}{\partial U}-L_\Omega^T(\varphi_C)\right)d\Omega\right)\delta U_p+(1-\beta)\sum_{q=1}^{N}\frac{\mathfrak{D}j_q}{\mathfrak{D}U_p}\Delta\Omega_l\Delta U_p \\ +\sum_{q=1}^{N}\varphi_{D_q}^T\frac{\mathfrak{D}\mathcal{R}_{T_q}^{(*)}}{\mathfrak{D}U_p}\Delta U_p+\sum_{q=1}^{N}\varphi_{\mu_{T_q}}^T\frac{\mathfrak{D}f_q}{\mathfrak{D}U_p}\Delta U_p\Delta\Omega_q &= 0,\end{aligned} \tag{B.76}$$

and finally making the assumption that $\delta U_p \approx \Delta U_p$ we can cancel out the flow perturbations and arrive at the hybrid adjoint equation for the flow and turbulence model variable adjoints

$$\begin{aligned}\int_{\Omega_p}\left(L_\Omega^*(\varphi_C)-\beta\left(\frac{\partial j_\Omega}{\partial U}\right)^T\right)d\Omega-(1-\beta)\sum_{q=1}^{N}\left(\frac{\mathfrak{D}j_q}{\mathfrak{D}U_p}\right)^T\Omega_q \\ -\sum_{q=1}^{N}\left(\frac{\mathfrak{D}\mathcal{R}_{T_q}^{(*)}}{\mathfrak{D}U_p}\right)^T\varphi_{D_q}-\sum_{q=1}^{N}\left(\frac{\mathfrak{D}f_q}{\mathfrak{D}U_p}\right)^T\varphi_{\mu_{T_q}}\Omega_q &= 0.\end{aligned} \tag{B.77}$$

Now considering the eddy viscosity adjoint equation, (B.70), we can discretize the integral and write

$$\sum_{p=1}^{N}\int_{\Omega_p}\left(\partial_i\varphi_C^T\right)\mathcal{C}_1\delta\mu_T d\Omega+\sum_{p=1}^{N}\varphi_{\mu_{T_p}}^T\Delta\mu_T\Delta\Omega_p=0. \tag{B.78}$$

We then drop the leading summation terms, giving

$$\int_{\Omega_p}\left(\partial_i\varphi_C^T\right)\mathcal{C}_1\delta\mu_T d\Omega+\varphi_{\mu_{T_p}}^T\Delta\mu_T\Delta\Omega_p=0, \tag{B.79}$$

and assuming $\delta\mu_T$ is piecewise constant, we may factor it out of the integral

$$\left(\int_{\Omega_p}\left(\partial_i\varphi_C^T\right)\mathcal{C}_1 d\Omega\right)\delta\mu_{T_p}+\varphi_{\mu_{T_p}}^T\Delta\mu_T\Delta\Omega_p=0, \tag{B.80}$$

and assuming $\delta\mu_{T_p}=\Delta\mu_{T_p}$, we can then cancel it out, giving

$$\int_{\Omega_p}\mathcal{C}_1^T\partial_i\varphi_C d\Omega+\varphi_{\mu_{T_p}}\Omega_p=0. \tag{B.81}$$

We can finally substitute equation (B.81) into equation (B.77) to remove the variable φ_{μ_T} and

produce a single set of adjoint equations,

$$\begin{aligned}\int_{\Omega_p}\left(L^*_\Omega(\varphi_C)-\beta\left(\frac{\partial j_\Omega}{\partial U}\right)^T\right)d\Omega-(1-\beta)\sum_{q=1}^{N}\left(\frac{\mathfrak{D}j_q}{\mathfrak{D}U_p}\right)^T\Omega_q \\ -\sum_{q=1}^{N}\left(\frac{\mathfrak{D}\mathcal{R}^{(*)}_{T_q}}{\mathfrak{D}U_p}\right)^T\varphi_{D_q}+\sum_{q=1}^{N}\left(\frac{\mathfrak{D}f_q}{\mathfrak{D}U_p}\right)^T\int_{\Omega_q}\mathcal{C}_1^T\partial_i\varphi_C d\Omega &= 0.\end{aligned} \tag{B.82}$$

Appendix C

Adjoint boundary condition derivations

This appendix presents the derivations of the continuous and hybrid adjoint boundary conditions for two- and three-dimensional flows in full detail.

C.1 Euler flow

C.1.1 Continuous adjoint boundary conditions

The boundary conditions on the adjoint equation are given by (B.15), however, we still need to manipulate these so as to remove the dependence on the flow perturbation. This can be done by considering each type of flow boundary in turn:

Euler wall At an Euler wall the flow boundary condition is that the flow velocity normal to the wall is zero. The consequence of this is that by considering characteristic velocities there is only one adjoint characteristic entering or leaving the wall, and thus only one boundary condition is needed here on the adjoint equation.

Since the shape is held fixed in these derivations, we also note that the linearized version of this flow boundary condition gives

$$\delta u_i \hat{n}_i = 0, \tag{C.1}$$

Writing the Jacobian

$$\frac{\partial F_i}{\partial U} = \begin{pmatrix} 0 & \delta_{ik} & 0 \\ -u_i u_j + \dfrac{\partial p}{\partial \rho}\delta_{ij} & \dfrac{1}{\rho}(\rho u_j \delta_{ik} + \rho u_i \delta_{jk}) + \dfrac{\partial p}{\partial(\rho u_k)}\delta_{ij} & \dfrac{\partial p}{\partial(\rho E)}\delta_{ij} \\ \rho u_i \dfrac{\partial H}{\partial \rho} & H\delta_{ik} + \rho u_i \dfrac{\partial H}{\partial(\rho u_k)} & \rho u_i \dfrac{\partial H}{\partial(\rho E)} \end{pmatrix}, \tag{C.2}$$

we can then use the wall boundary condition to get

$$\frac{\partial F_i}{\partial U}\hat{n}_i = \begin{pmatrix} 0 & \hat{n}_k & 0 \\ \dfrac{\partial p}{\partial \rho}\hat{n}_j & \dfrac{\partial p}{\partial(\rho u_k)}\hat{n}_j & \dfrac{\partial p}{\partial(\rho E)}\hat{n}_j \\ 0 & H\hat{n}_k & 0 \end{pmatrix}. \tag{C.3}$$

Noting that we can also write the flow perturbation as

$$\delta U = \begin{pmatrix} \delta\rho \\ (\delta\rho)u_k + \rho(\delta u_k) \\ \delta(\rho E) \end{pmatrix}, \tag{C.4}$$

we can multiply through, using the flow boundary condition and its linearized form to cancel terms, to obtain

$$\frac{\partial F_i}{\partial U}\hat{n}_i \delta U = \frac{\partial p}{\partial U}\hat{n}_j \delta U, \tag{C.5}$$

and the boundary integral finally becomes

$$\int_S \left(\frac{\partial j_\Gamma}{\partial U} - \phi^T_{\rho u_j} \frac{\partial p}{\partial U}\hat{n}_j \right) \delta U \, d\Gamma = 0. \tag{C.6}$$

We therefore introduce the adjoint boundary condition to remove the dependence on the flow perturbation:

$$\frac{\partial j_\Gamma}{\partial U} - \phi^T_{\rho u_j} \frac{\partial p}{\partial U}\hat{n}_j = 0. \tag{C.7}$$

Far field At the far field the usual characteristic rules apply, and thus for incoming flow across the boundary we require one adjoint boundary condition for subsonic conditions and none for supersonic, and for outgoing flow we require $N+1$ for subsonic and $N+2$ for supersonic conditions, where N is the number of dimensions. Considering objective functions not defined along the far field boundary,

we can also simplify the boundary condition to

$$-\int_{\Gamma_\infty} \phi^T \frac{\partial F_i}{\partial U} \hat{n}_i \delta U d\Gamma = 0. \tag{C.8}$$

C.2 Laminar Navier-Stokes flow

C.2.1 Frozen-viscosity continuous adjoint boundary conditions

The boundary conditions on the adjoint equation are given by (B.33), however, we must again manipulate this so as to remove the dependence on the flow perturbation. Considering each type of boundary condition in turn:

Viscous wall At a viscous wall the flow boundary condition is that the velocity at the wall is zero. The consequence of this is that by considering characteristic velocities there is only one adjoint characteristic entering or leaving the wall, and thus only one boundary condition is needed here on the adjoint equation.

Since the shape is held fixed in these derivations, we also note that the linearized version of this flow boundary condition gives

$$\delta u_i = 0. \tag{C.9}$$

In a similar way to Euler flow, we simplify the Jacobian of the convective flux term using the velocity boundary condition

$$\frac{\partial F_i}{\partial U} = \begin{pmatrix} 0 & \delta_{ik} & 0 \\ \frac{\partial p}{\partial \rho}\delta_{ij} & \frac{\partial p}{\partial(\rho u_k)}\delta_{ij} & \frac{\partial p}{\partial(\rho E)}\delta_{ij} \\ 0 & H\delta_{ik} & 0 \end{pmatrix}. \tag{C.10}$$

Noting now that we can write the flow perturbation as

$$\delta U = \begin{pmatrix} \delta\rho \\ (\delta\rho)u_i + \rho(\delta u_i) \\ \delta(\rho E) \end{pmatrix} = \begin{pmatrix} \delta\rho \\ 0 \\ \delta(\rho E) \end{pmatrix}, \tag{C.11}$$

we can then multiply through to obtain the same condition as for Euler flow, i.e., (C.7).

Now considering the viscous Jacobians we can write

$$\frac{\partial F_i^{v1}}{\partial U} = \begin{pmatrix} 0 & 0 & 0 \\ \dfrac{\partial \tau_{ij}}{\partial \rho} & \dfrac{\partial \tau_{ij}}{\partial (\rho u_l)} & 0 \\ u_k \dfrac{\partial \tau_{ik}}{\partial \rho} + \dfrac{\partial u_k}{\partial \rho}\tau_{ik} & u_k \dfrac{\partial \tau_{ik}}{\partial (\rho u_l)} + \dfrac{\partial u_k}{\partial (\rho u_l)}\tau_{ik} & 0 \end{pmatrix}, \tag{C.12}$$

$$\frac{\partial F_i^{v2}}{\partial U} = \begin{pmatrix} 0 & 0 & 0 \\ 0 & 0 & 0 \\ C_p \dfrac{\partial (\partial_i T)}{\partial \rho} & C_p \dfrac{\partial (\partial_i T)}{\partial (\rho u_l)} & C_p \dfrac{\partial (\partial_i T)}{\partial (\rho E)} \end{pmatrix}, \tag{C.13}$$

$$\frac{\partial F_i^{v1}}{\partial (\partial_m U)} = \begin{pmatrix} 0 & 0 & 0 \\ \dfrac{\partial \tau_{ij}}{\partial (\partial_m \rho)} & \dfrac{\partial \tau_{ij}}{\partial (\partial_m (\rho u_l))} & 0 \\ u_k \dfrac{\partial \tau_{ik}}{\partial (\partial_m \rho)} & u_k \dfrac{\partial \tau_{ik}}{\partial (\partial_m (\rho u_l))} & 0 \end{pmatrix}, \tag{C.14}$$

and

$$\frac{\partial F_i^{v2}}{\partial (\partial_m U)} = \begin{pmatrix} 0 & 0 & 0 \\ 0 & 0 & 0 \\ C_p \dfrac{\partial (\partial_i T)}{\partial (\partial_m \rho)} & C_p \dfrac{\partial (\partial_i T)}{\partial (\partial_m (\rho u_l))} & C_p \dfrac{\partial (\partial_i T)}{\partial (\partial_m (\rho E))} \end{pmatrix}. \tag{C.15}$$

Noting that

$$\frac{\partial u_k}{\partial \rho} = -\frac{u_k}{\rho}, \quad \frac{\partial u_k}{\partial (\rho u_l)} = \frac{1}{\rho}\delta_{kl}, \tag{C.16}$$

and using the viscous boundary condition that the flow velocity at the wall is zero, we can now write

$$F_i^{v1} = \begin{pmatrix} 0 \\ \tau_{ij} \\ 0 \end{pmatrix}, \tag{C.17}$$

$$\frac{\partial F_i^{v1}}{\partial U} = \begin{pmatrix} 0 & 0 & 0 \\ \dfrac{\partial \tau_{ij}}{\partial \rho} & \dfrac{\partial \tau_{ij}}{\partial (\rho u_l)} & 0 \\ 0 & \frac{1}{\rho}\tau_{il} & 0 \end{pmatrix}, \tag{C.18}$$

and

$$\frac{\partial F_i^{v1}}{\partial(\partial_m U)} = \begin{pmatrix} 0 & 0 & 0 \\ \dfrac{\partial \tau_{ij}}{\partial(\partial_m \rho)} & \dfrac{\partial \tau_{ij}}{\partial(\partial_m(\rho u_l))} & 0 \\ 0 & 0 & 0 \end{pmatrix}. \tag{C.19}$$

Collecting these we can then write

$$\mathcal{A}_2 \delta U = \mu \begin{pmatrix} 0 \\ \dfrac{\partial \tau_{ij}}{\partial U}\delta U \\ \left(\dfrac{\partial u_k}{\partial U}\tau_{ik} + \dfrac{C_p}{Pr}\dfrac{\partial(\partial_i T)}{\partial U}\right)\delta U \end{pmatrix}, \tag{C.20}$$

$$\mathcal{A}_3 \delta U = \mu \begin{pmatrix} 0 \\ \dfrac{\partial \tau_{ij}}{\partial(\partial_m U)}\delta U \\ \dfrac{C_p}{Pr}\dfrac{\partial(\partial_i T)}{\partial(\partial_m U)}\delta U \end{pmatrix}, \tag{C.21}$$

and

$$\mathcal{A}_3 \delta(\partial_m U) = \mu \begin{pmatrix} 0 \\ \dfrac{\partial \tau_{ij}}{\partial(\partial_m U)}\delta(\partial_m U) \\ \dfrac{C_p}{Pr}\dfrac{\partial(\partial_i T)}{\partial(\partial_m U)}\delta(\partial_m U) \end{pmatrix}. \tag{C.22}$$

Using these results we can then write

$$\begin{aligned} &\left(\phi^T \mathcal{A}_2 \hat{n}_i - \left(\partial_i \phi^T\right)\mathcal{A}_3 \hat{n}_j\right)\delta U + \phi^T \mathcal{A}_3 \delta(\partial_j U)\hat{n}_i \\ &= \phi^T_{\rho u_j}\left(\mu \frac{\partial \tau_{ij}}{\partial(\partial_m U)}\delta U + \mu \frac{\partial \tau_{ij}}{\partial(\partial_m U)}\delta(\partial_m U)\right)\hat{n}_i \\ &\quad + \phi_{\rho E}\left(\mu \frac{\partial u_k}{\partial U}\tau_{ik}\delta U + \mu \frac{C_p}{Pr}\frac{\partial(\partial_i T)}{\partial U}\delta U + \mu \frac{C_p}{Pr}\frac{\partial(\partial_i T)}{\partial(\partial_m U)}\delta(\partial_m U)\right)\hat{n}_i \\ &\quad - \mu\left(\partial_i \phi^T_{\rho u_j}\right)\frac{\partial \tau_{ij}}{\partial(\partial_m U)}\delta U \hat{n}_m - \mu\left(\partial_i \phi_{\rho E}\right)\frac{C_p}{Pr}\frac{\partial(\partial_i T)}{\partial(\partial_m U)}\delta U \hat{n}_m, \end{aligned} \tag{C.23}$$

and noting that $T(U)$, $\tau(U, \partial_m U)$, $\partial_i T(U, \partial_m U)$ and $u_k(U)$, we can collect terms together to give

$$\begin{aligned}
&\left(\phi^T \mathcal{A}_2 \hat{n}_i - \left(\partial_i \phi^T\right) \mathcal{A}_3 \hat{n}_j\right) \delta U + \phi^T \mathcal{A}_3 \delta(\partial_j U) \hat{n}_i \\
&\quad = \quad \phi^T_{\rho u_j} \mu \delta \tau_{ij} \hat{n}_i + \phi_{\rho E} \left(\mu \tau_{ik} \delta u_k + \mu \frac{C_p}{Pr} \delta(\partial_i T)\right) \hat{n}_i \\
&\qquad -\mu \left(\partial_i \phi^T_{\rho u_j}\right) \frac{\partial \tau_{ij}}{\partial(\partial_m U)} \delta U \hat{n}_m - \mu \left(\partial_i \phi_{\rho E}\right) \frac{C_p}{Pr} \frac{\partial(\partial_i T)}{\partial(\partial_m U)} \delta U \hat{n}_m.
\end{aligned} \tag{C.24}$$

With the boundary conditions on flow velocity and temperature this reduces to

$$\begin{aligned}
&\left(\phi^T \mathcal{A}_2 \hat{n}_i - \left(\partial_i \phi^T\right) \mathcal{A}_3 \hat{n}_j\right) \delta U + \phi^T \mathcal{A}_3 \delta(\partial_j U) \hat{n}_i \\
&\quad = \quad \phi^T_{\rho u_j} \mu \delta \tau_{ij} \hat{n}_i - \mu \left(\partial_i \phi^T_{\rho u_j}\right) \frac{\partial \tau_{ij}}{\partial(\partial_m U)} \delta U \hat{n}_m - \mu \left(\partial_i \phi_{\rho E}\right) \frac{C_p}{Pr} \frac{\partial(\partial_i T)}{\partial(\partial_m U)} \delta U \hat{n}_m.
\end{aligned} \tag{C.25}$$

We now need derivatives of τ_{ij} and $\partial_i T$ with respect to the gradients of the flow variables. First considering τ_{ij} we can expand this to be

$$\begin{aligned}
\tau_{ij} \quad = \quad & \frac{1}{\rho} \left(\left(\partial_i(\rho u_j) - (\partial_i \rho) \frac{\rho u_j}{\rho} \right) + \left(\partial_j(\rho u_i) - (\partial_j \rho) \frac{\rho u_i}{\rho} \right) \right. \\
& \left. -\frac{2}{3} \delta_{ij} \left(\partial_k(\rho u_k) - (\partial_k \rho) \frac{\rho u_k}{\rho} \right) \right),
\end{aligned} \tag{C.26}$$

and thus we can write the results

$$\frac{\partial \tau_{ij}}{\partial(\partial_m \rho)} = -\frac{1}{\rho} \left(\frac{\rho u_j}{\rho} \delta_{im} + \frac{\rho u_i}{\rho} \delta_{jm} - \frac{2}{3} \delta_{ij} \frac{\rho u_k}{\rho} \delta_{km} \right), \tag{C.27}$$

$$\frac{\partial \tau_{ij}}{\partial(\partial_m(\rho u_l))} = \frac{1}{\rho} \left(\delta_{im} \delta_{jl} + \delta_{jm} \delta_{il} - \frac{2}{3} \delta_{ij} \delta_{lm} \right), \tag{C.28}$$

and

$$\frac{\partial \tau_{ij}}{\partial(\partial_m(\rho E))} = 0. \tag{C.29}$$

Considering the boundary condition on flow velocity, then

$$\frac{\partial \tau_{ij}}{\partial(\partial_m \rho)} = 0, \tag{C.30}$$

and, noting that $\delta(\rho u_j) = 0$, we see that

$$\frac{\partial \tau_{ij}}{\partial(\partial_m U)}\delta U = 0. \tag{C.31}$$

Next we consider $\partial_i T$. We can write

$$T = \frac{(\gamma-1)}{R}\left(\frac{\rho E}{\rho} - \frac{\rho u_k \rho u_k}{2\rho^2}\right), \tag{C.32}$$

and thus $\partial_i T$ is given by

$$\partial_i T = \frac{(\gamma-1)}{R}\left(\left(\frac{\rho u_k \rho u_k}{\rho^3} - \frac{\rho E}{\rho^2}\right)\partial_i \rho - \frac{\rho u_k \partial_i(\rho u_k)}{\rho^2} + \frac{1}{\rho}\partial_i(\rho E)\right). \tag{C.33}$$

Therefore we can write out the results

$$\frac{\partial(\partial_i T)}{\partial(\partial_l \rho)} = \frac{(\gamma-1)}{R}\left(\frac{\rho u_k \rho u_k}{\rho^3} - \frac{\rho E}{\rho^2}\right)\delta_{il}, \tag{C.34}$$

$$\frac{\partial(\partial_i T)}{\partial(\partial_l(\rho u_m))} = -\frac{(\gamma-1)}{R}\frac{\rho u_m}{\rho^2}\delta_{il}, \tag{C.35}$$

and

$$\frac{\partial(\partial_i T)}{\partial(\partial_l(\rho E))} = \frac{(\gamma-1)}{\rho R}\delta_{il}. \tag{C.36}$$

Considering the boundary condition on flow velocity, then

$$\frac{\partial(\partial_i T)}{\partial(\partial_l \rho)} = -\frac{(\gamma-1)}{R}\frac{\rho E}{\rho^2}\delta_{il}, \tag{C.37}$$

and

$$\frac{\partial(\partial_i T)}{\partial(\partial_l(\rho u_m))} = 0, \tag{C.38}$$

and, noting that $\delta(\rho u_j) = 0$, we see that

$$\frac{\partial(\partial_i T)}{\partial(\partial_m U)}\delta U = \frac{\gamma-1}{\rho R}\left(\frac{\rho E}{\rho}\delta\rho - \delta(\rho E)\right)\delta_{im}. \tag{C.39}$$

Writing the perturbation to the pressure on the wall as

$$\delta p = (\gamma-1)\left(\delta(\rho E) + \frac{\rho u_k \rho u_k}{2\rho^2}\delta\rho - \frac{\rho u_k}{\rho^2}\delta(\rho u_k)\right), \tag{C.40}$$

and using the flow velocity boundary condition plus rearrangement gives

$$\delta(\rho E) = \frac{\delta p}{\gamma - 1}, \tag{C.41}$$

and thus

$$\frac{\partial(\partial_i T)}{\partial(\partial_m U)}\delta U = \frac{1}{\rho R}\left(\frac{p}{\rho}\delta\rho - \delta p\right)\delta_{im}. \tag{C.42}$$

Next, using the ideal gas law, $p = \rho RT$, we note

$$\delta p = \frac{p}{\rho}\delta\rho + \rho R\delta T, \tag{C.43}$$

and thus

$$\frac{\partial(\partial_i T)}{\partial(\partial_m U)}\delta U = -\delta T\delta_{im}. \tag{C.44}$$

This allows us to finally write

$$\begin{aligned}\left(\phi^T\mathcal{A}_2\hat{n}_i - \left(\partial_i\phi^T\right)\mathcal{A}_3\hat{n}_j\right)\delta U + \phi^T\mathcal{A}_3\delta(\partial_j U)\hat{n}_i \\ = \quad \phi^T_{\rho u_j}\mu\delta\tau_{ij}\hat{n}_i + \mu\left(\partial_i\phi_{\rho E}\right)\frac{C_p}{Pr}\hat{n}_i\delta T,\end{aligned} \tag{C.45}$$

and so finally we can collect terms and write the wall boundary condition as

$$\int_S\left(\frac{\partial j_\Gamma}{\partial U}\delta U - \phi^T_{\rho u_j}\delta p\hat{n}_i + \phi^T_{\rho u_j}\mu\hat{n}_i\delta\tau_{ij} + \mu\left(\partial_i\phi_{\rho E}\right)\frac{C_p}{Pr}\hat{n}_i\delta T\right)d\Gamma = 0. \tag{C.46}$$

We can therefore finally introduce the adjoint boundary condition to remove the dependence on the flow perturbation:

$$\frac{\partial j_\Gamma}{\partial U}\delta U - \phi^T_{\rho u_j}\hat{n}_i\delta p + \phi^T_{\rho u_j}\mu\hat{n}_i\delta\tau_{ij} + \mu\left(\partial_i\phi_{\rho E}\right)\frac{C_p}{Pr}\hat{n}_i\delta T = 0. \tag{C.47}$$

We therefore wish to consider objective functions for which we can write the perturbation in the form

$$\frac{\partial j_\Gamma}{\partial U}\delta U = \frac{\partial j_\Gamma}{\partial p}\delta p + \frac{\partial j_\Gamma}{\partial\tau_{ij}}\delta\tau_{ij} + \frac{\partial j_\Gamma}{\partial T}\delta T, \tag{C.48}$$

allowing the δp, $\delta\tau_{ij}$ and δT dependencies to be removed.

Far field At the far field the usual characteristic rules apply, and thus we require the same numbers of boundary conditions as for Euler flow. Considering objective functions not defined along the far field boundary, we can also simplify the boundary condition to

$$-\int_{\Gamma_\infty}\left(L^T_\Gamma(\phi)\delta U - \phi^T\mathcal{A}_5\delta(\partial_j U)\hat{n}_i\right)d\Gamma = 0, \tag{C.49}$$

and further, if the flow gradients are negligible at the far field we can write

$$-\int_{\Gamma_\infty} L_\Gamma^T(\phi)\delta U d\Gamma = 0. \tag{C.50}$$

C.2.2 Full continuous adjoint boundary conditions

The boundary conditions on the adjoint equation are again given by (B.33), though with the addition of the $\mathcal{A}_5$ term. Considering each type of boundary condition in turn:

Viscous wall At a viscous wall we now include the additional term

$$\mathcal{A}_5\delta U = \begin{pmatrix} 0 \\ \tau_{ij} \\ \dfrac{C_p}{Pr}\partial_i T \end{pmatrix} \frac{\partial \mu}{\partial T}\frac{\partial T}{\partial U}\delta U. \tag{C.51}$$

Carrying this term through the manipulation used before for the frozen-viscosity adjoint, and using the boundary condition $\partial_i T = 0$, we finally introduce the adjoint boundary condition to remove the dependence on the flow perturbation

$$\frac{\partial j_\Gamma}{\partial U}\delta U - \phi^T_{\rho u_j}\hat{n}_i\delta p + \phi^T_{\rho u_j}\mu\hat{n}_i\delta\tau_{ij} + \left(\phi^T_{\rho u_j}\tau_{ij}\frac{\partial \mu}{\partial T} + \mu\left(\partial_i\phi_{\rho E}\right)\frac{C_p}{Pr}\right)\hat{n}_i\delta T = 0. \tag{C.52}$$

We thus again wish to consider objective functions for which we can write the perturbation in the form

$$\frac{\partial j_\Gamma}{\partial U}\delta U = \frac{\partial j_\Gamma}{\partial p}\delta p + \frac{\partial j_\Gamma}{\partial \tau_{ij}}\delta\tau_{ij} + \frac{\partial j_\Gamma}{\partial T}\delta T, \tag{C.53}$$

allowing the δp, $\delta\tau_{ij}$ and δT dependencies to be removed.

Far field At the far field the usual characteristic rules apply, and thus we require the same numbers of boundary conditions as for Euler flow. Considering objective functions not defined along the far field boundary, we can also simplify the boundary condition to

$$-\int_{\Gamma_\infty}\left(L_\Gamma^T(\phi)\delta U - \phi^T\mathcal{A}_5\delta(\partial_j U)\hat{n}_i\right)d\Gamma = 0, \tag{C.54}$$

and further, if the flow gradients are negligible at the far field we can write

$$-\int_{\Gamma_\infty} L_\Gamma^T(\phi)\delta U d\Gamma = 0. \tag{C.55}$$

C.3 Reynolds-Averaged Navier-Stokes flow

C.3.1 Frozen-viscosity continuous adjoint boundary conditions

The boundary conditions on the adjoint equation are given by (B.54), however, we must manipulate this so as to remove the dependence on the flow perturbation. Considering each type of boundary condition in turn:

Viscous wall At the viscous wall the eddy viscosity must be zero and thus the boundary conditions for the RANS frozen-viscosity continuous adjoint reduce to those of the laminar Navier-Stokes frozen-viscosity continuous adjoint, (C.47).

Far field At the far field the usual characteristic rules apply, and thus we require the same numbers of boundary conditions as for Euler flow. Considering objective functions not defined along the far field boundary, we can also simplify the boundary conditions to

$$-\int_{\Gamma_\infty}\left(L_\Gamma^T(\phi)\delta U-\left(\phi_L^T\left(\mathcal{A}_3+\mathcal{B}_3\right)-\phi_T^T\frac{\partial T_i^{cv}}{\partial(\partial_j U)}\right)\delta(\partial_j U)\hat{n}_i\right)d\Gamma=0, \tag{C.56}$$

and further, if the flow and viscosity gradients are negligible at the far field we can write just

$$-\int_{\Gamma_\infty}L_\Gamma^T(\phi)\delta U d\Gamma=0. \tag{C.57}$$

C.3.2 Hybrid adjoint boundary conditions

The boundary conditions on the adjoint equation are given by (B.71) and (B.72), however, we must manipulate this so as to remove the dependence on the flow perturbation.

Viscous wall We can handle the mean-flow contribution to (B.71) in the same way as for laminar flow, noting that apart from the eddy viscosity, none of these depend on the turbulence variable. Therefore we can use the results (C.7) and (C.45). Importantly we also again note that the eddy viscosity must be zero on the wall (here the flow is laminar) and thus the terms dependent on this ($\mathcal{B}_2$ and $\mathcal{B}_3$) are all zero. This gives

$$\begin{aligned}\int_S\Bigg(&\beta\frac{\partial j_\Gamma}{\partial U}\delta U-\varphi_{\rho u_j}^T\delta p\hat{n}_i+\varphi_{\rho u_j}^T\mu\hat{n}_i\delta\tau_{ij}\\&+\left(\varphi_{\rho u_j}^T\tau_{ij}\frac{\partial\mu}{\partial T}+\mu\left(\partial_i\varphi_{\rho E}\right)\frac{C_p}{Pr}\right)\hat{n}_i\delta T\Bigg)d\Gamma\\+(1-\beta)\sum_{p=1}^{N_S}\sum_{q=1}^{N_S}\frac{\mathfrak{D}j_{\Gamma_q}}{\mathfrak{D}U_p}\Delta\Gamma_q\Delta U_p&+\sum_{p=1}^{N_S}\sum_{q=1}^{N_S}\varphi_{D_q}^T\frac{\mathfrak{D}(\hat{F}_T)_{\Gamma_q}}{\mathfrak{D}U_p}\Delta U_p\quad=\quad 0.\end{aligned} \tag{C.58}$$

Now considering the term ΔU_p in more detail we can write

$$\Delta U_p = \begin{pmatrix} \Delta U_{L_p} \\ \Delta U_{T_p} \end{pmatrix}, \tag{C.59}$$

and making the assumption that $\Delta U_p \approx \delta U_p$, and thus by implication $\Delta(\rho u_j)_p \approx \delta(\rho u_j)_p$, and using the boundary conditions on the flow velocity,

$$\Delta U_{L_p} = \begin{pmatrix} \Delta\rho_p \\ \Delta(\rho u_j)_p \\ \Delta(\rho E)_p \end{pmatrix} = \begin{pmatrix} \Delta\rho_p \\ 0 \\ \Delta(\rho E)_p \end{pmatrix}, \tag{C.60}$$

which can again be rewritten using the analytical equations for p and T as

$$\Delta U_p = \begin{pmatrix} \frac{\rho_p}{p_p}\Delta p_p - \frac{\rho_p}{T_p}\Delta T_p \\ 0 \\ \frac{1}{\gamma-1}\Delta p_p \end{pmatrix}. \tag{C.61}$$

We also note that there is no direct dependence of p, τ_{ij} or T on U_T, and therefore the boundary condition becomes

$$\begin{aligned} \int_S \Bigg(& \frac{\partial j_\Gamma}{\partial U}\delta U - \phi^T_{\rho u_j}\delta p\hat{n}_i + \phi^T_{\rho u_j}\mu\hat{n}_i\delta\tau_{ij} \\ & + \left(\phi^T_{\rho u_j}\tau_{ij}\frac{\partial\mu}{\partial T} + \mu\left(\partial_i\phi_{\rho E}\right)\frac{C_p}{Pr}\right)\hat{n}_i\delta T\Bigg) d\Gamma \\ & + (1-\beta)\sum_{p=1}^{N_S}\sum_{q=1}^{N_S}\frac{\mathfrak{D}j_{\Gamma_q}}{\mathfrak{D}U_p}\Delta\Gamma_q\Delta U_p \\ & + \sum_{p=1}^{N_S}\sum_{q=1}^{N_S}\varphi^T_{D_q}\left(\frac{\rho_p}{p_p}\frac{\mathfrak{D}(\hat{F}_T)_{\Gamma_q}}{\mathfrak{D}\rho_p} + \frac{1}{\gamma-1}\frac{\mathfrak{D}(\hat{F}_T)_{\Gamma_q}}{\mathfrak{D}(\rho E)_p}\right)\Delta p_p \\ & - \sum_{p=1}^{N_S}\sum_{q=1}^{N_S}\frac{\rho_p}{T_p}\varphi^T_{D_q}\frac{\mathfrak{D}(\hat{F}_T)_{\Gamma_q}}{\mathfrak{D}\rho_p}\Delta T_p \\ & + (1-\beta)\sum_{p=1}^{N_S}\sum_{q=1}^{N_S}\frac{\mathfrak{D}j_{\Gamma_q}}{\mathfrak{D}U_{T_p}}\Delta\Gamma_q\Delta U_{T_p} + \sum_{p=1}^{N_S}\sum_{q=1}^{N_S}\varphi^T_{D_q}\frac{\mathfrak{D}(\hat{F}_T)_{\Gamma_q}}{\mathfrak{D}U_{T_p}}\Delta U_{T_p} \quad = \quad 0. \end{aligned} \tag{C.62}$$

Discretizing this in the same way as the hybrid adjoint equation and dropping the summation

terms, we can write

$$\begin{aligned}
&\int_{S_p}\left(\frac{\partial j_\Gamma}{\partial U}\delta U-\phi^T_{\rho u_j}\delta p\hat{n}_i+\phi^T_{\rho u_j}\mu\hat{n}_i\delta\tau_{ij}\right.\\
&\left.+\left(\phi^T_{\rho u_j}\tau_{ij}\frac{\partial\mu}{\partial T}+\mu\left(\partial_i\phi_{\rho E}\right)\frac{C_p}{Pr}\right)\hat{n}_i\delta T\right)d\Gamma\\
&+(1-\beta)\sum_{q=1}^{N_S}\frac{\mathfrak{D}j_{\Gamma_q}}{\mathfrak{D}U_p}\Delta\Gamma_q\Delta U_p\\
&+\sum_{q=1}^{N_S}\varphi^T_{D_q}\left(\frac{\rho_p}{p_p}\frac{\mathfrak{D}(\hat{F}_T)_{\Gamma_q}}{\mathfrak{D}\rho_p}+\frac{1}{\gamma-1}\frac{\mathfrak{D}(\hat{F}_T)_{\Gamma_q}}{\mathfrak{D}(\rho E)_p}\right)\Delta p_p\\
&-\sum_{q=1}^{N_S}\frac{\rho_p}{T_p}\varphi^T_{D_q}\frac{\mathfrak{D}(\hat{F}_T)_{\Gamma_q}}{\mathfrak{D}\rho_p}\Delta T_p\\
&+(1-\beta)\sum_{q=1}^{N_S}\frac{\mathfrak{D}j_{\Gamma_q}}{\mathfrak{D}U_{T_p}}\Delta\Gamma_q\Delta U_{T_p}+\sum_{q=1}^{N_S}\varphi^T_{D_q}\frac{\mathfrak{D}(\hat{F}_T)_{\Gamma_q}}{\mathfrak{D}U_{T_p}}\Delta U_{T_p} \quad = \quad 0.
\end{aligned}\tag{C.63}$$

We then make the assumption that the continuous perturbations are step-wise constant, that is, they are constant within each cell. This allows them to be factored out, giving, after rearrangement,

$$\begin{aligned}
&\left(\int_{S_p}\frac{\partial j_\Gamma}{\partial U}d\Gamma\right)\delta U_p+(1-\beta)\sum_{q=1}^{N_S}\frac{\mathfrak{D}j_{\Gamma_q}}{\mathfrak{D}U_p}\Delta\Gamma_q\Delta U_p\\
&-\left(\int_{S_p}\phi^T_{\rho u_j}\hat{n}_i\right)\delta p_p+\sum_{q=1}^{N_S}\varphi^T_{D_q}\left(\frac{\rho_p}{p_p}\frac{\mathfrak{D}(\hat{F}_T)_{\Gamma_q}}{\mathfrak{D}\rho_p}+\frac{1}{\gamma-1}\frac{\mathfrak{D}(\hat{F}_T)_{\Gamma_q}}{\mathfrak{D}(\rho E)_p}\right)\Delta p_p\\
&+\left(\int_{S_p}\left(\phi^T_{\rho u_j}\tau_{ij}\frac{\partial\mu}{\partial T}+\mu\left(\partial_i\phi_{\rho E}\right)\frac{C_p}{Pr}\right)\hat{n}_i d\Gamma\right)\delta T_p-\sum_{q=1}^{N_S}\frac{\rho_p}{T_p}\varphi^T_{D_q}\frac{\mathfrak{D}(\hat{F}_T)_{\Gamma_q}}{\mathfrak{D}\rho_p}\Delta T_p\\
&+\left(\int_{S_p}\phi^T_{\rho u_j}\mu\hat{n}_i d\Gamma\right)\delta\tau_{ij_p}\\
&+(1-\beta)\sum_{q=1}^{N_S}\frac{\mathfrak{D}j_{\Gamma_q}}{\mathfrak{D}U_{T_p}}\Delta\Gamma_q\Delta U_{T_p}+\sum_{q=1}^{N_S}\varphi^T_{D_q}\frac{\mathfrak{D}(\hat{F}_T)_{\Gamma_q}}{\mathfrak{D}U_{T_p}}\Delta U_{T_p} \quad = \quad 0.
\end{aligned}\tag{C.64}$$

We thus wish to consider objective functions for which we can write the perturbation in the form

$$\frac{\partial j_\Gamma}{\partial U}\delta U=\frac{\partial j_\Gamma}{\partial p}\delta p+\frac{\partial j_\Gamma}{\partial\tau_{ij}}\delta\tau_{ij}+\frac{\partial j_\Gamma}{\partial T}\delta T+\frac{\partial j_\Gamma}{\partial U_T}\delta U_T,\tag{C.65}$$

allowing the δp, $\delta\tau_{ij}$, δT and δU_T dependencies to be removed.

Now considering the other boundary condition, (B.72), we note that at the wall the flow should be laminar and thus the eddy viscosity must be zero, implying $\delta\mu_T = 0$ and thus satisfying this condition.

Far field At the far field the usual characteristic rules apply, and thus we require the same number of boundary conditions as for Euler flow, to handle the mean-flow adjoint variables. Depending on the turbulence model being used, we will also need to consider additional boundary conditions to remove the dependence on the perturbations to the turbulence variables. Considering objective functions not defined along the far field boundary, we can also simplify the boundary conditions to

$$-\int_{\Gamma_\infty} \left(L_\Gamma^T(\varphi_C)\delta U - \phi_L^T \left(\mathcal{A}_3 + \mathcal{B}_3\right) \delta(\partial_j U)\hat{n}_i \right) d\Gamma + \sum_{p=1}^{N_{\Gamma_\infty}} \sum_{q=1}^{N_{\Gamma_\infty}} \varphi_{D_q}^T \frac{\mathfrak{D}(\hat{F}_T)_{\Gamma_q}}{\mathfrak{D}U_p} \Delta U_p = 0, \tag{C.66}$$

and

$$\int_{\Gamma_\infty} \phi_L^T \mathcal{C}_1 \hat{n}_i \delta\mu_T d\Gamma = 0, \tag{C.67}$$

and further, if the flow and viscosity gradients are negligible at the far field we can write just

$$-\int_{\Gamma_\infty} L_\Gamma^T(\varphi_C)\delta U d\Gamma + \sum_{p=1}^{N_{\Gamma_\infty}} \sum_{q=1}^{N_{\Gamma_\infty}} \varphi_{D_q}^T \frac{\mathfrak{D}(\hat{F}_T)_{\Gamma_q}}{\mathfrak{D}U_p} \Delta U_p = 0. \tag{C.68}$$

Appendix D

Analytic adjoints

This appendix presents work on analytic adjoints for both quasi-one-dimensional Euler flow and Rayleigh flow.

D.1 Quasi-one-dimensional Euler flow

The analytic adjoint approach and theory for quasi-one-dimensional Euler flow has been well explained and developed by Giles and Pierce[45], but is here extended to handle both reduced-interval and pointwise functionals.

D.1.1 Flow problem

We again consider quasi-one-dimensional Euler flow as previously defined in Section 4.1.1.1 with the boundary conditions given in Section 4.1.1.2.

D.1.1.1 Numerical implementation

Analytical results exist for quasi-one-dimensional flow, allowing us to solve the Euler equations exactly. These include the area-Mach number relation,

$$\frac{h}{h^*} = \frac{1}{M}\left(\frac{2}{\gamma+1}\left(1+\frac{\gamma-1}{2}M^2\right)\right)^{\frac{\gamma+1}{2(\gamma-1)}}, \tag{D.1}$$

the isentropic relation,

$$\frac{p_0}{p} = \left(1+\frac{\gamma-1}{2}M^2\right)^{\frac{\gamma}{\gamma-1}}, \tag{D.2}$$

noting that for smooth flow the stagnation enthalpy is constant, and, in the presence of a shock, the shock jump relations,

$$M_{x_{s^+}} = \frac{(\gamma-1)M_{x_{s^-}}^2 + 2}{2\gamma M_{x_{s^-}}^2 - (\gamma-1)}, \tag{D.3}$$

$$\frac{p_{0x_{s^+}}}{p_{0x_{s^-}}} = \left(\frac{(\gamma+1)M_{x_{s^-}}^2}{(\gamma-1)M_{x_{s^-}}^2+2}\right)^{\frac{\gamma}{\gamma-1}} \left(\frac{\gamma+1}{2\gamma M_{x_{s^-}}^2-(\gamma-1)}\right)^{\frac{1}{\gamma-1}}, \tag{D.4}$$

and

$$\frac{p_{x_{s^+}}}{p_{x_{s^-}}} = \frac{2\gamma M_{x_{s^-}}^2 - (\gamma-1)}{\gamma+1}. \tag{D.5}$$

These equations were implemented into a MATLAB code to calculate the flow for any given duct shape or flow conditions.

D.1.2 Continuous adjoint problem

The continuous adjoint equations for quasi-one-dimensional Euler flow were previously derived in Section 4.1.3.1 with the boundary conditions given in Section 4.1.3.1. Note that the development outlined here is based around using the 'lift' objective function given by equation (4.117).

D.1.3 Analytical adjoint solution

D.1.3.1 Approach

Full-interval functional Following the Green's function approach outlined in Section 2.1.3, we can obtain the continuous adjoint variables without needing to solve the adjoint problem.

The solution to the inhomogeneous equations (2.27) can be written in terms of uniform perturbations a, b and c to the mass flow, stagnation pressure and stagnation enthalpy, respectively, i.e.,

$$\delta U_p(x,\xi) = a(x,\xi)\frac{1}{h(x)}\left.\frac{\partial U}{\partial m}(x)\right|_{H,p_0} + c(x,\xi)\left.\frac{\partial U}{\partial H}(x)\right|_{p_0,M} + c(x,\xi)\left.\frac{\partial U}{\partial p_0}(x)\right|_{H,M}, \tag{D.6}$$

noting that on either side of ξ, the perturbations a, b and c must satisfy the homogeneous equations and are thus constant, but that there can be a discontinuous jump in their values at $x = \xi$. In the presence of a shock there may also be a jump in these values across the discontinuity.

Using this result, analytical solutions for $\mathcal{I}_p$ can be found from equation (2.28).

Now, integrating the inhomogeneous equations (2.27) from $x = \xi^-$ to $x = \xi^+$ gives

$$\begin{aligned} f_p(\xi) &= (a_2 - a_1)\frac{1}{h(x)}\left.\frac{\partial F}{\partial m}(\xi)\right|_{p,H} \\ &\quad +(b_2 - b_1)\left.\frac{\partial F}{\partial H}(x)\right|_{p_0,M} \\ &\quad +(c_2 - c_1)\left.\frac{\partial F}{\partial p_0}(x)\right|_{H,M}, \end{aligned} \tag{D.7}$$

noting that the subscript 1 denotes the value when $x < \xi$, and 2 the value when $x > \xi$. Thus, if we choose the three linearly independent source vectors to be

$$\begin{aligned} f_1(\xi) &= \left.\frac{\partial F}{\partial m}(\xi)\right|_{H,p_0}, \\ f_2(\xi) &= h(\xi)\left.\frac{\partial F}{\partial H}(\xi)\right|_{p_0,M}, \\ f_3(\xi) &= h(\xi)\left.\frac{\partial F}{\partial p_0}(\xi)\right|_{H,M}, \end{aligned} \tag{D.8}$$

this means that the perturbations have the simple properties

$$\begin{array}{lllll} f_1(\xi) & \rightarrow & a_2 - a_1 = 1, & b_2 = b_1, & c_2 = c_1, \\ f_2(\xi) & \rightarrow & a_2 = a_1, & b_2 - b_1 = 1, & c_2 = c_1, \\ f_3(\xi) & \rightarrow & a_2 = a_1, & b_2 = b_1, & c_2 - c_1 = 1. \end{array} \tag{D.9}$$

Using the results for $\mathcal{I}_p$ and f_p we can then derive exact values for the continuous adjoint variables, ϕ, from equation (2.29). This whole derivation is explained in greater detail by Giles and Pierce[45], and formulae for the $\mathcal{I}_p$ for different flow regimes are given in Appendix E.

Reduced-interval and pointwise functionals The general approach for reduced-interval and pointwise functionals is to define these problems as integrals over the full interval so that the approach of Giles and Pierce[45] can still be used, with only minor modifications.

Reduced-interval functionals for smooth flow If the objective function, $\mathcal{J}$, is now changed to an integral only over part of the duct, the interval between x_1 and x_2, we can write

$$\mathcal{J} = \int_{x_1}^{x_2} p dx, \tag{D.10}$$

or, using the Heaviside function, $\mathcal{H}$, define this as an integral over the full domain,

$$\mathcal{J} = \int_{x_i}^{x_e} \mathcal{H}\left(x - x_1\right) \mathcal{H}\left(x_2 - x\right) p dx. \tag{D.11}$$

The perturbation to this, $\mathcal{I}$, can be treated similarly, giving

$$\mathcal{I} = \int_{x_i}^{x_e} g^T \delta U dx, \tag{D.12}$$

where g^T is now equal to $\mathcal{H}\left(x - x_1\right) \mathcal{H}\left(x_2 - x\right) \dfrac{\partial p}{\partial U}$, and, using this new g^T in exactly the same Green's function approach explained previously, the analytic adjoints for reduced-interval functionals can be derived. The formulae for the $\mathcal{I}_p$ for different flow regimes in this case are also given in Appendix E.

Pointwise functionals for smooth flow Now considering a pointwise functional located at x_0, we can write

$$\mathcal{J} = p\left(x_0\right), \tag{D.13}$$

or, using the delta function, δ, define this as an integral over the full domain,

$$\mathcal{J} = \int_{x_i}^{x_e} \delta\left(x - x_0\right) p dx. \tag{D.14}$$

As in the reduced-interval case, the perturbation to this, $\mathcal{I}$, is again treated similarly, giving the same result as in equation (D.12), where g^T is now equal to $\delta\left(x - x_0\right) \dfrac{\partial p}{\partial U}$, and, using this new g^T in the Green's function approach, the analytic adjoints for pointwise functionals can be derived. The formulae for the $\mathcal{I}_p$ for different flow regimes in this case are also given in Appendix E.

Handling shocks When considering flow cases that are discontinuous, it is important to note that the assumptions of linearity used to derive the adjoint equation actually imply that the shocks do not move, though we do consider the sensitivity of their positions to changes in the flow variables. This removes the potential complication for reduced-interval and pointwise functionals of shocks crossing over the borders of the regions in which these functionals are defined.

For reduced-interval functionals, the result is that when the shock is located within the limits of the functional, i.e., $x_1 < x_s < x_2$, we thus include the shock movement, δx_s, in the derivation, whilst when the shock is outside this region, we do not need to consider this contribution. The formulae for the $\mathcal{I}_p$ for different flow regimes for this case are also given in Appendix E.

For pointwise functionals, there is no contribution due to shock movement.

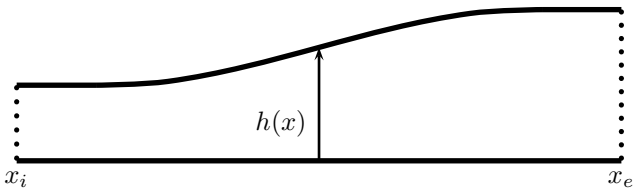

Figure D.1: Expansion nozzle.

D.1.3.2 Numerical implementation

Once the flow problem had been solved, the continuous adjoint variables were found using these analytical results. As for the flow solution, this was again done via MATLAB, and the required integrals were found by applying the trapezoidal quadrature rule.

D.1.4 Results

D.1.4.1 Flow test cases

The test cases used to analyze the quasi-one-dimensional analytic adjoint results are the converging-diverging nozzle previously shown in Figure 4.2 and defined in equation (4.114), and the expansion nozzle shown in Figure D.1 and defined by

$$h(x) = \begin{cases} 0.95 & \text{for } -0.1 \leq x \leq 0, \\ 0.6x^5 - 1.5x^4 + x^3 + 0.95 & \text{for } 0 < x < 1, \\ 1.05 & \text{for } 1 \leq x \leq 0.1. \end{cases} \tag{D.15}$$

For the converging-diverging nozzle, four different flow cases were considered:

- subsonic flow, with $H_i = 4$, $p_{0_i} = 2$ and $p_e = 1.98$,
- shocked flow, with $H_i = 4$, $p_{0_i} = 2$ and $p_e = 1.6$,
- transonic flow, with $H_i = 4$ and $p_{0_i} = 2$,
- supersonic flow, with $H_i = 4$, $p_{0_i} = 2$ and $M_i = 3$,

and the shapes of the analytic adjoint variables in each case were analyzed on an evenly spaced grid of 1,000 points. The pressure variation along the duct for these different situations can be seen in Figure D.2.

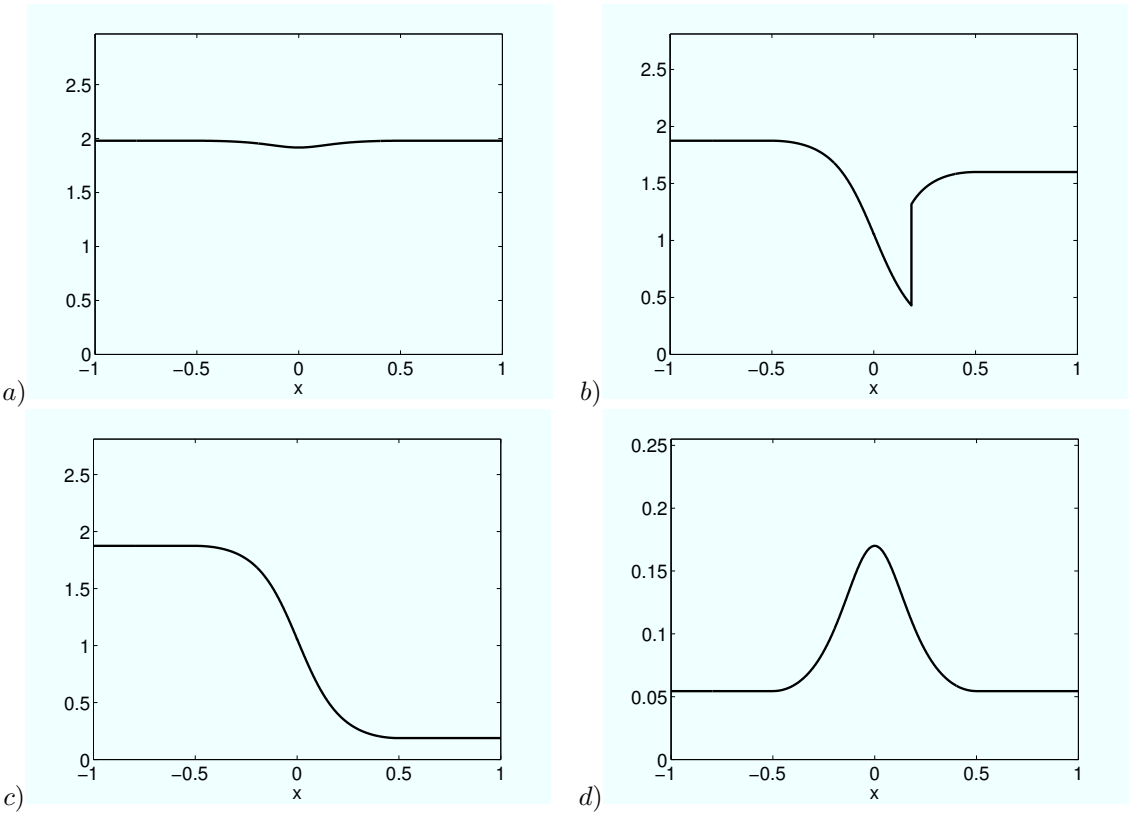

Figure D.2: Pressure variation along converging-diverging nozzle, with $H_i = 4$, $p_{0_i} = 2$: a) subsonic flow, $p_e = 1.98$; b) shocked flow, $p_e = 1.6$; c) transonic flow; d) supersonic flow, $M_i = 3$.

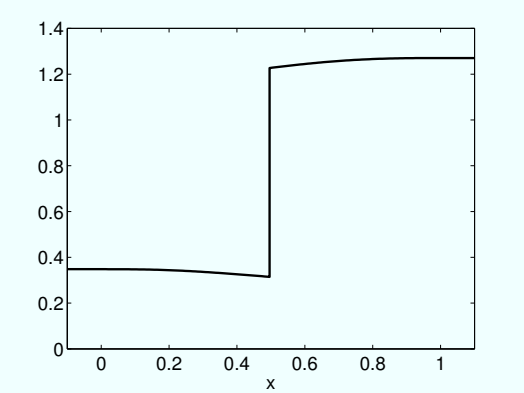

Figure D.3: Pressure variation along expansion nozzle for shocked flow with $H_i = 4$, $M_i = 1.8$ and $\frac{p_e}{p_i} = 3.65$.

For the expansion nozzle, the sensitivity of the objective function to the inlet Mach number, $\frac{\partial \mathcal{J}}{\partial M_i}$, and exit pressure, $\frac{\partial \mathcal{J}}{\partial p_e}$, was investigated over a range of Mach numbers and exit pressures, respectively, making comparison to results from finite differencing. For this comparison an evenly spaced grid of 10,000 points was used, and the finite difference step was 2×10^{-4}. The inlet stagnation enthalpy and stagnation pressure were kept fixed throughout: $H_i = 4$ and $p_{0_i} = 2$. Additionally, for a single shocked flow case ($H_i = 4$, $M_i = 1.8$ and $\frac{p_e}{p_i} = 3.65$), comparison was made between a discrete adjoint solution and the analytic results, with an evenly spaced grid of 160 cells. The pressure variation along the duct in this flow case is shown in Figure D.3.

D.1.4.2 Adjoint results

Full-interval functional The shapes of the adjoint variables along the converging-diverging nozzle for the different flow cases can be seen in Figure D.4. The results here demonstrate exact agreement with Giles and Pierce[45].

In Figure D.5, the analytic adjoint is used to predict the sensitivity of the objective function to the inlet Mach number and the exit presssure, with comparison made to results from finite differencing. It is seen that there is good agreement for both subsonic and supersonic flow, but that the finite difference results become oscillatory when a shock is present and no longer match the smooth analytic result. This is likely due to poor shock capturing because of insufficient resolution of the grid around the discontinuity, and the analytic sensitivity appears better because it is not affected by this problem.

Finally, analytic and discrete adjoint results are compared in Figure D.6, using the flow case shown in Figure D.3. The grids used here both contain 160 points, though in order to better show the two results on the same graph, the discrete results are only shown at every 10th point.

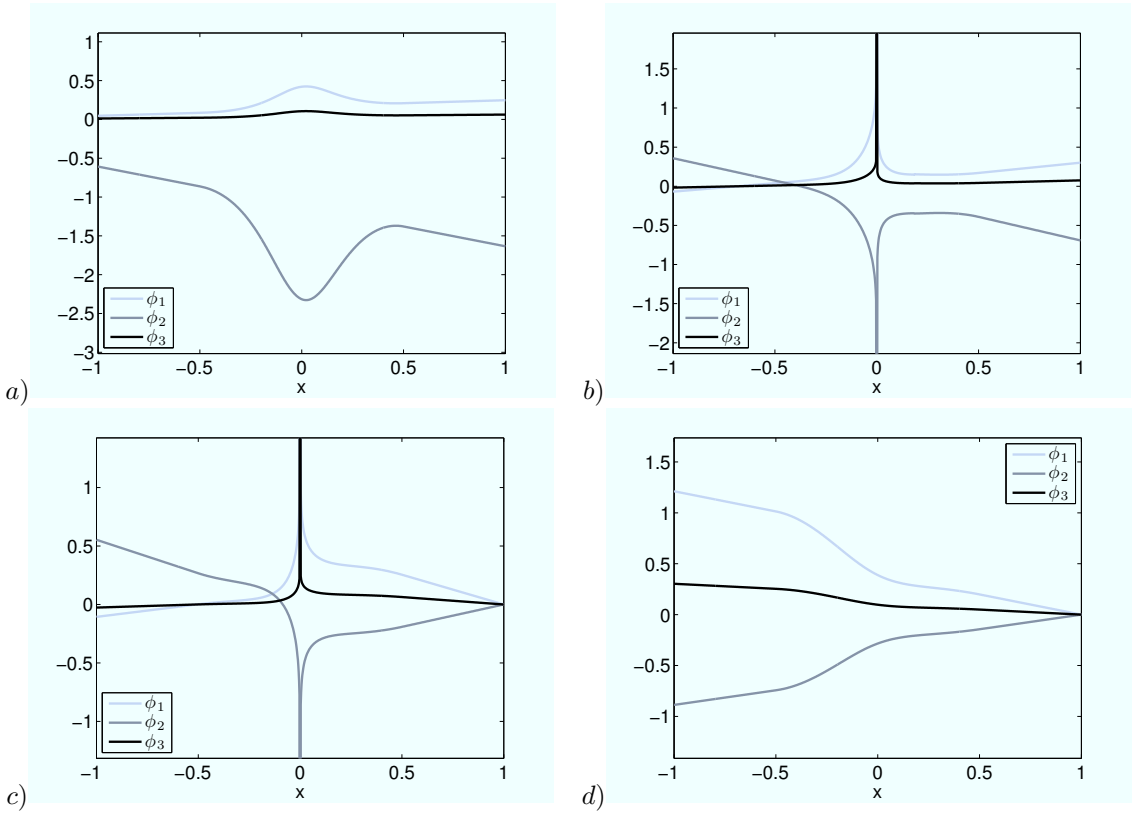

Figure D.4: Full-interval objective function adjoint variables along the converging-diverging nozzle, with $H_i = 4$, $p_{0_i} = 2$: a) subsonic flow, $p_e = 1.98$; b) shocked flow, $p_e = 1.6$; c) transonic flow; d) supersonic flow, $M_i = 3$.

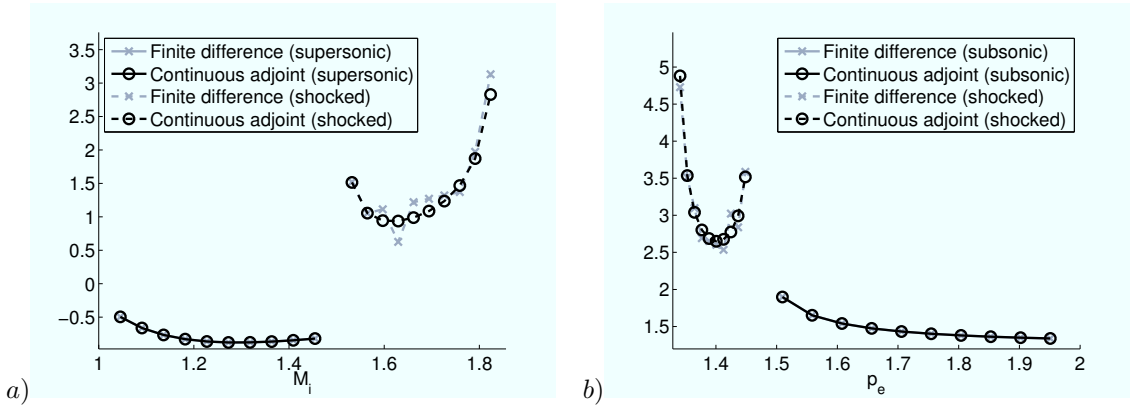

Figure D.5: Full-interval objective function sensitivity in expansion nozzle, with $H_i = 4$, $p_{0_i} = 2$: a) with respect to inlet Mach number, $\frac{dJ}{dM_i}$, b) with respect to exit pressure, $\frac{dJ}{dp_e}$.

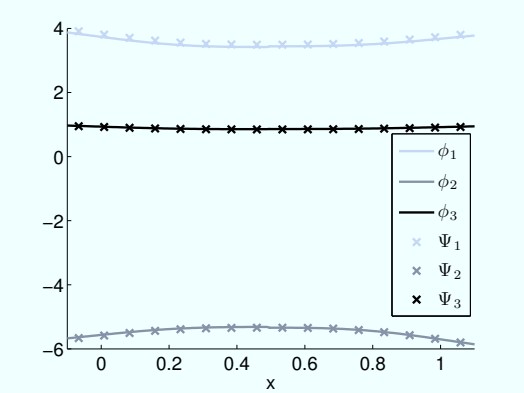

Figure D.6: Comparison between discrete (Ψ) and analytic (ϕ) adjoint variables for the expansion nozzle with shocked flow ($H_i = 4$, $M_i = 1.8$ and $\frac{p_e}{p_i} = 3.65$). The grid spacing used for both results is 160 points, but for clarity only every 10th point of the discrete solution is shown.

Reduced-interval functionals Figures D.7, D.8, D.9 and D.10 show the affect on the adjoint variables of changing the width of a reduced-interval functional centered at the throat of the converging-diverging nozzle for the subsonic, shocked, transonic and supersonic flow cases, respectively. An interesting feature to note in the shocked case is that the shape is similar to that for the full-interval objective function, but with the adjoint variables steadily decreasing in absolute value, until the interval no longer includes the shock. After this point, the adjoint variables are zero downstream of the shock.

The sensitivity of the reduced-interval objective function to both the inlet Mach number, M_i, and exit pressure, p_e, is plotted in Figure D.11, showing the comparison to finite differencing. This shows the same features as for the full-interval, i.e., that there is good agreement for subsonic and supersonic flow, but that where a shock is present the finite difference result poorly matches the analytic adjoint.

Finally, comparison with the discrete adjoint in Figure D.12 again shows generally good, though not perfect, matching for the reduced-interval functional.

Pointwise functionals The effect of moving the pointwise objective function along the converging-diverging nozzle is shown in Figures D.13, D.14, D.15 and D.16 for the subsonic, shocked, transonic and supersonic flow cases, respectively. The shocked case shows similarities to the previous situation with the reduced-interval functional, i.e., that passing through the sonic point or the shock changes which parts of the nozzle contribute to the functional.

The sensitivity of the pointwise functional to inlet Mach number and exit pressure is shown in Figure D.17. In contrast to the previous two situations, here the finite differencing agrees exactly with the analytic result. This is likely because it would only be affected by poor shock capturing in

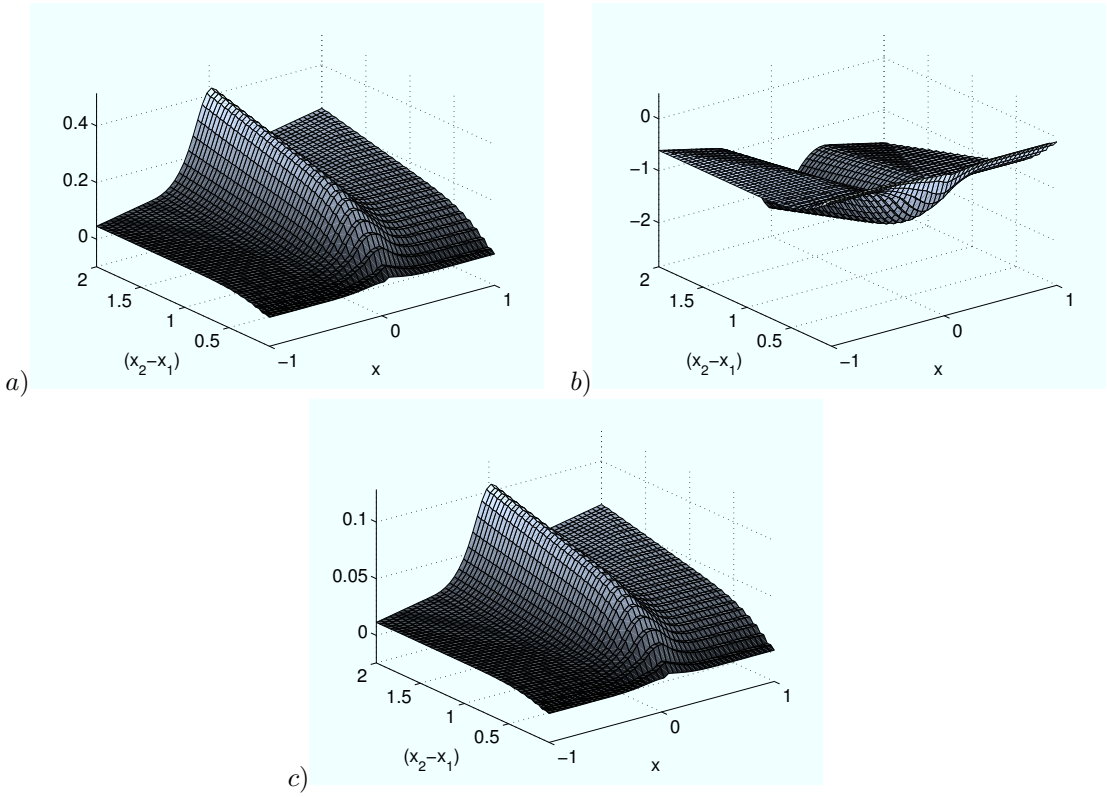

Figure D.7: Adjoint variables for reduced interval functionals located at the throat ($x = 0$) with varying widths, $x_2 - x_1$, along the converging-diverging nozzle, for subsonic flow: a) ϕ_1; b) ϕ_2; c) ϕ_3.

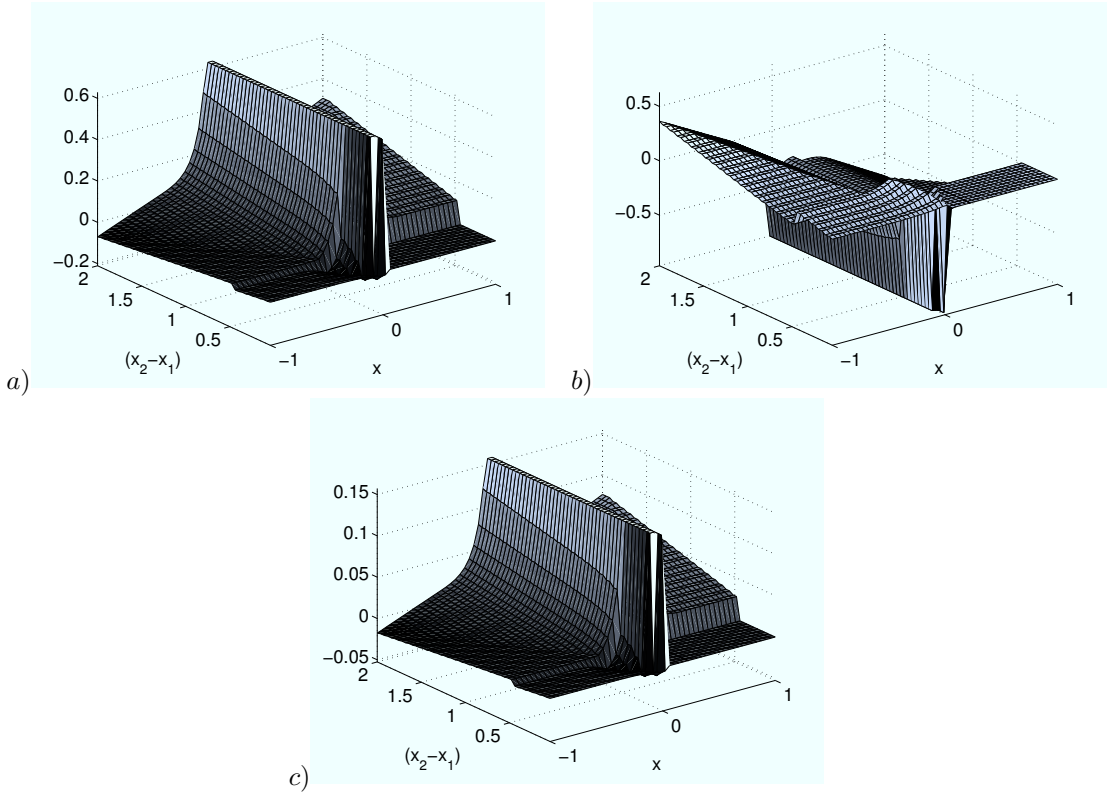

Figure D.8: Adjoint variables for reduced-interval functionals centered at the throat ($x = 0$) with varying widths, $x_2 - x_1$, along the converging-diverging nozzle, for shocked flow: a) ϕ_1; b) ϕ_2; c) ϕ_3.

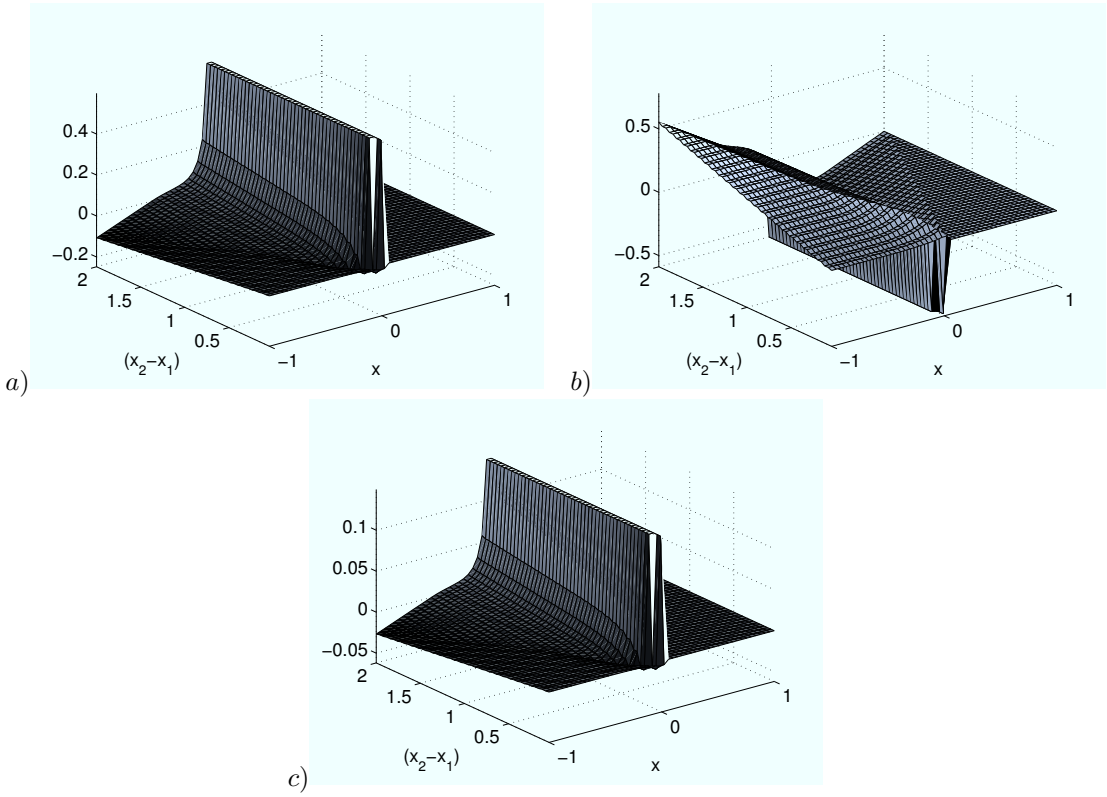

Figure D.9: Adjoint variables for reduced interval functionals located at the throat ($x = 0$) with varying widths, $x_2 - x_1$, along the converging-diverging nozzle, for transonic flow: a) ϕ_1; b) ϕ_2; c) ϕ_3.

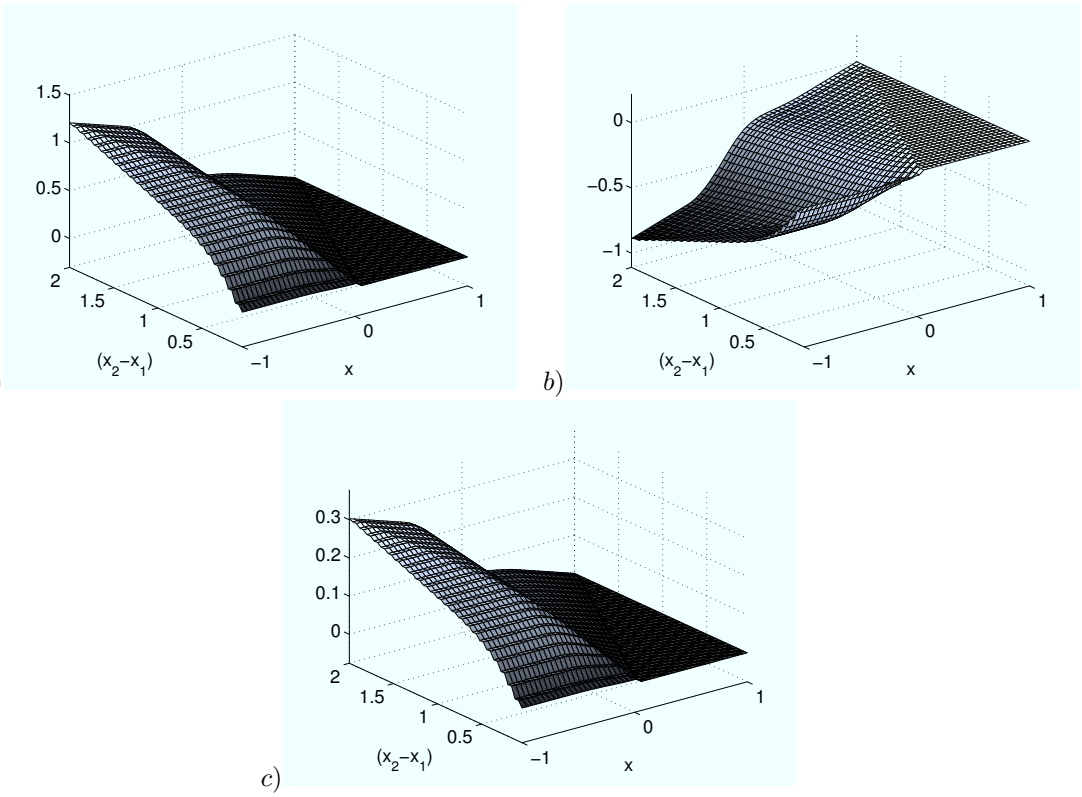

Figure D.10: Adjoint variables for reduced interval functionals located at the throat ($x = 0$) with varying widths, $x_2 - x_1$, along the converging-diverging nozzle, for supersonic flow: a) ϕ_1; b) ϕ_2; c) ϕ_3.

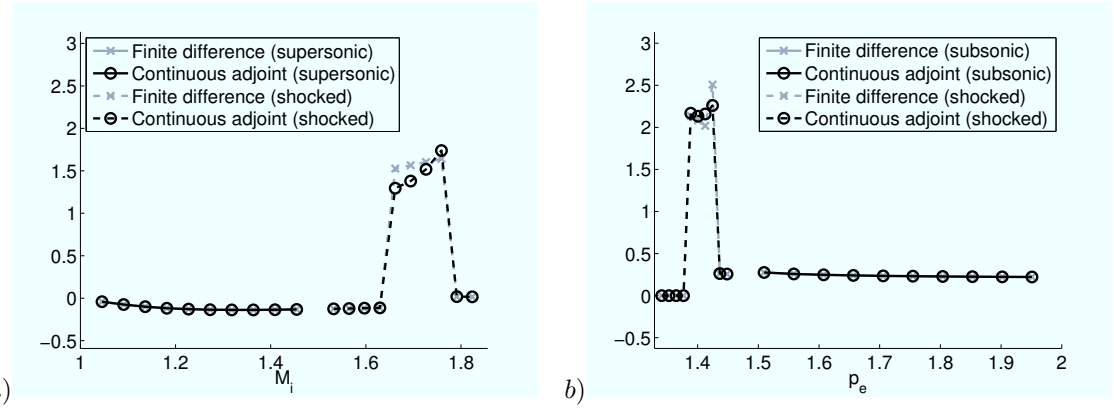

Figure D.11: Reduced-interval objective function ($x_1 = 0.4$, $x_2 = 0.6$) sensitivity in expansion nozzle, with $H_i = 4$, $p_{0_i} = 2$: a) to inlet Mach number, $\dfrac{dJ}{dM_i}$, b) to exit pressure, $\dfrac{dJ}{dp_e}$.

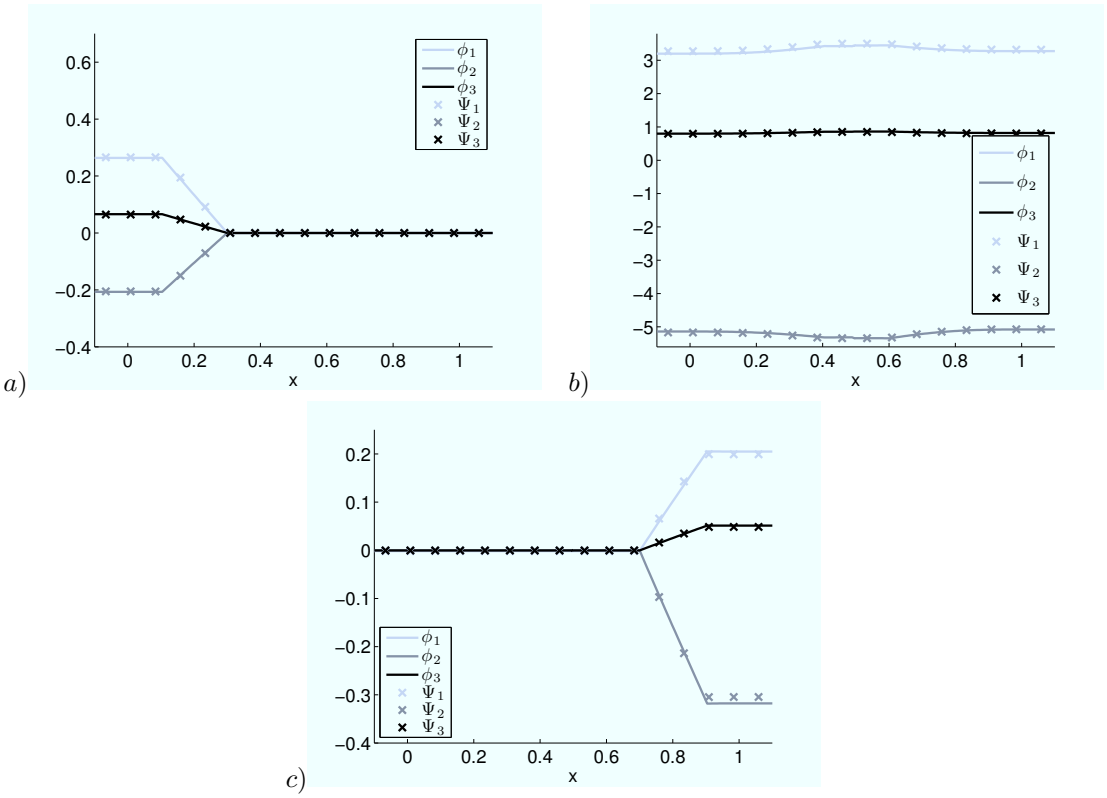

Figure D.12: Comparison between discrete (Ψ) and analytic (ϕ) reduced-interval adjoint variables for the expansion nozzle with shocked flow ($H_i = 4$, $M_i = 1.8$ and $\frac{p_e}{p_i} = 3.65$): a) $x_1 = 0.1$, $x_2 = 0.3$; b) $x_1 = 0.4$, $x_2 = 0.6$;. c) $x_1 = 0.7$, $x_2 = 0.9$. The grid spacing used for both results is 160 points, but for clarity only every 10th point of the discrete solution is shown.

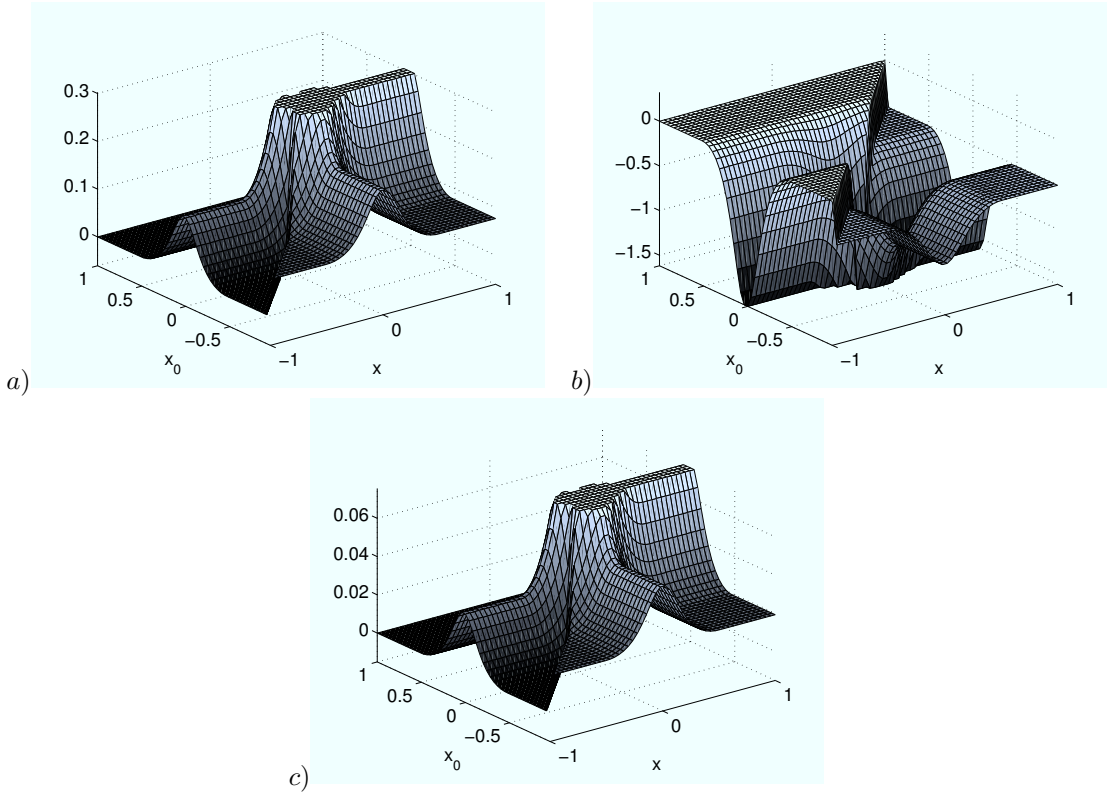

Figure D.13: Adjoint variables for pointwise functionals located as various positions (x_0) along the converging-diverging nozzle, for subsonic flow: a) ϕ_1; b) ϕ_2; c) ϕ_3.

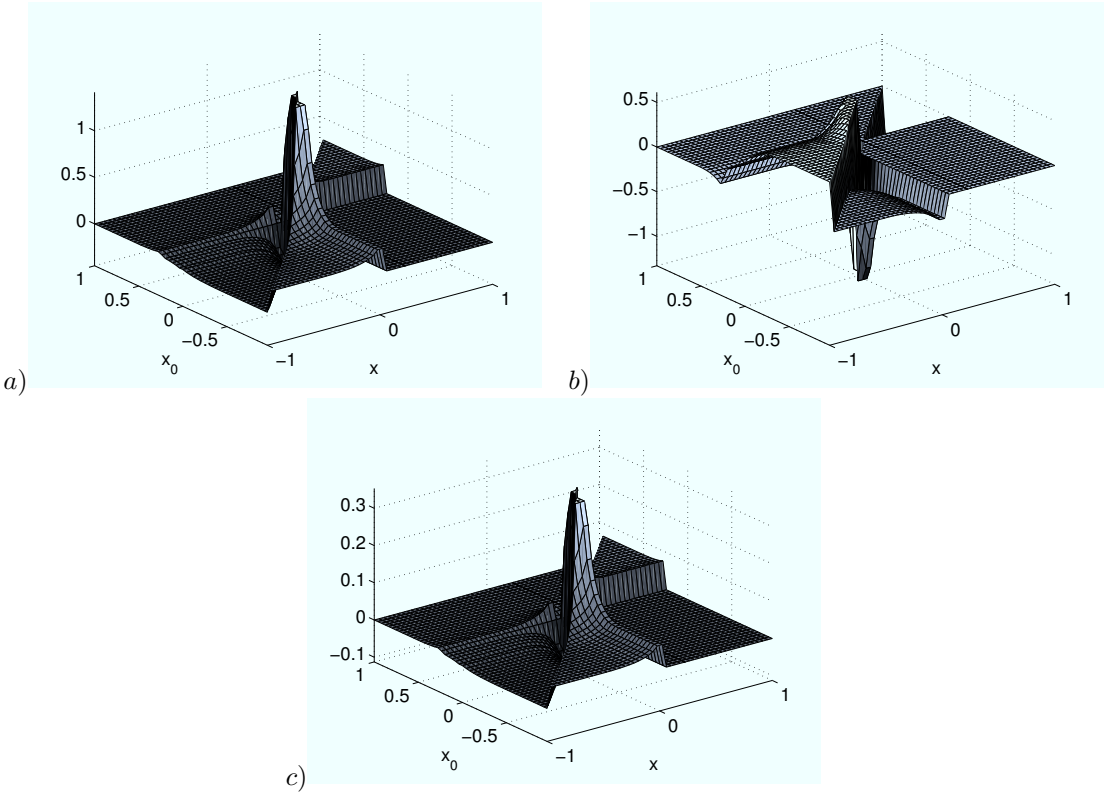

Figure D.14: Adjoint variables for pointwise functionals located as various positions (x_0) along the converging-diverging nozzle, for shocked flow: a) ϕ_1; b) ϕ_2; c) ϕ_3.

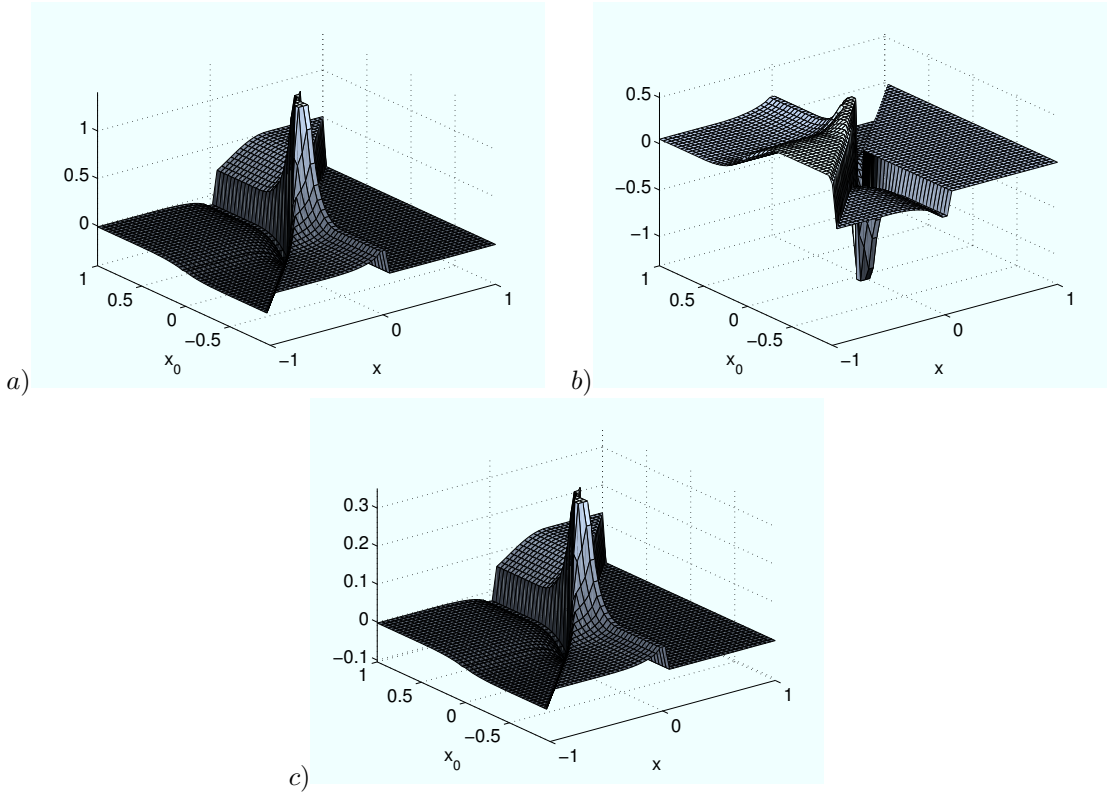

Figure D.15: Adjoint variables for pointwise functionals located as various positions (x_0) along the converging-diverging nozzle, for transonic flow: a) ϕ_1; b) ϕ_2; c) ϕ_3.

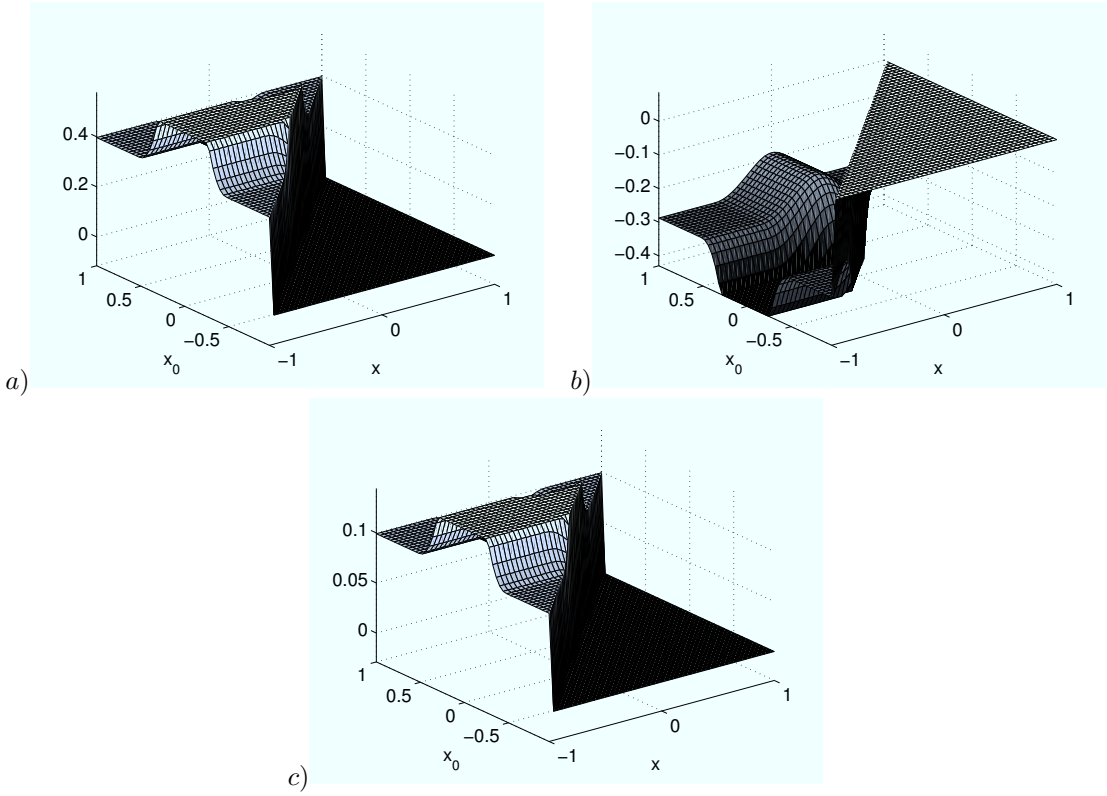

Figure D.16: Adjoint variables for pointwise functionals located as various positions (x_0) along the converging-diverging nozzle, for supersonic flow: a) ϕ_1; b) ϕ_2; c) ϕ_3.

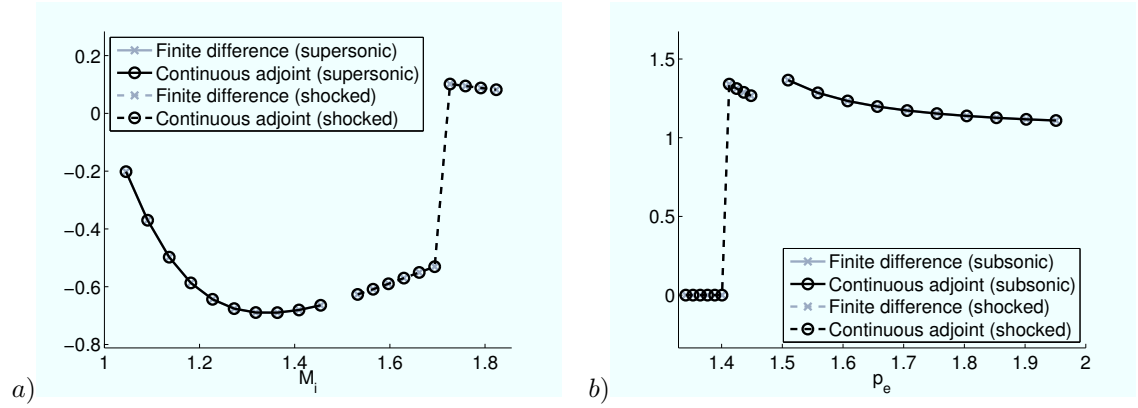

Figure D.17: Pointwise objective function ($x_0 = 0.5$) sensitivity in expansion nozzle, with $H_i = 4$, $p_{0_i} = 2$: a) to inlet Mach number, $\frac{dJ}{dM_i}$, b) to exit pressure, $\frac{dJ}{dp_e}$.

the very close vicinity of the shock.

Figure D.18 shows the comparison of the pointwise analytic adjoints with results from discrete adjoints, showing very close agreement.

D.1.5 Discussion

In the above theory and results we can see that it is possible to handle reduced interval and pointwise functionals relatively easily with the analytic adjoint approach. We can also note that the analytic adjoint is seen to be more accurate than finite differencing for shocked cases, especially where the grid is relatively coarse in the vicinity of the shock, and that on a coarse grid it gives close, but not perfect agreement with the discrete adjoint. Finally it may be useful to consider that solution through an analytic continuous adjoint may be much cheaper than solving either the continuous or discrete equations, and we can, for example, investigate a range of different reduced-interval or pointwise functionals quickly and easily.

D.2 Rayleigh flow

The Green's function approach for obtaining analytic adjoint solutions can also be applied to other simple one-dimensional flows, and here we extend it to handle Rayleigh flow, which is purely one-dimensional but with heat addition.

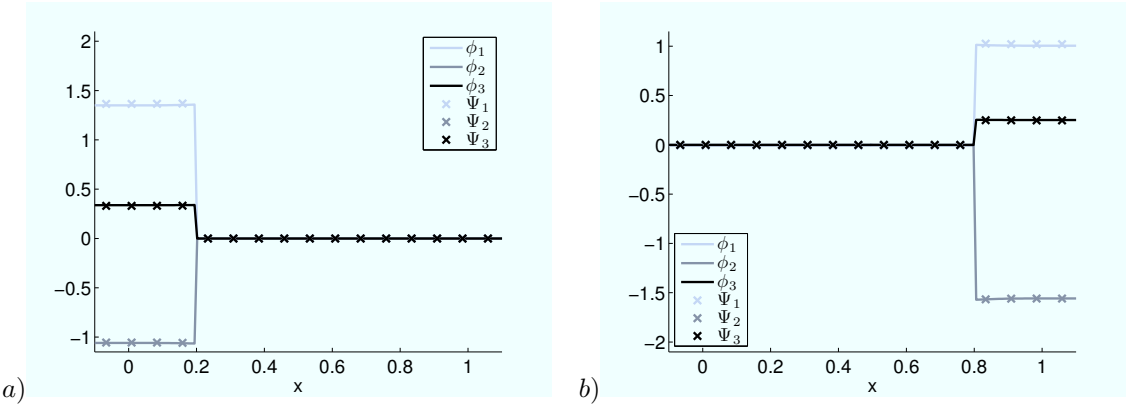

Figure D.18: Comparison between discrete (Ψ) and analytic (ϕ) pointwise adjoint variables for the expansion nozzle with shocked flow ($H_i = 4$, $M_i = 1.8$ and $\frac{p_e}{p_i} = 3.65$): a) $x_0 = 0.2$; b) $x_0 = 0.8$. The grid spacing used for both results is 160 points, but for clarity only every 10th point of the discrete solution is shown.

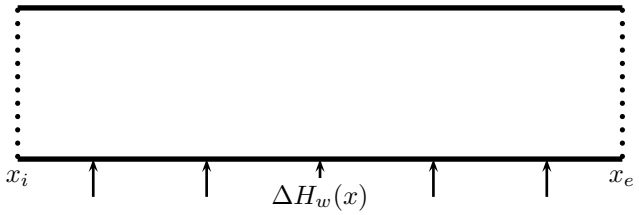

Figure D.19: Constant-height duct with heat addition.

D.2.1 Flow problem

D.2.1.1 Definition

We consider one-dimensional Rayleigh flow in the duct $x \in [x_i, x_e]$ of constant height with cumulative heat addition from the wall $\Delta H_w(x)$ as shown in Figure D.19.

The analytical governing equations for this are

$$\mathcal{N} \equiv \frac{dF}{dx} - \frac{dS_R}{dx} = 0, \quad x \in [x_i, x_e], \tag{D.16}$$

where the vectors of flow variables and fluxes are again given by (4.2), but we now include a heat

source term

$$S_R = \begin{pmatrix} 0 \\ 0 \\ m\Delta H_w \end{pmatrix}. \tag{D.17}$$

A feature of Rayleigh flow is that as the stagnation pressure increases along the duct the Mach number of the flow will approach unity for both subsonic and supersonic initial conditions. Adding further heat after the choked point will move the position of choking downstream, changing the inlet conditions. This simple flow type does not admit shocked solutions, or at least provides no way that the shock can be fixed at a set location by the boundary conditions and so we thus consider only subsonic and supersonic flows.

We define the same 'lift' integral functional used previously for quasi-one-dimensional flow, given in equation (4.117).

D.2.1.2 Boundary conditions

The characteristics for Rayleigh flow are the same as those for quasi-one-dimensional Euler flow, and thus we can use the same subsonic and supersonic boundary conditions as before, given in Section 4.1.1.2.

D.2.1.3 Numerical implementation

As for quasi-one-dimensional Euler flow, analytical results also exist for Rayleigh flow, allowing us to solve the equations exactly. These include the stagnation temperature-Mach number relation,

$$\frac{T_0}{T_0^*} = \frac{2(\gamma+1)M^2}{(1+\gamma M^2)^2}\left(1+\frac{\gamma-1}{2}M^2\right), \tag{D.18}$$

the stagnation pressure-Mach number relation,

$$\frac{p_0}{p_0^*} = \frac{\gamma+1}{1+\gamma M^2}\left(\frac{2}{\gamma+1}\left(1+\frac{\gamma-1}{2}M^2\right)\right)^{\frac{\gamma}{\gamma-1}}, \tag{D.19}$$

and the isentropic relation,

$$\frac{p_0}{p} = \left(1+\frac{\gamma-1}{2}M^2\right)^{\frac{\gamma}{\gamma-1}}. \tag{D.20}$$

These were implemented into a MATLAB code to calculate the flow for any given distribution of heat addition.

D.2.2 Continuous adjoint problem

D.2.2.1 Derivation

It is again possible to derive the continuous adjoint equation via a Lagrange multiplier approach as previously shown for quasi-one-dimensional Euler flow in Section 4.1.3.1. Again the development outlined here is based around using the 'lift' objective function given by equation (4.117). We will not show this process here since the results can be found by inspection, noting that it is very similar to quasi-one-dimensional Euler flow but with no height variation, and thus no pressure source term, an additional flux term from the heat addition and no shocks. We can therefore write down the continuous adjoint equation,

$$L^*(\phi) - g = 0, \quad x \in [x_i, x_e], \tag{D.21}$$

where

$$L^*(\phi) = \left(\frac{S_R}{m}\frac{\partial m}{\partial U} - \frac{\partial F}{\partial U}\right)^T \frac{d\phi}{dx}, \tag{D.22}$$

and

$$g = \left(\frac{\partial p}{\partial U}\right)^T, \tag{D.23}$$

with the boundary conditions

$$\left[\phi^T \left(\frac{S_R}{m}\frac{\partial m}{\partial U} - \frac{\partial F}{\partial U}\right)\delta U\right]_{x_i}^{x_e} = 0, \tag{D.24}$$

giving the perturbation to the objective function, assuming no explicit dependence of $\mathcal{J}$ on α, as

$$\mathcal{J} = \int_{x_i}^{x_e} \phi^T \frac{\partial \mathcal{N}}{\partial \alpha}\delta\alpha dx + \int_{x_i}^{x_e} \frac{\partial p}{\partial \alpha}\delta\alpha dx. \tag{D.25}$$

D.2.2.2 Boundary conditions

The continuous adjoint equations for Rayleigh flow are subject to the boundary conditions (D.24) at the inlet and outlet. As for quasi-one-dimensional flow, we note that the boundary conditions will be satisfied if the term in square brackets is zero at both the inlet and outlet, and this implies the same number of adjoint boundary conditions will be required.

Expanding the term in square brackets at just one of these locations we now get

$$\begin{pmatrix} \phi_\rho & \phi_m & \phi_\epsilon \end{pmatrix} \left(\frac{S_R}{m}\frac{\partial m}{\partial U} - \frac{\partial F}{\partial U}\right) \begin{pmatrix} \delta\rho \\ \delta m \\ \delta\epsilon \end{pmatrix} = 0. \tag{D.26}$$

As previously, appropriately applying the flow boundary conditions will give the required conditions on the adjoint variables. Rayleigh flow has the same adjoint boundary conditions as quasi-one-dimensional Euler flow (Section 4.1.3.2) except at a subsonic exit. Here a slight modification is needed to account for the change in the stagnation enthalpy along the duct, giving

$$-\left(\frac{m}{\rho}\right)^2 \phi_m - \left(\frac{m}{\rho}H + \frac{1}{2}\left(\frac{m}{\rho}\right)^3\right)\phi_\epsilon = 0, \tag{D.27}$$

and

$$\phi_\rho + 2\frac{m}{\rho}\phi_m + \left(H_i + \left(\frac{m}{\rho}\right)^2\right)\phi_\epsilon = 0, \tag{D.28}$$

where we note that the inlet stagnation enthalpy $H_i = H - \Delta H_w$.

D.2.2.3 Sensitivity formulae

Again by inspection, noting the result from quasi-one-dimensional Euler flow given in section 4.1.3.3, the sensitivity of the functional to a parameter α can be written as

$$\frac{d\mathcal{J}}{d\alpha} = \frac{\delta\mathcal{J}}{\delta\alpha} = \int_{x_i}^{x_e} \phi^T \frac{\partial}{\partial U}\left(F - S_R\right)\frac{\partial U}{\partial \alpha}dx, \tag{D.29}$$

assuming there is no explicit dependence of $\mathcal{J}$ on α. Thus the only additional information needed to calculate this sensitivity is the term $\dfrac{\partial U}{\partial \alpha}$, noting that the other required derivative terms make up the continuous adjoint equation and will have already been calculated.

When considering possible choices for α that are only defined at just one point in the flow, such as boundary conditions, this can again be further simplified to give just

$$\frac{d\mathcal{J}}{d\alpha} = h\phi^T\left(\frac{\partial F}{\partial U} - \frac{\partial S_R}{\partial U}\right)\frac{\partial U}{\partial \alpha}. \tag{D.30}$$

D.2.3 Analytical adjoint solution

D.2.3.1 Approach

This follows closely the Green's function approach outlined previously for quasi-one-dimensional flow, however, for Rayleigh flow, the solution to the inhomogeneous equation (2.27) is now written in terms of uniform perturbations a, b and c to the mass flow, the momentum, which we will call $\mu = p + \frac{m^2}{\rho}$, and the inlet stagnation enthalpy, respectively, i.e.,

$$\delta U_p(x,\xi) = a(x,\xi)\left.\frac{\partial U}{\partial m}\right|_{\mu,H_i} + b(x,\xi)\left.\frac{\partial U}{\partial \mu}\right|_{m,H_i} + c(x,\xi)\left.\frac{\partial U}{\partial H_i}\right|_{m,\mu}, \tag{D.31}$$

noting as before that on either side of ξ, the perturbations a, b and c must satisfy the homogeneous equations and are thus constant, but there can be a discontinuous jump in their values at $x = \xi$. From this result we can again find analytic solutions for the $\mathcal{I}_p$ using equation (2.28).

Integrating the inhomogeneous equations (2.27) from $x = \xi^-$ to $x = \xi^+$ gives, for Rayleigh flow,

$$\begin{aligned} f_p(\xi) &= (a_2 - a_1)\left(\frac{\partial F}{\partial m}(\xi)\bigg|_{\mu,H_i} - \frac{S_R}{m}\frac{\partial m}{\partial m}(\xi)\bigg|_{\mu,H_i}\right) \\ &\quad +(b_2 - b_1)\left(\frac{\partial F}{\partial \mu}(\xi)\bigg|_{m,H_i} - \frac{S_R}{m}\frac{\partial m}{\partial \mu}(\xi)\bigg|_{m,H_i}\right) \\ &\quad +(c_2 - c_1)\left(\frac{\partial F}{\partial H_i}(\xi)\bigg|_{m,\mu} - \frac{S_R}{m}\frac{\partial m}{\partial H_i}(\xi)\bigg|_{m,\mu}\right). \end{aligned} \tag{D.32}$$

Therefore we can choose the three linearly independent source vectors to be

$$\begin{aligned} f_1(\xi) &= \frac{\partial F}{\partial m}(\xi)\bigg|_{\mu,H_i} - \frac{S_R}{m}(\xi)\bigg|_{\mu,H_i}, \\ f_2(\xi) &= \frac{\partial F}{\partial \mu}(\xi)\bigg|_{m,H_i}, \\ f_3(\xi) &= \frac{\partial F}{\partial H_i}(\xi)\bigg|_{m,\mu}, \end{aligned} \tag{D.33}$$

so that the perturbations have the same simple properties given in (D.9).

Using the results for $\mathcal{I}_p$ and f_p we can then again derive exact values for the continuous adjoint variables, ϕ, from equation (2.29). Formulae for the $\mathcal{I}_p$ for both flow regimes are given in Appendix E.

D.2.3.2 Numerical implementation

As for quasi-one-dimensional Euler flow, once the flow problem had been solved, the continuous adjoint variables were found using these analytical results. This was again performed via MATLAB, and the required integrals were found by applying the trapezoidal quadrature rule.

D.2.4 Results

D.2.4.1 Flow test cases

The test case used to analyze the Raleigh flow analytic adjoint results was a straight duct with constant heating. Two different flow cases were considered:

- subsonic flow, with $H_i = 4$, $H_e = 5$, $p_{0_i} = 2$ and $p_e = 1.9$,

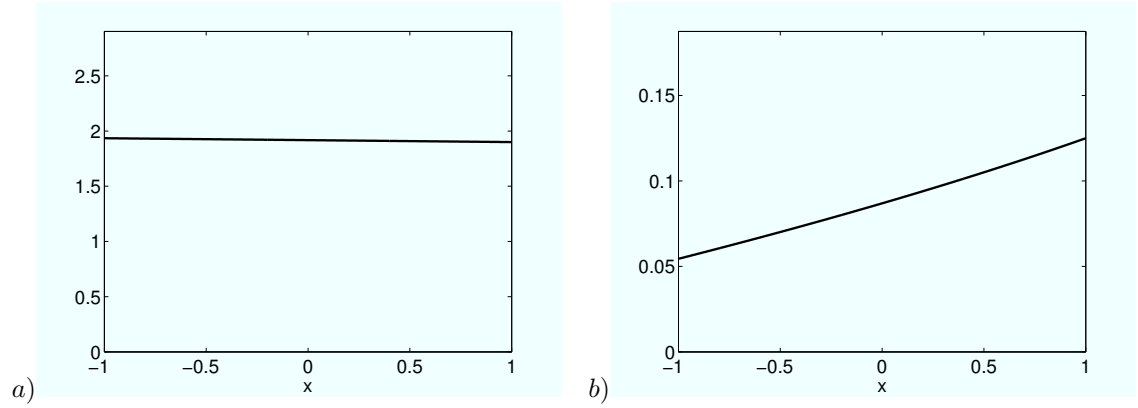

Figure D.20: Pressure variation along straight duct, with constant heating and $H_i = 4$, $H_e = 5$, $p_{0_i} = 2$: a) subsonic flow, $p_e = 1.9$; b) supersonic flow, $M_i = 3$.

- supersonic flow, with $H_i = 4$, $H_e = 5$, $p_{0_i} = 2$ and $M_i = 3$,

and the shapes of the analytic adjoint variables in each case were analyzed. The pressure variation along the duct for these different situations can be seen in Figure D.20.

The sensitivity of the objective function to the inlet Mach number, $\frac{\partial \mathcal{J}}{\partial M_i}$, and exit pressure, $\frac{\partial \mathcal{J}}{\partial p_e}$, was also investigated over a range of inlet Mach numbers and exit pressures, respectively, making comparison to results from finite differencing. The grid used was evenly spaced with 10,000 points, and the finite difference step was 2×10^{-4}.

D.2.4.2 Adjoint results

Figure D.21 show the shapes of the resultant adjoint variables for Rayleigh flow. We can note that as expected in the case of supersonic flow, all adjoint variables are zero at the exit.

The sensitivity of the objective function is shown in Figure D.22, with comparison to finite differencing. Exact agreement is seen for the supersonic case, but not for the subsonic.

D.2.5 Discussion

We have shown above that it is theoretically possible to create analytic adjoint solutions for Rayleigh flow, and the results have shown good agreement with finite differencing, thought with a discrepancy in the subsonic case. This also implies that we may be able to apply this approach to further one-dimensional flows, perhaps including other terms such as friction, as long as it is possible to write perturbations in terms of appropriate conserved quantities.

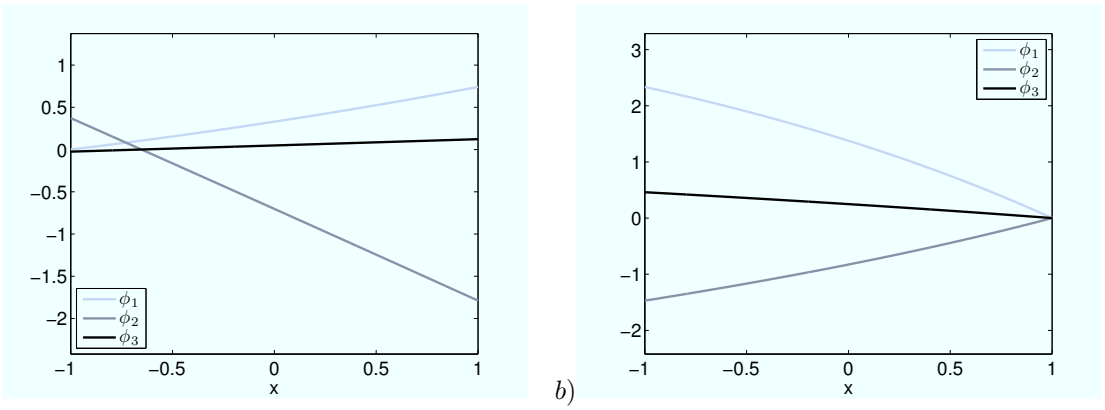

Figure D.21: Adjoint variables along the straight duct, with constant heating and $H_i = 4$, $H_e = 5$, $p_{0_i} = 2$: a) subsonic flow, $p_e = 1.9$; b) supersonic flow, $M_i = 3$.

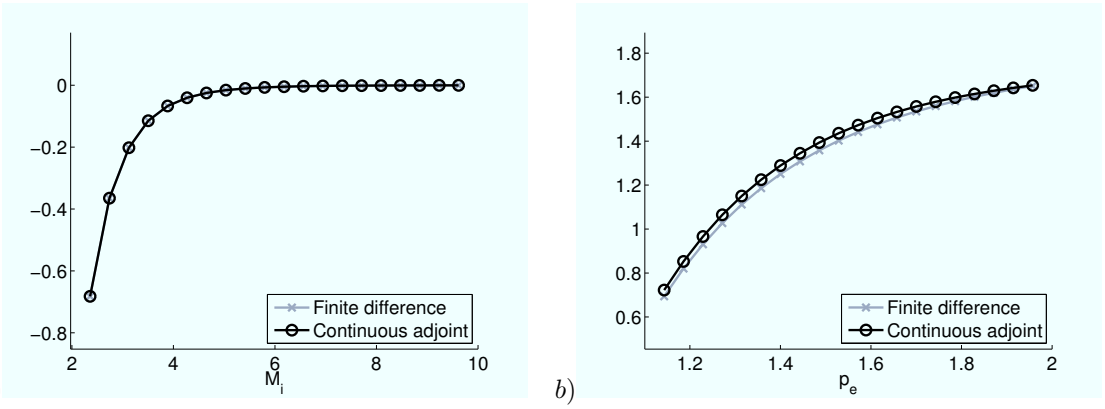

Figure D.22: Objective function sensitivity in the straight duct, with constant heating and $H_i = 4$, $H_e = 5$, $p_{0_i} = 2$: a) to inlet Mach number, $\frac{dJ}{dM_i}$; b) to exit pressure $\frac{dJ}{dp_e}$.

Appendix E

Analytic adjoint formulae

This appendix presents the formulae for obtaining the analytic adjoints for both quasi-one-dimensional Euler flow and Rayleigh flow.

E.1 One-dimensional flows

E.1.0.1 Quasi-one-dimensional Euler flow

Full-interval functionals

Supersonic

$\mathcal{I}_1$**:**

$$\mathcal{I}_1(\xi) = \int_{\xi}^{x_e} \frac{1}{h} \left.\frac{\partial p}{\partial m}\right|_{H,p_0} dx. \tag{E.1}$$

$\mathcal{I}_2$**:**

$$\mathcal{I}_2(\xi) = 0. \tag{E.2}$$

$\mathcal{I}_3$**:**

$$\mathcal{I}_3(\xi) = \int_{\xi}^{x_e} \left.\frac{\partial p}{\partial p_0}\right|_{H,M} dx. \tag{E.3}$$

Subsonic

$\mathcal{I}_1$**:**

$$\mathcal{I}_1(\xi) = -\int_{x_i}^{\xi} \frac{1}{h} \left.\frac{\partial p}{\partial m}\right|_{H,p_0} dx. \tag{E.4}$$

$\mathcal{I}_2$**:**

$$\mathcal{I}_2(\xi) = 0. \tag{E.5}$$

$\mathcal{I}_3$**:**

$$\mathcal{I}_3(\xi) = \int_{x_i}^{x_e} \frac{a}{h} \left.\frac{\partial p}{\partial m}\right|_{H,p_0} dx + \int_{\xi}^{x_e} \frac{\partial p}{\partial p_0}|_{H,M} dx, \tag{E.6}$$

where

$$a = \left(\frac{-h \left.\frac{\partial p}{\partial p_0}\right|_{H,M}}{\left.\frac{\partial p}{\partial m}\right|_{H,p_0}} \right)_{x_e}. \tag{E.7}$$

Isentropic Transonic

$\mathcal{I}_1$**:**

$\xi < 0$:

$$\mathcal{I}_1(\xi) = -\int_{x_i}^{\xi} \frac{1}{h} \left.\frac{\partial p}{\partial m}\right|_{H,p_0} dx. \tag{E.8}$$

$\xi > 0$:

$$\mathcal{I}_1(\xi) = \int_{\xi}^{x_e} \frac{1}{h} \left.\frac{\partial p}{\partial m}\right|_{H,p_0} dx. \tag{E.9}$$

$\mathcal{I}_2$**:**

$$\mathcal{I}_2(\xi) = 0. \tag{E.10}$$

$\mathcal{I}_3$**:**

$$\mathcal{I}_3(\xi) = \int_{\xi}^{x_e} \left.\frac{\partial p}{\partial p_0}\right|_{H,M} dx. \tag{E.11}$$

Shocked

$\mathcal{I}_1$**:**

$\xi < 0$:

$$\mathcal{I}_1(\xi) = -\int_{x_i}^{\xi} \frac{1}{h} \left.\frac{\partial p}{\partial m}\right|_{H,p_0} dx. \tag{E.12}$$

$0 < \xi < x_s$:

$$\begin{aligned}\mathcal{I}_1(\xi) &= \int_{\xi}^{x_s} \frac{1}{h}\left.\frac{\partial p}{\partial m}\right|_{H,p_0} dx \\ &\quad + \int_{x_s}^{x_e} \left(\frac{a_{2B}}{h}\left.\frac{\partial p}{\partial m}\right|_{H,p_0} + c_{2B}\left.\frac{\partial p}{\partial p_0}\right|_{H,M} \right) dx \\ &\quad -(p_B - p_A)\delta x_s,\end{aligned} \tag{E.13}$$

where

$$a_{2B} = 1 - c_{2B}\left(h\left.\frac{\partial m}{\partial p_0}\right|_{H,M} \right)_{x_{s^+}}, \tag{E.14}$$

$$c_{2B} = p_{0A} f_s^{'}(M_A)\left(\frac{dM}{dx}\delta x_s + \frac{1}{h}\left.\frac{\partial M}{\partial m}\right|_{H,p_0} \right)_{x_{s^-}}, \tag{E.15}$$

and

$$\left(\frac{a_{2B}}{h}\left.\frac{\partial p}{\partial m}\right|_{H,p_0} + c_{2B}\left.\frac{\partial p}{\partial p_0}\right|_{H,M} \right)_{x_e} = 0. \tag{E.16}$$

$\xi > x_s$:

$$\begin{aligned}\mathcal{I}_1(\xi) &= \int_{x_s}^{\xi} \frac{a_{1B}}{h}\left.\frac{\partial p}{\partial m}\right|_{H,p_0} dx + \int_{\xi}^{x_e} \frac{1 + a_{1B}}{h}\left.\frac{\partial p}{\partial m}\right|_{H,p_0} dx \\ &\quad + \int_{x_s}^{x_e} c_{1B}\left.\frac{\partial p}{\partial p_0}\right|_{H,M} dx - (p_B - p_A)\delta x_s,\end{aligned} \tag{E.17}$$

where

$$a_{1B} = -c_{1B}\left(h\left.\frac{\partial m}{\partial p_0}\right|_{H,M} \right)_{x_{s^+}}, \tag{E.18}$$

$$c_{1B} = p_{0A} f_s^{'}(M_A)\left.\frac{dM}{dx}\right|_{x_{s^-}} \delta x_s, \tag{E.19}$$

and

$$\left(\frac{1 + a_{1B}}{h}\left.\frac{\partial p}{\partial m}\right|_{H,p_0} + c_{1B}\left.\frac{\partial p}{\partial p_0}\right|_{H,M} \right)_{x_e} = 0. \tag{E.20}$$

$\mathcal{I}_2$**:**

$$\mathcal{I}_2(\xi) = 0. \tag{E.21}$$

$\mathcal{I}_3$**:**

$\xi < x_s$:

$$\begin{aligned}\mathcal{I}_3(\xi) &= \int_{x_s}^{x_e} \left(\frac{a_{2B}}{h} \left.\frac{\partial p}{\partial m}\right|_{H,p_0} + c_{2B} \left.\frac{\partial p}{\partial p_0}\right|_{H,M} \right) dx \\ &\quad + \int_{\xi}^{x_s} \left.\frac{\partial p}{\partial p_0}\right|_{H,M} dx - (p_B - p_A)\delta x_s,\end{aligned} \tag{E.22}$$

where

$$a_{2B} = \left(h \left.\frac{\partial m}{\partial p_0}\right|_{H,M} \right)_{x_{s^-}} - c_{2B} \left(h \left.\frac{\partial m}{\partial p_0}\right|_{H,M} \right)_{x_{s^+}}, \tag{E.23}$$

$$c_{2B} = f_s(M_A) + p_{0A} f_s^{'}(M_A) \left.\frac{dM}{dx}\right|_{x_{s^-}} \delta x_s, \tag{E.24}$$

and

$$\left(\frac{a_{2B}}{h} \left.\frac{\partial p}{\partial m}\right|_{H,p_0} + c_{2B} \left.\frac{\partial p}{\partial p_0}\right|_{H,M} \right)_{x_e} = 0. \tag{E.25}$$

$\xi > x_s$:

$$\begin{aligned}\mathcal{I}_3(\xi) &= \int_{x_s}^{x_e} \frac{a_{1B}}{h} \left.\frac{\partial p}{\partial m}\right|_{H,p_0} dx + \int_{x_s}^{\xi} c_{1B} \left.\frac{\partial p}{\partial p_0}\right|_{H,M} dx \\ &\quad + \int_{\xi}^{x_e} (1 + c_{1B}) \left.\frac{\partial p}{\partial p_0}\right|_{H,M} dx - (p_B - p_A)\delta x_s,\end{aligned} \tag{E.26}$$

where

$$a_{1B} = -c_{1B} \left(h \left.\frac{\partial m}{\partial p_0}\right|_{H,M} \right)_{x_{s^+}}, \tag{E.27}$$

$$c_{1B} = p_{0A} f_s^{'}(M_A) \left.\frac{dM}{dx}\right|_{x_{s^-}} \delta x_s, \tag{E.28}$$

and

$$\left(\frac{a_{1B}}{h} \left.\frac{\partial p}{\partial m}\right|_{H,p_0} + (1 + c_{1B}) \left.\frac{\partial p}{\partial p_0}\right|_{H,M} \right)_{x_e} = 0. \tag{E.29}$$

Reduced-interval functionals

Supersonic

$\mathcal{I}_1$**:**

$\xi < x_1$:

$$\mathcal{I}_1(\xi) = \int_{x_1}^{x_2} \frac{1}{h} \left.\frac{\partial p}{\partial m}\right|_{H,p_0} dx. \tag{E.30}$$

$x_1 < \xi < x_2$:

$$\mathcal{I}_1(\xi) = \int_{\xi}^{x_2} \frac{1}{h} \left.\frac{\partial p}{\partial m}\right|_{H,p_0} dx. \tag{E.31}$$

$\xi > x_2$:

$$\mathcal{I}_1(\xi) = 0. \tag{E.32}$$

$\mathcal{I}_2$**:**

$$\mathcal{I}_2(\xi) = 0. \tag{E.33}$$

$\mathcal{I}_3$**:**

$\xi < x_1$:

$$\mathcal{I}_3(\xi) = \int_{x_1}^{x_2} \left.\frac{\partial p}{\partial p_0}\right|_{H,M} dx. \tag{E.34}$$

$x_1 < \xi < x_2$:

$$\mathcal{I}_3(\xi) = \int_{\xi}^{x_2} \left.\frac{\partial p}{\partial p_0}\right|_{H,M} dx. \tag{E.35}$$

$\xi > x_2$:

$$\mathcal{I}_3(\xi) = 0. \tag{E.36}$$

Subsonic

$\mathcal{I}_1$**:**

$\xi < x_1$:

$$\mathcal{I}_1(\xi) = 0. \tag{E.37}$$

$x_1 < \xi < x_2$:

$$\mathcal{I}_1(\xi) = -\int_{x_1}^{\xi} \frac{1}{h} \left.\frac{\partial p}{\partial m}\right|_{H,p_0} dx. \tag{E.38}$$

$\xi > x_2$:

$$\mathcal{I}_1(\xi) = -\int_{x_1}^{x_2} \frac{1}{h} \left.\frac{\partial p}{\partial m}\right|_{H,p_0} dx. \tag{E.39}$$

$\mathcal{I}_2$**:**

$$\mathcal{I}_2(\xi) = 0. \tag{E.40}$$

$\mathcal{I}_3$**:**

$\xi < x_1$:

$$\mathcal{I}_3(\xi) = \int_{x_1}^{x_2} \left(\frac{a}{h} \left.\frac{\partial p}{\partial m}\right|_{H,p_0} + \left.\frac{\partial p}{\partial p_0}\right|_{H,M} \right) dx. \tag{E.41}$$

$x_1 < \xi < x_2$:

$$\mathcal{I}_3(\xi) = \int_{x_1}^{x_2} \frac{a}{h} \left.\frac{\partial p}{\partial m}\right|_{H,p_0} dx + \int_{\xi}^{x_2} \left.\frac{\partial p}{\partial p_0}\right|_{H,M} dx. \tag{E.42}$$

$\xi > x_2$:

$$\mathcal{I}_3(\xi) = \int_{x_1}^{x_2} \frac{a}{h} \left.\frac{\partial p}{\partial m}\right|_{H,p_0} dx. \tag{E.43}$$

Isentropic Transonic

$\mathcal{I}_1$**:**

$\xi < x_1$:

$\xi < 0$:

$$\mathcal{I}_1(\xi) = 0. \tag{E.44}$$

$\xi > 0$:

$$\mathcal{I}_1(\xi) = \int_{x_1}^{x_2} \frac{1}{h} \left.\frac{\partial p}{\partial m}\right|_{H,p_0} dx. \tag{E.45}$$

$x_1 < \xi < x_2$:

$\xi < 0$:

$$\mathcal{I}_1(\xi) = -\int_{x_1}^{\xi} \frac{1}{h} \left.\frac{\partial p}{\partial m}\right|_{H,p_0} dx. \tag{E.46}$$

$\xi > 0$:

$$\mathcal{I}_1(\xi) = \int_{\xi}^{x_2} \frac{1}{h} \left.\frac{\partial p}{\partial m}\right|_{H,p_0} dx. \tag{E.47}$$

$\xi > x_2$:

$\xi > 0$:

$$\mathcal{I}_1(\xi) = -\int_{x_1}^{x_2} \frac{1}{h} \left.\frac{\partial p}{\partial m}\right|_{H,p_0} dx. \tag{E.48}$$

$\xi > 0$:

$$\xi > 0 : \mathcal{I}_1(\xi) = 0. \tag{E.49}$$

$\mathcal{I}_2$**:**

$$\mathcal{I}_2(\xi) = 0. \tag{E.50}$$

$\mathcal{I}_3$**:**

$\xi < x_1$:

$$\mathcal{I}_3(\xi) = \int_{x_1}^{x_2} \left.\frac{\partial p}{\partial p_0}\right|_{H,M} dx. \tag{E.51}$$

$x_1 < \xi < x_2$:

$$\mathcal{I}_3(\xi) = \int_{\xi}^{x_2} \left.\frac{\partial p}{\partial p_0}\right|_{H,M} dx. \tag{E.52}$$

$\xi > x_2$:

$$\mathcal{I}_3(\xi) = 0. \tag{E.53}$$

Shocked

$\boldsymbol{x_s < x_1, x_2}$**:**

$\mathcal{I}_1$**:**

$\xi < x_s$:

$\xi < 0$:

$$\mathcal{I}_1(\xi) = 0. \tag{E.54}$$

$\xi > 0$:

$$\mathcal{I}_1(\xi) = \int_{x_1}^{x_2} \left(\frac{a_{2B}}{h} \left.\frac{\partial p}{\partial m}\right|_{H,p_0} + c_{2B} \left.\frac{\partial p}{\partial p_0}\right|_{H,M} \right) dx. \tag{E.55}$$

$x_s < \xi < x_1, x_2$:

$$\mathcal{I}_1(\xi) = \int_{x_1}^{x_2} \left(\frac{1 + a_{1B}}{h} \left.\frac{\partial p}{\partial m}\right|_{H,p_0} + c_{1B} \left.\frac{\partial p}{\partial p_0}\right|_{H,M} \right) dx. \tag{E.56}$$

$x_1 < \xi < x_2$:

$$\begin{aligned} \mathcal{I}_1(\xi) \quad = \quad & \int_{x_1}^{\xi} \frac{a_{1B}}{h} \left.\frac{\partial p}{\partial m}\right|_{H,p_0} dx + \int_{\xi}^{x_2} \frac{1 + a_{1B}}{h} \left.\frac{\partial p}{\partial m}\right|_{H,p_0} dx \\ & + \int_{x_1}^{x_2} c_{1B} \left.\frac{\partial p}{\partial p_0}\right|_{H,M} dx. \end{aligned} \tag{E.57}$$

$\xi > x_1, x_2$:

$$\mathcal{I}_1(\xi) = \int_{x_1}^{x_2} \left(\frac{a_{1B}}{h} \left.\frac{\partial p}{\partial m}\right|_{H,p_0} + c_{1B} \left.\frac{\partial p}{\partial p_0}\right|_{H,M} \right) dx. \tag{E.58}$$

$\mathcal{I}_2$**:**

$$\mathcal{I}_2(\xi) = 0. \tag{E.59}$$

$\mathcal{I}_3$**:**

$\xi < x_s$:

$$\mathcal{I}_3(\xi) = \int_{x_1}^{x_2} \left(\frac{a_{2B}}{h} \left.\frac{\partial p}{\partial m}\right|_{H,p_0} + c_{2B} \left.\frac{\partial p}{\partial p_0}\right|_{H,M} \right) dx. \tag{E.60}$$

$x_s < \xi < x_1, x_2$:

$$\mathcal{I}_3(\xi) = \int_{x_1}^{x_2} \left(\frac{a_{1B}}{h} \left.\frac{\partial p}{\partial m}\right|_{H,p_0} + (1 + c_{1B}) \left.\frac{\partial p}{\partial p_0}\right|_{H,M} \right) dx. \tag{E.61}$$

$x_1 < \xi < x_2$:

$$\begin{aligned} \mathcal{I}_3(\xi) &= \int_{x_1}^{x_2} \frac{a_{1B}}{h} \left.\frac{\partial p}{\partial m}\right|_{H,p_0} dx + \int_{x_1}^{\xi} c_{1B} \left.\frac{\partial p}{\partial p_0}\right|_{H,M} dx \\ &\quad + \int_{\xi}^{x_2} (1 + c_{1B}) \left.\frac{\partial p}{\partial p_0}\right|_{H,M} dx. \end{aligned} \tag{E.62}$$

$\xi > x_1, x_2$:

$$\mathcal{I}_3(\xi) = \int_{x_1}^{x_2} \left(\frac{a_{1B}}{h} \left.\frac{\partial p}{\partial m}\right|_{H,p_0} + c_{1B} \left.\frac{\partial p}{\partial p_0}\right|_{H,M} \right) dx. \tag{E.63}$$

$x_1 < x_s < x_2$:

$\mathcal{I}_1$:

$\xi < x_1$:

$\xi < 0$:

$$\mathcal{I}_1(\xi) = 0. \tag{E.64}$$

$\xi > 0$:

$$\begin{aligned} \mathcal{I}_1(\xi) &= \int_{x_1}^{x_s} \frac{1}{h} \left.\frac{\partial p}{\partial m}\right|_{H,p_0} dx \\ &\quad + \int_{x_s}^{x_2} \left(\frac{a_{2B}}{h} \left.\frac{\partial p}{\partial m}\right|_{H,p_0} + c_{2B} \left.\frac{\partial p}{\partial p_0}\right|_{H,M} \right) dx \\ &\quad - (p_B - p_A)\delta x_s. \end{aligned} \tag{E.65}$$

$x_1 < \xi < x_s$:

$\xi < 0$:

$$\mathcal{I}_1(\xi) = -\int_{x_1}^{\xi} \frac{1}{h} \left.\frac{\partial p}{\partial m}\right|_{H,p_0} dx. \tag{E.66}$$

$\xi > 0$:

$$\begin{aligned} \mathcal{I}_1(\xi) &= \int_{\xi}^{x_s} \frac{1}{h} \left.\frac{\partial p}{\partial m}\right|_{H,p_0} dx \\ &\quad + \int_{x_s}^{x_2} \left(\frac{a_{2B}}{h} \left.\frac{\partial p}{\partial m}\right|_{H,p_0} + c_{2B} \left.\frac{\partial p}{\partial p_0}\right|_{H,M} \right) dx \\ &\quad - (p_B - p_A)\delta x_s. \end{aligned} \tag{E.67}$$

$x_s < \xi < x_2$:

$$\begin{aligned}\mathcal{I}_1(\xi) &= \int_{x_s}^{\xi} \frac{a_{1B}}{h}\left.\frac{\partial p}{\partial m}\right|_{H,p_0} dx + \int_{\xi}^{x_2} \frac{1+a_{1B}}{h}\left.\frac{\partial p}{\partial m}\right|_{H,p_0} dx \\ &\quad + \int_{x_s}^{x_2} c_{1B}\left.\frac{\partial p}{\partial p_0}\right|_{H,M} dx - (p_B - p_A)\delta x_s.\end{aligned} \tag{E.68}$$

$\xi > x_2$:

$$\begin{aligned}\mathcal{I}_1(\xi) &= \int_{x_s}^{x_2} \left(\frac{a_{1B}}{h}\left.\frac{\partial p}{\partial m}\right|_{H,p_0} + c_{1B}\left.\frac{\partial p}{\partial p_0}\right|_{H,M}\right) dx \\ &\quad -(p_B - p_A)\delta x_s.\end{aligned} \tag{E.69}$$

$\mathcal{I}_2$**:**

$$\mathcal{I}_2(\xi) = 0. \tag{E.70}$$

$\mathcal{I}_3$**:** $\xi < x_1$:

$$\begin{aligned}\mathcal{I}_3(\xi) &= \int_{x_s}^{x_2} \left(\frac{a_{2B}}{h}\left.\frac{\partial p}{\partial m}\right|_{H,p_0} + c_{2B}\left.\frac{\partial p}{\partial p_0}\right|_{H,M}\right) dx \\ &\quad + \int_{x_1}^{x_s} \left.\frac{\partial p}{\partial p_0}\right|_{H,M} dx - (p_B - p_A)\delta x_s.\end{aligned} \tag{E.71}$$

$x_1 < \xi < x_s$:

$$\begin{aligned}\mathcal{I}_3(\xi) &= \int_{x_s}^{x_2} \left(\frac{a_{2B}}{h}\left.\frac{\partial p}{\partial m}\right|_{H,p_0} + c_{2B}\left.\frac{\partial p}{\partial p_0}\right|_{H,M}\right) dx \\ &\quad + \int_{\xi}^{x_s} \left.\frac{\partial p}{\partial p_0}\right|_{H,M} dx - (p_B - p_A)\delta x_s.\end{aligned} \tag{E.72}$$

$x_s < \xi < x_2$:

$$\begin{aligned}\mathcal{I}_3(\xi) &= \int_{x_s}^{x_2} \frac{a_{1B}}{h}\left.\frac{\partial p}{\partial m}\right|_{H,p_0} dx + \int_{x_s}^{\xi} c_{1B}\left.\frac{\partial p}{\partial p_0}\right|_{H,M} dx \\ &\quad + \int_{\xi}^{x_2} (1+c_{1B})\left.\frac{\partial p}{\partial p_0}\right|_{H,M} dx - (p_B - p_A)\delta x_s.\end{aligned} \tag{E.73}$$

$\xi > x_2$:

$$\begin{aligned}\mathcal{I}_3(\xi) &= \int_{x_s}^{x_2} \left(\frac{a_{1B}}{h}\left.\frac{\partial p}{\partial m}\right|_{H,p_0} + c_{1B}\left.\frac{\partial p}{\partial p_0}\right|_{H,M}\right) dx \\ &\quad -(p_B - p_A)\delta x_s.\end{aligned} \tag{E.74}$$

$x_1, x_2 < x_s$:

$\mathcal{I}_1$**:**

$\xi < x_1, x_2$:

$\xi < 0$:

$$\mathcal{I}_1(\xi) = 0. \tag{E.75}$$

$\xi > 0$:

$$\mathcal{I}_1(\xi) = \int_{x_1}^{x_2} \frac{1}{h} \left.\frac{\partial p}{\partial m}\right|_{H,p_0} dx. \tag{E.76}$$

$x_1 < \xi < x_2$:

$\xi < 0$:

$$\mathcal{I}_1(\xi) = -\int_{x_1}^{\xi} \frac{1}{h} \left.\frac{\partial p}{\partial m}\right|_{H,p_0} dx. \tag{E.77}$$

$\xi > 0$:

$$\mathcal{I}_1(\xi) = \int_{\xi}^{x_2} \frac{1}{h} \left.\frac{\partial p}{\partial m}\right|_{H,p_0} dx. \tag{E.78}$$

$x_1, x_2 < \xi < x_s$:

$\xi < 0$:

$$\mathcal{I}_1(\xi) = -\int_{x_1}^{x_2} \frac{1}{h} \left.\frac{\partial p}{\partial m}\right|_{H,p_0} dx. \tag{E.79}$$

$\xi > 0$:

$$\mathcal{I}_1(\xi) = 0. \tag{E.80}$$

$\xi > x_s$:

$$\mathcal{I}_1(\xi) = 0. \tag{E.81}$$

$\mathcal{I}_2$**:**

$$\mathcal{I}_2(\xi) = 0. \tag{E.82}$$

$\mathcal{I}_3$**:**

$\xi < x_1, x_2$:

$$\mathcal{I}_3(\xi) = \int_{x_1}^{x_2} \left.\frac{\partial p}{\partial p_0}\right|_{H,M} dx. \tag{E.83}$$

$x_1 < \xi < x_2$:

$$\mathcal{I}_3(\xi) = \int_{\xi}^{x_2} \left.\frac{\partial p}{\partial p_0}\right|_{H,M} dx. \tag{E.84}$$

$x_1, x_2 < \xi < x_s$:

$$\mathcal{I}_3(\xi) = 0. \tag{E.85}$$

$\xi > x_s$:

$$\mathcal{I}_3(\xi) = 0. \tag{E.86}$$

Pointwise functionals

Supersonic

$\mathcal{I}_1$**:**

$\xi < x_0$:

$$\mathcal{I}_1(\xi) = \frac{1}{h(x_0)} \frac{\partial p}{\partial m}(x_0)\bigg|_{H,p_0}. \tag{E.87}$$

$\xi > x_0$:

$$\mathcal{I}_1(\xi) = 0. \tag{E.88}$$

$\mathcal{I}_2$**:**

$$\mathcal{I}_2(\xi) = 0. \tag{E.89}$$

$\mathcal{I}_3$**:**

$\xi < x_0$:

$$\mathcal{I}_3(\xi) = \frac{\partial p}{\partial p_0}(x_0)\bigg|_{H,M}. \tag{E.90}$$

$\xi > x_0$:

$$\mathcal{I}_3(\xi) = 0. \tag{E.91}$$

Subsonic

$\mathcal{I}_1$**:**

$\xi < x_0$:

$$\mathcal{I}_1(\xi) = 0. \tag{E.92}$$

$\xi > x_0$:

$$\mathcal{I}_1(\xi) = -\frac{1}{h(x_0)} \frac{\partial p}{\partial m}(x_0)\bigg|_{H,p_0}. \tag{E.93}$$

$\mathcal{I}_2$**:**

$$\mathcal{I}_2(\xi) = 0. \tag{E.94}$$

$\mathcal{I}_3$: $\xi < x_0$:

$$\mathcal{I}_3(\xi) = \frac{a}{h(x_0)} \frac{\partial p}{\partial m}(x_0)\Big|_{H,p_0} + \frac{\partial p}{\partial p_0}(x_0)\Big|_{H,M}. \tag{E.95}$$

$\xi > x_0$:

$$\mathcal{I}_3(\xi) = \frac{a}{h(x_0)} \frac{\partial p}{\partial m}(x_0)\Big|_{H,p_0}. \tag{E.96}$$

Isentropic Transonic

$\mathcal{I}_1$:

$\xi < x_0$:

$\xi < 0$:

$$\mathcal{I}_1(\xi) = 0. \tag{E.97}$$

$\xi > 0$:

$$\mathcal{I}_1(\xi) = \frac{1}{h(x_0)} \frac{\partial p}{\partial m}(x_0)\Big|_{H,p_0}. \tag{E.98}$$

$\xi > x_0$:

$\xi < 0$:

$$\mathcal{I}_1(\xi) = -\frac{1}{h(x_0)} \frac{\partial p}{\partial m}(x_0)\Big|_{H,p_0}. \tag{E.99}$$

$\xi > 0$:

$$\mathcal{I}_1(\xi) = 0. \tag{E.100}$$

$\mathcal{I}_2$:

$$\mathcal{I}_2(\xi) = 0. \tag{E.101}$$

$\mathcal{I}_3$:

$\xi < x_0$:

$$\mathcal{I}_3(\xi) = \frac{\partial p}{\partial p_0}(x_0)\Big|_{H,M}. \tag{E.102}$$

$\xi > x_0$:

$$\mathcal{I}_3(\xi) = 0. \tag{E.103}$$

Shocked

$\boldsymbol{x_s < x_0}$:

$\mathcal{I}_1$:

$\xi < x_s$:

$\xi < 0$:

$$\mathcal{I}_1(\xi) = 0. \tag{E.104}$$

$\xi > 0$:

$$\mathcal{I}_1(\xi) = \frac{a_{2B}}{h(x_0)} \left.\frac{\partial p}{\partial m}(x_0)\right|_{H,p_0} + c_{2B} \left.\frac{\partial p}{\partial p_0}(x_0)\right|_{H,M}. \tag{E.105}$$

$x_s < \xi < x_0$:

$$\mathcal{I}_1(\xi) = \frac{1 + a_{1B}}{h(x_0)} \left.\frac{\partial p}{\partial m}(x_0)\right|_{H,p_0} + c_{1B} \left.\frac{\partial p}{\partial p_0}(x_0)\right|_{H,M}. \tag{E.106}$$

$\xi > x_0$:

$$\mathcal{I}_1(\xi) = \frac{a_{1B}}{h(x_0)} \left.\frac{\partial p}{\partial m}(x_0)\right|_{H,p_0} + c_{1B} \left.\frac{\partial p}{\partial p_0}(x_0)\right|_{H,M}. \tag{E.107}$$

$\mathcal{I}_2$**:**

$$\mathcal{I}_2(\xi) = 0. \tag{E.108}$$

$\mathcal{I}_3$**:** $\xi < x_s$:

$$\mathcal{I}_3(\xi) = \frac{a_{2B}}{h(x_0)} \left.\frac{\partial p}{\partial m}(x_0)\right|_{H,p_0} + c_{2B} \left.\frac{\partial p}{\partial p_0}(x_0)\right|_{H,M}. \tag{E.109}$$

$x_s < \xi < x_0$:

$$\mathcal{I}_3(\xi) = \frac{a_{1B}}{h(x_0)} \left.\frac{\partial p}{\partial m}(x_0)\right|_{H,p_0} + (1 + c_{1B}) \left.\frac{\partial p}{\partial p_0}(x_0)\right|_{H,M}. \tag{E.110}$$

$\xi > x_0$:

$$\mathcal{I}_3(\xi) = \frac{a_{1B}}{h(x_0)} \left.\frac{\partial p}{\partial m}(x_0)\right|_{H,p_0} + c_{1B} \left.\frac{\partial p}{\partial p_0}(x_0)\right|_{H,M}. \tag{E.111}$$

$\boldsymbol{x_0 < x_s}$**:**

$\mathcal{I}_1$**:**

$\xi < x_0$:

$\xi < 0$:

$$\mathcal{I}_1(\xi) = 0. \tag{E.112}$$

$\xi > 0$:

$$\mathcal{I}_1(\xi) = \frac{1}{h(x_0)} \left.\frac{\partial p}{\partial m}(x_0)\right|_{H,p_0}. \tag{E.113}$$

$x_0 < \xi < x_s$:

$\xi < 0$

$$\mathcal{I}_1(\xi) = -\frac{1}{h(x_0)} \left.\frac{\partial p}{\partial m}(x_0)\right|_{H,p_0}. \tag{E.114}$$

$\xi > 0$

$$\mathcal{I}_1(\xi) = 0. \tag{E.115}$$

$\xi > x_s$:

$$\mathcal{I}_1(\xi) = 0. \tag{E.116}$$

$\mathcal{I}_2$**:**

$$\mathcal{I}_2(\xi) = 0. \tag{E.117}$$

$\mathcal{I}_3$**:**

$\xi < x_0$:

$$\mathcal{I}_3(\xi) = \left.\frac{\partial p}{\partial p_0}(x_0)\right|_{H,M}. \tag{E.118}$$

$x_0 < \xi < x_s$:

$$\mathcal{I}_3(\xi) = 0. \tag{E.119}$$

$\xi > x_s$:

$$\mathcal{I}_3(\xi) = 0. \tag{E.120}$$

E.1.0.2 Rayleigh flow

Supersonic

$\mathcal{I}_1$:

$$\mathcal{I}_1(\xi) = \int_\xi^{x_e} \left.\frac{\partial p}{\partial m}\right|_{\mu,H_i} dx. \tag{E.121}$$

$\mathcal{I}_2$:

$$\mathcal{I}_2(\xi) = \int_\xi^{x_e} \left.\frac{\partial p}{\partial \mu}\right|_{m,H_i} dx. \tag{E.122}$$

$\mathcal{I}_3$:

$$\mathcal{I}_3(\xi) = \int_\xi^{x_e} \left.\frac{\partial p}{\partial H_i}\right|_{m,\mu} dx, \tag{E.123}$$

where

$$\left.\frac{\partial p}{\partial m}\right|_{\mu,H_i} = \frac{m}{\rho}\left(\frac{(\gamma-1)\mu+(\gamma+1)p}{\mu-(\gamma+1)p}\right), \tag{E.124}$$

$$\left.\frac{\partial p}{\partial \mu}\right|_{m,H_i} = \frac{(\gamma-1)\mu+p}{(\gamma+1)p-\mu}, \tag{E.125}$$

and

$$\left.\frac{\partial p}{\partial H_i}\right|_{m,\mu} = \frac{m^2(\gamma-1)}{\mu-(\gamma+1)p}. \tag{E.126}$$

Subsonic

$\mathcal{I}_1$:

$$\mathcal{I}_1(\xi) = \int_{x_i}^{\xi} a_1 \left.\frac{\partial p}{\partial m}\right|_{\mu,H_i} dx + \int_{\xi}^{x_e} (1+a_1) \left.\frac{\partial p}{\partial m}\right|_{\mu,H_i} dx + \int_{x_i}^{1} b \left.\frac{\partial p}{\partial \mu}\right|_{m,H_i} dx, \tag{E.127}$$

where

$$\left(a_1 \left.\frac{\partial p_0}{\partial m}\right|_{\mu,H_i} + b \left.\frac{\partial p_0}{\partial \mu}\right|_{m,H_i}\right)\Bigg|_{x_i} = 0, \tag{E.128}$$

$$\left(a_2 \left.\frac{\partial p}{\partial m}\right|_{\mu,H_i} + b \left.\frac{\partial p}{\partial \mu}\right|_{m,H_i}\right)\Bigg|_{x_e} = 0, \tag{E.129}$$

and $a_2 = 1 + a_1$.

$\mathcal{I}_2$:

$$\mathcal{I}_2(\xi) = \int_{x_i}^{1} a \left.\frac{\partial p}{\partial m}\right|_{\mu,H_i} dx + \int_{x_i}^{\xi} b_1 \left.\frac{\partial p}{\partial \mu}\right|_{m,H_i} dx + \int_{\xi}^{1} (1+b_1) \left.\frac{\partial p}{\partial \mu}\right|_{m,H_i} dx, \tag{E.130}$$

where

$$\left(a \left.\frac{\partial p_0}{\partial m}\right|_{\mu,H_i} + b_1 \left.\frac{\partial p_0}{\partial \mu}\right|_{m,H_i}\right)\Bigg|_{x_i} = 0, \tag{E.131}$$

$$\left(a \left.\frac{\partial p}{\partial m}\right|_{\mu,H_i} + b_2 \left.\frac{\partial p}{\partial \mu}\right|_{m,H_i}\right)\Bigg|_{x_e} = 0, \tag{E.132}$$

and $b_2 = 1 + b_1$.

$\mathcal{I}_3$:

$$\mathcal{I}_3(\xi) = \int_{x_i}^{1} \left(a \left.\frac{\partial p}{\partial m}\right|_{\mu,H_i} + b \left.\frac{\partial p}{\partial \mu}\right|_{m,H_i}\right) dx + \int_{\xi}^{x_e} \left.\frac{\partial p}{\partial H_i}\right|_{m,\mu} dx, \tag{E.133}$$

where

$$\left(a \left.\frac{\partial p_0}{\partial m}\right|_{\mu,H_i} + b \left.\frac{\partial p_0}{\partial \mu}\right|_{m,H_i} \right)\Bigg|_{x_i} = 0, \tag{E.134}$$

$$\left(a \left.\frac{\partial p}{\partial m}\right|_{\mu,H_i} + b \left.\frac{\partial p}{\partial \mu}\right|_{m,H_i} + \left.\frac{\partial p}{\partial H_i}\right|_{m,\mu} \right)\Bigg|_{x_e} = 0, \tag{E.135}$$

and

$$\left.\frac{\partial p_0}{\partial m}\right|_{\mu,H_i} = \frac{p_0}{p}\left(\frac{(\gamma-1)(\gamma+1)p-(\gamma-1)\mu}{(\gamma-1)((\gamma-1)\mu+(\gamma+1)p)}\right)\left.\frac{\partial p}{\partial m}\right|_{\mu,H_i}, \tag{E.136}$$

$$\left.\frac{\partial p_0}{\partial \mu}\right|_{m,H_i} = \frac{p_0}{p}\left(\frac{(\gamma-1)(2\gamma+1)p-(\gamma-1)\mu}{(\gamma-1)((\gamma-1)\mu+(\gamma+1)p)}\right)\left.\frac{\partial p}{\partial \mu}\right|_{m,H_i}. \tag{E.137}$$

Bibliography

[1] Lions, J. L., *Optimal Control of Systems Governed by Partial Differential Equations*, Springer Verlag, New York, 1971.

[2] Pironneau, O., "On optimum design in fluid mechanics," *Journal of Fluid Mechanics*, Vol. 64, No. 1, 1974, pp. 97–110.

[3] Jameson, A., "Aerodynamic Design via Control Theory," *Journal of Scientific Computing*, Vol. 3, No. 3, 1988, pp. 233–260.

[4] Jameson, A., Martinelli, L., and Pierce, N. A., "Optimum aerodynamic design using the Navier-Stokes equations," *Theoretical and Computational Fluid Dynamics*, Vol. 10, 1998, pp. 213–237.

[5] Zymaris, A. S., Papadimitriou, D. I., Giannakoglou, K. C., and Othmer, C., "Continuous adjoint approach to Spalart-Allmaras turbulence model for incompressible flows," *Computers and Fluids*, Vol. 38, 2009, pp. 1528–1538.

[6] Bueno-Orovio, A., Castro, C., Palacios, F., and Zuazua, E., "Continuous Adjoint Approach for the Spalart-Allmaras Model in Aerodynamic Optimization," *AIAA Journal*, Vol. 50, No. 3, March 2012.

[7] Duraisamy, K. and Alonso, J. J., "Adjoint Based Techniques for Uncertainty Quantification in Turbulent Flows with Combustion," *42nd AIAA Fluids Dynamics Conference*, New Orleans, LA, June 2012.

[8] Spalart, P. R. and Allmaras, S. R., "A One-equation Turbulence Model for Aerodynamic Flows," *La Recherche Aerospatiale*, 1994.

[9] Elliot, J. and Peraire, J., "Practical 3D Aerodynamic Design and Optimization Using Unstructured Meshes," *AIAA Journal*, Vol. 35, 1997, pp. 35–39.

[10] Giles, M. B., Duta, M. C., Müller, J.-D., and Pierce, N. A., "Algorithm Developments for Discrete Adjoint Methods," *AIAA Journal*, Vol. 41, No. 2, 2003, pp. 198–205.

[11] Giles, M. B., Ghate, D., and Duta, M. C., "Using Automatic Differentiation for Adjoint CFD Code Development," Technical Report 05/25, Oxford University Computing Laboratory, 2005.

[12] Baysal, O. and Eleshaky, M. E., "Aerodynamic Sensitivity Analysis Methods for the Compressible Euler Equations," *Journal of Fluids Engineering*, Vol. 113, 1991, pp. 681–688.

[13] Martins, J. R. R. A. and Hwang, J. T., "Review and Unification of Methods for Computing Derivatives of Multidisciplinary Systems," *53rd AIAA/ASME/ASCE/AHS/ASC Structures, Structural Dynamics and Materials Conference*, Honolulu, HI, April 2012.

[14] Reuther, J. and Jameson, A., "Supersonic Wing and Wing-Body Shape optimization Using an Adjoint Formulation," *International Mechanical Engineering Congress and Exposition*, 1995.

[15] Jameson, A. and Alonso, J. J., "Aerodynamic Shape Optimization Techniques Based On Control Theory," *AIAA*, 1998.

[16] Reuther, J. J., Jameson, A., Alonso, J. J., Rimlinger, M. J., and Saunders, D., "Constrained Multipoint Aerodynamic Shape Optimization Using an Adjoint Formulation and Parallel Computers, Part 1," *Journal of Aircraft*, Vol. 36, No. 1, January-February 1999, pp. 51–60.

[17] Reuther, J. J., Jameson, A., Alonso, J. J., Rimlinger, M. J., and Saunders, D., "Constrained Multipoint Aerodynamic Shape Optimization Using an Adjoint Formulation and Parallel Computers, Part 2," *Journal of Aircraft*, Vol. 36, No. 1, January-February 1999, pp. 61–74.

[18] Giles, M. B. and Pierce, N. A., "On the Properties of Solutions of the Adjoint Euler Equations," *Numerical Methods for Fluid Dynamics*, Vol. IV, 1998, pp. 1–16.

[19] Giles, M. B. and Pierce, N. A., "Improved lift and drag estimates using adjoint Euler equations," *AIAA*, 1999.

[20] Venditti, D. A. and Darmofal, D. L., "Anisotropic Grid Adaptation for Functional Outputs: Application to Two-dimensional Viscous Flows," *Journal of Computational Physics*, Vol. 187, 2002, pp. 22–46.

[21] Nemec, M., Aftosmis, M. J., and Wintzer, M., "Adjoint-Based Adaptive Mesh Refinement for Complex Geometries," *46th AIAA Aerospace Sciences Meeting*, Reno, NV., January 2008.

[22] Wintzer, M., Nemec, M., and Aftosmis, M. J., "Adjoint-Based Adaptive Mesh Refinement for Sonic Boom Prediction," *26th AIAA Applied Aerodynamics Conference*, Honolulu, HI, August 2008.

[23] Duraisamy, K. and Chandrashekar, P., "Goal-oriented uncertainty propagation using stochastic adjoints," *Computers and Fluids*, Vol. 66, 2012, pp. 10–20.

[24] Palacios, F., Duraisamy, K., Alonso, J. J., and Zuazua, E., "Robust Grid Adaptation for Efficient Uncertainty Quantification," *AIAA Journal*, Vol. 50, No. 7, 2012, pp. 1538–1546.

[25] Pierce, N. A. and Giles, M. B., "Adjoint and defect error bounding and correction for functional estimates," *Journal of Computational Physics*, Vol. 200, 2004, pp. 769–794.

[26] Giles, M. B. and Pierce, N. A., "An Introduction to the Adjoint Approach to Design," *Flow, Turbulence and Combustion*, Vol. 65, 2000, pp. 393–415.

[27] Giles, M. B. and Süli, E., "Adjoint methods for PDEs: a posteriori error analysis and postprocessing by duality," *Acta Numerica*, Vol. 11, January 2002, pp. 145–236.

[28] Anderson, W. K. and Venkatakrishnan, V., "Aerodynamic Design Optimization on Unstructured Grids with a Continuous Adjoint Formulation," *Computers and Fluids*, Vol. 28, No. 4-5, May-June 1999, pp. 443–480.

[29] Martins, J. R. R. A., Sturdza, P., and Alonso, J. J., "The Complex-Step Derivative Approximation," *ACM Transactions on Mathematical Software*, Vol. 29, 2003, pp. 245–262.

[30] Mader, C. A., Martins, J. R. R. A., Alonso, J. J., and Weide, E. V. D., "ADjoint: An Approach for the Rapid Development of Discrete Adjoint Solvers," *AIAA Journal*, Vol. 46, April 2008, pp. 4.

[31] Belegundu, A. D. and Arora, J. S., "A Sensitivity Interpretation of Adjoint Variables in Optimal Design," *Computer Methods in Applied Mechanics and Engineering*, Vol. 48, 1985, pp. 81–89.

[32] Hascoët, L. and Pascual, V., "TAPENADE 2.1 user's guide," Technical Report 0300, INRIA, http://www.inria.fr/rrrt/rt-0300.html, 2004.

[33] Griewank, A., Juedes, D., and Utke, J., "Algorithm 755: ADOL-C: A Package for the Automatic Differentiation of Algorithms Written in C/C++," *ACM Transactions on Mathematical Software*, Vol. 22, No. 2, 1996, pp. 131–167.

[34] Hicken, J. E. and Zingg, D. W., "Superconvergent functional estimates from summation-by-parts finite-difference discretizations," *SIAM Journal on Scientific Computing*, Vol. 33, No. 2, 2011, pp. 893–922.

[35] Nadarajah, S. K. and Jameson, A., "A Comparison of the Continuous and Discrete Adjoint Approach to Automatic Aerodynamic Optimization," *38th AIAA Aerospace Sciences Meeting*, No. AIAA-2000-0667, Reno, NV., January 2000.

[36] Lozano, C. and Ponsin, J., "Remarks on the numerical solution of the adjoint quasi-one-dimensional Euler equations," *International Journal for Numerical Methods in Fluids*, Vol. 69, 2011, pp. 966–982.

[37] Arian, E. and Salas, M. D., "Admitting the Inadmissible: Adjoint Formulation for Incomplete Cost Functionals in Aerodynamic Optimization," Technical Report 97-69, Institute for Computer Applications in Science and Engineering, NASA Langley Research Center, December 1997.

[38] Nielsen, E. J. and Anderson, W. K., "Aerodynamic Design Optimization on Unstructured Meshes Using the Navier-Stokes Equations," *AIAA*, 1998.

[39] Taylor, T. W. R., Palacios, F., Duraisamy, K., and Alonso, J. J., "Towards a Hybrid Adjoint Approach for Arbitrarily Complex Partial Differential Equations," *42nd AIAA Fluids Dynamics Conference*, New Orleans, LA, June 2012.

[40] Castro, C., Lozano, C., Palacios, F., and Zuazua, E., "Systematic Continuous Adjoint Approach to Viscous Aerodynamic Design on Unstructured Grids," *AIAA Journal*, Vol. 45, No. 9, September 2007, pp. 2125–2139.

[41] Baeza, A., Castro, C., Palacios, F., and Zuazua, E., "2D Euler Shape Design on Non-Regular Flows Using Adjoint Rankine-Hugoniot Relations," *AIAA Journal*, Vol. 47, No. 3, March 2009, pp. 522–562.

[42] Taylor, T. W. R., Palacios, F., Duraisamy, K., and Alonso, J. J., "Towards a hybrid adjoint approach for complex flow simulations," *Center for Turbulence Research Annual Research Briefs*, 2012, pp. 333–345.

[43] Taylor, T. W. R., Palacios, F., Duraisamy, K., and Alonso, J. J., "A hybrid adjoint approach applied to turbulent flow simulations," *43rd AIAA Fluids Dynamics Conference*, San Diego, CA, June 2013.

[44] Cook, P. H., McDonald, M. A., and Firmin, M. C. P., "Aerofoil RAE 2822 — Pressure Distributions, and Boundary Layer and Wake Measurements," Advisory Report 138, AGARD, 1979.

[45] Giles, M. B. and Pierce, N. A., "Analytic adjoint solutions for the quasi-one-dimensional Euler equations," *Journal of Fluid Mechanics*, Vol. 426, 2001, pp. 327–345.

[46] Giles, M. B. and Pierce, N. A., "Adjoint equations in CFD: duality, boundary conditions and solution behaviour," *AIAA*, 1997.

[47] Fidkowski, K. J. and David L, D., "Output-Based Error Estimation and Mesh Adaptation in Computational Fluid Dynamics. Overview and Recent Results," *47th AIAA Aerospace Sciences Meeting*, January 2009.

[48] Powers, J. M. and Aslam, T. D., "Exact Solution for Multidimensional Compressible Reactive Flow for Verifying Numerical Algorithms," *AIAA Journal*, Vol. 44, No. 2, February 2006, pp. 337–344.

[49] Roe, P. L., "Approximate Riemann Solvers, Parameter Vectors, and Difference Schemes," *Journals of Computational Physics*, , No. 43, 1981, pp. 357–372.

[50] Wang, Q., Duraisamy, K., Alonso, J. J., and Iaccarino, G., "Risk Assessment of Scramjet Unstart Using Adjoint-Based Sampling Methods," *AIAA Journal*, Vol. 50, No. 3, 2012, pp. 581–592.

[51] Palacios, F., Colonno, M. R., Aranake, A. C., Campos, A., Copeland, S. R., Economon, T. D., Lonkar, A. K., Lukaczyk, T. W., Taylor, T. W. R., and Alonso, J. J., "Stanford University Unstructured (SU2): An open-source integrated computational environment for multi-physics simulation and design," *51st AIAA Aerospace Sciences Meeting*, Grapevine, TX, January 2013.

[52] Jameson, A., Schmidt, W., and Turkel, E., "Numerical Solution of the Euler Equations by Finite Volume Methods Using Runge-Kutta Time-Stepping Schemes," *14th AIAA Fluid and Plasma Dynamic Conference*, Palo Alto, CA, June 1981.

[53] Haase, W., Bradsma, F., Elsholz, E., Leschziner, M., and Schwamborn, D., editors, *EUROVAL: An European Initiative on Validation of CFD Codes*, Vol. 42, Wiley, New York, 1993.

[54] Hicks, R. M. and Henne, P. A., "Wing Design by Numerical Optimization," *Journal of Aircraft*, Vol. 15, No. 7, 1978, pp. 407–412.